Universidade da Coruña

E.T.S. Ingenieros de Caminos, Canales y Puertos
Departamento de Tecnología de la Construcción

Simultaneous Utilization of Fine and Coarse Recycled Concrete Aggregate for the Fabrication and Experimental Analysis of the Structural Performance of Precast Reinforced and Prestressed Concrete Elements

Author

Pablo Vázquez Burgo

Advisors

Cristina Vázquez Herrero

Mª Isabel Martínez Lage

A Coruña, May 2016

Universidade da Coruña

E.T.S. Ingenieros de Caminos, Canales y Puertos
Departamento de Tecnología de la Construcción

Memoria presentada por Pablo Vázquez Burgo, bajo la dirección de las Doctoras Cristina Mercedes Vázquez Herrero y Mª Isabel Martínez Lage

Pablo Vázquez Burgo

Dra. Cristina Mercedes Vázquez Herrero

Dra. Mª Isabel Martínez Lage

A Coruña, mayo de 2016

"There are no secrets to success. It is the result of preparation, hard work, and learning from failure"

Coling Powell

Acknowledgements

Financial support for this study was provided by project FEDER-INNTERCONECTA ITC-20113055, Program "Development of value adding technologies for RCDs for innovative applications", which was convened by the Centre for Industrial and Technological Development (CDTI in Spanish), a subsidiary of the Ministry of Economics and Competitiveness, and the Technological Fund – FEDER Funds. I would like to thank the companies in the project consortium, SACYR Construcción S.A.U., Castelo Soluciones Estructurales Sociedad de Responsabilidad, Prefabricados Faro S.L. and CIMARQ Consultora de Ingeniería, Medio Ambiente y Arquitectura, S.L., for their participation in this study.

It is a pleasure to express my deep sense of thanks and gratitude to my advisors Dr. Isabel Martínez-Lage and Dr. Cristina Vázquez-Herrero for their full support, expert guidance, understanding and encouragement through my study and research. My thesis work would have not been possible without their incredible patience and counsel.

I would also like to thank my workmate Miriam Velay-Lizancos for her friendship and team spirit during this last four years. The work included in this dissertation would not have been possible without her priceless support.

Thanks also go to Dr. Fernando Martínez-Abella and Dr. Javi Eiras-López for their great involvement and significant help, as well as the rest of the members of the Group of Construction.

I am thankful to all the students who shared their valuable time to develop this project: Cristina, Marcos, Lidia, Jorge, Pablo, Conchi, Xacobe, Sara, Andrea and Eva; the technical staff of the CITEEC: Jose, Dani, Gonzalo, Miguel, Esteban and Félix; and specially, to the laboratory technician of the School of Civil Engineering, María Recarey.

The workmates who were sharing different offices with me during these years deserve special mention for all those hours trying to solve problems together: Ibuki, Antonio, Alba, Miguel and Rubén; as well as the members of the Group of Calculus: Adrián, Guille L., Guille V., Hugo, Carles and Jiangping Xu.

Finally, I would like to thank all my family and friends, specially my parents Alvaro and Conchi, mi sister Iria and my girlfriend Paula for their unconditional support. They are the people who best know me and have always been there in good and bad times.

All the above-mentioned people and institutions have made possible this doctoral thesis.

Summary

This doctoral thesis aims at taking a step forward in concrete recycling, since it is proposed to replace simultaneously the fine and coarse fraction of the aggregate without having to previously sieve the raw recycled aggregate. The structural behaviour of both precast reinforced and prestressed concrete elements was assessed, compared to conventional concretes with similar compressive strength.

A first experimental campaign was performed with self-compacting recycled concrete. Different percentages of the total amount of natural aggregates (0, 20, 35 and 50%, including fine and coarse fraction) were replaced with recycled aggregates from rejected members of a precast plant. Fresh and hardened concrete properties were compared in laboratory for the different replacement levels. The mechanical properties were not significantly affected. So, the resulting recycled concrete was utilised for the fabrication of reinforced concrete beams in a precast plant with replacement levels of 0, 10, 20, 35 and 50%. Reinforced beams were subjected to quality control shear and flexural failure tests in the precast plant showing a similar ultimate bending moment and shear strength regardless of the replacement ratio. However, the ductility factor of flexural beams and cracking moment decreased for higher replacement levels. Flexural tests were repeated with displacement control and accurate monitoring in the CITEEC at the University of A Coruña, including strain gauges on concrete surface to obtain the flexural behaviour up to failure, the ductility factors, and moment vs. curvature relationships. The results obtained showed a lower cracking moment and ductility for the higher replacement levels but similar ultimate moments.

A second experimental campaign was performed with vibrated concrete and prestressed precast concrete beams. In this case, the source of the recycled aggregate was old concrete sleepers. Different percentages of the total amount of natural aggregates (0, 8, 20 and 31%, including fine and coarse fraction) were replaced by recycled aggregates and fresh and hardened properties were compared in laboratory for the different replacement levels. The mechanical properties did not experience considerable decrease depending on the replacement percentage. So, the resulting recycled concrete was utilised for the fabrication of prestressed concrete beams, as well as Pull-Out test samples with replacement levels of 0

and 8%. The aim was to evaluate the loss of bond performance between prestressed strands and surrounding concrete when recycled aggregates are introduced in the mix.

Pull-Out tests showed that the bond stress at which the first slip occurs is approximately 24% lower when 8% of the total aggregate is replaced with recycled aggregate. Prestressed beams were monitored to evaluate transfer and development length. Transfer length was evaluated measuring the strain values with DEMEC points at different ages. It was determined to be 717 mm in natural concrete beams and 957 mm in recycled beams. That is, there is an increase of 33% in transfer length when 8% recycled aggregate is incorporated in the concrete mix. Development length was evaluated performing flexural tests at different embedment lengths and measuring the strand end slips during the tests. It was determined to be 1475 mm in natural concrete beams and 1850 mm in recycled concrete beams. That is, there is an increase of 25% in development length when 8% recycled aggregate is incorporated in the concrete mix.

From this research it may be concluded that it is feasible to replace up to 50% of the total aggregate (fine and coarse) in reinforced concrete beams. However, the incorporation of recycled aggregate in prestressed concrete significantly reduces the bond between prestressed strands and surrounding concrete in beams fabricated with 8% replacement of the total aggregate. Consequently, further research is recommended in this subject.

Resumen

Esta tesis doctoral busca llevar un paso adelante el reciclado del hormigón ya que propone reemplazar simultáneamente la fracción fina y gruesa del árido, sin tener que cribar previamente el árido reciclado bruto. El comportamiento estructural, tanto de vigas prefabricadas armadas como pretensadas fue evaluado, comparándolo al de un hormigón convencional con una resistencia a compresión similar.

Se realizó una primera campaña experimental con hormigón autocompactante reciclado. Diferentes porcentajes de la cantidad total de árido natural (0, 20, 35 y 50%, incluyendo la fracción fina y gruesa) fueron reemplazados por árido reciclado de elementos rechazados de una planta de prefabricados. Las propiedades del hormigón fresco y endurecido fueron comparadas en el laboratorio para los diferentes porcentajes de sustitución. Las propiedades mecánicas no se vieron significativamente afectadas. Por lo tanto, el hormigón reciclado resultante fue utilizado para la fabricación de vigas de hormigón armado en una planta de prefabricados con porcentajes de sustitución del 0, 10, 20, 35 y 50%. Las vigas armadas fueron sometidas a ensayos de control de calidad de flexión y cortante en la planta, mostrando un momento último y resistencia a cortante similares, independientemente del porcentaje de sustitución. Sin embargo, el factor de ductilidad y el momento de fisuración disminuyeron para los porcentajes más altos. Los ensayos a flexión fueron repetidos mediante control de desplazamiento y una instrumentación más precisa en el CITEEC de la Universidade da Coruña, incluyendo galgas de deformación en la superficie del hormigón para obtener el comportamiento a flexión hasta rotura, factores de ductilidad, y la relación Momento-Curvatura. Los resultados obtenidos mostraron un momento de fisuración y ductilidad más bajo para los porcentajes de sustitución más altos, pero igual momento último.

Una segunda campaña experimental fue realizada con hormigón convencional y vigas prefabricadas pretensadas de hormigón. En este caso, el origen del árido reciclado fue viejas traviesas de hormigón. Diferentes porcentajes de la cantidad total de árido natural (0, 8, 20 y 31%, incluyendo la fracción fina y gruesa) fueron sustituidos por árido reciclado, comparando las propiedades en estado fresco y endurecido para los diferentes porcentajes. Las propiedades mecánicas no se vieron excesivamente afectadas. Por lo tanto, el hormigón resultante fue utilizado para la fabricación de las vigas pretensadas y de las probetas para

ensayos Pull-Out, con sustituciones del 0 y 8%. La finalidad fue evaluar la pérdida de comportamiento adherente entre los cordones pretensados y el hormigón que los envuelve cuando el árido reciclado se introduce en la mezcla.

Los ensayos Pull-Out reflejaron que la tensión adherente a la que se produce el primer deslizamiento es aproximadamente un 24% inferior cuando se introduce un 8% de árido reciclado en la mezcla. Las vigas pretensadas fueron instrumentadas interna y externamente para evaluar la longitud de transmisión y de anclaje. La longitud de transmisión se evaluó midiendo las deformaciones con puntos DEMEC a diferentes edades. Se determinó un valor de 717 mm en las vigas de hormigón natural y 957 mm en las de reciclado. Por lo tanto, hay un incremento del 33% en la longitud de transmisión cuando el 8% de árido reciclado se incorpora a la mezcla. La longitud de anclaje se evaluó realizando ensayos a flexión con diferentes puntos de aplicación de las cargas y midiendo la penetración de los cordones durante el ensayo. Se determinó un valor de 1475 mm en las vigas de hormigón natural y 1850 mm en las vigas de hormigón reciclado. Es decir, hay un incremente del 25% en la longitud de anclaje cuando el 8% de árido reciclado se incorpora a la mezcla.

De esta investigación se puede concluir que es viable reemplazar hasta un 50% del árido total (fino y grueso) en vigas armadas. Sin embargo, incluir árido reciclado en hormigón pretensado disminuye significativamente la adherencia en las vigas fabricadas con un 8% de sustitución del árido total. Por consiguiente, es recomendable realizar una investigación más profunda sobre este tema.

Resumo

Esta tese doutoral busca levar un paso adiante o reciclado do formigón xa que propón substituír simultaneamente a fracción fina e grosa do árido, sen ter que cribar previamente o árido reciclado bruto. O comportamento estrutural tanto de vigas prefabricadas armadas como pretensadas foi avaliado, comparándoo co dun formigón convencional cunha resistencia a compresión similar.

Realizouse una primeira campaña experimental con formigón autocompactante reciclado. Diferentes porcentaxes da cantidade total do árido natural (0, 20, 35 e 50%, incluíndo a fracción fina e grosa) foron substituídos por árido reciclado de elementos rechazados dunha planta de prefabricados. As propiedades do formigón fresco e endurecido foron comparadas no laboratorio para os diferentes porcentaxes de substitución. As propiedades mecánicas non foron significativamente afectadas. Polo tanto, o formigón reciclado resultante foi utilizado para a fabricación das figas de formigón armado nunha planta de prefabricados con porcentaxes de substitución do 0, 10, 20, 35 e 50%. As vigas armadas foron sometidas a ensaios de control de calidade a flexión e cortante na planta, amosando un momento último e resistencia a cortante similares, independentemente do porcentaxe de substitución. Sen embargo, o factor de ductilidade e o momento de fisuración diminuíron para os porcentaxes máis altos. Os ensaios a flexión foron repetidos mediante control de desprazamento e cunha instrumentación máis precisa no CITEEC da Universidade da Coruña, incluíndo galgas de deformación na superficie do formigón para obter o comportamento a flexión ata rotura, os factores de ductilidade e a relación Momento-Curvatura. Os resultados obtidos amosan un momento de fisuración e ductilidade más baixo para os porcentaxes de substitución máis altos, pero igual momento último.

Unha segunda campaña experimental foi realizada con formigón convencional e vigas prefabricadas pretensadas de formigón. Neste caso, a orixe do árido reciclado foi travesas vellas de formigón. Diferentes porcentaxes da cantidade total do árido natural (0, 8, 20 e 31%, incluíndo a fracción fina e grosa) foron substituídos por árido reciclado, comparando as propiedades en estado fresco e endurecido para os diferentes porcentaxes. As propiedades mecánicas non se viron excesivamente afectadas. Polo tanto, o formigón resultante foi utilizado para a fabricación das vigas pretensadas e probetas para ensaios Pull-Out, con substitucións do 0 e 8%. A finalidade foi avaliar a pérdida do comportamento adherente

entre os cordóns pretensados e o formigón que os envolve cando o árido reciclado é introducido no formigón.

Os ensaios Pull-Out reflexaron que a tensión adherente á que se produce o primeiro deslizamento é aproximadamente un 24% inferior cando se introduce un 8% de árido reciclado no formigón. As vigas pretensadas foron instrumentadas interna e externamente para avaliar a lonxitude de transmisión e de ancoraxe. A lonxitude de transmisión avaliouse medindo as deformación con puntos DEMEC a diferentes idades. Determinouse un valor de 717 mm nas vigas de formigón natural e 957 mm nas de reciclado. Polo tanto hai un incremento do 33% na lonxitude de transmisión cando o 8% do árido reciclado se incorpora no formigón. A lonxitude de ancoraxe avaliouse realizando ensaios a flexión con diferentes puntos de aplicación das cargas e medindo a penetración dos cordóns durante o ensaio. Determinouse un valor de 1475 mm nas vigas de formigón natural e 1850 mm nas vigas de formigón armado. É dicir, hai un incremento do 25% na lonxitude de ancoraxe cando o 8% do árido reciclado se incorpora no formigón.

Desta investigación pódese concluír que é viable substituír ata un 50% do árido total (fino e groso) en vigas armadas. Sen embargo, non é aconsellable incluír árido reciclado en formigón pretensado debido á gran pérdida de adherencia observada cun 8% de substitución do árido total. Por conseguinte, é recomendable realizar unha investigación mais profunda neste tema.

Table of contents

List of Tables

List of Figures

Chapter 1. Introduction

1.1. Background

Concrete is a composite material obtained basically from the mix of a binder, generally cement, coarse aggregates, sand and water. When all these elements are mixed together in appropriate proportions, they form a fluid mass. Cement reacts chemically with water, forming a hard matrix which blinds all the materials together into a new material with stone-like aspect. In many cases, additives and admixtures are included to improve the physical properties of the fluid mass or the final material.

Concrete has very high compressive strength but it is very fragile when submitted to tensile splitting forces. Therefore, when necessary, it is poured with reinforcing materials embedded, such as steel bars, to provide tensile strength and ductility. This is known as reinforced concrete. Other method to overcome concrete's weakness in tension is prestressing the concrete element. Prestressing tendons (wires or strands) are used to introduce a previous compressive stress that balances the tensile stress that concrete element would experience due to a bending load.

The urban development of the last decades, especially in developing countries (Figure 1.1), with concrete as its main construction material, has caused a huge demand of aggregates, which has led to the exhaustion of these natural resources in some sites, and to critical environmental impact worldwide. The extraction of these materials has an important impact on the environment, causing modifications to the landscape shape; pollution of the air, water and soil; deforestation; in sum, an overall damage to the natural landscape. At the same time, millions of tonnes of debris from construction and demolition wastes are generated and go directly to landfills without a previous treatment or selection that might result in their reutilization (Figures 1.2 and 1.3).

Approximately half of the construction and demolition waste produced in Spain is made of brick, tiles and ceramic, and by 20% are made of concrete and mortar. These waste can be

reused as recycled aggregates for the fabrication of concrete after being crushed and sieved. Several studies have been performed to date by different authors with very promising results [GEAR 2002].

Many countries have regulations on the use of recycled aggregates in concrete. In particular, the Spanish Regulation EHE-08 defines “recycled concrete” as a concrete produced with coarse recycled aggregate from the crushing of concrete waste, and recommends to limit the replacement ratio to 20% when used in structural concrete. Therefore, it excludes fine recycled concrete aggregates (FRA) and aggregates with a source different from concrete (mixed recycled aggregate, asphalt, etc.).

Figure 1.1. Elevated highways, Segundos Pisos at Mexico City

In other countries, the regulations with regard to the use of recycled concrete are different. Some of them allow higher replacement levels of coarse recycled concrete aggregate in structural concrete, such as Germany and Japan with 35% replacement, or even the Netherlands and Denmark with full replacement. With regard to the use of FRA, it is allowed in Brazil with a 100% replacement for non-structural concrete, in Japan for less demanding structures up to 100%, in the Netherlands only if the coarse aggregate is natural, in Switzerland with a 100% replacement even in structural concrete, 20% in Denmark for non-aggressive environments, and 100% in Russia for non-prestressed concrete.

Figure 1.2. Rejected precast concrete slabs at Tyconsa precast plant, Mexico City

Figure 1.3. Rejected precast concrete pillar at Pretencreto. Precast Plant. Mexico City

After several studies on the use of fine recycled aggregate, it was concluded that, with the right approach, it is feasible to make concrete with FRA and get a similar behaviour to concrete made of solely natural aggregates. Therefore, it is too conservative to consider unacceptable the use of FRA in concrete production.

On the other hand, the use of recycled concrete to produce reinforced and prestressed concrete members is conditioned by the structural performance and durability of these structures. Structural performance is key, especially in seismic zones. Seismic design objectives are met by "judicially equipping structures with adequate and appropriately distributed (in plan and in elevation) stiffness, strength, and ductility" [VILL 2009]. The structural requirements for structures built in seismic zones are more restrictive than those included in non-seismic zones [EHE 08]. In this thesis, the use of recycled aggregate concrete in both reinforced and prestressed concrete structures is studied, focused on the structural properties that must be assessed in seismic zones. This research is conducted comparing these structural in recycled aggregates concrete structures, compared to conventional concrete ones.

The following structural properties are addressed regarding reinforced and prestressed precast concrete structural elements:

- An adequate level of stiffness for flexural behaviour, analysing the experimental load vs. displacement behaviour of recycled aggregate concrete reinforced and prestressed concrete beams under increasing load up to failure. In particular, moment vs. curvature relationships are attained and compared to analytical predictions, after performance based seismic design.
- An appropriate level of strength of the tested structural members is assessed, as well as its ductility capacity, namely the "ability of the structure to undergo large inelastic deformations without significant reduction of its stiffness and strength during repetitive

dynamic loading-unloading-reloading cycles" [AVRA 2016, page 9]. Ductility factors are determined with respect to displacement and curvature for each tested material structural member.

- Adequate bond properties in the precast prestressed concrete beams that were monitored, produced and tested at a precast concrete facility, from recycled aggregate concrete and conventional concrete, have been assessed: transfer length and development length. Also, instantaneous prestress losses have been quantified during the production of these beams. These parameters are paramount in the design of prestressed precast concrete structures with recycled aggregate concrete, a possible use that accounts for no published previous research so far.

1.2. Research significance and aim of thesis

The research significance of this doctoral thesis is to take a step forward in concrete recycling. So far, most of research performed on concrete recycling has been focused on replacing solely different ratios of the coarse fraction from different sources. Few studies have been performed on the fine fraction and when both fractions have been replaced in the same mix composition, this substitution has been done independently. This procedure implies an important waste of energy since aggregates need to be sieved to obtain the desired fractions.

In this doctoral thesis, it is proposed to replace simultaneously the fine and coarse fraction by weight without having to sieve the raw recycled aggregate. It is necessary to analyse the particle size distribution of the recycled aggregate to determine its percentage of fine particles (< 4 mm). Then, the recycled aggregate will be introduced in the mix as a replacement of the total aggregate, removing the corresponding fine and coarse fractions from the natural aggregates, according to the percentage of fines previously determined.

With this method, it is possible to obtain similar joint particle size distributions of the total aggregate regardless of the replacement level. Moreover, the fine fraction is introduced in the mix instead of being dismissed and the corresponding waste of energy at sieving is avoided.

This replacement method has not only been tested in reinforced concrete, but also in prestressed concrete. So far, no studies have been found on the use of recycled aggregates for prestressed concrete. Therefore, this research offers a first approach to analyse the stiffness, strength, ductility and bond behaviour of prestressed concrete when recycled concrete aggregates are introduced in the mix.

1.3. General objectives

This doctoral thesis has two main objectives related to the use of recycled concrete aggregates for structural concrete.

The first objective is to analyse the feasibility of replacing higher ratios than the limit of 20% recommended by the Spanish Code EHE-08 for the coarse aggregate in reinforced concrete. However, in this case, both the fine and coarse fraction will be replaced. The substitution will be simultaneous in both fractions according to the particle size distribution of the raw recycled aggregate, without having been submitted to a previous sieving process. Accordingly, structural testing will be performed so as to characterize the stiffness, strength and ductility of reinforced recycled concrete beams compared to conventional concrete ones. Thus, the structural performance of recycled aggregate concrete beams will be assessed.

The second objective consists of studying the feasibility of producing prestressed concrete beams when recycled aggregates are introduced in the mix. Prestressed concrete beams will be produced and monitored at a precast concrete plant, using both a recycled aggregate concrete and a reference concrete with a similar compressive strength. After prestress transfer at the plant, the prestress losses and transfer length will be determined. Then, beams will be monitored and subjected to flexural tests by displacement control, allowing to determine their stiffness, strength, ductility, and development length. In this case, 8% percent of the total aggregate (fine and coarse) will be replaced. In conclusion, the structural behaviour of pretensioned concrete beams made of recycled aggregate concrete will be assessed.

These goals surpass the scope of the current standard EHE-08, both in the materials and the seismic requirements included in this national standard. The results of this thesis may support an increase beyond the maximum 20% replacement recommended by the EHE-08 for coarse recycled aggregate, and even permit the incorporation of the fine fraction of recycled aggregates.

1.4. Organisation

This doctoral thesis is organised in six chapters.

Chapter 1 is an introductory chapter to the main topic of this thesis, with a first approach to the recycling of construction and demolition waste (CDW) and the current situation in the Spanish standards with regard to its incorporation in structural concrete. The general objectives and the aim of this research work are explained as well as the methodology followed to achieve the goals.

Chapter 2 includes a detailed analysis on the studies performed to date on recycled concrete and bond behaviour between concrete and prestressing strand. It is divided in two parts. The first part is focused on recycled concrete; in particular, recycled concrete including fine recycled concrete aggregates. The second part is focused on the bond performance between prestressing strands and surrounding concrete, especially studies related to transfer and development length. In particular, studies on the incorporation of recycled aggregate in prestressed concrete have not been found so far.

Chapter 3 is focused on the use of fine and coarse recycled concrete aggregates in reinforced concrete. It includes the main properties of the materials utilised for this study and the mechanical properties of the mix compositions, preliminary shear and flexural tests of reinforced beams in the precast plant where they were fabricated, and a more accurate analysis on the flexural behaviour, monitoring the whole failure process.

Chapter 4 presents a similar study, but in this case, the materials utilised are different and the beams are prestressed. The main properties of the materials and the mechanical properties of the mix compositions are included in this chapter, as well as the fabrication process, where the beams where internally and externally monitored. Pull-out bond tests are also included, with the fabrication procedure and a description of the test to evaluate the loss of bond performance when recycled aggregate is introduced in the mix.

Chapter 5 includes a description and results of the transfer length test, based on strain measurements and strand slip values at transfer; and the development length test, based on flexural failure tests with different embedment lengths at the same time that strand slips are measured. The experimental values are compared with the values obtained from equations proposed by different authors.

Chapter 6 summarises the conclusions drawn from this investigation and the proposed future lines of research.

Finally, references and bibliography are included at the end of this document as well as several appendices with information necessary to follow the line of the investigation.

1.5. Methodology

The methodology followed to achieve the aforementioned objectives can be summarised in four stages which took place in a chronological order.

The first stage includes an analysis of the current standards and studies performed up to now on the use of recycled concrete aggregates for the fabrication of concrete as well as the bond behaviour between prestressed strands and concrete. The information was searched on books, scientific journals and conference papers. After analysing all this information, an

experimental campaign was designed to study the possibility of substituting higher replacement levels of recycled aggregate than those permitted by the current regulations in structural concrete and including the fine fraction.

The second stage depicts the first part of the experimental campaign. This part includes:

- Detailed study of the main properties of the materials utilised in the mixes according to the UNE-EN Standards.
- Laboratory tests to assess the evolution of the concrete mechanical properties when 0, 20, 35 and 50% of the total aggregate (fine and coarse) was replaced. These tests were performed according to the UNE-EN Standards.
- Fabrication of reinforced beams with replacement ratios of 0, 10, 20, 35 and 50% in a precast plant.
- In-situ flexural and shear failure tests, performed on force control, measuring the deflection at mid-span as a preliminary study of the loss of mechanical properties when recycled aggregate is introduced in different ratios.
- Flexural tests performed at the university following the displacement control procedure described in Appendix 2. The applied load was monitored with load cells, the deflection at mid span measured with a linear potentiometric transducer and the strain values measured with strains gauges fixed to the concrete surface.

The third stage depicts the second part of the experimental campaign. This part includes:

- A preliminary study of the mechanical performance of prestressed concrete when recycled aggregate is introduced in the mix in ratios lower than 10% of the total aggregate. For this purpose, prestressed pre-slabs with replacement levels of 0, 2, 4, 6, 8 and 10% of the total aggregate which were subjected to flexural and shear tests.
- A detailed study of the main properties of the materials utilised in the mixes according to the UNE-EN Standards.
- Laboratory tests were performed to assess the evolution of the mechanical properties when 0, 8, 20 and 31% of the total aggregate (fine and coarse) was replaced. These tests were performed according to the UNE-EN Standards.
- The fabrication and monitoring of prestressed I-beams with replacement ratios of 0 and 8% in a precast plant, following the procedures described in Appendices 4 and 5.
- The measurement of the strands slips and transfer length immediately after prestress transfer.
- The measurement of the strain values with the DEMEC points adhered to the concrete surface on both sides of the beam. These measures were taken immediately before transfer, after transfer, at 7, 14, 28, 90 and 300 days.
- Flexural tests controlled by displacement with different embedment lengths following the procedure described in Appendix 2. The deflection was measured at

mid span with linear potentiometric transducer, the load applied to the beam registered with load cells or an oil pressure transducer, the strands slips measured with linear displacement sensors attached to the strands and the strain values measured with strains gauges fixed to the concrete surface.

The last stage includes a deep analysis of the data obtained from the experimental campaign and its comparison with analytical predictions. These results were compared with those of previous authors and a series of conclusions were drawn together with several recommendations.

Chapter 2. Literature Review

This chapter includes a detailed analysis on the studies performed to date on recycled concrete and bond behaviour between concrete and prestressing strand. It is divided in two parts. The first part is focused on recycled concrete; in particular, recycled concrete including fine recycled concrete aggregates. The second part is focused on the bond performance between prestressing strands and surrounding concrete, especially studies related to transfer and development length. Studies on the incorporation of recycled aggregate in prestressed concrete have not been found so far.

2.1. Recycled aggregate

2.1.1. Environmental sustainability

Sustainable development can be defined as "a process of change in which the exploitation of resources, the direction of investments, the orientation of technological development; and institutional change are all in harmony and enhance both current and future potential to meet human needs and aspirations". This definition was used on the World Commission on Environment and Development: Our Common Future [BRUN 1987].

The boom of the urban development in the last decades has caused a fast reduction in the available natural resources in some parts of the world. The construction industry needs a considerably amount of raw materials whose extraction causes modifications in the course and bed of the rivers, damages the natural landscape and affects slope stability. At the same time, millions of tonnes of debris from construction and demolition wastes are generated and go directly to landfills (Figure 2.1), without a previous treatment or selection that might result in their reutilization.

Figure 2.1. Debris in landfill
(*http://www.20minutos.es/noticia/1047474/0/ladrillos/basura/proyecto)*

In 1999, a study into "Construction and Demolition Waste Management Practises, and their Economic Impacts" was published and it is known as the Symonds Report [SYMO 1999]. This study was undertaken between January 1998 and March 1999 and shows that in the European Union (15 countries at that time) 180 million tonnes of Construction and Demolition Wastes were produced each year with different levels of reuse or recycling depending on the country (Table 2.1). This is over 480 kg per person per year, and only about 28% across the EU-15 as a whole is re-used or recycled. Landfilling comprises the other 72%.

On the basis of this report, detailed studies have been done by the countries with the aim of having a more accurate value of the amount of CDW produced as well as CDW recycled. The report of the European Commission (DG ENV) [EURO 2011] ""Service Contract on Management of Construction and Demolition Waste – SR1, February 2011 written by the BIO Intelligence Service in association with ARCADIS and Institute European Environmental Policy, shows this increase in the production and recycling of CDW in every country (Table 2.1) in comparison with the previous report. The value for the CDW produced by the 27 countries is 532 million tonnes each year and 423 are solely produced by the 15 countries of the Symonds Report, which represents 1000 Kg per person per year.

Table 2.1. CDW Arising and Recycling

Member State Country	Symonds Report Arising (million tonnes)	Symonds Report % Re-Used or Recycled	European Comission (DG ENV) Arising (million tonnes)	European Comission (DG ENV) % Re-used or recycled
Austria	4.70	41	6.60	60
Belgium	6.75	87	11.02	68
Denmark	2.64	81	5.27	94
Finland	1.35	45	5.21	26
France	23.60	15	85.65	45
Germany	59.00	17	72.40	86
Greece	1.80	< 5	11.04	5
Ireland	0.57	< 5	2.54	80
Italy	20.00	9	46.31	(*)
Luxembourg	0.30	n/a	0.67	46
Netherlands	11.17	90	23.9	98
Portugal	3.20	< 5	11.42	5
Spain	12.80	< 5	31.34	14
Sweden	1.69	21	10.23	(*)
UK	30.00	45	99.10	75
EU-15	179.70	28	422.70	53
Bulgaria			7.80	(*)
Cyprus			0.73	1
Czech Republic			14.70	23
Estonia			1.51	92
Hungary			10.12	16
Latvia			2.32	46
Lithuania			3.45	60
Malta			0.80	(*)
Poland			38.19	28
Romania			21.71	(*)
Slovak Republic			5.38	(*)
Slovenia			2.00	53
EU 27			531.38	46

(*) No data available

Nowadays, this amount has increased and construction and demolition waste (CDW) is one of the most significant waste streams in the EU, accounting for approximately 750 million tonnes per year according to the EU Commission. It is estimated that CDW accounts for approximately 25% - 30% of all waste generated each year in the EU and consists of numerous materials, including concrete, bricks, gypsum, wood, glass, plastic, solvents, asbestos and excavated soil, many of which can be recycled.

One of the objectives of the Waste Framework Directive (2008/98/EC) was to provide a framework for moving towards a European recycling society with a high level of resource

efficiency. In particular, Article 11.2 stipulates that "Member States shall take the necessary measures designed to achieve that by 2020 a minimum of 70% (by weight) of non-hazardous construction and demolition waste excluding naturally occurring material defined in category 17 05 04 in the List of Wastes shall be prepared for re-use, recycled or undergo other material recovery" (including backfilling operations using waste to substitute other materials).

As observed in the Symonds Report, the level of recycling and material recovery of CDW varies greatly (between less than 10% and over 90%) across the Union. If not separated at source, CDW can contain small amounts of hazardous wastes, the mixture of which can pose particular risks to the environment and can hamper recycling. The Figure 2.2 shows the levels of recycling and backfilling in the EU Members in 2011 published by the European Commission.

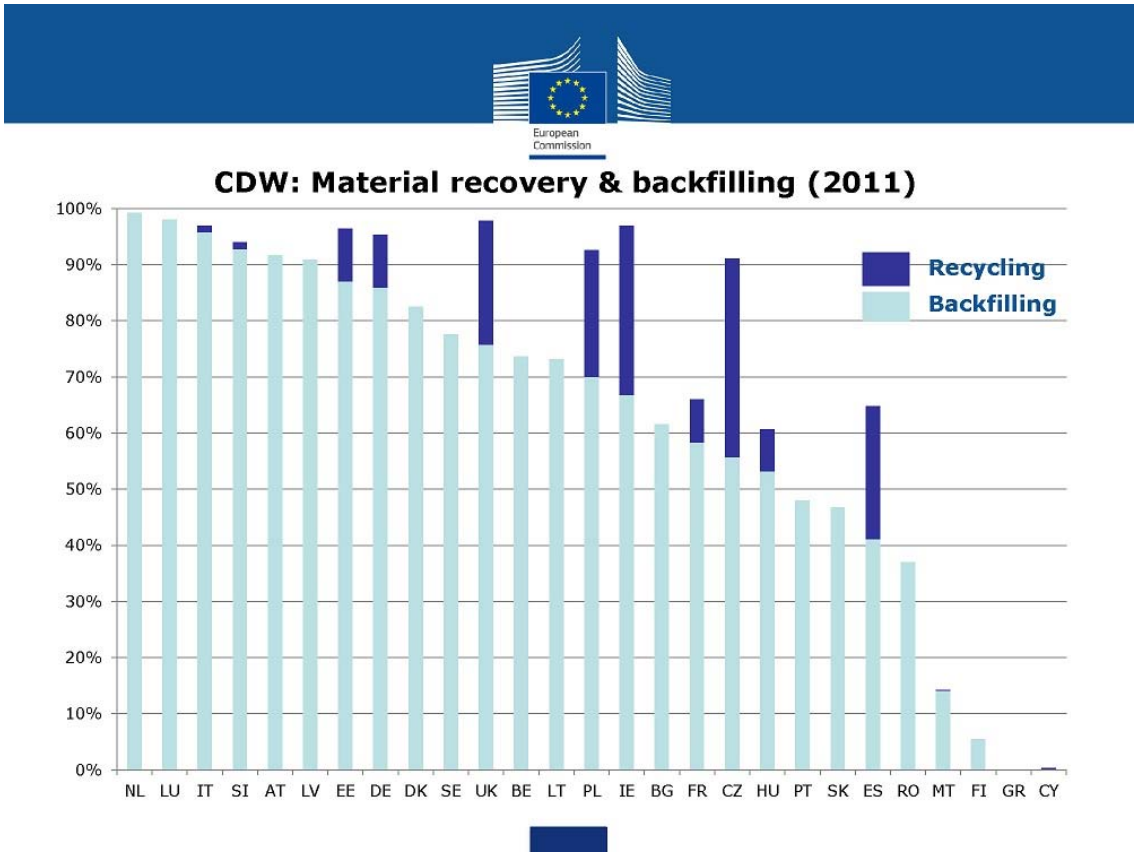

Figure 2.2. CDW: Material recovery & backfilling (2011)

A new project of the European Commission 'Resource Efficient Use of Mixed Waste' led by BIO by Deloitte in partnership with BRE, ICEDD, VTT, RPS and FCT of NOVA University of Lisbon has been conducted until April 2016. The aim of the study is to investigate the current CDW management situation in EU Member States, identifying the obstacles and deficiencies that could lead to non-compliance with EU waste legislation. Good practises and recommendations will be formulated to increase CDW recycling.

In Spain, according to the National Plan of Concrete and Demolition Waste Management (2001-2006). The composition of the CDWs that usually go to landfill is shown in Figure 2.3.

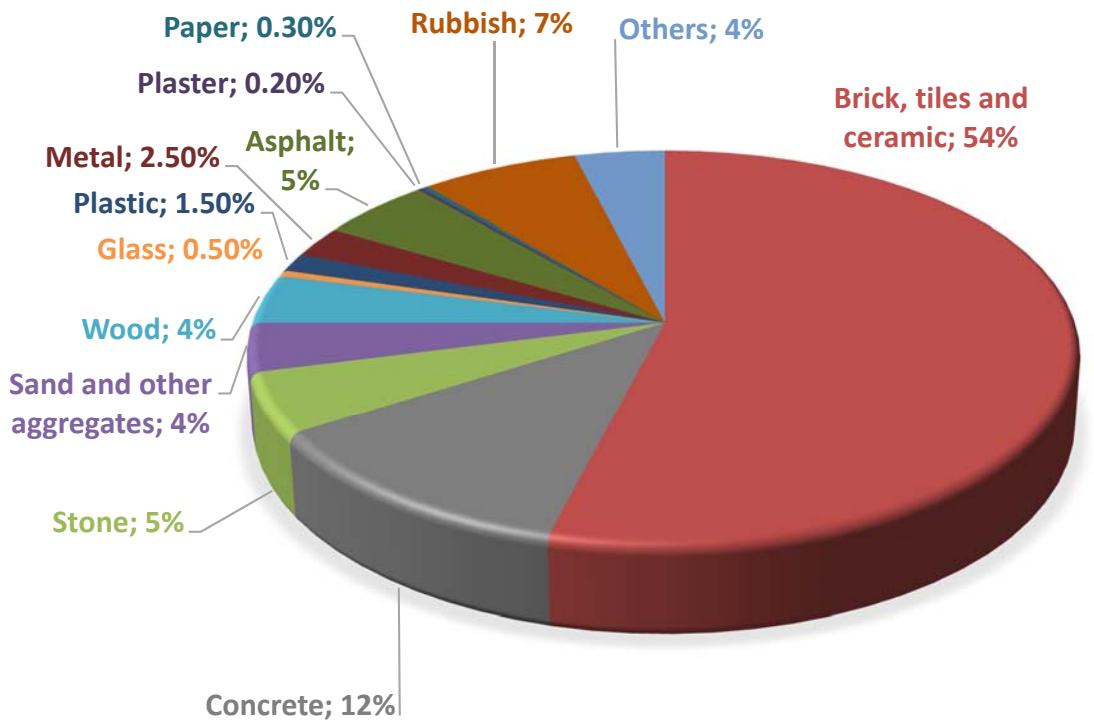

Figure 2.3. Composition of CDW

Martínez-Lage et al. [MART 2010] designed a procedure to determine the annual production construction and demolition debris in any region and applied this method to Galicia, one of Spain's autonomous communities, and similar results were obtained.

In Figure 2.3, it can be observed that more than half of the total CDWs (54%) are made of brick, tiles and ceramic, which is commonly known as mixed recycled aggregates. Several authors [GOME 2009, MAS 2012, GONZ 2014, ETXE 2015, AGRE 2015] have studied the possibility of replacing mixed recycled coarse aggregates in concrete composition. Martínez-Lage et al. [MART 2012], as part of the study conducted for the research project "Spanish Guide on Recycled Aggregates from Construction and Demolition Waste" [GEAR 2012] observed a linear decrease in mechanical properties as mixed recycled aggregates were replaced. Compressive strength and modulus of elasticity decreased approximately 20-30% and 30-40%, respectively, in concrete with 100% replacement.

In Figure 2.3, it can also be observed that 12% of CDW is made of concrete, 5% of stone, and 4% of sand and other aggregates. Hence, 21% of CDWs is made of concrete and mortar or what is most commonly known as concrete recycled aggregate. The incorporation of recycled aggregates for the fabrication of vibrated and self-compacting concrete has been extensively studied on different research programmes, noticing a decrease in its mechanical and durability properties as the replacement level increases.

In the previous paragraphs, the situation in Spain has been explained. However, the composition of CDW varies greatly depending on the country. In Table 2.2 the composition of RCDs at different countries is included. This information is part of the report "Service Contract on Management of Construction and Demolition Waste – SR1" [EURO 2011].

Table 2.2. Material composition of some European countries (after the exclusion of excavation material)

Country	Netherlands	Flanders	Denmark	Estonia	Finland	Czech Republic	Ireland	Spain	Germany
Year	**2001**	**2000**	**20003**	**20006**	**20006**	**2006**	**1996**	**2005**	**2007**
Concrete	40%	41%	32%	17%	33%	33%	80%	12%	70%
Masonry	25%	43%	8%			35%		54%	
Other mineral waste	2%	--	0%	0%	--		0%	9%	--
Total mineral waste	**67%**	**84%**	**40%**	**17%**	**33%**	**68%**	**80%**	**75%**	**70%**
Asphalt	26%	12%	24%	9%	--	--	4%	5%	27%
Wood	2%	2%	--	--	41%	--	--	4%	--
Metal	1%	0.2%	--	40%	14%	--	4%	3%	--
Gypsum	--	0.3%	--	--	--	--	--	0.2%	0.4%
Plastics	--	0.1%	--	--	--	--	--	2%	--
Miscellaneous	7%	2%	36%	34%	12%	32%	12%	12%	3%

Recycled aggregates are obtained from the treatment of CDW, only from the mineral waste. According to their compositions, they can be classified in 4 groups:

- Recycled concrete aggregates
- Recycled mixed aggregates
- Recycled ceramic aggregates
- Recycled asphalt aggregates

In this thesis, only concrete recycled aggregates will be utilised. Therefore, from now on, when recycled aggregate will be mentioned, it will be referred to recycled concrete aggregate.

2.1.2. Existing regulations

Several countries have regulations on the use of recycled aggregates in concrete. The Spanish Regulation EHE-08 defines "recycled concrete", as a concrete produced with coarse recycled aggregate from the crushing of concrete wastes. Regarding its utilization in non-structural concrete, it does not set a limit in the replacement level. However, in structural concrete, it is recommended that the content of recycled coarse aggregate will be limited to 20% by weight of the total amount of coarse aggregate. However, further specific studies and supplementary experimental tests are required for higher replacement levels.

With this limitation, the final properties of concrete are barely affected in comparison with the properties of conventional concrete. Both types concrete require a characteristic strength lower than 40 MPa to incorporate recycled aggregates and their incorporation is not allowed in prestressed concrete.

The Spanish Regulation EHE does not consider as recycled concretes:

- Concretes fabricated with fine recycled aggregates.
- Concretes fabricated with recycled aggregates with a source different from concrete (mixed recycled aggregate, asphalt, etc.).
- Concretes fabricated with recycled aggregates from concrete structures with pathologies affecting the concrete quality, such as alkali-aggregate, sulphate attack, fire, etc.
- Concretes fabricated with recycled aggregates form special concretes such as particular concretes, such as aluminous, with fibres, with polymers, etc.

With regard to the particle size, recycled aggregates must have a content of non-classified materials lower or equal 10% and the content of particles lower than 4 mm must not be higher than 5%.

In other countries, the regulations with regard to the use of recycled concrete are different. Gonçalves and de Brito [GONÇ 2010] compared the normative standards existing in several countries and summarised the information in the Table 2.3. It can be observed that some countries allow replacement levels of coarse recycled concrete aggregate in structural concrete higher than 20%, such as Germany with 35% replacement and Japan, the Netherlands and Denmark with full replacement. With regard to the use of fine recycled concrete aggregates, it is allowed in Brazil with a 100% replacement for non-structural concrete, in Japan (up to 100%) for less demanding structures, in the Netherlands only if the coarse aggregate is natural, in Switzerland with a 100% replacement even in structural concrete, in Denmark with 20% replacement for non-aggressive environments, and in Russia with 100% for non-prestressed concrete.

Table 2.3. Existing regulations on the use of recycled aggregates [GONÇ 2010]

Specification	Classification	Maximum replacement of natural with recycled aggregates		Use conditions [b]	Maximum strength class
		Coarse	Fine		
Brazil	RCA	100%	100%	Non-structural concrete	15 MPa
	MRA				
Germany	RCA	20 to 35%, depending on the application	0%	X0, XC1 to XC4, XF1 to XF3, XA1; prestressed concrete not allowed	C30/37 (20% replacement); C25/30 (35% replacement)
	RCA				
	RMA	n.a	n.a	Non-structural concrete	n.a
	MRA				
Hong-Kong	RCA	20 or 100%	0%	Less demanding solutions or structural concrete, for 100 or 20% replacement, respectively	20 MPa (100% replacement); 35 MPa (20% replacement)
Japan BCSJ	MRA	100%	Up to 100%, depending on the application	Foundations and less demanding solutions	18 MPa
Japan JIS 5021	MRA	n.a	n.a	No limitations	45 MPa
Japan JIS 5022	MRA	n.a	n.a	Members not subjected to drying or freezing-and-thawing action	n.a
Japan JIS 5023	MRA	n.a	n.a	Backfill concrete; blinding concrete; leveling concrete	n.a
RILEM	RCA+AP	100%	Only if the natural aggregate requirements are met	Dry and wet environment; non aggressive soils and/or water environment	No limit
	RCA				C50/60
	RMA			Dry and wet environment; non-aggressive soils and/or water not exposed to frost	C16/20
United Kingdom	RCA	20%	0%	X0, XC1 a XC4, XF1, DC-1	C40/50
	RA	n.a	0%	Non-structural concrete	n.a
The Netherlands	RCA	100%	Only if applied with natural coarse aggregates	Non-aggressive environments	C40/50
	RMA				C20/25
Portugal	RCA	25%	0%	X0, XC1 to XC4, XS1, XA1	C40/50
	RCA	20%	0%		C35/45
	MRA	n.a	0%	Non-structural concrete	n.a
Switzerland	RCA	100%	100%	Reinforced concrete; prestressed concrete only with additional tests	C30/37
	MRA			Not allowed in reinforced concrete	n.a
Denmark	RCA with testing	100%	20%	Non-aggressive environments	40 MPa
	RCA without testing				
	MRA				20 MPa
Russia	MRA	100%		Not allowed in prestressed concrete	15 MPa
		50%			20 MPa
Spain[a]	RCA	20%	0%	Not allowed in prestressed concrete	40 MPa

[a] proposed recommendation not yet being used;

[b] conforming with EN 206-1.

n.a - not available.

In 2014, Evangelista and de Brito [EVAN 2014] published a complete review of the studies on the use of fine recycled concrete aggregate in concrete production up to that moment. Initial works on the subject and an overview of the existing regulations are presented and the production, treatment and properties of the fine recycled aggregates are described. They conclude that it is too conservative to consider unacceptable the use of FRA in concrete

production. Since, with the right approach to the problem, it is possible to make concrete with fine recycled aggregates and similar behaviour to a high-performance concrete.

2.1.3. Mix designs analysed

The aim of this research is to study de feasibility of incorporating simultaneously the fine and coarse fraction of the concrete recycled aggregate. Therefore, this part of literature review will be only focused on the analysis of the mechanical and durability properties of vibrated concrete with fine recycled concrete aggregate and self-compacting concrete with fine and/or coarse recycled concrete aggregate. However, in the case of the flexural and shear behaviour of reinforced recycled concrete beams exposed at the end of this part of the chapter, beams made of recycled aggregate with solely replacement of the coarse fraction has also been included and their mix compositions are described in their corresponding section.

Vibrated concrete

One of the first studies on the influence of fine recycled aggregates on the properties of concrete was performed by Corinaldesi and Marconi and presented in a conference paper [CORI 2004]. The authors examine the possibility of reusing the fine fraction of recycled aggregates from building demolition as aggregates for either structural concrete or mortar. A coarse fraction (15 mm maximum size) and a fine fraction (6 mm maximum size) of recycled aggregate were used. Three Series of concrete are fabricated. Series I includes three mixtures with no recycled aggregates and water-to-cement (w/c) ratios (0.40, 0.50 and 0.60). In Series II the fine and coarse fractions are fully replaced with recycled aggregate and water-to-cement ratios are again 0.40, 0.50 and 0.60. Finally, in Series III, the natural aggregate is again fully replaced with recycled aggregate, water-to-cement ratios are 0.40, 0.50 and 0.60 and a superplasticizer is added to the mixtures at a dosage of 1.8% by weight of cement.

Khatib [KHAT 2005] reports the effect of replacing fine aggregate (sand) with either fine crushed concrete (CC) or brick (CB) on the properties of the concrete. The replacement ratios are 0, 25, 50 and 100%. The recycled aggregates were obtained from demolished structures and were further crushed in the laboratory to produce fine CC and CB with particle size of less than 5 mm in diameter.

This study carried out by Evangelista and de Brito [EVAN 2007] concerns the use of fine recycled concrete aggregates to partially or fully replace natural fine aggregates (sand) in the production of structural concrete. The fine recycled aggregates (FRA) were obtained from an original concrete (OC), of standard composition and properties, which was made solely for the purpose of being crushed afterwards. Only the fractions between 0.074 mm and 1.19 mm were used in order to have the same particle size than natural fine aggregates (FNA). The replacement ratios are 0, 10, 20, 30, 50 and 100%.

In 2009, Corinaldesi and Marconi [CORI 2009] studied concrete specimens that were manufactured by completely replacing fine and coarse aggregates simultaneously with recycled aggregates from a rubble recycling plant. Recycled aggregate concrete (RAC) with fly ash (RA + FA) or silica fume (RA + SF) were also studied. The coarse fraction maximum size of recycled aggregate was 15 mm and the fine fraction 5 mm.

Kou and Poon [KOU 2009a] compared the properties of concretes prepared with the use of river sand, crushed fine stone (CFS), furnace bottom ash (FBA), and fine recycled aggregate (FRA) as fine aggregates in recycled concrete. Replacement ratios were 0, 25, 50, 75 and 100% by mass. Two methods were used to design the concrete mixes: fixed water-cement ratio (W/C = 0.53) in Series I and fixed slump ranges (60 – 80 mm) in Series II. The concrete mixes were designed based in the saturated surface dried condition and water compensation was made during the batching.

In 2010, Evangelista and de Brito [EVAN 2010] studied the durability of different concrete mixes with 30% and 100% replacement ratios of fine natural aggregates with fine recycled aggregates. The recycled aggregates were obtained by crushing the original concrete (OC) produced in the laboratory for that purpose and only the fractions up to 1.19 mm were used. Workability was fixed as a common characteristic, within the interval 80 ± 10 mm.

Yaprak et al. [YAPR 2011] investigated the effects of the fine recycled concrete aggregate (FRA) on the concrete properties. In concrete mixtures, 0, 10, 20, 30, 40, 50 and 100% by weight of fine recycled aggregate (FRA) were used instead of river sand. Effective water amount in each concrete type was kept constant (w/c = 0.53).

Pereira et al. [PERE 2012a, PERE 2012b] carried out a research to limit the disadvantages associated with the performance of concrete containing fine recycled concrete aggregates through the use of superplasticizers. Two types of latest generation superplasticizers (regular superplasticizer SP1 and high performance superplasticizer SP2) were used and the replacement ratios of fine natural aggregates (FNA) by fine recycled concrete aggregates (FRA) were 0, 10, 30, 50 and 100%. The slump was tried to keep constant for all mixes as a levelling parameter.

The aim of the CLEAM project [ALAE 2011] was to study the influence of the content of fine recycled aggregate, as part of the coarse recycled aggregate, on the properties of concrete. In the experimental campaign two types of concrete were made with water/cement ratios of 0.55 and 0.45. The replacement ratios of coarse recycled aggregate were 0, 20, 50 and 100% and the replacement ratios of fine recycled aggregate with respect to this coarse recycled aggregate were 5, 10 and 20%. The coarse recycled aggregate was presaturated and the fine recycled aggregated was introduced completely dry in the mixture.

Chan and Poon [CHAN 2013] studied the influence of fine recycled aggregate (FRA) on the properties of concrete prepared with coarse natural aggregate. The replacement ratios of FRA were 0, 50 and 100%. Two series of concrete were prepared with a water-to-binder (w/b) ratio of 0.55, replacing in series II the 25% of cement with fly ashes.

Mardani-Aghabaglou et al. [MARD 2014] investigated the effects of fine recycled concrete and glass aggregate on mechanical and durability performance of concrete. The waste concrete and glass were crushed, sieved and re-mixed in order to fulfil the same gradation as the available 0-4 mm crushed limestone aggregate size fraction. In test mixtures, 15, 30, 45 and 60% by weight of the fine aggregate was replaced with recycled concrete (RC) or recycled glass (RC) having the similar gradation as the limestone aggregate and a water/cement ratio of 0.45. The slump of the concrete was kept constant in the range of 100 ± 20 mm.

Khoshkenari et al. [KHOS 2014] studied the effects of using 0-2 mm fine recycled concrete aggregate instead of natural aggregate on the compressive and tensile strengths of normal and high strength concretes. Two groups of mix proportions were considered in this study: group A includes four normal strength mixes with the same cement content and a fixed slump value of 80-100 mm for all mixes. Mix N (0% FRA and 0% CRA), mix N-RW (100% FRA and 100% CRA and additional water), mix NR-S (100% FRA and 100% CRA and superplasticizer), mix N-RP (100% RA > 2 mm, 0% RA < 2 mm). The aim of making the three high strength mixes in group B was to investigate the effect of using silica fume and the reduction of water to binder ratio on the quality of RCA concrete. In this group, mixes of H, H-R and H-RP are the same as the mixes of N, N-RS and N-RP, respectively, but with a different type of binder, as well as water and SP contents.

Jang and Yun [JANG 2014] investigated the fresh and hardened properties of recycled aggregate concrete (RAC) with fine recycled aggregates. Two types of fine recycled aggregates (FRA) were used: one of them with a lower water absorption ratio of 5.83% (FRAL) and the other with a higher water absorption ratio of 7.95% (FRAH). The replacement ratios for FRAL are 0, 30, 60 and 100% by volume and the replacement ratios for FRAH were 35% and 70% by volume. The water/cement ratio was 0.44 aiming for a 28 days compressive strength of at least 27 MPa.

Bravo et al. [BRAV 2015a, BRAV 2015b] analysed the mechanical and durability performance of concrete made with recycled aggregates from various locations in Portugal. The replacement levels were 10, 25, 50 and 100% of fine natural aggregate (FNA) by fine recycled aggregate (FRA) and 10, 25, 50 and 100% of coarse natural aggregate (CNA) by coarse recycled aggregate (CRA), separately.

Lotfy and Al-Fayez [LOTF 2015] studied the fresh, mechanical and durability performance of structural concrete made with controlled quality recycled concrete aggregate (RCA). Five

mixes with a water-to-cementing material (w/cm) of 0.40 were produced with various RCA contents and tested against two 0% RCA control mixes made with General Use (GU) cement, and General Use Limestone cement (GUL). The RCA contents in the mixes were 10, 20 and 30% by coarse aggregate volume replacement, as well as 10% and 20% fine and coarse (granular) replacement. All of them incorporate 35% Ground Granulated Blast furnace slay (GGBF slay) by mass of the total cementing material.

Self-compacting concrete

Self-compacting concrete has become widely used in recent years. This concept of concrete that does not require vibrating was proposed by Professor Okamura of Kochi University of Technology, Japan, in 1986. It was a solution to durability problems that some Japanese structures had due to inadequate consolidation of concrete and unskilled labour. Consolidation is achieved in all parts of the structure, including the most inaccessible parts, with no additional external force, except gravity. These properties are achieved by addition of chemical additives, such as superplasticizers, combined with additives for modification of viscosity and through the application of a certain amount of fine mineral additive powder.

One of the first studies on the influence of recycled aggregates on the properties of self-compacting concrete was also performed by Corinaldesi and Marconi and presented in this conference paper [CORI 2004]. The authors examine the possibility of reusing the dust produced during the rubble processing as a filler for manufacturing self-compacting concrete. Two concretes were prepared with 100% replacement of limestone powder with rubble powder and a w/c ratio of 0.45.

Kou and Poon [KOU 2009b] evaluated the fresh and hardened properties of self-compacting concrete (SCC) using recycled concrete aggregate as both fine and coarse aggregates. Three series were prepared with 100% coarse recycled aggregates (CRA) and different levels of fine recycled aggregates (FRA) (0, 25, 50, 75 and 100% for series I and II, and 100% for series III). The corresponding water-to-binder ratios (W/B) were 0.53 for SCC mixtures in Series I, 0.44 for Series II and 0.44, 0.40 and 0.35 for Series III. Two fly ashes were used in this study, a fine fly ash with most of the particles < 45 μm (f-FA) and a rejected fly ash with most of the particles > 45 μm (r-FA). The f-FA was treated as binder together with cement in Series II and III, while r-FA was treated as a filler in the three Series. The recycled fine aggregates had a particle size of <5 mm. All aggregates were introduced in the mixture in a saturated surface dry condition. The amounts of water added to the mixture were higher as the replacement ratios increased due to the high water absorption of the recycled aggregates.

Corinaldesi and Marconi [CORI 2009b] analysed the feasibility of utilising self-compacting concrete with recycled aggregates for the rehabilitation of concrete structures. This self-compacting concretes were prepared only with recycled aggregates and without any filler addition, since other very-fine material required to achieve cohesiveness was supplied by

the recycled aggregates themselves. Three types of recycled aggregate were compared: A fine recycled rubble aggregate (RecRub) with maximum particle size of 8 mm, a fine recycled concrete aggregate (RecCon) with maximum particle size of 8 mm and combination of fine recycled rubble fraction and a recycled concrete aggregate (RecRub+Con) with a maximum grain size equal to 12 mm. A common water-reducing admixture was used for preparing concrete admixtures (1.15% by weight of cement). All mixtures were prepared with a water-to-cement ratio of 0.54.

Grdic et al. [GRDI 2010] studied the usage of coarse recycled aggregate (CRA) obtained from crushed concrete for making self-compacting concrete. The replacement ratio of coarse aggregate by recycled aggregate was 0, 50 and 100%.

Kim et al. [KIM 2011] investigated the use of recycled fine aggregates (RFA) from waste concrete as a new cementitious material by using the characteristic that the powder contained from the RFA can increase the strength and flowability of Self-Compacting concrete. Five mixes were prepared with 0, 25, 50, 75 and 100% RFA replacement. A water-reducing admixture and a viscosity modifier were used for concrete and fly ash was used to improve the workability. The water-binder ratio was 0.35.

Gheidari and Salkhordeh [GHEI 2012] studied the influence of fine recycled aggregate on the compressive strength of recycled self-compacting concrete. Three series of self-compacting concrete mixtures were prepared with 100% coarse recycled concrete aggregates and different percentages of 0, 20, 40, 60, 80 and 100% fine recycled aggregates (FRA). In series I and II the water-to-binder ratios were 0.50 and 0.45, respectively, while in series III, the FRA replacement was 100% for all mixes and the water-to-binder ratios were 0.35, 0.40 and 0.45. Fly ashes were incorporated to Series II and III in order to increase the cementation content.

The aim of the research carried out by Yuan et al. [YUAN 2012] was to seek the proper way in preparation Self-Compacting concrete (SCC) with recycled concrete aggregate (RCA), preparation of RCA, composition design, microstructure evolution with hydration and mechanical properties. Two series of mixtures with 100% coarse recycled aggregate replacement were prepared. Series I with a water-to-binder (w/b) ratio of 0.55 and replacement levels of 0, 10 and 20% of fly ash instead of cement and Series II with a w/b ratio of 0.45 and, again replacement levels of 0, 10 and 20% of fly ash instead of cement. For each of the Series there was also one mixture with 0% replacement of FRA and 0% replacement of fly ash.

Tang [TANG 2013] evaluated the fresh properties of self-compacting concrete (SCC) using recycled coarse aggregate (RCA). The replacement ratios of natural coarse aggregate by RCA were 0, 25, 50, 75 and 100% and all mixes included silica fine and fly ash. The cement content, water to binder (w/b) ratio 0.40 and superplasticizer dosage were kept constant for all mixes.

Khafaga [KHAF 2014] evaluated the fresh and hardened properties of self compacting-concrete (SCC) using recycled concrete aggregates (RCA) as coarse and fine aggregates. 0, 25, 50 and 75% of natural coarse aggregate was replaced with coarse recycled aggregate (CRA) and for each series, 0, 25, 50 and 75% of fine natural aggregate was replaced with fine recycled aggregate (FRA). The water-to-binder (w/b) ratio of the mixture was 0.30 and silica fume (SF) and superplasticizer (SP) were also added to produce self-compacting concrete.

The aim of the study carried out by Gesoglu et al. [GESO 2015a, GESO 2015b] was to evaluate the durability, shrinkage performance and mechanical properties of self-compacting concretes (SCCs) with 0% and/or 100% replacement of fine and/or coarse natural aggregates by recycled aggregates. A total of 16 SCCs mixtures were produced and classified into four series (Series I without recycled aggregates, Series II with 100% CRA, Series III with 100% FRA and Series IV with 100% CRA and FRA), each of which included four mixes designed with two water-to-binder (w/b) ratios of 0.3 and 0.43 and two silica fume (SF) replacement levels of 0 and 10%. In all mixes a Ground granulated blast furnace slag (GGBFS) was used as a replacement for 25% of the total binder content and a slump flow of 680±30 mm was kept constant.

Carro-López et al. [CARR 2015] studied the effect of incorporating fine recycled aggregates on the rheology of self-compacting concrete (SCC) over time and the compressive strength. 0, 20, 50 and 100% of the fine natural fraction was replaced with recycled sand.

2.1.4. Properties of fresh concrete

Vibrated concrete

Khatib [KHAT 2005] was one of the first to study the fresh properties of concrete incorporating fine recycled aggregate. It was noticed that at a free water/cement ratio of 0.5, all mixtures exhibit good workability without the use of admixtures, showing an increase of up to 11% in slump as the content of fine recycled concrete aggregate in the mixes increases.

In the study performed by Kou and Poon [KOU 2009a], at the fixed w/c (free water/cement ratio) the slump of the fine recycled aggregate (FRA) concrete was increased with an increase in FRA content due to these materials has higher water absorption values than those of river sand making more free water available to increase the fluidity of fresh concrete. In Series II (fixed slump range), mixes were maintained at approximately the same value by reducing the added free water.

Yaprak et al. [YAPR 2011] observed that the air content of the fresh concretes produced varies between 1.8% and 2.5%. This variation increased linearly as the FRA quantity in the concrete mixture raised. Unit weight values of fresh concretes produced changes between 2.350 and 2.510 kg/dm^3. The unit weight value decreased as the FRA quantity was increased

because of the lower specific gravity of the FRA compared to the FNA and increasing air content of the fresh concrete. The slump values of the fresh concrete varied between 85 to 165 mm. The slump decreased as the FRA increased probably due to the shape, texture and dust content of the crushed sand when compared to river sand.

In the CLEAM project [ALAE 2011], the slump value increases when the coarse aggregate replacement ratio rises because the coarse recycled aggregate is presaturated. When w/c = 0.55, replacement ratios of fine aggregate up to 10% keeps or increases the slump value. However, when the replacement ratio of fine aggregate is 20%, the slump value always decreases. When w/c = 0.45, replacement ratios of fine aggregate up to 5% keeps or increases the slump value. However, when the replacement ratio of fine aggregate is ≥20%, the slump value always decreases.

Chan and Poon [CHAN 2013] observed that in both series, concrete containing 50% FRA had the highest initial slump while the initial slump of concrete with 100% FRA was the lowest. A comparison among the slump losses values shows that the use of fly ash as cement replacement reduced the slump loss of concrete made with FRA and it could be attributed to the retarding effect of fly ash.

Mardani-Aghabaglou [MARD 2014] noticed that since the RC aggregate was used in saturated surface dry condition, there was not a significant change in the slump of the concrete upon increasing RC aggregate content.

In the research carried out by Jang and Yun [JANG 2014], the air content of the conventional concrete (CC) was similar to the values for the concrete mixture made with FRA, varying within 4.76 ± 0.17%. The CC slump value was 200 mm but the slump of all the RAC mixtures varied from 175 mm to 195 mm, according to the replacement level and type of FRA used. All the concretes thus showed good initial workability. Incorporating a high proportion of FRA was observed to decrease slump by as much as about 10% due to the fact that FRA has a poor shape and higher water absorption characteristics.

In the study carried out by Bravo et al. [BRAV 2015a] all mixes were produced with a slump of 125±15 mm in order to be more fairly compared, being necessary to increase the water/cement ratio as the RA increased, but this increase was not identical in all families of mixes with RA. It was concluded that the shape and composition influenced the mixes' workability. The fresh-state density of concrete decreases as the RA incorporation ratio increases. This was justified by the lower particles density of the RA.

Lotfy and Al-Fayez [LOTF 2015] noticed that mixtures maintaining a w/c ratio of 0.40 (through the use of a HRWR admixture), exhibited equivalent fresh properties in terms of slump retention and measured air stability, regardless of the RCA replacement level.

Self-compacting concrete

In the conference paper published by Corinaldesi and Marconi [CORI 2004], in relation to the slump flow test, both concretes showed enough fluidity; however, a certain flow-segregation was observed for the concrete with limestone powder, while the concrete with rubble powder seemed to behave as a quite viscous system. With regard to the L-Box test, both concretes showed good results in terms of mobility through narrow sections.

Kou and Poon [KOU 2009b] noticed that the slump flow diameter increased as the fine recycled concrete aggregate content increased due to the higher absorption capacity of the FRA compared to river sand. The RA-SCC mixtures achieved adequate passing ability and maintained sufficient resistance to segregation which increased in both Series I and II with an increase in the fine recycled concrete due to the higher absorption of the FRA. The wet density of RA-SCC mixtures decreases with the increase in the percentage of FRA due to the difference of densities between the FRA and the river sand. Furthermore, the wet density slightly increased as the W/B ratio decreased.

Corinaldesi and Marconi [CORI 2009b] observed that all the concrete mixtures fulfil SCC requirements and in particular the RecRub+Con (combination of fine recycled rubble fraction and a recycled concrete aggregate) mixture performed very well in terms of fluidity and the RecCon (fine recycled concrete aggregate) mixture performs very well in terms of mobility through narrow sections. Any segregation phenomena were never noticed.

In the study carried out by Grdic et al. [GRDI 2010], wet density slightly decreases as the replacement ratio increases (1% and 1.5% with 50% and 100% replacement respectively). In the three replacement ratios (0, 50 and 100%), the slump-flow achieved 73 cm and all of them matched the requirement of having a T_{50} inside an interval of 3.5 – 6.0 s, related to viscosity. All the mixtures meet the criterion that the ratio of heights of concrete at the ends of L-Box is no less than 0.8 and they are resistant to segregation.

Kim et al. [KIM 2011] noticed that the values achieved in the slump flow test for 25% FRA and 50% FRA only decreased 3% and 5%, respectively. However, for replacements of 75% and 100%, the values were 11% and 17% lower than that of the reference concrete, respectively. The L-Box and U-Box tests exhibit the required values regardless of a high replacement of the RFA at mixes 0%, 25% and 50% FRA. The high level of RFA obviously inhibits the workability of the mix.

For Tang [TANG 2013], the slump-flow test showed no significant difference in slump flow values between control and recycled mixtures. No segregation or water separation was observed in mixtures with recycled aggregate and in general displayed similar flowability as compared to control concrete. However, the T_{50} values which represent the mixture viscosity tended to increase with the recycled aggregate content. This might be due to the

angular shape and, possibly, the higher water absorption of the recycled aggregate. Shorter time of T_{50} indicates the better flow capacity, but lower viscosity.

The L-Box test, similarly showed no significant difference in the blocking ratio between natural and recycled concrete mixtures in the initial measurements. The results demonstrate that all mixes were resistant to segregation. It can also be seen that the segregation ratio of the concrete mixtures decreased with an increase in the recycled aggregate content due to the higher water absorption capacity. Wet density of RCA-SCC mixtures decreased with an increase in the percentage of recycled aggregate content, which is consequence of its increased porousness.

The author concludes that RCA can be used to produce SCC substituting up to 100% natural coarse aggregates without affecting the key fresh properties of concrete.

Khafaga [KHAF 2014] noticed that the slump flow decreased by 4.9%, 9.70% and 10.40% for mixes with 25%, 50% and 75% CRA, respectively. This is mainly attributed to the decrease of the free water content in SCC mix due to the high water absorption of RCA. In addition, both the greater surface roughness and angularity of RCA increase the friction between coarse aggregates and cement paste. The increase in the percentage of the used fine RCA as a replacement of sand in concrete mixes decreased the slump flow, due to the reduction in the free water content in the SCC mix because of the high water absorption of RCA. The V-funnel flow times were within the acceptable limits except for the mix with 75% CRA and 75% FRA. A high flow time can be caused by either a low flowing ability or a blockage of the flow. The results of the J-ring test show that all SCC mixes possessed reasonably good passing ability except for the mix with 75% CRA and 75% FRA. The increasing in FRA and CRA led to a decrease in the passing ability.

In the study carried out by Carro-López et al. [CARR 2015], the fresh-state empirical tests (slump flow, V-funnel, J-Ring, L-Box and sieve segregation analysis) showed that mixes with 100% replacement totally lost their SCC characteristics at 90 min and this loss of passing and filling ability also partly occurred at 45 min. In the 50% recycled sand mix, the effect was not so severe but the loss of properties was strongly noticeable after 45 min. This radical change of properties is produced by the very high absorption of the recycled sand. 0% and 20% mixes show similar behaviour.

2.1.5. Properties of hardened concrete

2.1.5.1. Compressive strength

Vibrated concrete

In the study performed by Corinaldesi and Marconi [CORI 2004], by comparing the compressive strength after 28 days of the mixtures prepared with the same dosage, it can be

clearly noted that the strength loss due to the fully replacement of fine and coarse recycled aggregates (24 - 28%) can be compensated by the w/c decrease obtained by adding the superplasticizer. In general, the strength loss of RA (without superplasticizer) with respect to NA concrete decreases for high w/c or early curing time. The reason could be that a weak cement matrix tends to attenuate the negative effect of a poor-quality aggregate.

Khatib [KHAT 2005] observed that a systematic reduction in 28 days strength occurs when natural sand is replaced with fine crushed concrete with particle size of less than 5 mm in diameter. This reduction reaches 24%, 25%, 25% and 35% when 25%, 50%, 75% and 100% is replaced, respectively.

The results obtained by Evangelista [EVAN 2007], showed an insignificant variation and no visible trend in the compressive strength due to the FNA replacement with FRA (fraction between 0.074 mm and 1.19 mm). Decreases of only 0.6%, 3.4%, 3.7%, 0.8% and 7.6% for 10%, 20%, 30%, 50% and 100% replacement ratios were obtained, respectively. The reference concrete compressive strength almost stabilizes after 28 days of age. In opposition, the compressive strength of concrete mixes made with FRA continues to increase after that age because there is non-hydrated cement mixed with the fine recycled aggregates that contributes to the overall resistance.

Corinaldesi and Marconi [CORI 2009] noted that there is a strength reduction of 18% in the recycled concrete without mineral additions compared to the reference concrete. This effect is not evident in the case of silica fume addition (increases 20%) and it is not even noticeable in the presence of fly ash (decreases 6%) because of its pozzolanic activity. In a second experimental part, with a reduced water/cement relationship, the compressive strengths are similar for the three concretes because the compositions of the mixtures were intentionally chosen to achieve almost the same strength class value.

Kou and Poon [KOU 2009a] observed that when using the same w/c ratio, the compressive strength of the FRA concrete decreased at all ages with an increase in the FRA contents. For concrete designed with a fixed slump range, the compressive strength decreased with an increase in the FRA content at all the test ages.

In the study performed by Yaprak et al. [YAPR 2011], compressive strength values decreases as the FRA quantity in the concrete mixture raises. The highest value was obtained as 44.10 MPa for the CC, the concretes produced by using the FRA show lower strength by 4.3% for 10FRA, 5.9% for 20 FRA, 9.8% for 30 FRA, 12.7% for 40 FRA, 18.6% for 50 FRA and 35.4% for 100 FRA.

The research carried out by Pereira et al. [PERE 2012a] show that compressive strength gains occurred in concrete with fine recycled aggregate, and were greater the higher the water reduction capacity of the superplasticizer. Concrete mixes made with a regular

superplasticizer experienced bigger relative compressive strength losses than those made with a high-performance superplasticizer that proved to be more robust in the presence of FRA. Moreover, the effect of superplasticizers on the compressive strength is the more pronounced the lower the FRA incorporation in the mix.

The CLEAM Project [ALAE 2011] shows that the compressive strength always decreases when the coarse natural aggregate is replaced with presatured recycled coarse aggregate. In concretes with w/c = 0.55 and a 20% coarse aggregate replacement, the presence of up to 10% of fine recycled aggregate increases the compressive strength. However, with the same replacement ratios and w/c = 0.45, the compressive strength slightly decreases. The differences in the compressive strength of recycled concretes are higher when their w/c = 0.45 than in concretes with w/c = 0.55.

Chan and Poon [CHAN 2013] noticed that the strength of the concrete mixtures decreased 12% as the replacement ratio of FRA increased from 0 to 100% for both concretes with and without fly ash. Moreover, the strength of concrete containing fly ash was developed at a slower rate compared to that of concrete without fly ash due to the pozzolanic properties of fly ash.

In the study performed by Mardani-Aghabaglou et al. [MARD 2014], the compressive strength of mixtures with fine recycled aggregate RC-15, RC-30, RC-45 and RC-60 was 0.6, 1.8, 4.2 and 7.6% lower than that of the control mixture, respectively.

Khoshkenari et al. [KHOS 2014] noticed that in normal strength concrete, the concrete derived from replacing normal coarse and fine aggregates with RCAs has lower compressive strength than normal concrete for the same slump value. The reduction at 28 days is significant if the whole natural aggregate is replaced and additional water is added (27% for N-RW) and is negligible if superplasticizer (13% for N-RS) or normal sand of 0-2 mm (10% for N-RP) is used. In high strength concrete containing wholly RCA (group B), if silica fume is used as a cement replacement together with a reduction of water content (by using a superplasticizer), with the same slump value, the compressive strength could be significantly increased. Mix H, H-R and H-RP had a compressive strength at 28 days of about 114, 57 and 39% higher than mix N, N-RS and N-RP, respectively, due to the significant effect of silica fume in terms of filling and pozzolanic reaction. However, the reduction is significant if recycled aggregate is replaced, 38% and 41% for H-R and H-RP, respectively. In conclusion, the use of RCA instead of normal aggregates in high strength concrete mixtures significantly decreases the compressive strength. However, it is negligible in a normal strength concrete.

In the research carried out by Jang and Yun [JANG 2014] observed that the concrete compressive strength gradually decreased with increasing the content of FRA (13% and 8% for 100% replacement of FRAL and 75% replacement of FRAL, respectively).

Bravo et al. [BRAV 2015a] realised that the compressive strength is affected by the incorporation of RA, independently of the aggregates' size fraction. This is due to the RA's composition and the increase of w/c ratio as the RA incorporation increases. The results demonstrate that the scale of the compressive strength's decrease varies with two factors: the RA's source and the size of the RA. The compressive strength drops was significantly greater in the mixes with FRA (up to 50% for 100% replacement) than in those with CRA (up to 44.5% for 100% replacement).

Lotfy and Al-Fayez [LOTF 2015] noticed that compressive strength performance remains unaffected with either, coarse or granular RCA replacement levels.

Self-compacting concrete

Corinaldesi and Marconi [CORI 2004] observed that in terms of mechanical performance, both concretes (0 and 100% replacement of limestone powder with rubble powder) performed similarly, with a 28-day compressive strength of 40 MPa.

Kou and Poon [KOU 2009b] noticed that in Series I, the incorporation of 25% and 50% of FRA as sand replacement did not significantly affected the 28 days compressive strength and at replacement levels of 75% and 100% was approximately 10% lower than that of control-I. The compressive strength in Series II was higher than that of Series I (20% in control mixes) due to reduced W/B ratios. For RA-SCC mixtures prepared with 25% and 50% FRA, the compressive strengths were 18% higher than that of the control-II. For those prepared with 75% and 100% FRA were close to the control-II. This may be due to the presence of f-FA and the pozzolanic reaction between $Ca(OH)_2$ in the fine recycled aggregate and the fly ash forming additional C-S-H and enhancing strength. The compressive strength in Series III, prepared with 100% FRA, increased as the W/B ratio decreased at all test ages.

Corinaldesi and Marconi [CORI 2009b] observed that the concrete mixtures RecRub and RecRub+Con achieved a concrete strength class equal to 30 MPa, while the concrete mixture RecCon achieved a concrete strength class equal to 25 MPa.

Grdic et al. [GRDI 2010] noticed differences in compressive strength for the same age that cannot be characterized as significant; it decreased 3.88% with 50% replacement and 8.55% with full replacement at 28 days of age.

In the research performed by Kim et al. [KIM 2011], the compressive strength at 28 days increased 7% for 25% FRA replacement and reduced 2, 5 and 10% for 50, 75 and 100% FRA replacement, respectively. The reason for the large increase in strength using recycled fine aggregate 25% can be found in the good fitness modulus 2.8, which is filled with large and fine aggregates into the matrix concrete. The high level of RFA obviously inhibits the strength of the mix.

Gheidari and Salkhordeh [GHEI 2012] concluded from the results in Series I that adding between 20 and 40% of the FRA has a little effect on 28-day compressive strength (decreases less than 3%). However for higher replacement level, the loss of compressive strength is significant (8, 10 and 13% with 60, 80 and 100% FRA replacement, respectively). The highest strength was achieved with 20% replacement.

The results in Series II show that the compressive strength increases 18, 14, 12 and 1% for FRA replacement levels of 20, 40, 60 and 80% respectively. However it decreases 2% for 100% FRA replacement.

The results of test conducted on samples of Series III show that with a decrease of the water-to-binder ratio, the compressive strength of SCC made with 100% of fine recycled aggregates increases 12% and 21% for w/b 0.40 and w/b 0.35, respectively, with respect to the reference mixture with w/b 0.45.

The authors conclude that the compressive strengths of self-compacting concrete made with fine recycled concrete aggregates have a little reduction in comparison with natural aggregates.

Yuan et al. [YUAN 2012] noticed that the compressive strength increases for lower w/b ratios and when fine natural aggregates are incorporated instead of fine recycled aggregates. However, it decreases as the content of fly ashes rises.

Khafaga [KHAF 2014] observed that the compressive strength at 28 days decreased with increasing the percentage of CRA (8%, 10% and 18% for replacement levels of 25%, 50% and 75% respectively). The compressive strength also decreased in each of the series when fine natural aggregate was replaced by FRA as the replacement level increased, being this effect more noticeable when 0% coarse aggregate was replaced (8%, 10% and 18% when 25%, 50% and 75% of fine natural aggregate is replaced, respectively).

Gesoglu et al. [GESO 2015b] realised that the incorporation of recycled aggregates adversely affected the compressive strength. It was reduced 11.8-16.9% in Series II (100% CRA), 15.8–26.9% in Series III (100% FRA) and 27.0–30.9% in Series IV (100% CRA and FRA) with respect to Series I (0% CRA and FRA). The reduction in strength may be due to the strength and volume of the aggregate used in the production of the old concrete. Moreover, the poor quality of the adhered mortar to recycled aggregates which had experienced the crushing process, and consequently created weak areas in the concrete, as well as the weak interfacial transition zone (ITZ). The compressive strength was higher as the w/b ratio decreased irrespective of the matrix type and aggregate type. The incorporation of silica fume also enhanced the compressive strength.

Carro-López et al. [CARR 2015] observed that the mix with 20% recycled sand only showed a reduction of 8% of compressive strength at 28 days, relative to the reference concrete, whereas the one with 100% exhibited a reduction of 47%.

2.1.5.2. Modulus of elasticity

Vibrated concrete

From the results obtained by Evangelista [EVAN 2007], it can be noticed that there is a slight reduction of the modulus of elasticity for concrete with 30% of FNA replacement with FRA (3.7%), while for the concrete with full replacement the loss was significant (18.5%), indicating that the modulus of elasticity decreases with the replacement ratio. Evangelista justifies this decrease saying that the concrete's modulus of elasticity is deeper related to the stiffness of the coarse aggregates, the stiffness of the mortar, their porosity and bond. Therefore, for small replacement ratios, it is possible that the overall stiffness is not significant influenced, because the mortar stiffness is only one of several factors, while for total replacement the mortar withstands such a big stiffness loss that the concrete's modulus of elasticity is considerably affected.

Corinaldesi and Marconi [CORI 2009] measured the dynamic modulus of elasticity after 28 days of curing. The recycled aggregate concretes had 20% or 30% lower elastic modulus than the reference concrete depending on the absence or presence of fly ash.

Pereira et al. [PERE 2012b] drew the conclusion that the use of superplasticizers significantly increased the modulus of elasticity value, even in FRAC, with improvements of up to 20.7% for SP1 (C10) and 33.0% for SP2 (C100). On the other hand, the replacement of FNA with FRA resulted in losses of up to 13.2% for mixes without admixture, 17% for SP1 and 9.5% for SP2, all of them with 100% replacement. It is observed that for all mixes there is a relationship between a decrease in the modulus of elasticity and FRA incorporation.

The CLEAM research project [ALAE 2011] drew the conclusion that the modulus of elasticity decreases when replacing natural coarse aggregate with recycled coarse aggregate. In concretes with w/c = 0.55 and with a 20% of recycled coarse aggregate, the presence of fine recycled aggregate up to 10% keeps the value of the elastic modulus. However, with the same replacement ratios and w/c = 0.45 the value of the elastic modulus slightly decreases.

The study carried out by Chan and Poon [CHAN 2013] drew the conclusion that the incorporation of FRA reduced the elastic modulus of concrete. However, the use of fly ash as cement replacement increased the elastic modulus of the concrete mixtures prepared with FRA at 29 and 90 days when compared with the corresponding concrete mixtures without fly ash.

Bravo et al. [BRAV 2015a] notices that the replacement of NA with RA reduces the concrete's modulus of elasticity (up to 47.9 for 100% CRA replacement and up to 42.5% for 100% FRA replacement). The RA's composition is the factor that most influences the modulus when the RA contains ceramic material, the loss is greater because of the lower particles density of the material. The modulus of mixes with CRA and FRA from the same source are similar. Therefore, the aggregates' size did not have influence on the modulus.

Self-compacting concrete

In the study carried out by Corinaldesi and Marconi [CORI 2009b], elastic modulus values are about 20% less than the expected values for ordinary concretes belonging to strength class of 30 and 25 MPa. The reason probably lies on the kind of aggregate used. For the design of an efficient repair system the modulus of elasticity of both the repair concrete and the concrete substrate should be similar.

Gesoglu et al. [GESO 2015b] noticed that mixes with recycled aggregates had lower modulus of elasticity. It was reduced 13-18% in Series II (100% CRA), 23-25% in Series III (100% FRA) and 28-34% in Series IV (100% CRA and FRA). Decreasing the w/b ratio enhanced the modulus of elasticity. Similarly, replacing 10% of the binder by silica fume resulted in an improvement on the modulus.

2.1.5.3. Splitting tensile strength

Vibrated concrete

Evangelista and Brito [EVAN 2007] observe a clear decrease in the concrete's splitting tensile strength with the increase of FRA (5.2% and 30.5%, for 30% and 100% replacement, respectively) due to the more porous structure of the recycled aggregates.

Corinaldesi and Marconi [CORI 2009] notice small differences in the tensile strength values which confirm that for equal compressive strength, RAC is approximately 10% weaker than virgin aggregate concrete.

In the research carried out by Pereira et al. [PERE 2012a] the splitting tensile strength increases when using superplasticizers, regardless of the replacement ratio, with increases of 26.6% for SP1 and 52.8% for SP2 with 0% FRA replacement. However, regardless of the SP used, the splitting tensile strength decreases when increasing the amount of FRA. It decreases 15.6% without superplasticizer, 19% for SP1 and 24.3 for SP2, all of them with 100% replacement.

Mardani-Aghabaglou et al. [MARD 2014] noticed that the splitting tensile strength of RC-15, RC-30, RC-45 and RC-60 mixtures were 0.8, 2.8, 3.8 and 7.6% lower than that of the control mixture, respectively.

Khoshkenari et al. [KHOS 2014] drew the conclusion that the reduction in the splitting strength due to the use of RCAs instead of normal aggregates in a normal strength concrete (33%, 26% and 19% for N-RW, N-RS and N-RP, respectively) is more pronounced than the reduction in compressive strength. However, using silica fume and reducing the water to binder ratio, splitting strength improves to be equivalent to the control (H, H-R and H-RP vary 35%,-5% and 0% with respect to N). The use of 0-2 mm normal sand in RCA concrete reduces the splitting tensile strength loss. This positive effect is more pronounced in high strength concrete than for normal strength concrete.

For Jang and Yun [JANG 2014] the replacement content of FRA has little effect on the splitting tensile strength.

In the study carried out by Bravo et al. [BRAV 2015a] the incorporation of CRA and FRA causes a decrease of the splitting tensile strength (up to 34.6 for 100% CRA replacement and up to 36.1% for 100% FRA replacement) due to the increase in the effective w/c ratio and the negative effect of the composition of some of the RA. The loss of tensile strength increases as the fine RA's replacement ratio goes up, due the worst quality of the paste of cement and FRA, which is essential to this property.

Lotfy and Al-Fayez [LOTF 2015] observe a decline in splitting tensile strength occurred with increasing RCA content.

Self-compacting concrete

For Kou and Poon [KOU 2009b] the splitting tensile strength of the RA-SCC mixtures in Series I were slightly lower than of the control-I mixture. However, in series II mixes the values were higher than that of the control-II. In series III mixes, the splitting tensile strength increased as the W/B ratio decreased.

In the study carried out by Corinaldesi and Marconi [CORI 2009b], in terms of tensile strength the mean values of the results were 2.29, 2.64 and 2.24 MPa for the RecRub, RecRub+Con and RecCon mixtures respectively. The positive effect on tensile strength of the coarse recycled concrete fraction is quite evident in the mixture RecRub+Con.

In the research of Grdic et al. [GRDI 2010], the results of the tensile strength testing by bending indicate that hardness of control concrete after 28 days is 2.49 % higher in respect to the concrete with 50% of CRA and 13.95% higher than the concrete with 100% CRA.

Khafaga [KHAF 2014] noticed that the splitting tensile strength at 28 days decreased with increasing the percentage of CRA used by 26, 31.3 and 36.3% for replacement percentages of 25, 50 and 75% respectively.

Gesoglu et al. [GESO 2015b] observed that the splitting tensile strength diminished due to the presence of CRA and/or FRA. It was reduced 7.4-16.6% in Series II (100% CRA), 19.5–

27.7% in Series III (100% FRA) and 29.1-37.1% in series IV (100% CRA and FRA). The concretes with silica fume and a w/b ratio lower performed better.

2.1.5.4. Density

Vibrated concrete

Khatib [KHAT 2005] noticed a decrease of up 4% in density at 28 days as the replacement of sand with fine recycled concrete aggregate increases.

In the study carried out by Yaprak et al. [YAPR 2011], the unit weight of the hardened concrete decreased as the FRA quantity in the concrete mixtures increased. The reason is lower specific gravity of the FRA and the higher air content ratio of the mixtures as the FRA replacement increased.

In the CLEAM project [ALAE 2011], the density of the concrete with fine recycled aggregate up to 20% replacement ratio is barely modified.

Chan and Poon [CHAN 2013] observed that the use of FRA as sand replacement slightly reduced the density of concrete without fly ash by about 3.6% when the replacement level increased from 0 to 100%. However, the incorporation of fly ash as cement replacement did not cause a noticeable change in the density of concrete.

For Khoshkenari et al. [KHOS 2014] the density of recycled concrete aggregates was about 20% less than that of normal aggregates. Therefore, it was expected that by substituting the natural aggregate with such RCAs the density of concrete would reduce. In groups A and B, the concretes containing RCAs showed 7.9 – 13.6% and 10.6 – 11% lower density, respectively, compared to the control concrete mix.

Self-compacting concrete

Grdic et al [GRDI 2010] realised that density in hardened state decreases 2.12% with 50% replacement of coarse recycled aggregate and 3.4% with full replacement.

In the study carried out by Khafaga [KHAF 2014], density of hardened concrete also decreased as the rate of coarse natural aggregates replacement with CRA increased. The reason is the lower density of CRA compared to the natural coarse aggregates, due to the higher porosity and lower density of cement paste adhered to the aggregates surface.

2.1.5.5. Flexural strength

Vibrated concrete

In the study carried out by Jang and Yun [JANG 2014], the rupture modulus at 28 days for FRA concrete decreased with an increase of FRA replacement level, being this reduction more notable for concretes made with FRA with the higher absorption ratio.

Lotfy and Al-Fayez [LOTF 2015] noticed a minimal impact in terms of flexural strength performance with either, coarse or granular recycled concrete aggregate replacement levels.

Self-compacting concrete

Khafaga [KHAF 2014] observed that the use of CRA had slight effect on the flexural strength for ratio up to 50%. When the replacement percentage increased to 75%, a reduction of 18% was observed in the flexural strength. Otherwise, the use of FRA with CRA simultaneously had clarified effects on the tensile and flexural strength.

Gesoglu et al. [GESO 2015b] noticed that the net flexural strength also diminished due to the presence of CRA and/or FRA. It was reduced 16.3–23.7% in Series II (100% CRA), 20.3–27.7% in Series III (100% FRA) and 31.9–39.7% in Series IV (100% CRA and FRA). The concretes with silica fume and a w/b ratio lower performed better.

2.1.6. Durability of concrete with fine recycled aggregates

2.1.6.1. Shrinkage performance

Vibrated concrete

According to the test performed by Khatib [KHAT 2005] the shrinkage mainly occurs during the first 10 days for all concretes, and it increases with the increase of CC content, namely 25% and 58% for 50% and 100% replacement percentages, respectively.

Corinaldesi and Marconi [CORI 2009] noticed that regarding the drying shrinkage, the greatest strains occurred prepared with recycled aggregate and fly ash, due to the largest volume of micro pores contained in the concrete structure.

Kou and Poon [KOU 2009a] notice that at fixed w/c ratio of 0.53 the drying shrinkage values of FRA concretes increased with an increase in FRA content due to the adhered old mortar. At fixed slump range, the drying shrinkage values of FRA concrete also increased with an increase in the FRA concrete probably due to the instability of the old adhered cement mortar in the FRA.

Jang and Yun [JANG 2014] observe that drying shrinkage increases with an increase in FRA replacement due to the higher water absorption ratio of FRA than that of river sand. In particular, the 43-day drying shrinkage of concrete with 100% FRAL was almost twice of the CC made with river sand.

The study carried out by Lotfy and Al-Fayez [LOTF 2015], mixtures containing RCA, where a constant w/c ratio was maintained, displays consistent performance in terms of linear drying shrinkage. Higher shrinkage occurrence was observed in mixtures containing granular RCA primarily due to the presence of finer particulates.

Self-compacting concrete

Kou and Poon [KOU 2009b] notice that, at all test ages, the drying shrinkage increased with an increase in the FRA content. This can be explained by the mortar adhering to the fine recycled aggregates which contributed to an increase in the volume of paste (old and new) as the FRA increased, thus increasing the drying shrinkage.

Corinaldesi and Marconi [CORI 2009b] obtain too high shrinkage strains, affecting the SCC potential compatibility with concrete substrate. If the fresh repair material tends to shrink, the concrete substrate restrains it and the differential movements cause tensile stresses within the concrete. This could cause cracks and failure if exceed the tensile capacity of the repair material or the bond strength at the interface.

Gesoglu et al. [GESO 2015a] observed that the drying shrinkage of SCCs with RAs was much higher than that of concrete with natural aggregates. Moreover, for all SCC mixes, the drying shrinkage rate was reduced gradually over time.

2.1.6.2. Abrasion resistance

Vibrated concrete

Evangelista and de Brito [EVAN 2007] notice that concretes with FRA have greater abrasion resistance than the reference concrete (5.1% and 30.1% for 30% and 100% replacement, respectively). Evangelista says that this increase may have to do with the fact that the abrasion resistance is deeply connected with the bond of the cement paste with the fine aggregates, which is better when recycled aggregates are used.

The results obtained by Pereira et al. [PERE 2012b] for abrasion resistance reveal that FRA incorporation has an unfavourable influence on concrete performance, the worst of all the FRAC mechanical properties evaluated. The abrasion resistance decreased up to 21.7% (no admixture), 39.5% (SP1) and 25.3% (SP2) with 100% replacement. On the other hand, the addition of superplasticizers led to increases in the abrasion resistance of up to 23.7% and 33.2% for mixes with SP1 and with SP2 and without FRA replacement.

Bravo et al. [BRAV 2015a] observe that the abrasion resistance increases with the use of CRA. However, the replacement of the FNA by FRA led to an abrasion resistance loss between 18% and 53%.

2.1.6.3. Chloride-ion penetration

Vibrated concrete

Kou and Poon [KOU 2009a] realised that at the same w/c, the resistance to chloride-ion penetration of the concrete mixes decreased with increasing the percentage of FRA replacement. At a fixed slump range, due to the initial free water required was decreased,

the resistance to chloride-ion penetration of all FRA concrete mixes was better than that of the control.

In the study carried out by Evangelista and de Brito [EVAN 2010], an increase of around 12% was observed in terms of the mitigation coefficient when comparing the concrete with a 30% replacement ratio with the reference concrete, a difference that increases to 33.8% when the concrete with 100% replacement ratio is compared.

Chan and Poon [CHAN 2013] noticed that the incorporation of FRA increased chloride ion penetration for concrete mixtures without fly ash. In contrast, for concrete mixtures with fly ash, the increasing use of FRA decreased the chloride ion penetration.

In the tests carried out by Mardani-Aghabaglou [MARD 2014], Chloride-ion penetration values of the concrete mixtures were lower than 1000 Coulomb, the limit specified for very good chloride-ion penetration resistance of concrete mixtures in accordance with [ASTM 1202] standard.

Bravo et al. [BRAV 2015b] observed that the use of recycled aggregate in concrete causes a slight increase of the chloride diffusion coefficient relative to the RC. The replacement of fine aggregates led to values higher than those in mixes with coarse recycled aggregates.

Lotfy and Al-Fayez [LOTF 2015] noticed that due to the nature of RCAs, an increase in chloride-ion penetration was observed with increasing RCA content, especially for granular RCA.

Self-compacting concrete

In the study carried out by Kou and Poon [KOU 2009b], the resistance to chloride ion penetration in Series I can be classified as moderate or low and increased with the fine recycled aggregate content, contrary to compressive strength. This can likely be attributed to the filler effect of the FRA as it was comprised of a higher percentage of small particles than the river sand. Similarly, it was found that the resistance to chloride ion penetration of the Series II increased as the fine recycled aggregate content increased. In Series III, it also increased as the W/B ratio decreased from 0.44 to 0.33.

Gesogly et al. [GESO 2015a] observed that Incorporating RCA and/or CRA resulted in a systematic increase in chloride-ion permeability for SCCs. Compared to Series III, Series II seemed to be more resistant to chloride penetration. Moreover, the negative effect diminished with the decrease of the w/b ratio and incorporating SF.

2.1.6.4. Water absorption and water penetration

Vibrated concrete

Evangelista and Brito [EVAN 2010] noticed that the water absorption by immersion increased 16.8% when 30% FNA was replaced and 46% when 100% FNA was replaced with FRA. Water absorption through capillarity increased 34.4% for concrete with a 30% replacement ratio and 70.3% for complete replacement.

In the study carried out by Yaprak et al. [YAPR 2011], the water absorption rate values increased as the FRA quantity in concrete mixtures rose because of the higher absorption of the recycled aggregate (the water absorption varied between 1.67% and 1.97%).

Chan and Poon [CHAN 2013] observed that the 28-day water absorption of the concrete mixtures without fly ash increases with an increase in the FRA content. The corresponding increase was over 34% when the FRA content increased from 0 to 100%. However, with the incorporation of fly ash as cement replacement, using 100% fine RA only increased the absorption by about 15% compared to that of the control mixture.

Mardani-Aghabaglou et al. [MARD 2014] noticed that the water absorption values of concrete mixtures incorporating RC aggregate up to 45% are in the range of 3-5%, the limit specified for the average concrete in accordance with the [CEB-FIB]. However, the mixtures with 60% of RC, water absorption is greater than 5%, the limit specified for poor concrete.

In the study performed by Bravo et al. [BRAV 2015b] the replacement of NA with RA caused an increase of the water absorption by immersion. Moreover, it increased as the size of the replaced aggregates decreased. With replacement ratios of CRA lower than 25% and FRA lower than 10% the results were similar to the reference concrete. The water absorption by capillarity increased as the replacement ratio of NA with RA grew. The mixes with FRA have much higher absorption than those with CRA. The incorporation of 10% RA caused a decrease of the capillarity water absorption in almost all mixes evaluated due to the filler effect.

Lotfy and Al-Fayez [LOTF 2015] noticed that due to the nature of RCAs, an increase in water absorption by capillarity was observed with increasing RCA content, especially for granular RCA.

Self-compacting concrete

In the study carried out by Grdic et al. [GRDI 2010], the highest water absorption was noted at the test of 100% CRA which is 0.15% higher than the test of 50% CRA and 0.37% higher than the control sample. This is consequence of the implementation of recycled aggregate which has higher water absorption with respect to the river aggregate. On samples with 50% CRA and 100% CRA no water penetration was recorded, whereas the control sample had a

penetration of 10 mm, so it can be concluded that all the samples are water-proof which is in full accordance with the structure of self-compacting concrete.

Gesoglu et al. [GESO 2015a] noticed that with regard to the water absorption by capillarity test, the SCCs incorporating RCAs and/or RFA revealed a systematic increase in sorptivity coefficient values. Increasing mean pore size and total porosity increases capillarity of RAs concrete. The lowest water penetration depth was measured for the mix with 0% CRA, 0% FRA, w/b 0.3 and 10% SF as 4 mm whereas the highest was measured for the mix with 100% CRA, 100% FRA, w/b 0.43 and 0% SF as 55 mm at 56 days.

2.1.6.5. Carbonation resistance

Vibrated concrete

Evangelista and de Brito [EVAN 2010] observed that carbonation depth increased with replacement ratio, which was to be expected since both capillary absorption and chloride penetration exhibited the same trend. It increases almost linearly with the replacement ratio, with a maximum increase of about 110% measured at 21 days for concrete made only with FRA, and a maximum increase of about 40%, measured at the same age, for concrete with 30% replacement of FNA by FRA.

In the study of Bravo et al. [BRAV 2012b] the mixes with recycled aggregate had lower carbonation resistance than the reference concrete and this decrease strongly depended on the type of RA used. There is a significant increase of carbonation depth as the size of the replaced aggregates decreases and this increase is also linear with the replacement ratio.

Self-compacting concrete

Gesoglu et al. [GESO 2015a] noticed that the highest value obtained in the gas permeability test was at mix with 100% CRA, 100% FRA, w/b 0.43 and 0% SF, since the transport properties of concretes are strongly dependent on their pore structure. The raising of gas permeability of concrete can be attributed to the increase pore structure in concrete due to RAs addition.

2.1.7. Flexural behaviour of reinforced beams made with recycled concrete aggregate

2.1.7.1. Studies analysed

Sato et al. (2007)

Sato et al. [SATO 2007] performed flexural loading tests of recycled reinforced concrete members in order to evaluate whether concrete with recycled aggregate can be applied for concrete structures. Two types of recycled aggregate were used in this study; in Series A, recycled aggregates obtained from natural concrete with the same mixture composition

than that of the recycled concretes were studied and, in Series B, the recycled aggregates came from beams, columns and slab of reinforced concrete buildings built in 1961. The fine and/or coarse natural aggregate was totally replaced with fine and/or coarse recycled aggregates and different water-to-cement ratios were studied (0.25, 0.30, 0.45 and 0.60). The size of the specimens is 200 x 200 x 2800 mm with a full span length of 2200 mm, a pure bending moment zone of 800 mm, and a reinforcement ratio of 1.06% for all the flexural tests.

Choi et al. (2012)

The study performed by Choi et al. [CHOI 2012] evaluates the flexural performance of reinforced concrete (RC) beams made with fine and/or coarse recycled aggregate. 8 full-scale beams were cast using 3 different types of recycled aggregate. In type 1 beams, two beams were cast with a 0% and 100% replacement of coarse natural aggregate with a mixture of high-grade and low-grade coarse recycled aggregate. In type 2 beams, three beams were made with a 0%, 100% and 70% replacement of fine natural aggregate with a high-grade and a low-grade fine recycled aggregate, respectively. Finally, for type 3 beams, three beams were made with: a 0% replacement of the total aggregate, a 15% and 60% replacement of coarse and fine aggregates, respectively and a 100% replacement of the total aggregate. The dimensions of the cross section of the reinforced concrete beams were 400 mm width and 300 depth, with a total length of 6400 mm and a net span length of 6000 mm.

Choi and Yun (2013)

Choi and Yun [CHOI 2013] present experimental results on the long-term deformations and flexural behaviour of RAC beams, after exposure to sustained loading of 50% of their nominal flexural capacity for 380 days. The recycled aggregates were obtained from demolished concrete structures. Three reinforced beams specimens were fabricated with different replacement levels of aggregate: 100% natural aggregate (C30), 100% recycled coarse aggregate (RL30) and 50% recycled fine aggregate (RH30) and a design compressive strength of 30 MPa. The beams are 170 mm wide and 200 mm high, with a total length of 2300 mm and a net span length of 200 mm.

Ignjatovic et al. (2013)

Ignjatovic et al. [IGNJ 2013] present the results of an investigation on the flexural behaviour of recycled aggregate concrete (RAC) beams when compared to the behaviour of natural aggregate concrete (NAC) beams under short-term loading. Three different percentages of coarse recycled aggregate by weight were replaced (0, 50 and 100%) and three different reinforcement ratios for each of them (0.28, 1.46 and 2.54%). Thus, 9 full-scale tests were performed on 9 beams until failure. The beams are 200 mm wide and 300 mm high, with a total length of 3500 mm and a net span length of 3000 mm.

Lee et al. (2013)

The study performed by Lee et al. [LEE 2013] presents the results of an investigation on the change of strength in high strength reinforced concrete beams when coarse natural aggregates are replaced with coarse recycled aggregates. The replacement ratios are 0%, 30%, 50% and 100%. The beams are 150 mm wide and 250 mm high, with a total length of 2400 mm and a net span length of 1960 mm.

Knaack and Kurama (2014)

Knaack and Kurama [KNAA 2014] investigate the flexural and shear behaviour of reinforced concrete beams that use recycled concrete aggregates (RCA) as replacement for coarse natural aggregates (NAC). The replacement levels are 0%, 50% and 100%. The target NAC mix was designed with a water-to-cement ratio of 0.44 for a target strength of 40 MPa and a slump of 125±25 mm. The dimensions of the beams are 150 mm wide and 230 mm high, with a total length of 2000 mm and a net span length of 1680 mm.

Kang et al. (2014)

The main objectives of the research of Kang et al. [KANG 2014] are the investigation of flexural performance and the evaluation of the potential application of recycled concrete aggregates (RCA) for concrete structures. The parameters for investigating their flexural behaviour are: the replacement ratio (0, 15, 30 and 50%), the tensile reinforcement ratio (0.5, 1, 1.5 and 1.8%) and the specified concrete compressive strength (27 and 54 MPa). The dimensions of the beams are 135 mm wide and 270 mm high, with a total length of 3030 mm and a net span length of 2700 mm.

Arezoumandi et al. (2015a)

Arezoumandi et al. [AREZ 2015a] present the results of an experimental investigation of the flexural strength of full-scale reinforced concrete beams fabricated with 0% (CC) and 100% coarse recycled aggregate (RCA), and with two different longitudinal reinforcement ratios of 0.47% and 0.64%. The concrete target compressive strength is 35 MPa. The dimensions of the beams are 300 mm wide and 460 mm deep, with a net span length of 2700 mm. As a result, a total of 8 beams were fabricated (2 of each type)

Seara-Paz (2015)

Seara-Paz [SEAR 2015] presents an analysis on flexural beam tests with 0, 20, 50 and 100% replacement of coarse natural aggregates with coarse recycled aggregates. Two different water/cement ratios were used 0.50 and 0.65. The dimensions of the cross section of the beams were 200 mm wide and 300 mm deep, with a total length of 3600 mm and a net span length of 3400 mm. Short-term and long-term analysis under sustained load for 1000 days were performed.

2.1.7.2. Flexural strength

In Sato et al. [SATO 2007] tests, ultimate moment of recycled concrete beams (in series A and B) were almost the same as those of beams with natural aggregates. In the study of Choi et al. [CHOI 2012], similar results of nominal strength were observed, regardless of the replacement ratio and type of recycled aggregate.

In the tests carried out by Choi and Yun [CHOI 2013], flexural performance of the beams made with recycled aggregate is comparable to that of the beam with natural aggregate. The initial flexural stiffness values and maximum flexural strength values are similar regardless of the type of aggregate, whereas the maximum flexural strength of the beam with natural aggregate is 20% higher than that of the beams with recycled aggregate.

Ignjatovic et al. [IGNJ 2013] observed that at service load, the cracking load is not affected significantly by the quantity of recycled aggregate, the beam with 100% coarse recycled aggregate replacement has 10% lower cracking load. At failure, the differences in the ultimate load of beams failed in flexure, made of NAC and RAC with the same reinforcement ratio are negligible.

Lee et al. [LEE 2013] concluded that if the load at which initial cracks occurred is compared with the failure strength for each of the beams (50.6, 55.47, 52.8, 47.1% for 0, 30, 50 and 100% replacement, respectively), it can be observed that the crack occurs earlier depending on the replacement level of recycled aggregates.

Knaack and Kurama [KNAA 2014] noticed that recycled concrete aggregate does not cause an observable change in the progression of nonlinear behaviour and failure in flexure-critical reinforced concrete beams. Increased amounts of RCA result in a reduction in the initial stiffness, but the effect on the flexural or shear strength of the beams is relatively small.

Kang et al. [KANG 2014] observed that with the exception of the specimens using 50% RCA, it is concluded that none of the other specimens demonstrated a significant difference in the moment strength. Similarly, cracked stiffness was not adversely affected by the use of RCA.

In the Arezoumandi et al. [AREZ 2015a] tests, the RCA beams showed lower stiffness after the cracking moments that can be attributed to lower modulus of elasticity of the RCA mix compared with the CC mix.

Seara-Paz [SEAR 2015] observed that in the short-term analysis, the cracking moment decreases as the replacement level increases due to the lower splitting tensile strength of recycled concrete. However, the recycled aggregate content barely affects to maximum moments. In long-term analysis, it was also noted that the cracking moment decreases as the replacement level increases.

2.1.7.3. Crack pattern

Cracks spacing observed by Sato et al. [SATO 2007] of CRC (coarse) and CFRC (coarse and fine) in Series A and B, was 0.92 – 1.37 times and 0.74 – 1.26 times, respectively, that of concrete with natural aggregates. So there was no significant difference. The crack width of recycled concrete beams with CRC and CFRC (in Series A and B) was 0.57 – 1.3 times and 1.1 – 1.7 times that of reference concrete, respectively. The crack width was greater in recycled concrete beams. Under the sustained bending moment, recycled concrete beams with CFRC under wet condition did not show cracking nor an increase in deflection for 1 year, but in drying condition, they developed many cracks. The crack width of recycled concrete beams with CFRC was not different from of natural concrete beams and the increase in the crack width was also the same (0.06 mm after 1-year-loading).

In the tests carried out by Choi and Yun [CHOI 2013], under the sustained loading, a single crack was observed in the C30 beam immediately after applying the superimposed load, and two cracks in each of the RL30 and RH30 beams. Over time, there were fewer cracks in the beam with natural aggregate than in the beams with recycled aggregate. During the failure test, the crack in the beam with recycled coarse aggregate is slightly wider than that of the beam with natural aggregate. However, overall results indicate that the crack propagation of the beam with natural aggregate is similar to those of the recycled aggregate beams, regardless of the type of recycled aggregate.

In Choi et al. tests [CHOI 2012], the crack propagation of reinforced concrete members was similar to those of recycled aggregate concrete, regardless of the replacement ratio. Ignjatovic et al. [IGNJ 2013] concluded that the crack spacing and width of NAC and RAC beams of the same reinforcement ratio can be considered similar in cases of average and maximum ratios. Lee et al. [LEE 2013] noticed that in the crack occurrence and failure progress, generally crack shapes were found similar. Kang et al. [KANG 2014] observed that although the RCA specimens showed greater number of cracks and lower cracking moments, the overall crack pattern were similar. Arezoumandi et al. [AREZ 2015a] noticed that the behaviour of the both CC and RCA was similar except for cracking space (the RCA beams cracks were closer to each other compared with the CC beams cracks).

2.1.7.4. Deflection

Sato et al. [SATO 2007] noticed that deflections of recycled concrete beams were larger than those with natural aggregates under the same conditions of moment and water-to-cement ratio. Under the sustained bending moment, recycled concrete beams with CFRC under wet condition did not show an increase in deflection for 1 year, but in drying condition, they developed an increase in deflection. This increased deflection was twice that of beams with natural aggregates.

In the tests carried out by Choi and Yun [CHOI 2013], under the sustained loading, the instant deflection values were 1.01, 0.91 and 1.18 mm for C30, RL30 and RH30 beams, respectively. With an increase in the loading time, the deflections at mid-span increased continuously and reached 2.10, 1.80 and 2.29 mm for C30, RL30 and RH30 beams, respectively. After the sustained load is stopped, the ratios of the recovery amounts to the instant deflection values are 0.65, 1.04 and 0.89 for the C30, RL30 and RH30 beams, respectively. So the 1.04 and 0.89 of the beams with recycled aggregate are 60% and 37% higher, respectively than the beam without recycled aggregate.

Ignjatovic et al. [IGNJ 2013] observed that at failure, the load-deflection behaviour is not significantly affected by the concrete type, the beam with 100% coarse recycled aggregate replacement has 13% higher service deflection. Knaack and Kurama [KNAA 2014] also noticed that for flexure-critical beams, deflection at ultimate moment increases as the replacement level increase. In the Arezoumandi et al. [AREZ 2015a] tests, the RCA beams showed higher ultimate deflection compared with the CC beams around 5% for F-6 (0.47% longitudinal reinforcement ratio) and 22% for F-7 (0.64% longitudinal reinforcement ratio). They claim that this phenomenon can be attributed to both the lower modulus of elasticity and the lower effective moment inertia (more cracks) of the RCA beams.

For Choi et al. [CHOI 2012], similar results of load-deflection relationships and moment-curvature relationship were observed regardless of the replacement ratio and type of recycled aggregate.

Seara-Paz [SEAR 2015] observed that in the short-term tests, the deflections increases slightly in concretes with replacement levels higher than 20%. In long-term analysis, it is concluded that the recycled aggregate content has a significant influence on the specific long-term deflection. Compared to the conventional concrete at 1000 days, it increases 21%, 29% and 76% for 20, 50 and 100% replacement in concretes with w/c = 0.65, respectively. In the same way, in series with a w/c ratio = 0.50, it showed increments of 18%, 34% and 72% for 20, 50 and 100% replacement levels, respectively.

2.1.7.5. Ductility factors

Sato et al. [SATO 2007] noticed that the ductility factors of recycled concrete beams were almost the same as those of beams with natural aggregates. Similarly, Lee et al. [LEE 2013] observed that ductility does not tend to decrease or increase at constant interval depending on substitution rate, and it is affected more by other factors than recycled aggregates. Ignjatovic et al. [IGNJ 2013] tests showed that at failure, the difference in ductility between the beams with the same reinforcement ratio, regardless of the amount of RCA in concrete, can be considered negligible.

However, in the study of Choi et al. [CHOI 2012], there is a decrease in the ductility ratio as the replacement ratio increases. In particular, the degradation is significant when both

coarse and fine aggregates are replaced with recycled aggregates. Kang et al. [KANG 2014] also observed that increasing the RCA replacement ratios of the specimens resulted in a decrease in displacement ductility. This was due in part to the bond deterioration between aggregate interface and mortar, as evidenced by the steel and concrete strain measurements.

2.1.8. Shear behaviour of reinforced beams made with recycled concrete aggregate

2.1.8.1. Studies analysed

González-Fonteboa and Martínez-Abella [GONZ 2007] present the results of shear behaviour tests of concrete beams made with 0% and 50% replacement levels of coarse natural aggregate with coarse recycled aggregate (RCA). For each of the two mixtures, 4 different amounts of transverse reinforcement were used (stirrups spaced 100 mm, 130 mm, 170 mm and 240 mm, respectively), with a diameter of 6 mm in one span and 8 mm in the other). In order to achieve a similar degree of workability for both types of concretes (CC and RC), the water content of the recycled concrete was increased. The cement content was also correspondingly increased (6.2%) to maintain the required water-to-cement (w/c) ratio and the percentage of superplasticizer. The dimensions of the beams are 200 mm wide and 350 mm high, with a total length of 3050 mm and a net span length of 2600 mm.

González-Fonteboa et al. [GONZ 2009] presents the results of a second stage of studies carried out on the shear behaviour of concrete beams made with coarse recycled aggregates [GONZ 2007]. In this case, apart from the replacement of coarse recycled aggregates (0 and 50%), an 8% of silica fume by cement weight was added to all mixtures in order to study its effect on the shear behaviour. The same transverse reinforcement and dimensions of the beams than in [GONZ 2007] were used for these tests.

In the study performed by Choi et al. [CHOI 2008] the effects of coarse recycled aggregate (CRA) on concrete shear strength are studied experimentally on 20 CRA concrete beams with various combinations of span-to-depth ratios (a/d = 1.50, 2.50, 3.25), longitudinal reinforcement ratios (s = 0.53, 0.83 and 1.61%) and CRA replacement ratios (0, 30, 50 and 100%). The cross section of the beams is 200 mm wide and 400 mm deep. The test specimens were not reinforced with stirrups along the length of the beams in order to allow assessment of the shear strength contribution of the concrete. Only a couple of stirrups were placed near the support to prevent premature bond failure and to secure the main bars before the concrete was cast.

Fathifazl et al. [FATH 2011] investigate the applicability of some major concrete design standards and other pertinent methods to calculate the concrete contribution to shear resistance of reinforced recycled concrete (RRC) beams without stirrups. The test variables

included in this experimental program are shear-span/depth ratio (1.5, 2, 2.7 and 4), beam size, recycled concrete aggregate (RCA) source and coarse aggregate type. For each RCA source, one companion control beam was made of concrete with 100% coarse natural aggregate.

Al-Zahraa et al. [AL-ZA 2011] present the results of an investigation on shear strength of concrete beams with recycled coarse concrete aggregates. In this study, 4 groups of beams were made with replacement levels of 0, 25 and 50% of recycled coarse aggregate. Group 1 (no shear reinforcement and shear span/depth (a/d) = 2), group 2 (6 mm diameter stirrups each 200 mm (μ_{st} = 0.3%) and a/d = 2), group 3 (6 mm diameter stirrups each 200 mm (μ_{st} = 0.5%) and a/d = 2) and group 4 (6 mm diameter stirrups each 200 mm (μ_{st} = 0.3%) and a/d = 2.5). The dimensions of the beams are 100 mm wide and 200 mm deep, with a total length of 1700 mm and a net span length of 1500 mm.

Arezoumandi et al. [AREZ 2014] conduct an experimental investigation to study the shear strength of 6 full-scale beams constructed with 100% coarse recycled concrete aggregate (RCA) as well as 6 beams with conventional concrete (CC). The test parameters are: longitudinal reinforcement ratio (1.27, 2.03 and 2.71%) and concrete type. The dimensions of the beams are 300 mm wide and 460 mm high, with a total length of 4300 mm and a net span length of 3600 mm and a shear span-depth ratio of 3.0 or greater.

Arezoumandi et al. [AREZ 2015b] present again the results of [AREZ 2014], but in this case, 6 beams with 50% replacement level of coarse natural aggregate with coarse recycled aggregate are also studied. The longitudinal reinforcement ratios are 1.3, 2.0 and 2.7% and the cross section is 300 mm wide and 460 mm high with shear span-depth ratios of 3.0 or greater.

2.1.8.2. Shear strength

González-Fonteboa and Martínez-Abella [GONZ 2007] noticed that recycled concrete beams present almost the same shear force at failure and deflections as the conventional concrete beams with an equal amount of transverse reinforcement. All the beams with shear reinforcement had the ratio shear force at stirrup yield (V_{yield}) to shear force at cracking (V_{crack}) somewhat greater than 1.0. However, these ratios are lower when recycled concrete is used. The ratio of shear force at failure (V_u) to shear force at cracking (V_{crack}) indicates that the recycled concrete beams reached shear force at cracking in earlier load stages than conventional concrete beams.

In the study performed by Choi et al. [CHOI 2008], the shear strength of the recycled concrete beams was lower than that of the natural concrete beams with the same reinforcement ratio and shear span-to-depth (a/d) ratio. In particular, the shear strength reduction caused by the recycled aggregate was higher in beams with smaller a/d ratio. The shear strength of the recycled aggregate beams decreased with increasing a/d value but the

reduction was smaller in concrete with higher recycled aggregate replacement. The recycled aggregate yielded no difference in flexural stiffness prior to the formation of either diagonal shear cracks or shear tension cracks, but it caused faster degradation of the shear after the formation of a diagonal shear crack.

Fathifazl et al. [FATH 2011] observed that, generally, the reinforced RCA-beams had a higher shear strength compared to the companion reinforced concrete beams. The shear strength of reinforced RCA-beams had a tendency to increase with decreasing a/d ratio mainly due to the contribution of an arch action mechanism at lower a/d ratios, which conforms to the known behaviour of conventional reinforced concrete beams. The shear resistance of reinforced RCA-concrete beams had a tendency to increase with decrease in the overall depth of the beam, which is well-known in conventional reinforced concrete beams, and is referred to as size effect.

Al-Zahraa et al. [AL-ZA 2011] noticed that the experimental failure loads for beams without shear reinforcement and with RCA are higher than that with natural aggregates because of better interlocking. For beams with low shear reinforcement (G2 and G4), the experimental failure loads of all of the beams with 25% RCA are higher than that with natural aggregates except beam with high shear reinforcement ratio. Beams with 50% RCA give almost the same failure loads as than beams with natural aggregates. For beams with high shear reinforcement (μ_{st} = 0.5%) (G3), the recorded failure loads for both percentages of substitutions are 15% lower than beams with natural aggregates. Increasing the shear reinforcement ratio from zero in group 1 to 0.3% in group 2, increased the shear capacity for beams with RCA by an average of 17%. The average increase for beams with RCA in group 3 with 0.5% shear reinforcement ratio was 52%.

In general, beams tested with higher shear span-depth ratio gave lower failure loads. For smaller (a/d) ratios, part of the concentrated force can be transmitted directly to the support by forming a compression strut allowing larger capacity. Mean shear capacity values of beams in G4 tested with a/d = 2.5 was 13% lower than that of beams in G2 tested with a/d = 2.0. This is applicable for beams with natural aggregates and beams with RCA.

Arezoumandi et al. [AREZ 2014] conclude that for a given standard, the ratios of experimental-to-code predicted capacity are approximately 12% higher for the conventional concrete beams compared with the RAC beams with the same amount of longitudinal reinforcement. The same conclusion in [AREZ 2015b], for a given standard, the ratios of experimental-predicted to code-predicted capacity for RAC100 are lower than the RAC50 and CC beams with the same amount of longitudinal reinforcement. Statistical data analysis indicate that the RAC100 beams have lower shear capacity compared with the CC and RAC50 beams tested, however there is no significant difference between RAC50 and CC beams.

2.1.8.3. Crack pattern

González-Fonteboa and Martínez-Abella [GONZ 2007] noticed that premature cracking and notable splitting cracks were observed in recycled concrete beams in comparison with conventional concrete beams. In the second stage of this study [GONZ 2009], the authors conclude that the notable splitting cracks along the tension reinforcement observed in recycled concrete beams of the first phase were mitigated by the addition of silica fume.

In the study performed by Choi et al. [CHOI 2008], the extent of shear-tension cracks was more severe in the concrete with higher recycled aggregate content and less reinforcement.

In the studies carried out by Arezoumandi et al. [AREZ 2014, AREZ 2015b], it was observed that in terms of crack morphology and crack progression, the behaviour of the RAC100, RAC50, and CC beams was similar to each other.

2.1.8.4. Deflection

In the study performed by González-Fonteboa et al. [GONZ 2009], the recycled concrete beams always present greater deflections than the natural concrete beams, in the middle of the shear span and in the centre of the beam because of the deformability of the mortar adhered to the aggregate. On the other hand, the shear deformation of recycled concrete beams with high quantity of reinforcement are lower than those obtained with conventional concrete, being, however, higher in the case of beams with low transverse reinforcement.

Arezoumandi et al. [AREZ 2014] observed that in terms of load deflection response, the behaviour of the RAC and CC beams was virtually identical. However, in [AREZ 2014], where 50% replacement was also studied, there was slight difference in slope of load-deflection graphs after cracking.

2.1.9. Conclusions

Properties of fresh concrete

Fresh properties of vibrated and self-compacting concrete are affected by the replacement of recycled aggregates in the mix due to the higher water absorption of the recycled aggregates which reduces the free water content in the mix and the greater surface roughness and angularity which increase the friction between coarse aggregates and cement paste. Therefore, water compensation, presaturation of the aggregates or the use of admixtures is needed in order to mitigate this effect.

In both, vibrated and self-compacting concrete with constant free water/cement content, the slump and slump flow, had a general tendency to decrease as the amount of fine and coarse recycled aggregate increases, being this decrease more noticeable in some of them for higher replacement levels. However, Khatib [KHAT 2005], Kou and Poon [KOU 2009a, KOU 2009b] noticed the opposite effect; the slump was higher as the replacement level

increased. While in the CLEAM project [ALAE 2011] and [CHAN 2013], it was observed an increase in the slump for low replacement levels (20% and 50%, respectively) and a decrease for higher replacement levels 20% and 100%, respectively). Fresh-state density of concrete decreases as the RA incorporation ratio increases because of the lower particles density of the RA due to the higher porosity. In terms of passing ability, self-compacting concretes with recycled aggregates generally showed good results and maintained sufficient resistance to segregation, being noticed a decrease in same of them for replacement levels higher than 50%.

Properties of hardened concrete

Hardened properties of vibrated and self-compacting concrete are affected by the replacement of fine recycled aggregates in the mix due to the lower quality of the recycled aggregate in comparison with the natural aggregate. Compressive strength was generally reduced as the replacement level on fine and coarse recycled aggregate increases. This decrease can be compensated by reducing the water/cement ratio or by incorporating fly ash. On the other hand, in the CLEAM Project [ALAE 2011] and in the study of Yuan et al. [YUAN 2012], it was noticed that the presence of small amounts of fine recycled aggregate slightly increased the compressive strength.

According to Evangelista [EVAN 2007], the concrete modulus of elasticity is related to the stiffness of the aggregates, the stiffness of the mortar, their porosity and bond performance. In all the studies analysed the elastic modulus was reduced as the amount of recycled aggregate increases, being this decrease more noticeable for higher replacement levels.

The splitting tensile strength and flexural strength were also reduced as the replacement level increases due to the worst quality of the paste of cement and fine recycled aggregate.

The lower density of concrete recycled aggregates compared to the natural aggregates, due to the higher porosity and lower density of cement paste adhered to the aggregates surface, caused a reduction in the density of hardened recycled concrete.

Durability performance

The durability of vibrated and self-compacting concrete is also affected by the incorporation of fine and coarse recycled aggregates. The drying shrinkage increases due to the instability of the old adhered mortar in the fine recycled aggregates and the presence of finer particles.

In terms of abrasion resistance, Evangelista and de Brito [EVAN 2007] noticed that concretes with FRA have greater abrasion resistance than the reference concrete (5.1% and 30.1% for 30% and 100% replacement, respectively). However, Pereira et al. [PERE 2012b] and Bravo et al. [BRAV 2015a] observed FRA incorporation have an unfavourable influence on this property.

With regard to chloride-ion penetration in vibrated concrete, all authors coincide that the resistance to chloride-ion penetration decreases as the replacement level rises. However, in self-compacting concrete, Kou and Poon [KOU 2009b] observe that the resistance to chloride ion penetration increases as the fine recycled aggregate content rises, probably due to the filler effect of the FRA as it was comprised of a higher percentage of small particles than the river sand.

The water absorption by immersion and capillarity is generally increased as the replacement level of recycled aggregate increases. However, Bravo et al. [BRAV 2015b] observed that with replacement ratios of CRA lower than 25% and FRA lower than 10% the results were similar to the reference concrete. In terms of water penetration, on the study performed by Grdic et al. [GRDI 2010], on samples with 50% CRA and 100% CRA no water penetration was recorded, whereas the control sample had a penetration of 10 mm. While Gesoglu et al. [GESO 2015a] observed that water penetration is increased when recycled aggregates are introduced in the mix.

All the studies performed on carbonation resistance show a decrease of this property as the replacement level increases.

Flexural behaviour of reinforced beams

In most of the studies analysed, it was noticed that cracking load was slightly affected by the incorporation of recycled aggregates, since the crack occurs earlier as the replacement level increases. At failure, the differences in the ultimate load of the beams, made with natural or recycled aggregates with the same reinforcement ratio are negligible.

In terms of crack pattern, in some studies such as the research performed by Choi and Yun [CHOI 2013] that the crack width in the beams with recycled coarse aggregate is slightly wider than that of the beam with natural aggregate. Moreover, in terms of crack spacing, Arezoumandi et al. [AREZ 2015a], noticed that the RCA beams cracks were closer to each other compared with the CC beams cracks. However, most authors conclude that overall crack pattern is similar regardless of the replacement level.

With regard to the deflection observed at failure, most authors conclude that the deflections observed at failure are higher in beams with recycled aggregates than in beams with only natural aggregates. Arezoumandi et al. [AREZ 2015a] claim that this phenomena can be attributed to lower modulus of elasticity and also lower effective moment inertia (more cracks) of the RCA beams.

In terms of ductility factors of recycled concrete beams, some authors noticed that the differences between beams with the same reinforcement ratio, regardless of the amount of RCA in concrete, can be considered negligible. However, Choi et al. [CHOI 2012] and Kang et

al. [KANG 2014] noticed a decrease that noticed a decrease that could be due to the bond deterioration between aggregate interface and mortar.

Most of authors conclude that the utilization of RAC in reinforced concrete beams is technically feasible the existing analytical models and code-bases procedures for conventional reinforced concrete beams can also be applied to RCA concrete beams. However, further testing to increase the database of test results for recycled aggregates should be done.

Shear behaviour of reinforced beams

With regard to the shear strength of the beam with and without recycled aggregates, different results were obtained in the studies analysed. Choi et al. [CHOI 2008] and Arezoumandi et al. [AREZ 2014, AREZ 2015b] observe that shear strength of the recycled concrete beams was lower than that of the natural concrete beams with the same reinforcement ratio and shear span-to-depth ratio. González-Fonteboa and Martínez-Abella [GONZ 2007] noticed that recycled concrete beams present almost the same shear force at failure as the conventional concrete beams with an equal amount of transverse reinforcement. However, Fathifazl et al. [FATH 2011] and Al-Zahraa et al. [AL-ZA 2011] conclude that the reinforced RCA-beams had a higher shear strength compared to conventional reinforced concrete beams, especially in beams with lower shear reinforcement in [AL-ZA 2011]. The shear strength of reinforced RCA-beams had a tendency to increase with decreasing span-to-depth ratio.

In terms of crack pattern, González-Fonteboa and Martínez-Abella [GONZ 2007, GONZ 2009] observe noticed that premature cracking and notable splitting cracks. The extent of shear-tension cracks was more severe in the concrete with higher recycled aggregate [CHOI 2008]. However, for Arezoumandi et al. [AREZ 2014, AREZ 2015b], crack morphology and crack progression of the RAC100, RAC50, and CC beams was similar to each other.

With regard to the measured deflections, González-Fonteboa et al. [GONZ 2009] observed that recycled concrete beams always present greater deflections than the natural concrete beams. However, Arezoumandi et al. [AREZ 2014, AREZ 2015b] observed that in terms of load deflection response, the behaviour of the RAC and CC beams was similar.

Most authors conclude that the existing code methods for determining the concrete contribution to the shear resistance can be applied without alteration to recycled concrete beams because they are always conservative.

2.2. Bond behaviour between concrete and prestressing strands

The bond performance between the prestressed steel and concrete is essential in order to get an appropriate transfer of the prestressing force and an appropriate behaviour of the concrete element. Both the appearance of cracks along the element and the transfer length are directly related to this phenomenon.

Janey was one of the first to study the physical characteristics of bond between pretensioned strand and concrete and its relationship to the transfer and development lengths. According to the study published in 1954 [JANE 1954], the bond between the prestressed steel and the surrounding concrete, is due to three key factors:

- Chemical adhesion on the concrete and steel interface, due to the interconnection between the cement paste particles and the roughness at a microscopic level of the steel in the contact surface.
- Friction between the concrete and steel.
- Mechanical resistance due to interlocking of the spiral twisting of the outer wires forming the strand.

Janey highlights that the chemical adhesion disappears in the region which covers the transfer length, since that, when the prestressing force is releasing a relative slip between concrete and steel occurs. Therefore, this phenomenon is only present in the central zone in which the steel strain keeps constant.

Friction between concrete and steel is enhanced by the Hoyer effect [HOYE 1939]. The tensioning of the strand in the pretensioning bed causes a reduction in the strand diameter due to Poisson's effect. After the concrete reaches sufficient strength, the strands are released from the abutments and the diameter of the strand expands and wedges against the surrounding concrete. This wedging action caused by the lateral expansion, results in improved bond performance over the transfer length. Therefore, the friction force depends on the normal force to the surface and the friction coefficient concrete-steel. This coefficient varies according to the surface characteristics of the strand or wire and that of the cement paste. Russell and Burns [RUSS 1997] made the surface conditions of the strands responsible for variances of around 20% in the mean values of transfer length.

Before releasing the prestressing force, the steel is subjected to an initial stress σ_{po}. When the strands are released, they tend to regain their original state of zero stress. As stated previously, this recovery is only partly produced, since the steel is compressed inside the concrete, being the steel subjected to a stress σ_{pi}, lower than σ_{po}, due to the instantaneous

losses by elastic shortening of concrete. This strain becomes null at the free ends varying linearly from a zero value in the free end of the specimen to σ_{pi}, at a certain distance. This distance is known as **transfer length (L_t)**. It is the distance from the end of the member over which the fully effective prestressing force is developed (Figure 2.4).

The tensioning force of the steel tends to be approximately 75% of its ultimate strength. Considering the instantaneous losses when releasing and the deferred losses along the lifespan of the specimen, there is an additional tension of the steel available until it reaches ultimate strength. This additional tension can only be developed by bond and may be used applying external loads on the element, producing an increase in tensions.

Therefore, it is necessary to define a new distance from the free end of the beam, the **development length (L_d)**. It is the distance required to develop the strand stress to ultimate stress at the ultimate flexural strength of the member. The tension reached at this point has to be the maximum stress of the prestressing steel.

The difference between the transfer length and the development length is known as the **flexural bond length (L_{fb})**.

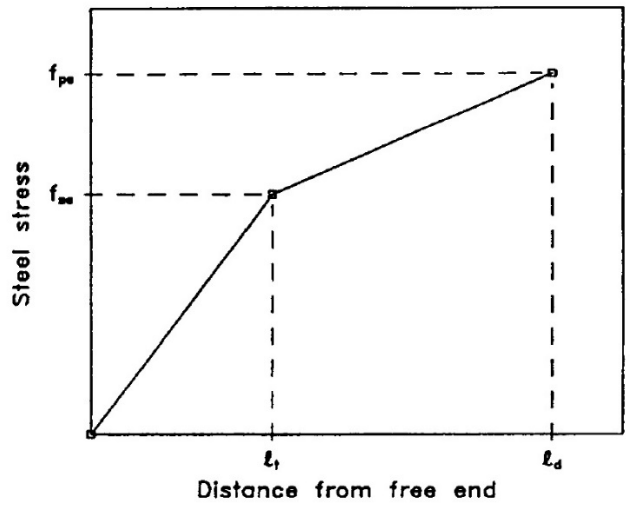

Figure 2.4. Transfer length and development length of pretensioned strands [ABRI 1993]

Several authors proposed analytical predictions of transfer and development length based on the strand end slip, pull out tests or strand stress. However, there is not a common agreement about the equation that offers the most reliable estimation of these values.

2.2.1. Previous studies

Based on the test results previously reported by Hanson and Kaar [HANS 1959] and Kaar et al. [KAAR 1963], an empirical relationship was for the development length was adopted by the ACI Building Code in 1963 [ACI 318-63] (Eq. 2.1).

$$L_d = \left(f_{ps} - \frac{2}{3} f_{se}\right) d_b \qquad [2.1]$$

where, L_d is the development length, in in.;f_{ps} is the stress in ksi, in the prestressed reinforcement at the critical section; f_{se} is the effective stress, in ksi, in the prestressed reinforcement after all losses; and d_b is the nominal diameter of the strand, in in.

The previous equation can be expressed as Eq. 2.2:

$$L_d = \left(\frac{f_{se}}{3}\right) d_b + (f_{ps} - f_{se}) d_b \qquad [2.2]$$

In this form, the first term $\left(\frac{f_{se}}{3}\right) d_b$ is the transfer length and the second term $(f_{ps} - f_{se}) d_b$ is the flexural bond length.

Zia and Mostafa [ZIA 1977] developed empirical equations for transfer length and flexural bond length of prestressing strand based on a linear regression analysis of available research data published before 1977. The proposed equations for transfer length, L_t, and flexural bond length, L_{fb}, were Eq. 2.3 and 2.4:

$$L_t = \left[1.5 \left(\frac{f_{si}}{f_{ci}}\right) d_b\right] - 4.6 \qquad [2.3] \qquad L_{fb} = 1.25(f_{su} - f_{se}) d_b \qquad [2.4]$$

where, f_{si} is the initial stress in strand before losses, in ksi; f_{ci} is the compressive strength of concrete at transfer, in ksi; d_b is the nominal diameter of prestressing strand, in in.; f_{su} is the ultimate strength of prestressing strand, in ksi; and f_{se} is the effective stress in prestressing strand after losses, in ksi.

Zia and Mostafa's equation for transfer length allows for adjustment for different concrete strengths at release, different strand sizes and different initial prestressing. This equation is more conservative than the ACI equation for larger strand sizes, but gives similar results for smaller size strands. Their equation for flexural bond length is based on a re-evaluation of test results from Hansson and Kaar [HANS 1959]. They concluded that the flexural bond length given in the ACI Coded needed to be increased 25%.

Martin and Scott [MART 1976] re-evaluated the available test results and proposed a transfer length of 80 strand diameter for all sizes of strand, which is considerably more conservative than the ACI Code equation.

In mid-1980s, Cousins et al. [COUS 1990] measured and presented the development of analytical equations for transfer length (L_t), flexural bond length (L_{fb}) and development length (L_d) of pretensioned strand in prestressed concrete, and compared them to the experimental results in the literature. Both the L_t and the L_{fb} equation assume a plastic and an elastic zone.

The proposed analytical equation (Eq. 2.5) for the entire transfer length is:

$$L_t = 0.5\left(\frac{U_t}{B}\right) + \frac{f_{se}A_s}{\pi d U_t} \qquad [2.5]$$

This equation for transfer length appears to be independent of the concrete compressive strength (f'_c). However, research on bond has suggested that bond strength is proportional to $\sqrt{f'_c}$. Thus, U_t can be redefined as $U'_t\sqrt{f'_{ci}}$, where f'_{ci} is the concrete compressive strength at transfer. Then, the equation for transfer length becomes in Eq. 2.6.

$$L_t = 0.5\left(\frac{U'_t\sqrt{f'_{ci}}}{B}\right) + \frac{f_{se}A_s}{\pi d U'_t\sqrt{f'_{ci}}} \qquad [2.6]$$

Where U_t is the plastic transfer bond stress, in psi; B is the bond modulus (slope of bond stress curve in the elastic zone), in psi/in.; f_{se} is the effective prestress, in psi; A_s is the cross-sectional area of strand, in sq in.; and d is the nominal diameter of the strand, in in.

The flexural bond length is given by Eq. 2.7:

$$L_{fb} = (f_{ps} - f_{se})\left(\frac{A_s/\pi d}{U_d}\right) \qquad [2.7]$$

Or restating the equation as a function of f'_c (Eq. 2.8):

$$L_{fb} = (f_{ps} - f_{se})\left(\frac{A_s/\pi d}{U'_d\sqrt{f'_c}}\right) \qquad [2.8]$$

Where f_{ps} is the stress in strand at flexural failure, in ksi; and U'_d is the plastic bond stress for development, in psi.

Combining these previous equations, the development length is $L_t + L_{fb}$, or Eq. 2.9:

$$L_t = 0.5\left(\frac{U'_t\sqrt{f'_{ci}}}{B}\right) + \frac{f_{se}A_s}{\pi d U'_t\sqrt{f'_{ci}}} + (f_{ps} - f_{se})\left(\frac{A_s/\pi d}{U'_d\sqrt{f'_c}}\right) \qquad [2.9]$$

The transfer and development length models predicted lengths within acceptable degree of accuracy. However, the authors conclude that due to the limited amount of research in this area, more experimental verifications of the development length parameters would be desirable because the transfer length measured exceeded the standard design predictions by a wide margin.

Their findings and a lack of data supporting the behaviour of pretensioned concrete beams caused by the interaction of this new size strand with concrete, led Federal Highway Administration (FHWA) to adopt a moratorium on the use of 0.6 in. (15.2 mm) diameter strands in October 1988 by FHWA memorandum [FHWA 1988]. This memorandum also included the impose a minimum strand spacing of 4 times the nominal strand diameter and to increase 1.6 and 2.0 times the development length for other sizes of bonded and debonded prestressing strands, respectively.

The FHWA action led to the creation of a large number of research programs with the intent on measuring the transfer and development length of prestressing strands. Research was performed at the University of Texas [RUSS 1996, RUSS 1997], Florida DOT [SHAH 1992], McGill University [MITC 1993], and Auburn University [COUS 1993]. The arbitrary 1.6 multiplier from the original FHWA moratorium is now incorporated into the [AASHTO 2007]. In 1996, this prohibition was lifted by another memorandum [FHWA 1996] as a result of the numerous studies that had been conducted using 0.6 in. (15 mm) strand.

Neither the [ACI 318-95] nor the AASHTO Standard Specifications for Highway Bridges [AASHTO 92] compel a transfer length requirement. However, both codes suggest a transfer length of 50 strand diameter, or 50 d_b.

2.2.2. Bond stress tests in concrete samples

Since the mid-1990s, the development of standardized tests to evaluate the bond characteristics of individual prestressing strands has also been the main objective several researchers. Abrishami and Mitchell [ABRI 1993] tried to introduce a simple test method to determine the bond stress-versus-slip response for pretensioned strand embedded in concrete along the transfer and flexural bond length. They concluded that the bond strength in the transfer length is 1.5, 2 and 2.3 times greater than the bond strength in the flexural bond length, for strand sizes of 9.5, 13 and 16 mm, respectively.

Testing programs were carried out with the aim of evaluating the viability and suitability of several standardized tests for predicting the bond behaviour of the prestressing strand. These tests are: the Moustafa Test [LOGA 1997] (untensioned strands pulled from large concrete blocks); the PTI Bond Test [PTI 2006] (untensioned strands are pulled from a neat cement mortar); and the NASP Bond Test [RAMI 2007] (untensioned strands are pulled from a sand cement mortar). Blind trial tests were performed at different laboratories in the United States in order to determine their reproducibility, being the NASP Bond Test the most reliable of the three [RAMI 2007].

It is also worth mentioning the ECADA test developed by Martí-Vargas et al. [MART 2006]. The aim of this test is to determine the transfer and development lengths by measuring the force in the strand in a series of test specimens with different embedment lengths. The test

sequentially reproduces the transfer of prestress in a specimen and simulates service load through a pull-out test on the same specimen.

Girgis and Tuan (2005)

The aim of this research [GIRG 2005] is to study the bond strength and transfer length of pretensioned bridge girders cast with self-consolidating concrete (Mixes 1 and 2) and conventional concrete (Mix 3). Moustafa pull out tests were conducted to determine the bond capacity of 0.6 in. (15.2 mm) diameter low-relaxation, untensioned strands with an embedment length of 18 in. (457 mm). The tests did not reveal any early bond strength reduction when using SCC with prestressing strands.

Martí-Vargas et al. (2006)

The research developed by Martí-Vargas et al. [MART 2006] proposes a test (ECADA: "*Ensayo para Caracterizar la Adherencia mediante Destesado y Arrancamiento*") to characterize the bond between prestressing strand and concrete. The proposed test determines the transfer and development lengths by measuring the force in the strand in a series of test specimens with different embedment lengths. The test sequentially reproduces the transfer of prestress in a specimen and simulates service load through a pull-out test on the same specimen. The study included 12 different concretes in the experimental program to validate this method and a prestressing strand of 0.5 in. (13 mm).

For the materials used and the established test parameters, good correlation to experimental results is shown in the following expressions (Eq. 2.10 and 2.11):

$$l_t = 29.85 - 0.0016 f'_{ci} \qquad [2.10]$$

$$l_d = 35.08 - 0.0014 f'_{ci} \qquad [2.11]$$

where: l_t is transfer length, in in.; l_d is development length, in in.; and f'_{ci} is the compressive strength of concrete at time of testing, in psi.

An increase in the compressive strength at the time of testing results in a decrease of strand transfer and development lengths. For concretes with compressive strengths from 3481 psi to 7977 psi (24 MPa to 55 MPa) at the time of testing, the transfer length results are between 50% and 80% of those calculated by [ACI 318-05] equations, and the test development lengths are between 45% and 65% of those calculated by [ACI 318-05] equations.

The authors conclude that the ECADA test is a valid method, systematic and reliable for measuring the transfer and development lengths of prestressing strands.

Eiras-López (2009)

Eiras-López [EIRA 2009] developed a procedure for evaluating the bond strength of prestressing reinforcement through pull-out tests. The test is called GCONS-A Bond Test. On the one hand, this test may register variations that modify bond capacity and, on the other hand, the goodness-of-fit of its results is related to the right value of transfer length according to the test UNE 7-436-82, performed following the procedure of the GCONS-P bond test.

The author concludes that the developed procedure permits the quality control of the bond capacity in prestressing reinforcement at every stage of the construction process. However, the procedure requires at least three experimental values because it considers the dispersion of results and informs about qualitative and quantitative aspects related to the bond properties of the reinforcement.

Martí-Vargas et al. (2012b)

Martí-Vargas et al. [MART 2012b] presents an experimental program to determine the transfer and development lengths, as well as the average bond stress along both the transfer and the flexural bond length. The study was made in 12 concretes of different compositions and properties and a concentric 13 mm single prestressing strand, by means of the ECADA test method [MART 2006]. The experimental results were compared with other theoretical and experimental studies found in the literature.

From the experimental results, it can be concluded that an increase of the concrete compressive strength at the testing time results in an increase of the bond stress along both the transfer length and the flexural bond lengths. An average bond stress along the transfer length as a function of the concrete compressive strength at the time of the prestress transfer was obtained as Eq. 2.12:

$$U_t = 0.4 {f_{ci}}^{2/3} \qquad [2.12]$$

Similarly, an average bond stress along the flexural bond length as a function of the concrete compressive strength at loading was obtained as Eq. 2.13:

$$U_c = 0.25 {f_{cl}}^{2/3} \qquad [2.13]$$

The following equation (Eq. 2.14) to predict the transfer length of 13 mm prestressing strand is proposed:

$$L_T = \frac{2.5 A_p \sigma_{pi}}{\Sigma_p {f_{ci}}^{2/3}} \qquad [2.14]$$

Where σ_{pi} the effective stress in prestressing strand is just after prestress transfer (MPa) and Σ_p is the perimeter of the prestressing reinforcement (mm).

The following equation to predict the development length of 13 mm prestressing steel strand when the testing loading time coincides with the prestress transfer time is proposed (Eq. 2.15):

$$L_A = \frac{2.5A_p}{\Sigma_p f_{ci}^{\,2/3}}\left[\sigma_{pi} + 1.6\left(\sigma_{pa} - \sigma_{pi}\right)\right] \qquad [2.15]$$

Where σ_{pa} is the maximum stress in strand at loading (MPa).

The test results obtained in this study were compared with the theoretical predictions obtained from the different equations proposed by several authors and codes to the determine transfer and development lengths. Predictions give values that vary considerably and differ from each other. The predicted transfer length generally overestimates the measured transfer length, with predictions that provide values more than twice the measured transfer length.

Vázquez-Herrero et al. (2013a)

The aim of the research carried out by Vázquez-Herrero et al. [VAZQ 2013a and VAZQ 2001] is to study the strand bond properties along the transfer length of prestressed lightweight concrete members. In this research 3 different lightweight concrete mixes with 0.6 in. (15.2 mm) strand were studied. Bond tests were performed in push-in (transfer length test) and push-out (flexural bond length test) types of specimens. The variables studied were the type of concrete, the test age and the delayed effects of bond.

The results obtained from the two types of bond testing in specimens were substantially different, the bond capacity in specimens for the same material was far superior in the push-in test than in the push-out test, between 1.7 and 2.7 higher, which is in agreement with other investigations that justify this effect due to the wedging of the strand occurred in the interior of the specimen in the push-in test that is not produced in the push-out test.

The push-in test allowed the bond behaviour in the transfer length to be characterized for different types of concrete. Assuming that the bond strength is constant along the transfer length, which agrees with the results of the study, the authors propose delimiting the transfer length using the equations 2.16 and 2.17.

$$l_{t,\max}(t) = \pi_1 \pi_2 f_{pe} d_b / \left(4\tau_{min,TL}\right) \qquad [2.16]$$

$$l_{t,\min}(t) = f_{pe} d_b / \left(4\tau_{max,TL}\right) \qquad [2.17]$$

where $l_{t,\max}(t)$ and $l_{t,\min}(t)$ are the upper and lower bond for the transfer length at a generic age t; π_1 is a coefficient that takes the bond conditions into account; π_2 is a coefficient that accounts for whether the transfer is gradual of sudden; $\tau_{min,TL}$ and $\tau_{max,TL}$ are the minimum and maximum value of the average bond stress that is expected for the transfer length at a generic age t.

During the experimental procedure, the higher bond capacity of the lightweight concrete was corroborated, as was the tendency of this material to experience pull-outs. This result, together with the reduced values of the tensile strength and the fracture energy of these types of concretes with respect to the conventional concretes, implies a greater risk in prestressed lightweight concrete structures to experience cracking by bursting/splitting and slips of the prestressing strand with respect to the concrete, compromising its structural security and durability. Therefore, the results obtained discourage the use of the studied lightweight concrete for a production of pretensioned elements.

2.2.3. Transfer length estimations

Russell and Burns (1996)

Russell and Burns [RUSS 1996] present the results obtained from measuring transfer lengths for both 0.5 and 0.6 in. (12.7 and 15.2 mm) diameter strands for a wide variety of research variables (strand spacing, debonding strand, confining reinforcement, number of strands per specimen and size and shape of the cross section).

They conclude that the average transfer length for 0.5 and 0.6 in. were 29.5 and 40.0 in. respectively (749 and 1020 mm). For debonded strands, they were measurably shorter than those of fully bonded strands: 25.8 and 32.7 in. (655 and 831 mm) for 0.5 and 0.6 in. diameter strands, respectively.

The data indicated that a correlation does exist between transfer length and strand end slips (Eq. 2.18):

$$L_t = 294.9 L_{es} \qquad [2.18]$$

Where L_{es} is the measured end slip, in in. The above equation is nearly identical to the theoretical relationship (Eq. 2.19):

$$L_t = \frac{2E_{ps}}{f_{si}}(L_{es}) \qquad [2.19]$$

where E_{ps} is the elastic modulus of the steel strand, and $f_{si}$is the strand stress immediately before release. Note that this theoretical relationship is independent of strand size. For those tests, the equation was simplified to the following (Eq. 2.20):

$$L_t = 290 L_{es} \qquad [2.20]$$

From the data, a rational and safe expression (Eq. 2.21) was determined and recommended for use in design applications:

$$L_t = \frac{f_{se}}{2} d_b \qquad [2.21]$$

where is the effective stress in prestressed reinforcement (after allowance for all prestress losses).

Kahn et al. (2002)

The aim of this research [KAHN 2002] is to verify that the transfer and development length of 15 mm (0.6 in.) diameter prestressing strand was lower than the calculated by the [AASHTO 96], when used in high performance concrete bridge girders. The tests were carried out with 4 AASHTO Type II girders (two made from 70 MPa and two made from 100 MPa design strength concretes). Transfer length was determined by measuring strand end slip (which failed) and concrete surface strain (with DEMEC gauge points and using the 95% average maximum strain (95%AMS) method discussed by [RUSS 1992]).

The transfer length averaged 447 mm (17.6 in.) and 371 mm (14.6 in.) for the 70 MPa and 100 MPa girders, respectively. It was determined to be 41 and 51% less than that calculated by the [AASHTO 96] specification of 50 strand diameters for the 70 MPa and 100 MPa concretes, respectively.

So, the current AASHTO provisions for transfer length is recommended for high performance concrete girders with concrete strength less than 100 MPa because of their simplicity and accuracy.

Kose and Burkett (2005)

In this study [KOSE 2005], the transfer and development length results from various studies were collected in addition to the results obtained in regional laboratories. New equations for transfer and development length are proposed and compared with current equations in ACI, AASHTO, and other codes.

The selected method to determine the transfer length was the 95% AMS method [RUSS 1992]. From the collected transfer length data, the following general trends were observed:

- For the 0.5 and 0.6 in. (13 and 15 mm) diameter strand data, an increase in the diameter of the prestressing strand decreased the transfer length.
- An increase in the concrete strength decreased the transfer length.
- An increase in the effective prestress force increased the transfer length.

Based on those observations, the proposed equation (Eq. 2.22) to predict the transfer length of strands is:

$$L_t = 95\frac{f_{pi}(1-d_b)^2}{\sqrt{f'_c}} \quad (in.) \qquad [2.22]$$

Where f_{pi} is the stress in the prestressing strands prior to release (ksi) and $\sqrt{f'_c}$ is the square root of 28-day concrete compressive strength for the long-term transfer length measurements (psi)

The authors conclude that the proposed transfer length equation was conservative for all the transfer length values, but not overly conservative for low-strength concrete members. [ACI 318-02], [AASHTO 92] and [AASHTO 97] ($50d_b$, $50d_b$ and $60d_b$, respectively) are very unconservative for 0.5 in. and slightly unconservative for 0.6 in.

Girgis and Tuan (2005)

The aim of this research [GIRG 2005] is to study the bond strength and transfer length of pretensioned bridge girders cast with self-consolidating concrete (Mixes 1 and 2) and conventional concrete (Mix 3). The transfer lengths of 3 pretensioned girders were measured using DEMEC points and determined with the 95% AMS method [RUSS 1992]. The diameter of the prestressing strands is 0.6 in. (15.2 mm).

The average transfer lengths of Mixes 1 and 2 were determined to be 36 and 43 in. (914 and 1092 mm), respectively. These values are longer than the transfer lengths specified by [ACI 318-02] and the [AASHTO 96], about 50 strand diameters or 30 in. (762 mm). Mix 2 has a transfer length greater than 60 strand diameters, or 36 in. (914 mm), specified by the [AASHTO 98]. The average transfer length of the conventional concrete (Mix 3) was determined to be 20 in. (508 mm), which is less than the required by both the AASHTO Specifications and ACI 318. Mix 3 had a higher early compressive strength compared to that of Mix 2. Short transfer lengths may cause excessive concrete stress at transfer and may result in splitting or bursting cracks in the girder end zone. Long transfer lengths may reduce girder shear resistance and imply long development lengths, which may adversely affect the flexural strength of the girder.

Martí-Vargas et al. (2007a)

The purpose of this research [MART 2007a] is to develop an analytical bond model to predict the transfer length of 13 mm prestressing strand. An elastic zone included in the transfer length equation proposed by [COUS 1990] has not been observed in the results of the tests made with the ECADA test method [MART 2006], so an inelastic bond stress distribution along the transfer length was considered for the analytical model. A relationship between the plastic bond stress and the concrete compressive strength at the time of prestress

transfer was also found. The equation proposed (Eq. 2.23) to predict the average and both the lower bound and the upper bound values of transfer length is:

$$L_t = \lambda \frac{f_{pi} A_p}{(4/3)\pi d_b 0.4 f'^{0.67}_{ci}} \qquad [2.23]$$

λ=1 for the average value of transfer length
λ=0.5 for the upper bound value of transfer length
λ=1.5 for the lower bound value of transfer length
f_{pi} = effective stress in prestressing strand (MPa)
f'_{ci} = concrete compressive strength at the time of prestress transfer (MPa)

by substituting A_p = 0.779 $\pi {d_b}^2/4$ and d_b = 12.9 mm, this equation can be expressed as Eq. 2.24:

$$L_t = \lambda \frac{4.7 f_{pi}}{f'^{0.67}_{ci}} \qquad [2.24]$$

A tendency of reduction of transfer length when f'_{ci} increases was observed.

The test results obtained in this study were compared with the theoretical predictions from different proposed equations by several authors to determine transfer length. The predictions gave transfer length values which vary considerably and are very different to each other. Generally, predicted transfer lengths are greater than measured transfer lengths.

Martí-Vargas et al. (2007b)

Martí-Vargas et al. [MART 2007b] analyse the reliability of transfer length determination from free end slips according with proposed expressions in the literature [MARS 1969, BALA 1992, BALA 1993 and ROSE 1997]. Variation in strand stress along the transfer length involves slip between the strand and the concrete. The measurement of the strand end slip is an indirect method to determine the transfer length. Guyon [GUYO 1953] proposed the following expression (Eq. 2.25) from a theoretical analysis:

$$L_t = \alpha \frac{\delta}{\varepsilon_{pi}} \quad , which\ can\ be\ rewritten\ as \quad L_t = \alpha \frac{\delta E_p}{f_{pi}} \qquad [2.25]$$

Where L_t is the transfer length, δ is the strand end slip at the free end of a prestressed concrete member, ε_{pi} is the initial strand strain, E_p is the modulus of elasticity of the prestressing strand, f_{pi} is the strand stress immediately before release and the α coefficient represents the shape factor of the bond stress distribution along the transfer zone (α=2 for uniform bond distribution and α=3 for linear descending bond distribution).

Transfer length test results of 0.5 in. (12.7 mm) diameter strands on twelve different concrete mixtures were analysed. The ECADA test method [MART 2006] was used to obtain the transfer length with a series of specimens with different embedment lengths.

The authors conclude that an average $\alpha = 2.44$ for Guyon's formula has been obtained from the experimental results. However, a great variability of results for some concrete mixture has been observed in transfer length estimation from the experimental free end slips when Guyon's formula was applied. The prediction range of transfer lengths from expression proposed by several authors is very ample.

The authors also conclude that the sequence of free end slip values versus the embedment length is not a reliable assurance procedure for the experimental determination of transfer length. However the sequence of stressed end slip values versus the embedment length in the ECADA method is a reliable assurance procedure.

Larson et al. (2007)

Larson et al. [LARS 2007] present the results of an experimental program conducted to determine the material and bond characteristics of a proposed self-compacting concrete mixture for bridge girders. Twelve single-strand (top or bottom strand and rectangular section) and four multiple-strand (T-shape) specimens were cast to investigate the transfer and development length. The strand diameter is 0.5 in. (13 mm).

To experimentally determine the transfer length of the girders, end-slip values were obtained by measuring the distance that the strand slipped into the specimen at the member ends. The following equations (Eq. 2.26) were used to determine the implied transfer length values from the end-slip measurement data:

$$\Delta = avg\ f_{si} \frac{L_{tr}}{E_{ps}} \qquad [2.26]$$

Where Δ is the end slip, in in.; $avg\ f_{si}$ is the average initial strand stress over the transfer length after release of prestressing, in ksi; L_{tr} is the transfer length, in in.; and E_{ps} is the elastic modulus of the strand, in ksi.

Assuming straight line variation of strand stress from zero at the end of the beam to full prestressing (Eq. 2.27):

$$\Delta = \frac{0.5 f_{si} L_{tr}}{E_{ps}} \qquad \rightarrow \quad L_{tr} = \frac{\Delta E_{ps}}{0.5 f_{si}} \qquad [2.27]$$

The average 21-day implied transfer length measured through end-slip was 21 in. (530 mm) for the bottom strand specimens, 30 in. (760 mm) for the top strand specimens, and 29 in. (740 mm) for the T-shape specimens. There was an increase in implied transfer lengths

during the first 21 days after releasing. For bottom strand specimens and T-shape specimens, the average increase in transfer length was 10% to 20%, while for the top strand specimens, the increase was 40% to 45%.

The authors conclude that transfer length estimated from 21-day strand end slip measurements were in general accordance with the value assumed by [AASHTO 2004] and [ACI 318-02].

Ramirez and Russell (2007)

This is a report of a NCHRP Project [RAMI 2007] with the objective of developing recommended revisions to the AASHTO LRFD Bridge Design Specifications for normal-weight concrete having compressive strengths up to 15 ksi (103 MPa), relative to transfer and development length of prestressing strand with diameters up to 0.62 in. (15.75 mm).

The authors conclude that the current AASHTO transfer length equation of $60d_b$ is adequate when using normal strength concrete. However, the data support that it is necessary to consider variations in concrete release strength, since the bond strength improves in proportion to the square root of the concrete strength. Therefore, it is proposed the following expression (Eq. 2.28) for transfer length, limiting the value to 10 ksi (69 MPa) concrete, which was the highest 1-day strength tested:

$$l_t = \frac{120}{\sqrt{f'_{ci}}} d_b \geq 40 d_b \qquad [2.28]$$

Where l_t is the transfer length (in.); f'_{ci} is the release concrete strength (ksi); and d_b is the diameter of prestressing strand (in.).

Pozolo and Andrawes (2011)

In this study, Pozolo and Andrawes [POZO 2011a] present an analytical method for predicting the transfer length of steel strands in prestressed girders using pull-out test results. 56 pull-out tests were used to get bond stress-slip relationships for 12.7 mm steel strands embedded in Self-compacting concrete (SCC) and conventional concrete (CC). These relationships were used to define parameters for finite element (FE) analyses of large-scale prestressed members.

The girder's transfer length at each day was also calculated using the 95% Average Maximum Strain Method [RUSS 1992] through the use surface target points spaced 50 mm apart were attached to both sides of the girder. The 28-day experimental transfer length for the box girder was found to be 532 mm, a value below both the ACI ($50d_b$ = 635 mm) and AASHTO ($60d_b$ = 762 mm) limits. Using the modified bond stress-slip relationships, transfer lengths predicted via FE analysis for a SCC T-beam and hollow box beam were 952 mm and 519 mm, respectively, with errors of 6.7% and 2.4%, respectively. Strand performance in SCC is

comparable with CC. Normalized pull-out loads differed by as little as 1% after 3 days of curing.

Pozolo and Andrawes (2011b)

This research [POZO 2011b] aims to investigate the transfer length of 12.7 mm (0.5 in.) diameter steel strands in full-scale prestressed box and I-beams cast with self-compacting concrete (SCC).

Transfer length was measured attaching surface-strain target points, which were used to obtain longitudinal strain profiles at the beam ends. The transfer length (Table 2.4) at each age was calculated using the 95% Average Maximum Strain Method [RUSS 1992]:

Table 2.4. Transfer length [POZO 2011b]

	Average measured transfer length (mm)	
	7 days	28 days
Box 1	535	564
Box 2	488	501
I-1	526	525
I-2	636	-

This results were compared to the analytical predictions and the [ACI 318-08] and [AASHTO 04] required transfer lengths. The experimental transfer lengths at seven of the eight girders ends were below the ACI 318-08 and AASHTO LRFD required transfer lengths. Only at one end (which had the lowest compressive strength of all locations) did the experimental results consistently and significantly exceed the code provisions (greater than $50d_b$ by up to 30% and greater than $60d_b$ by up to 8.3%). Overall, the experimental transfer lengths were 86% of $50d_b$, 72% of $60d_b$, and 69% of $f_{pe}d_b/20.7$ (SI units). No correlation was observed between transfer length and girder type.

According to the analytical comparison study, the experimental transfer lengths showed a better correlation to predictions incorporating initial prestress and concrete compressive strength than to predictions incorporating effective prestress or no concrete strength.

Floyd et al. (2011)

The objective of this research [FLOY 2011] is to examine the bond of prestressed strand with self-compacting concrete (SCC). For this investigation, 26 rectangular concrete beams were constructed, instrumented and tested over the course of several projects. The same cross-section was used for all specimens, but SCC using Type I and Type III cements and a conventional high strength concrete mixture were tested using a 0.6 in. (15.2 mm) prestressed strand and a lightweight SCC was used along with a 0.5 in. (12.7 mm) prestressed strand.

Transfer length was measured using concrete surface strains and the 95% Average Maximum Strain method [RUSS 1992]. The results obtained were compared to the transfer length equations proposed from nine different research projects conducted using different sets of variables.

The experimental values obtained for transfer length are included in Table 2.5.

Table 2.5. Transfer length [FLOY 2011]

	Transfer length (mm)		
	Min.	**Max.**	**Avg.**
SCC I	432	711	546
SCC III	381	660	500
HSC	432	737	602
LWSCC	330	686	511

The authors conclude that several of the proposed equations are adequate for predicting transfer length of prestressed strands cast using these different concrete types.

Martí-Vargas et al. (2012a)

In this research, Martí-Vargas et al. [MART 2012a] present the results of an experimental study to analyse the influence of the composition of concretes made with varying cement contents and with different water/cement (w/c) ratios on the bond behaviour in transmission of 13 mm diameter 7-wire prestressing steel strands. Four families of concrete were analysed. Each family was characterized by its cement content (350, 400, 450 and 500 kg/m^3) and was composed of concretes with different w/c ratios (0.3, 0.35, 0.40, 0.45 and 0.50).

For each transfer length determination a series of specimens with a variable embedment length are casted and tested with the ECADA test method [MART 2006].

It was observed that the greater the w/c ratio, the greater the transfer length obtained. However, the transfer length decreases when compressive strength at release increases. It was also observed that the transfer length is of 550 mm for all concretes with 350 kg of cement, irrespectively of the w/c ratio. The transfer length for the rest of the concrete mix designs depends as much on the cement content as on the w/c ratio. If the w/c ratio is high, the transfer length increases when the cement content increases; if the w/c ratio is low, it diminishes when the cement content increases. A general tendency is that the transfer length increases when the water content increases.

A relationship between the average bond stress in transmission and the variables cement content and concrete compressive strength at release was observed.

Vázquez-Herrero et al. (2013b)

Vázquez-Herrero et al. [VAZQ 2013b and VAZQ 2010] discuss an analytical model that relates the transfer length and the prestressing strand draw-in immediately after transfer. The model is based on the elastic confinement hypothesis of the prestressing strand using concrete or confinement reinforcement. The analytical model and the expressions proposed are compared with experimental results.

Two expressions that enable the establishment of lower and upper bounds for the transfer length were proposed (Eq. 2.29 and 2.30):

$$L_{t,min} = 2E_p\delta/(2f_{pi} - f_{pe}) \qquad [2.29]$$

$$L_{t,max} = \beta E_p\delta/(2f_{pi} - f_{pe}) \qquad [2.30]$$

where δ is the strand draw-in (mm); E_p is the elastic modulus of the strand (MPa); f_{pi} is the strand stress immediately before transfer (MPa); f_{pe} is the effective stress of the strand at the central zone of the structure; and β is an experimental coefficient.

β has to be experimentally adjusted for each pretensioned element as a function of the concrete type and the presence of confining reinforcement. From the Eurocode 2 [CEN 1996], this value would be β = 3, and from the Model Code [MC 2010], this value would be β = 4. However, the experimental results of this paper show a minimum value of 2 for all studied cases, and a maximum value greater than 4 in all lightweight concrete prism (no confining reinforcement) and all lightweight concrete beams. The maximum value of β was 3 in all conventional concrete elements, prisms and beams. Therefore, the formulation of the Eurocode 2 [CEN 1996] provides values resulting in the unsafe fabrication of lightweight concrete elements without confinement reinforcement.

It is important to highlight that upper bound equation is not valid if cracking by splitting/bursting is produced during the transfer in the absence of confining reinforcement. In this case, all the tested lightweight members presented structural insecurity due to splitting cracks, which were detected after the prestress release. This cracks compromise the durability of the prestressing, reducing its service life.

The advantages of the equations proposed in this paper is that they account for the effective prestressing force and the prestressing instantaneous losses. Therefore, they can be applied to concretes others than the conventional concrete.

Oh et al. (2014)

Oh et al. [OH 2014] propose a realistic estimation and appropriate prediction equation for transfer length in pretensioned, prestressed concrete members. Several series of tests were conducted to measure the transfer length in pretensioned members and a finite element

analysis was also conducted. For this study, a single strand was embedded at the middle of the cross section of each beam with a designated bottom cover of 30, 40 or 50 mm. The strand diameter studied were 12.7 mm (0.5 in.) and 15.2 mm (0.6 in.). The transfer length was measured with DEMEC gauge points and using the 95% average maximum strain method discussed by [RUSS 1992].

The equation 2.31 is derived for transfer length:

$$l_t = 8\sqrt{f_{pe}}\left(\frac{1}{f_{ci}}\right)^{1/3} {d_b}^{1.28}\left(\frac{1}{C-20.0}+0.25\right) \qquad [2.31]$$

where l_t is transfer length (mm); f_{pe} is effective prestress (MPa); f_{ci} is the compressive strength; d_b is strand diameter (mm); and C is concrete cover to the strand centre (mm).

The study also indicates that there are good correlations between the transfer lengths and end slip values in pretensioned members. Therefore, it may be possible to calculate the transfer length from the end slip value. A good regression equation (Eq. 2.32) was obtained from the data, where Δ is end-slip in mm:

$$l_t = 183\Delta + 340 \qquad [2.32]$$

The authors conclude that:

- The transfer length increases with an increase of the strand diameter (30% from 12.7 to 15.2 mm)
- The transfer length increases with an increase of prestress magnitude. This increase is proportional to the square root of prestress magnitude.
- The transfer length decreases with an increase of cover depth for all prestress magnitudes.
- The transfer length decreases with an increase of concrete strength for all prestress magnitudes and strand diameters.

2.2.4. Development length estimations

Kahn et al. (2002)

The aim of this research [KAHN 2002] is to verify that the transfer and development length of 15 mm (0.6 in.) diameter prestressing strand was lower than the calculated by the [AASHTO 96], when used in high performance concrete bridge girders. The tests were carried out with 4 AASHTO Type II girders (two made from 70 MPa and two made from 100 MPa design strength concretes). Development length was determined by performing 8 flexure tests with varying embedment lengths.

The minimum embedment length at which the girder failed in a flexural mode while reaching its theoretical flexural capacity with less than 2 mm bond slip was defined as the development length. The experimental development length (2032 mm) resulted to be 20% lower than that calculated by the current AASHTO code equation (2441 mm).

So, the current AASHTO provisions for development length is recommended for high performance concrete girders with concrete strength less than 100 MPa because of their simplicity and accuracy.

Kose and Burkett (2005)

In this study [KOSE 2005], the transfer and development length results from various studies were collected in addition to the results obtained in regional laboratories. New equations for transfer and development length are proposed and compared with current equations in ACI, AASHTO, and other codes.

From the collected flexural bond length data, the following general trends were observed:

- For the 0.5 and 0.6 in. (13 and 15 mm) diameter strand data, an increase in the diameter of the prestressing strand decreased the flexural bond length.
- An increase in concrete strength did not have any significant effect on the flexural bond length.
- An increase in $(f_{ps} - f_{se})$ led to a slight decrease in the flexural bond length. However, it is theoretically known that the flexural bond length is directly proportional to $(f_{ps} - f_{se})$.

Based on those observations, the proposed equation (Eq. 2.33) to predict the flexural bond length, L_{fb}, becomes:

$$L_{fb} = 8 + 400\frac{(f_{pu} - f_{pi})(1 - d_b)^2}{\sqrt{f'_c}} \quad (in.) \qquad [2.33]$$

Where f_{pu} is the ultimate tensile strength of the prestressing strand (ksi).

The development length: $L_d = L_t + L_{fb}$

$$L_d = 95\frac{f_{pi}(1 - d_b)^2}{\sqrt{f'_c}} + 8 + 400\frac{(f_{pu} - f_{pi})(1 - d_b)^2}{\sqrt{f'_c}} \quad (in.) \qquad [2.34]$$

The proposed development length equation (Eq. 2.34) values were conservative for development lengths that resulted in slip/shear and bond failures, except two values that resulted in slip/shear failure that were slightly non-conservative. For the development length values that resulted in flexural failure, the proposed equation, was not overly conservative as others.

Larson et al. (2007)

Larson et al. [LARS 2007] present the results of an experimental program conducted to determine the material and bond characteristics of a proposed self-compacting concrete mixture for bridge girders. Twelve single-strand (top or bottom strand and rectangular section) and four multiple-strand (T-shape) specimens were cast to investigate the development length. The strand diameter is 0.5 in. (13 mm).

All flexural specimens tests failed by strand rupture and the maximum end slip recorded for all specimens during testing was less than 0.01 in. (0.25 mm). In each case, the failure moment exceeded the calculated nominal moment capacities by 10% and 20% for specimens with an embedment length of 6 ft. 1 in. (1850 mm). All specimens with an embedment length of 4 ft. 10 in. (1470 mm) presented an increase of 25% to 35% in nominal capacity.

The authors conclude that all of the specimens with an embedment length equal to 80% of the ACI development length failed in flexure by strand rupture.

Ramirez and Russell (2007)

This is a report of a NCHRP project [RAMI 2007] with the objective of developing recommended revisions to the AASHTO LRFD Bridge Design Specifications for normal-weight concrete having compressive strengths up to 15 ksi (103 MPa), relative to transfer and development length of prestressing strand with diameters up to 0.62 in. (15.75 mm).

The results indicate that the development length diminishes with increasing the concrete strength. The development length expression can be rewritten as follows (Eq. 2.35) and it limited by a minimum value that corresponds to a concrete strength of approximately 14.9 ksi (103 MPa),

$$l_d = \left[\frac{120}{\sqrt{f'_{ci}}} + \frac{225}{\sqrt{f'_c}}\right] d_b \geq 100 d_b \qquad [2.35]$$

where l_d is development length (in.); and f'_c is design concrete strength (ksi).

Floyd et al. (2011)

The objective of this research [FLOY 2011] is to examine the bond of prestressed strand with self-compacting concrete (SCC). For this investigation, 26 rectangular concrete beams were constructed, instrumented and tested over the course of several projects. The same cross-section was used for all specimens, but SCC using Type I and Type III cements and a conventional high strength concrete mixture were tested using a 0.6 in. (15.2 mm) prestressed strand and a lightweight SCC was used along with a 0.5 in. (12.7 mm) prestressed strand.

Development length was determined using iterative flexural tests. The results obtained were compared to the development length equations proposed from nine different research projects conducted using different sets of variables.

The experimental values obtained for development length are included in Table 2.6.

Table 2.6. Development length [FLOY 2011]

	Development length (mm)
SCC I	889 - 953
SCC III	762-826
HSC	762-889
LWSCC	635-699

The authors conclude that several of the proposed equations are adequate for predicting development length of prestressed strands cast using these different concrete types.

Vázquez-Herrero et al. (2013c)

The aim of this research [VAZQ 2013c and VAZQ 2010] is to evaluate the feasibility of producing structural lightweight concrete prestressed girders with load-bearing capacities similar to conventional concrete girders. The principal objectives are estimating the upper bound for the development length of 15.2 mm (0.6 in.) diameter strands and evaluating the ductility of beams made with two different mixes of lightweight concrete (LC10-1 and LC10-2) and one mix of conventional concrete (NC). The ductility factor was defined by Meli [MELI 2010] as the quotient between the final strain and the elastic deformation of the material.

All of the beams tested exceeded the nominal flexural capacity. The maximum development length of the NC beams was 2.75 m and not exhibited splitting cracks. However the development length of the LC10-1 and LC10-2 beams did not exceed 4 and 3.25 m respectively, and splitting cracks were observed along the entire length of the beams. Moreover, lower strand slips were detected at ends in LC10-2 beams. The ductility factor of the LC10-1 and LC10-2 beams was 50% and 60% that of the NC beams.

Although all of the LC10-2 beams developed the full strength of the prestressed strands, showed a remarkably ductility behaviour and exceeded their nominal flexural capacities, its manufacturing it is not recommended. This is due to the splitting cracks observed in all the beams that might affect the durability and load-bearing capacities in case of strand corrosion.

Andrawes et al. (2013)

This paper [ANDR 2013] reports the findings of a study investigating the development length of 12.7 mm diameter prestressing steel strands in SCC full-scale prestressed bridge girders.

Iterative flexural tests with different embedment lengths were conducted on the two long box girders and two I-girders. Experimental results were compared with requirements of the [ACI-2008] and [AASHTO 04] and analytical expressions for development length proposed in the literature.

The results of the study revealed that for all studied development lengths, the box girders were able to resist moments in the range of 81-106% of the nominal moment capacity of the girder. The types of damage observed varied between excessive bond-slip of the strand associated with significant shear cracks and excessive flexural cracking associated with negligible end-slip if the strands.

The tests conducted on the two I-girders were all dominated by excessive flexural cracking, which was preceded by minor diagonal shear cracks that were initiated at the midheight of the web and did not propagate through the bottom flange. They resisted moments in the range of 101-107% of the girder's nominal moment capacity and the end-slip of the strands was negligible (below 1.6 mm).

The experimental and predicted development lengths in the box and I-girders are shown in the Table 2.7:

Table 2.7. Development length [ANDR 2013]

	Box-girder (mm)	**I-girder (mm)**
Experimental	< 2120	< 1461
ACI/AASHTO	1843 (-15%)	1948 (+25%)
Buckner [BUCK 1995]	1839 (-15%)	1935 (+24%)
Zia and Mostafa [ZIA 1977]	1945 (-9%)	2181 (+33%)
Deatherage et al. [DEAT 1994]	2524 (+16%)	2656 (+45%)
Shahawy [SHAH 2001]	2753 (+23%)	3746 (+61%)

The authors conclude that based on the results of the study, the use of SCC in prestressed full-scale girders provides significant advantage in terms of eliminating the need for mechanical vibration without impacting the flexural behaviour of full-scale girders. However, the discrepancy between the experimental results and the code requirements for both box and I-girders suggests the need for further research that could lead to expressions that are specifically developed for SCC prestressed members.

2.2.5. Formulations for transfer and development length in the current codes

ACI 318-14

The current Building Code Requirements for Structural Concrete [ACI 318-14] published by the American Concrete Institute maintain the following expression for development length (Eq. 2.36) of pretensioned seven-wire strands in tension:

$$L_d = \left(\frac{f_{se}}{3000}\right) d_b + \left(\frac{f_{ps} - f_{se}}{1000}\right) d_b \qquad [2.36]$$

Where f_{se} is the effective stress in the prestressed reinforcement after all losses (psi); f_{ps} is the stress in the prestressed reinforcement at the critical section (psi); and d_b = is the nominal diameter of the strand (in.).

The first term represents the transfer length and the second term the flexural bond length.

AASHTO LFRD 2012

The current "AASHTO LRFD Bridge Design Specification" [AASHTO 12] published by the American Association of State Highway and Transportation Officials proposes the following equations (Eq. 2.37 and 2.38) for transfer length and development length, respectively:

$$L_t = 60 d_b \qquad [2.37]$$

$$L_d = \kappa \left(f_{ps} - \frac{2}{3} f_{pe}\right) d_b \qquad [2.38]$$

Where d_b is the nominal diameter of the strand, in in.; κ = 1.0 for pretensioned members with a depth of less than or equal to 24.0 in. or κ = 1.6 for pretensioned members with a depth greater than 24.0 in.; f_{ps} is the average stress in prestressing steel at the time for which the nominal resistance of the member is required (ksi); and f_{pe} is the effective stress in prestressing steel after losses (ksi).

Eurocode 2 (2004)

The current "Eurocode 2: Design of concrete structures – Part 1-1: General rules and rules for buildings" [CEN 2004] published by the European Committee for Standardization proposes the following equations (Eq. 2.39 and 2.40) for transfer and development length, respectively:

$$L_t = \alpha_1 \alpha_2 \phi \frac{\sigma_{pm0}}{\eta_{p1} \eta_l f_{ctd}} \qquad [2.39]$$

$$L_d = 1.2 L_t + \alpha_2 \phi \frac{(\sigma_{pd} - \sigma_{pm\infty})}{\eta_{p1} \eta_l f_{ctd}} \qquad [2.40]$$

Where α_1= 1.0 (gradual release) or 1.25 (sudden release); α_2 = 0.25 (circular prestressed wires) or 0.19 (3 and 7 wires strands); ϕ is the nominal diameter of the prestressing reinforcement (mm); σ_{pm0} is the stress in prestressing strand just after release (MPa); η_{p1} = coefficient that accounts for the tendon type, 2.7 (wires) or 3.2 (3 and 7 wires strands); η_l = coefficient that accounts for the bond conditions, 1.0 (good conditions) or 0.7 (bad conditions); f_{ctd} is the concrete tensile strength at transfer (MPa); σ_{pd} is the stress in prestressed reinforcement at nominal strength (MPa); $\sigma_{pm\infty}$ is the stress in prestressed reinforcement after all losses (MPa).

EHE 08

The Spanish Code on Structural Concrete [EHE 08] proposes the following expressions (Eq. 2.41 and 2.42) for transfer and development length, respectively:

$$L_t = \alpha_1 \alpha_2 \alpha_3 \phi \frac{\sigma_{pi}}{4 f_{bpd}(t)} \qquad [2.41]$$

$$L_d = L_t + \alpha_4 \phi \frac{(\sigma_{pd} - \sigma_{pcs})}{4 f_{bpd}} \qquad [2.42]$$

Where: α_1= 1.0 (gradual release) or 1.25 (sudden release); α_2= 1.0 (ultimate limit state) or 0.5 (service limit state); ϕ is the nominal diameter of the prestressing reinforcement (mm); α_3 = 0.5 (for strands) or 0.7 (for indented or crimped wires); σ_{pi} is the tendon stress before release (MPa); $f_{bpd}(t)$ is bond stress when releasing (MPa) (Table 70.2.3 [EHE 2008]); σ_{pd} is the stress in prestressed reinforcement at nominal strength (MPa); and σ_{pcs} is the stress of the strand due to prestress after all losses.

Model Code 2010

The Model Code 2010 [MC 2010], published by the International Federation for Structural Concrete proposes the following expressions (Eq. 2.43 and 2.44) for transfer and development length of prestressing strands, respectively:

$$L_t = \alpha_{p1} \alpha_{p2} \alpha_{p3} \frac{7}{36} \phi \frac{\sigma_{pi}}{\eta_{p1} \eta_{p2} f_{ctd}} \qquad [2.43]$$

$$L_d = L_t + \frac{7}{36} \phi \frac{(\sigma_{pd} - \sigma_{pcs})}{\eta_{p1} \eta_{p2} f_{ctd}} \qquad [2.44]$$

Where: α_{p1}= 1.0 (gradual release) or 1.25 (sudden release); α_{p2}= 1.0 (moment and shear capacity considered) or 0.5 (verification of transverse stress in anchorage zone); α_{p3} = 0.5 (for strands) or 0.7 (for indented or crimped wires); η_{p1} = 1.2 (for 7-wire strands) or 1.4 (for indented and crimped wires); η_{p2} = 1.0 (for all tendons with an inclination of 45°-90° with respect to the horizontal during concreting, 1.0 (for all horizontal tendons which are up to

250 mm from the bottom or at least 300 mm below the top of the concrete section during concreting), 0.7 (for all other cases); ϕ = nominal diameter of the prestressing reinforcement (mm); σ_{pi} = tendon stress before releasing (MPa); f_{ctd} = f_{ctk} (t) / 1.50 is the lower design concrete tensile strength, for the transmission length at the time of release and for the anchorage length at 28 days; σ_{pd} = is de tendon stress under design load (MPa); and σ_{pcs} = tendon stress due to prestress after all losses (due to creep and shrinkage) (MPa).

2.2.6. Conclusions

The following conclusions have been drawn from the analysis of the different studies:

- The transfer and development lengths decrease as the concrete compressive strength increases because of a decrease of the bond strength along both length [MART 2006, MART 2012a, MART 2012b, OH 2014 and RAMI 2007].
- Short transfer lengths may cause excessive concrete stress at transfer and may result in splitting or bursting cracks in the beam end zone, compromising the structural security and durability [MART 2012b, VAZQ 2013a, and GIRG 2005].
- The greater the w/c ratio, the greater the transfer length obtained. If the w/c ratio is high, the transfer length increases when the cement content increases, if the w/c ratio is low, it diminishes when the cement content increases [MART 2012a].
- A general tendency is that the transfer length increases when the water content increases [MART 2012a].
- The transfer length increases with an increase of the strand diameter [OH 2014]. However, an increase in the diameter of the prestressing strand decreases the flexural bond length [KOSE 2005].
- The transfer length increases with an increase of prestress magnitude. This increase is proportional to the square root of prestress magnitude [OH 2014].
- The transfer length decreases with an increase of cover depth for all prestress magnitudes [OH 2014].
- Most authors conclude that the use of self-compacting concrete (SCC) has not a detrimental effect on the bond strength between the prestressing strand and the surrounding concrete [GIRG 2005, LARS 2007, POZO 2011a, FLOY 2011]. However, the use of lightweight concrete showed higher bond capacity than conventional concrete but reduced values of tensile strength and fracture energy, causing cracking by bursting/splitting and slips in prestressing strands. This cracks compromise the durability of the prestressed element, reducing its service life [VAZQ 2010, VAZQ 2013a, VAZQ 2013b, VAZQ 2013c].
- The proposed formulations for transfer, flexural bond, and development length by the studied authors and codes are summarised in Appendix 1.

To date, studies on bond behaviour, transfer length and development length of prestressed concrete with recycled aggregates have not been found. Therefore, the aim of the present

study is to analyse these properties on recycled concrete with fine and coarse recycled concrete aggregates.

2.3. Specific objectives

The main goal of this research will be to analyse the feasibility of utilising the fine and coarse fraction of recycled concrete aggregate for the fabrication of structural concrete, without a previous sieving process of the recycled aggregate.

This investigation will be divided into two parts.

The objective of the first part of this research will be to compare the mechanical performance of recycled concrete made of up to 39% replacement of the fine fraction and 62% replacement of the coarse fraction, that is, 50% replacement of the total aggregate with recycled concrete aggregate. As mentioned before, replacement levels of the coarse fraction higher than 20% are not recommended by the Spanish Regulation EHE-08 for reinforced concrete.

This part will include:

- Analysis of the main properties of the materials: particle size distribution, particle density and water absorption, particle shape (flakiness index), resistance to fragmentation, classification of the constituents of the coarse recycled aggregate and chemical composition.
- Quality control tests performed in the laboratory to evaluate the fresh and hardened properties: workability, density, compressive strength, splitting tensile strength and modulus of elasticity.
- Fabrication of reinforced concrete beams with the different substitutions in the precast plant.
- Flexural and shear tests performed in situ in the precast plant measuring the applied load and the deflection at mid span.
- Flexural tests controlled by displacement will be performed at university. The applied load will be monitored with load cells on both supports, strains registered with strain gauges adhered to the concrete surface and deflections measured at mid span. All of them synchronized and registered with a data acquisition device.

The incorporation of recycled aggregates in prestressed concrete is forbidden by most of the concrete regulations. Therefore, the second part of this research will be focused on assessing the loss of bond performance between prestressed steel and concrete when recycled aggregates (fine and coarse) are introduced in the mix.

This part will include:

- Preliminary study in a precast plant with prestressed pre-slabs. These elements will be fabricated with replacement levels of up to 10% of the fine fraction and 10% of the coarse fraction, that is, 10% replacement of total aggregate with recycled aggregate. The pre-slabs will be subjected to flexural and shear tests and if the results are promising, prestressed I-beams will be fabricated for a more detailed study.
- Analysis of the main properties of the materials: particle size distribution, particle density and water absorption, particle shape (flakiness index), resistance to fragmentation, classification of the constituents of the coarse recycled aggregate and chemical composition.
- Quality control tests performed in the laboratory to evaluate the fresh and hardened properties: workability, density, compressive strength, flexural strength, modulus of elasticity and depth of penetration of water under pressure.
- Fabrication of prestressed concrete I-beams with the selected replacement levels. The beams will be internally monitored with strain gauges adhered to the prestressing strands and externally monitored with load cells continuously registering the prestressing force.
- Determination of transfer length measuring the strain values with DEMEC points, adhered to bottom flange of the beam along the first 1500 mm.
- Determination of the strand end slips at transfer with linear displacement sensors attached to the strands.
- Determination of the bond stress loss through pull-out tests.
- Determination of development length subjecting the beams to flexural tests at different embedment lengths. This tests will be controlled by displacement, the load applied by the actuator and deflection at mid-span will be monitored, strains will be measured with strain gauges on the concrete surface and strands slips registered during the test. All of them synchronized and registered with a data acquisition device.

The data obtained from both parts will be processed and deeply analysed. If the final results are positive, an increase in the 20% limit established by the EHE-08 has to be considered, as well as the incorporation of the fine recycled fraction in structural concrete.

Chapter 3. Reinforced Concrete Beams

3.1. Introduction

After analysing the studies on the use of fine and coarse recycled concrete aggregates, it was decided to perform an experimental program with a self-compacting concrete. For this study, different percentages of the total amount of natural aggregates were replaced by high-quality recycled aggregates, including fine and coarse fraction, and fresh and hardened properties were compared among the different replacement levels. The resulting recycled concrete was utilised for the fabrication of reinforced concrete beams.

3.2. Materials

The materials used for the present study were provided by a nearby precast plant and are usually employed by this plant for the fabrication of precast elements. A detailed study was performed in the laboratory in order to analyse their properties and design a good mix composition.

The following materials were used in this study:

- Cement CEM-I 52.5 N/SR. (Cementos COSMOS)
- Limestone filler.
- Natural quartzite sand: 0/2.5 mm (NA-1 0/2.5) and 0/5 mm (NA-1 0/5) fractions (Figures 3.1 and 3.2).
- Natural granite gravel: 6/12 mm fraction (NA-1 6/12) (Figure 3.3).
- Recycled concrete aggregate: 0/12 mm fraction (RCA-1 0/12) (Figure 3.4).
- Sika Visocrete 20 HE superplasticizer.

The recycled concrete aggregate for this study was obtained from the existing waste of the precast plant: structures and member that were rejected or not sold with a compressive

strength between 35 and 45 MPa. These elements were taken to a construction and demolition waste (CDW) plant for recycling, where they were crushed, removed from impurities and sieved. After this process, the recycled aggregates were taken again to the precast plant. So, it is a high-quality recycled aggregate.

Figure 3.1. NA-1 0/2.5

Figure 3.2. NA-1 0/5

Figure 3.3. NA-1 6/12

Figure 3.4. RCA-1 0/12

The following properties were analysed for the materials used in this study:

- Particle size distribution
- Particle density and water absorption
- Particle shape. Flakiness index
- Resistance to fragmentation
- Classification of the constituents of coarse recycled aggregate
- Chemical composition

Particle size distribution

The particle size distribution of the aggregates was determined following the procedure of the UNE-EN 933-1:2012 and UNE-EN 933-2/1M:1999 Standards. The results are shown in Table 3.1 and Figure 3.5.

Table 3.1. Particle Size Distribution

	Percentage passing (by weight) (%)			
Sieve size (mm)	**NA-1 0/2.5**	**NA-1 0/5**	**NA-1 6/12**	**RCA-1 0/12**
0.063	1.9	1.5	0.4	3.6
0.125	3	5	1	6
0.25	10	17	1	9
0.5	33	41	1	13
1	62	63	2	17
2	90	80	3	24
2.5	96	84	-	-
4	100	92	4	41
5	100	96	5	53
5.6	100	98	6	56
6.3	100	100	12	68
8	100	100	35	84
10	100	100	86	98
11.2	100	100	99	100
12.5	100	100	100	100
14	100	100	100	100
16	100	100	100	100
20	100	100	100	100
25	100	100	100	100
31.5	100	100	100	100
63	100	100	100	100
Percentage of fines passing the 0,063 mm sieve (%)	1.9	1.4	0.5	3.7

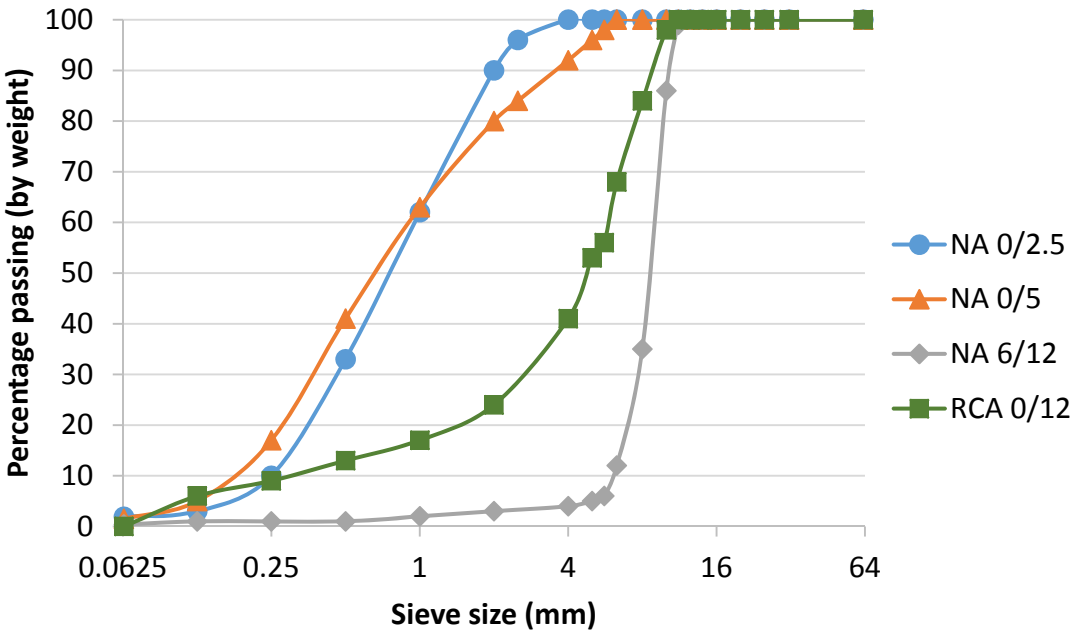

Figure 3.5. Particle size distribution

Particle density and water absorption

The particle density and water absorption of the aggregates was determined following the procedure of the UNE-EN 1097-6: 2001/A1:2006 Standard. The results are shown in Table 3.2.

Table 3.2. Particle density and water absorption

	NA-1 0/2.5	NA-1 0/5	NA-1 6/12	RCA-1 0/12
Bulk density of particles (ρa) Mg/m³	2.79	2.90	2.62	2.56
Density of particles after oven drying (ρrd) Mg/m³	2.74	2.88	2.55	2.21
Density of particles in saturated surface-dry condition (ρssd) Mg/m³	2.76	2.88	2.58	2.35
Water Absorption (WA24) %	0.7	0.3	1.0	6.06

It is important to highlight that the water absorption of the recycled aggregates is more than 6 times higher than the absorption of the natural aggregates. Therefore, it is an important factor to consider when designing the mix composition.

Particle shape. Flakiness index

The particle shape test to obtain the flakiness index of the recycled aggregate was performed following the UNE-EN 933-3:2012 Standard. The result is shown in Table 3.3.

Table 3.3. Particle shape test

Gravel	Flakiness index (%)
RCA-1 0/12	5

Resistance to fragmentation

The resistance to fragmentation of the recycled aggregate was calculated following the UNE-EN 1097-2:2010, which proposes Los Angeles abrasion test. A coefficient obtained after the test indicates the abrasion resistance of the aggregate. The value obtained is shown in Table 3.4.

Table 3.4. Resistance to fragmentation

Gravel	L.A. Coefficient
RCA-1 0/12	38

Classification of the constituents of coarse recycled aggregate

The classification of the constituents of the concrete recycled aggregate was performed following the procedure of the UNE-EN 933-11:2009/AC:2010 Standard. The results of the test are shown in Table 3.5.

Table 3.5. Classification of the constituents

Constituents	Description	RCA-1 0/12
FL (cm^3/kg)	Floating material	0.35
Rc (%)	Concrete, concrete products, mortar	93
Ru (%)	Unbound aggregate, natural stone	6.7
Rb (%)	Clay masonry units (bricks and tiles)	0
Ra (%)	Bituminous materials	0
Rg (%)	Glass	0
X (%)	Other: Cohesive (clay and soil), Miscellaneous: metals, non-floating wood and rubber, Gypsum plaster	0.1

The results in Table 2 show that almost all of the particles could be classified as Rc or Ru, as expected.

Chemical composition

Table 3.6 shows the chemical analysis results from X-ray fluorescence for all of the materials that were used for this study.

Table 3.6. Chemical composition of the materials (wt. %)

Component	Cement	Filler	NA-1 0/2.5	NA-1 0/5	NA-1 6/12	RCA-1 0/12
CaO	65.5	55.4	0.031	0.031	1.2	16.0
SiO_2	18.6	1.3	97.5	97.5	67.8	53,2
Fe_2O_3	4.7	0.25	0.40	0.40	2.3	2.1
SO_3	3.6	0.11			0.03	0.74
Al_2O_3	3.0	0.53	1.2	1.2	15.9	8.3
MgO	0.79	0.58			0.70	0.82
K_2O	0.65	0.11	0.14	0.14	6.0	3.1
Na_2O	0.45				3.8	1.2
TiO_2	0.31		0.094	0.094	0.35	0.26
ZnO	0.14	0.009	0.009	0.009	0.012	0.012
P_2O_5	0.12				0.26	0.15
CuO	0.089	0.011	0.004	0.004	0.008	0.008
SrO	0.082	0.029			0.015	0.153
MnO	0.042	0.028			0.055	0.033
Cl	0.042					
MoO_3	0.021					
ZrO_2	0.011	0.002	0.008	0.008	0.020	0.018
CO_2		41.6				
Rb_2O					0.051	0.025
LOI	1.7		0.31	0.31	1.3	13.4

The Spanish Code on Structural Concrete [EHE 08] establishes a series of requirements that the coarse aggregates should meet in order to achieve an appropriate concrete strength and durability. These requirements and the values obtained for the recycled aggregate used in this study are compared in Table 3.7.

Table 3.7. Aggregates Requirements

Property	Requirement	RCA-1 0/12
Fines content (< 0,063 mm) (%)	≤ 1,5	3.6
Sand content (< 4 mm) (%)	≤ 5	41
Flakiness index (%)	≤ 35	5
Los Angeles Coefficient	≤ 40	38
Water absorption (%)	≤ 5	6.06
Lightweight particles content (%)	≤ 1	0
Ceramic material content (%)	≤ 5	0
Asphalt content (%)	≤ 1	0
Other materials (glass, plastic, metal, etc.) (%)	≤1	0

As can be observed, RCA-1 0/12 does not meet all the established requirements. Fines content, sand content and water absorption are higher than the recommended values in the EHE 08. The reason for a high sand content, was the state of the aggregate before the sieving process in the CDW plant. Just before sieving, the recycled aggregate was extremely wet because of the weather conditions. Due to this fact, most of the fine particles were adhered to the coarse particles and the sieving process was not as effective as it should, with a final content of particles < 4 mm of 41%. The final recycled aggregate is shown in Figure 3.6.

Figure 3.6. Recycled aggregate after sieving

3.3. Experimental program in laboratory

3.3.1. Mix proportions

The mix used in the precast concrete plant for self-compacting concrete elements was used as a reference in the laboratory. In this way, 4 concrete mixes were fabricated with a water-to-cement ratio (w/c) of 0.50. One of the mixed was used as a reference, without recycled aggregate (M-0), and the others with a replacement level of the total amount of aggregate by recycled aggregate of 20, 35 and 50% for M-20, M-35 and M-50, respectively.

The excessive sand content (41%) in RCA-1 0/12, in comparison to the 5% recommended by the EHE-08, presents a great problem if solely the coarse natural aggregate is replaced, since the joint particle size distribution of the mix would be modified to a large extent. Hence, the decision was taken to replace the recycled aggregate in both, the coarse natural aggregate 6/12 and the fine natural aggregate 0/5 with a proportion of 60% and 40%, respectively, of the total amount of recycled aggregate introduced in the mixture. The goal of this kind of adjustment is getting a joint particle size distribution as similar as possible to the distribution of the reference concrete (M-0) as can be seen in Figure 3.7.

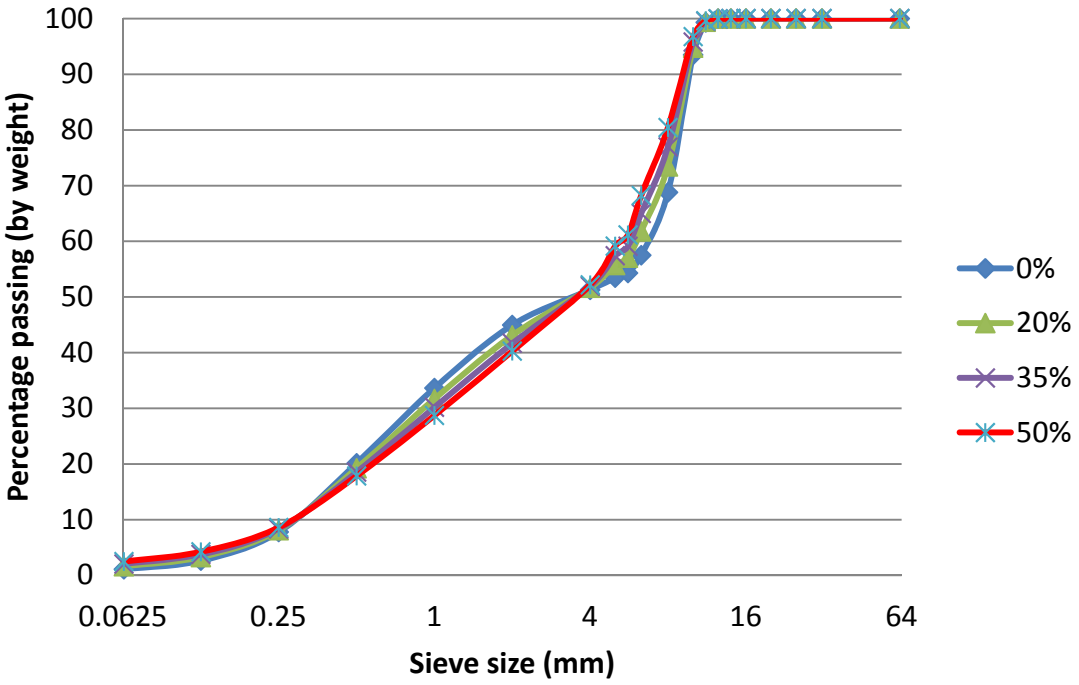

Figure 3.7. Joint particle size distribution

Due to the higher absorption of recycled aggregates compared to natural aggregates, the workability of the mixture is reduced. To compensate this effect, some authors such as Alaejos et al. [ALAE 2006] and even national Codes [EHE 08] propose presaturating the aggregates or put them in water for a determined time. This option is not economically

feasible in a precast plant. The other option found in the bibliography proposes adding an extra amount of water to the mixture in order to get a fixed water-to-cement content in all the substitutions studied. For most authors this value is in the range of 70-100% of the water necessary to saturate the recycled aggregate [ALAE 2011, MEDI 2014, FONS 2011, MART 2012]; in this particular case, it was decided to consider the 100%. Even so, it was also necessary to increase the amount of superplasticiser in M-35 and M-50 mixes to achieve similar workability to the previous substitutions. The mix proportions for each replacement level are shown in Table 3.8 and the corresponding replacement level for each fraction, fine and coarse, are shown in Table 3.9.

Table 3.8. Mix proportions of reinforced concrete beams

	M-0 (Kg/m^3)	**M-20** (Kg/m^3)	**M-35** (Kg/m^3)	**M-50** (Kg/m^3)
CEM-I 52.5 N/SR	335	335	335	335
Limestone filler	320	320	320	320
NA-1 0/2.5	370	370	370	370
NA-1 0/5	510	375	273	172
NA-1 6/12	810	607	455	303
RCA-1 0/12	0	338	592	845
Water	167.5	167.5	167.5	167.5
Extra water	0	20.1	36.85	50.25
Superplasticizer	5,4	5.4	6.0	6.0
Effective w/c	0.50	0,50	0.50	0.50
w/c	0.50	0.56	0.61	0.65

Table 3.9. Replacement ratios of reinforced concrete beams

	M-20	**M-35**	**M-50**
% recycled aggregate with respect to total amount of aggregate	20	35	50
% recycled fine aggregate with respect to total amount of fine aggregate	15.7	27.4	38.9
% recycled coarse aggregate with respect to total amount of coarse aggregate	24	43.2	62.1

3.3.2. Mixing procedure and casting

For each of the mix proportions, it was decided to fabricate a batch of 60 litres with the aim of having enough concrete to perform the slump-flow test and to cast 10 cylinders 150 x 300

mm cm for the mechanical tests. The previous day to the concrete fabrication, the water content of each of the materials was determined following the UNE-EN 1097-5: 2009 Standard, and the amount of water that would be added to the mix was adjusted in order to have the desired mix proportions.

The mixing was made in a vertical axis mixer with two mixing blades. The mixing procedure for each of the replacement levels was as follows:

1. Moisten the mixer with a wet cloth.
2. Add natural sand and mix for 30 seconds.
3. Add filler and mix for 60 seconds (Figure 3.8).
4. Add cement and mix for 60 seconds (Figure 3.9).
5. Add coarse natural aggregate and recycled aggregate, and mix for 60 seconds (Figure 3.10).
6. Without stopping the mixer, add water slowly for 30 seconds and mix for 60 seconds.
7. Without stopping the mixer, add the superplasticiser slowly for 30 seconds and mix the necessary time until the power consumed by the mixer will be stabilized (Figure 3.11).

Figure 3.8. Filler incorporation

Figure 3.9. Cement incorporation

Figure 3.10. Coarse aggregates incorporation

Figure 3.11. Mix completed

Immediately after mixing the materials, the slump-flow test was performed according to the UNE-EN 12350-8:2011 Standard to evaluate the workability of the mixture. The cylinders were cast following the UNE-EN 12390-2:2009 Standard (Figure 3.12) and kept inside an environmental chamber between 16 hours and 3 days before demoulding. The curing conditions inside the chamber are 20±2 °C temperature and relative humidity higher than 95%. After demoulding (Figure 3.13), the samples continued inside the environmental chamber for an appropriate curing until the age of testing.

Figure 3.12. Fresh concrete samples

Figure 3.13. Demoulded samples

3.3.3. Fresh and hardened properties

For each of the mixes analysed, the workability through the slump-flow test was studied in order to evaluate the fresh state properties; and the density, compressive strength, splitting tensile strength and elastic modulus were studied to evaluate the hardened state properties.

Workability

The slump-flow test was performed according to the UNE-EN 12350-8:2011 Standard to assess the viscosity and flowability of the concrete mix. In this test, when the cone is lifted, the SCC spreads out on a base plate of at least 900 x 900 mm. The longest diameter (D) of the spread and the perpendicular diameter to that one (d) are measured to obtain a mean value (Figures 3.14 and 3.15), which is an indicative of the concrete flowability.

Figure 3.14. Slump-flow test (D)

Figure 3.15. Slump-flow test (d)

The measured values for the different mixes are shown in Table 3.10.

Table 3.10. Slump-flow test

Mix	Slump-flow (mm)	Δ (%)
M-0	620	
M-20	695	12.1
M-35	630	1.6
M-50	610	-1.6

As observed in Table 3.10, the slump-flow increases by 12% for 20% replacement of the total aggregate, keeping the same proportion of superplasticiser (5.4 kg/m^3) and increasing the water content to compensate the absorption of the recycled aggregates. However, no flow-segregation was noticed. This may be due to the higher initial free water content. However, for the remaining replacement levels, the slump-flow value is similar to the value obtained for the reference concrete M-0, even having increased the proportion of superplasticiser to 6 kg/m^3. The reason may be that the effect of water absorption of the recycled aggregates on the flowability is more noticeable for higher replacement levels.

Density

The mean density of hardened concrete was measured following the UNE-EN 12390-7:2009 Standard for all the cylinders at the age of 28 days. The measured values are shown in Table 3.11.

Table 3.11. Mean density

Mix	Mean density (Kg/m^3)	Δ (%)
M-0	2274	
M-20	2250	-1.0
M-35	2248	-1.1
M-50	2244	-1.3

As expected, the mean density of hardened concrete slightly decreases as the replacement level increases because of the lower particle density of the recycled aggregate in comparison with the natural aggregate.

Compressive strength

The compressive strength was evaluated according to the UNE-EN 12390-3:2009/AC:2011. Two cylinders were tested at 7 days and 3 samples at 28 days, calculating the mean value for each age. The mean values of the test at 28 days are shown in Table 3.12 and Figure 3.16.

Table 3.12. Compressive strength at 28 days

Mix	Compressive strength (MPa)	Δ (%)
M-0	58,8	0,00
M-20	57,2	-2,7
M-35	55,9	-4,9
M-50	56,4	-4,1

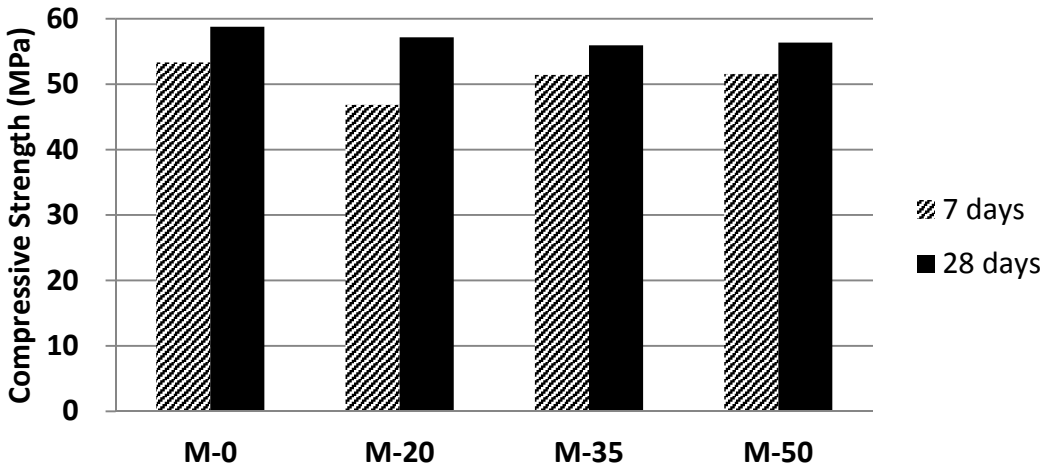

Figure 3.16. Compressive strength

The data depicted in Figure 3.16 indicate that the compressive strength at 28 days slightly decreases when the natural aggregate is replaced by the recycled aggregate. It decreases by 2.7, 4.9 and 4.1% for 20, 35 and 50% replacement, respectively. This decrease is negligible considering that half of the total aggregate is substituted in M-50.

Splitting tensile strength

The splitting tensile strength was tested following the UNE-EN 12390-6:2010 Standard. Three cylinders were tested at the age of 28 days and the mean value is shown in Table 3.13 and Figure 3.17.

Table 3.13. Splitting tensile strength

Mix	Splitting tensile strength (MPa)	Δ (%)
M-0	4.3	
M-20	4.1	-4.7
M-35	4.0	-7.0
M-50	3.9	-9.3

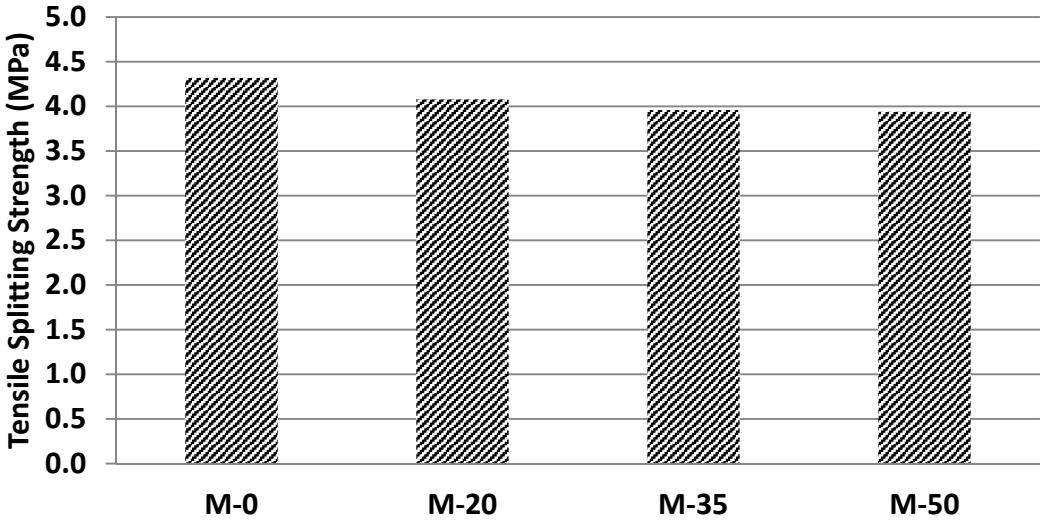

Figure 3.17. Splitting tensile strength

From the data depicted in Figure 3.17, it can be observed that the splitting tensile strength decreases as the replacement level increases, with a maximum loss of 9.3% for 50% replacement.

Modulus of elasticity

The modulus of elasticity was calculated in 2013 following the procedure of UNE 83316:1996, still valid when the modulus tests were performed. This UNE Standard became invalid in 2014 and was replaced by UNE-EN 12390-13:2014. Two cylinders were tested and the mean value was calculated. The results are shown in Table 3.14 and Figure 3.18.

Table 3.14. Modulus of elasticity

Mix	Elastic modulus (MPa)	Δ (%)
M-0	27000	
M-20	25250	-6,5
M-35	26000	-3,7
M-50	24500	-9,3

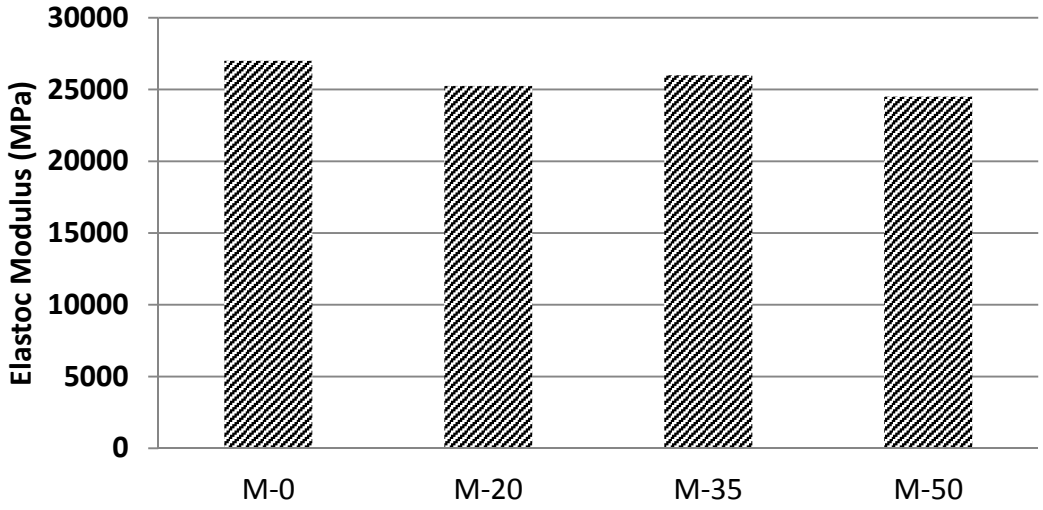

Figure 3.18. Modulus of elasticity

From the previous data, it can be concluded that the modulus of elasticity decreases as the replacement level increases, with a maximum loss of 9.3% for 50% replacement. The loss is similar to that obtained in the splitting tensile strength.

3.3.4. Results and discussion

The following conclusions can be drawn from the experimental program performed in laboratory to evaluate the properties of the self-compacting recycled concrete used for the fabrication of the reinforced beams:

- All recycled concretes showed enough fluidity at a fixed water-to-cement content 0.50. For M-20 mix, the slump-flow increased 12% but no flow-segregation was noticed. This increase in the slump flow diameter may be due to the higher initial free water content and agrees with the results obtained for self-compacting concrete by Kou and Poon [KOU2009b]. For the remaining substitutions (M-35 and M-50) the measured value was in the order of the reference concrete M-0 (620 mm). These results agree with the results obtained by Grdic et al. [GRDI 2010] and Tang [TANG 2013].
- The density of hardened concrete decreased up to 1.3% for 50% replacement of the total aggregate. It is expected since the density of the recycled aggregate is lower than that of the natural aggregate. All of authors who studied this property reached the same conclusion. Khatib [KHAT 2005] and Chan and Poon [CHAN 2013] registered weight losses up to 4% and 3.6%, respectively, when the total content of sand is replaced in vibrated concrete. On the other hand, Grdic et al [GRDI 2010] registered a decrease of 3.4% with full replacement of coarse aggregate in self-compacting concrete.
- The compressive strength slightly decreased by 2.7, 4.9 and 4.1% for 20, 35 and 50%, replacement of the total natural aggregate, respectively. This loss of strength agrees

with the results obtained for vibrated concrete by Chan and Poon [CHAN 2013] who noticed that the strength of the concrete mixtures decreased 12% as the replacement ratio of FRA increased from 0 to 100%; Mardani-Aghabaglou et al. [MARD 2014] with a decrease of 0.6, 1.8, 4.2 and 7.6% with a replacement of 15, 30, 45 and 60% of FRA, respectively; and Jang and Yun [JANG 2014] who noticed a strength loss of 13% and 8% for 100% and 75% replacement of FRA, respectively. With regard to self-compacting concrete, the strength loss agrees with the results obtained by Kou and Poon [KOU 2009b] who noticed that at replacement levels of 75% and 100% FRA, the compressive strength was approximately 10% lower than that of the control mix; Grdic et al. [GRDI 2010] observed losses of 4% with 50% replacement and by 9% with full replacement of CRA; and Kim et al. [KIM 2011] noticed that the compressive strength at 28 days increased 7% for 25% FRA replacement and reduced 2, 5 and 10% for 50, 75 and 100% FRA replacement, respectively.

- The splitting tensile strength decreased up to 9.3% for 50% replacement of the total aggregate content. The loss of splitting tensile strength agrees with the results obtained by several authors. Grdic [GRDI 2010] noticed losses of 2.5% and 14% for 50% and 100% replacement, respectively, of the coarse natural aggregate in self-compacting concrete. Mardani-Aghabaglou et al. [MARD 2014] registered losses up to 7.6% for 60% replacement of the natural sand in vibrated concrete. Other authors registered higher losses by 25-35% [PERE 2012a, KHOS 2014, BRAV 2015a, KHAF 2014 and GESO 2015b] when fine and/or coarse natural aggregate is fully replaced.
- The modulus of elasticity decreased as the replacement level increased, with a maximum loss of 9.3% for 50% replacement. The loss is similar to that obtained in the splitting tensile strength. These results agree with the values obtained by Pereira et al. [PERE 2012b] for vibrated concrete, with losses between 9.5 and 17% when the fine natural aggregate is fully replaced. However, they are lower than the obtained for self-compacting concrete by Corinaldesi and Marconi [CORI 2009b] with values 20% lower than the reference concrete; and Gesoglu et al. [GESO 2015b] with values 13-18% lower in Series II (100% CRA), 23-25% lower in Series III (100% FRA) and 28-34% lower in Series IV (100% CRA and FRA).

Considering that the properties of this concrete are not badly affected by the simultaneous replacement of this type of fine and coarse concrete recycled aggregates, it might be concluded that it is feasible to replace up to 50% of the total amount of natural aggregate by this particular recycled aggregate. However, it would be interesting to perform durability tests in order to evaluate the long-term behaviour.

3.4. Experimental program in precast plant

This experimental part was performed in the precast plant which provided the materials for the current study. Fifteen beams were fabricated with the studied recycled self-compacting concrete and replacement levels of 0, 10, 20, 35 and 50% of the total aggregate (three beams with each mix). Ten of the beams were fabricated with a higher shear reinforcement ratio and subjected to flexural behaviour tests (5 beams were tested in the precast plant and the other 5 in the Centro de Innovación Tecnolóxica en Edificación e Enxeñería Civil (CITEEC)). The five beams with a lower shear reinforcement ratio were subjected to shear tests in the precast plant.

3.4.1. Geometry and reinforcement layout

The reinforced concrete beams were fabricated in the precast plant according to the geometry and reinforcement layout designed by CIMARQ S.L. (Figures 3.19 to 3.22). For each replacement level, 2 beams were fabricated with higher shear reinforcement (ø8/200) for flexural testing and the other beam with lower shear reinforcement (ø8/600) was fabricated for shear testing.

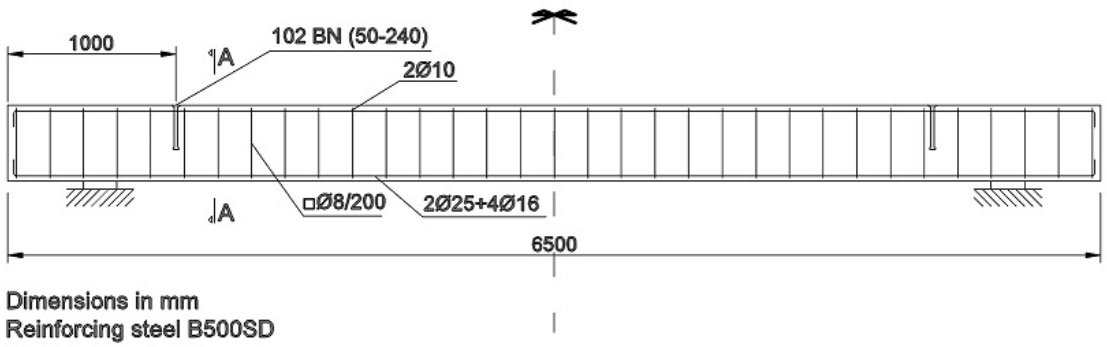

Figure 3.19. Geometry and reinforcement layout for flexural behaviour test beams

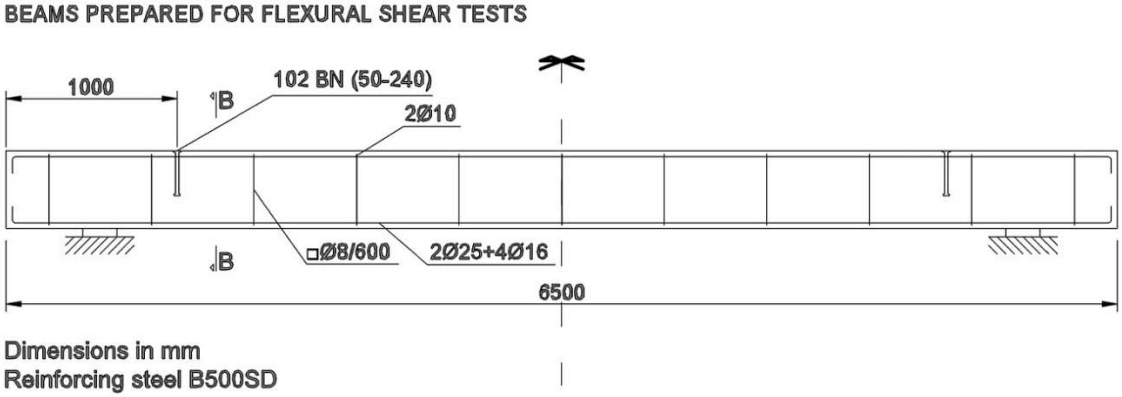

Figure 3.20. Geometry and reinforcement layout for shear behaviour test beams

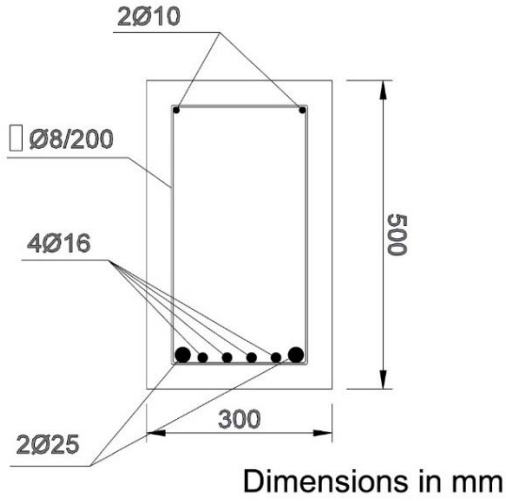

Figure 3.21. Flexural cross-section A-A

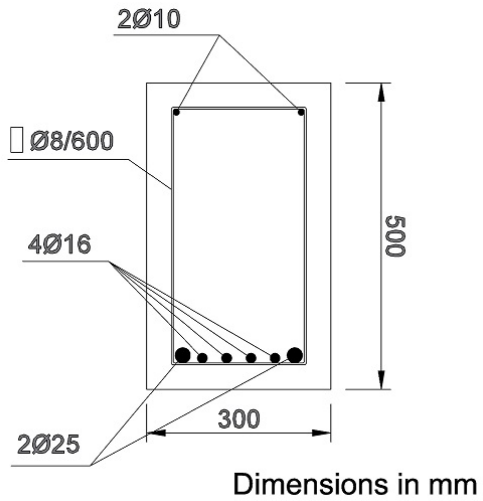

Figure 3.22. Shear cross-section B-B

The reinforcing steel supplied by the manufacturer fulfilled the requirements demanded by the Spanish Code EHE (Table 3.15).

Table 3.15. EHE requirements for reinforcing steel

	B 500S D
Yield stress, f_y (MPa)	≥ 500
Ultimate stress f_s (MPa)	≥ 575
Ultimate strain, $\varepsilon_{u,5}$ (%)	≥ 16
Maximum strain, ε_{max} (%)	≥ 10.0
Elastic's modulus, E_s (GPa)	≥ 200

3.4.2.Fabrication of beams

In the precast plant, 3 reinforced concrete beams of 6.5 m were fabricated for each substitution according to the mix composition studied in the laboratory (0%, 20%, 35% and 50% replacement) and an extra mix with 10% replacement. Two batches of 0.5 m^3 were prepared in an industrial mixer (Figures 3.23 to 3.25) for each of the beams and quality control cylindrical samples were casted in order to check the compressive strength and modulus of elasticity (Figure 3.26). It is important to mention that the extra amount of water to compensate the higher water absorption of the recycled aggregate was not added to the mixture. The aim of this decision was to keep the mixing procedure followed by the workforce in the plant.

Figure 3.23. Industrial mixer

Figure 3.24. Aggregate hopper

Figure 3.25. Weighting hopper

Figure 3.26. Quality control samples

The beams were casted (Figures 3.27 and 3.28) and cured the necessary time to remove the formwork and be transported.

Figure 3.27. Flexural beam casting

Figure 3.28. Flexural beam after casting

After removing the formwork, the beams were named as “FB M-x” and “SB M-x” for higher shear reinforcement (flexural test) and lower shear reinforcement (shear test), respectively, being “x” the replacement level of recycled aggregate. Finally, they were transported to a safe place for an adequate curing until the age of testing (Figures 3.29 – 3.30).

Figure 3.29. Flexural beams

Figure 3.30. Shear beams

3.4.3.Quality control of the elements

For each of the mix compositions, nine 15x30 cm cylindrical samples were tested in order to evaluate the compressive strength at different ages (3, 7 and 28 days) and the modulus of elasticity at 28 days. Samples were kept inside an environmental chamber between 16 hours and 3 days before demoulding according to the UNE-EN 12390-2:2009 Standard. The curing conditions inside the chamber are 20±2 °C temperature and relative humidity higher than 95%. After demoulding, the samples continued inside the environmental chamber for an appropriate curing until the age of testing.

Compressive strength

The compressive strength was evaluated according to the UNE-EN 12390-3:2009/AC:2011. For each of the recycled mixes used in the flexural and shear beams tested in the precast plant and the flexural beams tested in the CITEEC, 3 cylindrical samples were tested at the age of 28 days. The mean results of the compressive strength are shown in Table 3.16 and are compared with the value obtained for the reference concrete (FB M-0).

Table 3.16. Compressive strength FB (MPa)

	28 days	Δ (%)
FB M-0	58.4	
FB M-10	60.0	2.7
FB M-20	61.8	5.8
FB M-35	59.4	1.7
FB M-50	56.6	-3.1

As can be observed in Table 3.16, the compressive strength shows a clear tendency to slightly increase for replacement levels up to 20% of the total aggregate. For higher substitutions (35 and 50%), the compressive strength was decreased again achieving values similar to that of the reference concrete or even 3% lower as in the case of FB M-50. These

results do not agree with the decrease observed in the laboratory for all the replacement levels. This may be caused by the lower effective water-to-cement ratio in the recycled concrete mixes, since the water absorption of the recycled aggregate was not considered in the plant. A reduced water content tends to increase the compressive strength. For higher replacement levels (35 and 50%), the influence of the poorer quality of the recycled aggregate is more noticeable on the compressive strength, counteracting the effect of a reduced water content.

Modulus of elasticity

The modulus of elasticity was calculated following the procedure of UNE 83316:1996. Two cylindrical samples were tested at 28 days for each of the recycled mixes used in the flexural beams tested in the precast plant. The results of the mean values are shown in Table 3.17 and compared with the value obtained in the laboratory for the reference concrete (M-0).

Table 3.17. Modulus of elasticity of reinforced concrete beams

	Modulus of elasticity (MPa)	Δ (%)
M-0	27000	
FB M-10	28500	5.6
FB M-20	27500	1.9
FB M-35	26000	-3.7
FB M-50	24000	-11.1

As can be observed in Table 3.17, the evolution of the modulus is similar to the trend noticed in the compressive strength. The elastic modulus increases for replacement levels up to 20% and then decreases for 35 and 50%. However, this decrease is sharper than the observed in the compressive strength, reaching values up to 11% lower than M-0 for 50% replacement.

The reason for the increase observed when 10 and 20% of the aggregate is replaced may be the same than that of the compressive strength, a reduced water content tends to increase the compressive strength and the elastic modulus. However, for higher replacement levels the detrimental effect of the recycled aggregate is more noticeable than that of the reduced water content.

3.4.4.Beam tests in the precast plant

Ten beams were subjected to a four-point bending test, with a total span length of 6.10 m loading by two symmetrical concentrated loads. Two beams were tested for each substitution percentage: the beam oriented for flexural failure (FB) with 1.50 m load spacing and higher shear reinforcement; and the beam oriented for shear failure (SB) with 3.50 m load spacing and lower shear reinforcement. Both testing schemes for FB and SB type beams

are depicted in Figures 3.31 and 3.32, respectively. Load control was applied to failure in 2 ton (19.62 kN) increments with a hydraulic actuator attached to a steel frame. This shortcoming was further solved testing the remaining beams applying displacement control. The deflection at mid-span was measured for each test with a linear displacement sensor connected to a data acquisition device. During the tests, the crack widths and crack patterns were observed and marked on the surface of the beam.

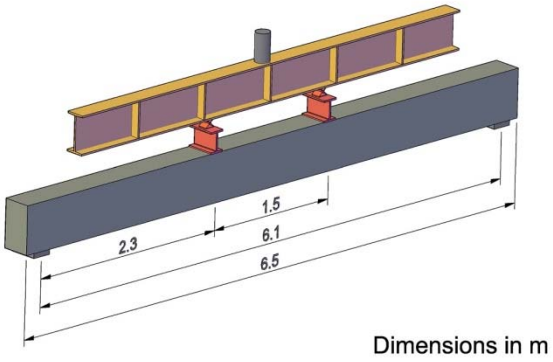

Figure 3.31. Schematic test set-up for flexural testing

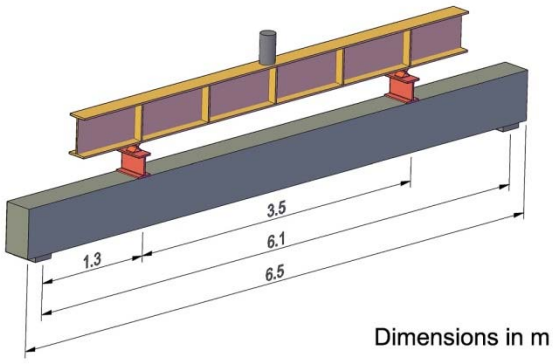

Figure 3.32. Schematic test set-up for flexural testing

3.4.4.1. Flexural behaviour tests

The results of the flexural behaviour tests for each of the mix compositions are shown in Table 3.18 and the bending moment vs. deflection diagrams at mid-span are depicted in Figure 3.33. The moment included in table and figure considers the bending moment produced by the self-weight of the beam.

Table 3.18. Load vs. Deflection in flexural behaviour tests

Load		M (m·kN)	Deflection (mm)				
ton	kN		FB M-0	FB M-10	FB M-20	FB M-35	FB M-50
0	0.0	16.1	0.00	0.00	0.00	0.00	0.00
2	19.6	38.7	0.91	0.59	1.81	1.51	1.36
4	39.3	61.2	1.31	1.61	3.72	3.42	2.98
6	58.9	83.8	2.67	3.03	5.76	4.98	5.20
8	78.6	106.4	5.91	5.55	7.56	7.31	7.90
10	98.2	129.0	8.08	9.11	9.57	10.21	10.46
12	117.8	151.6	11.76	12.78	11.52	13.43	13.52
14	137.5	174.2	13.73	14.94	13.85	16.45	15.49
16	157.1	196.8	16.35	18.15	16.10	18.71	18.53
18	176.8	219.3	18.97	21.19	18.80	21.74	21.31
20	196.4	241.9	21.73	24.73	21.48	24.30	25.04
22	216.0	264.5	23.82	26.41	23.86	27.40	27.38

24	235.7	287.1	26.21	29.44	26.33	29.82	29.42
26	255.3	309.7	28.84	32.14	29.12	32.22	31.73
28	275.0	332.3	31.62	35.19	31.98	34.66	34.63
30	294.6	354.9	34.65	38.94	34.73	38.84	39.15
32	314.2	377.4	38.05	43.59	38.31	41.50	42.70
34	333.9	400.0	42.30	58.93	43.57	43.10	48.96
36	353.5	422.6	70.55	100.61	72.77		68.71
38	373.2	445.2	-	162.61	128.00	128.00	127.71
38.5	378.1	450.9	174.14				

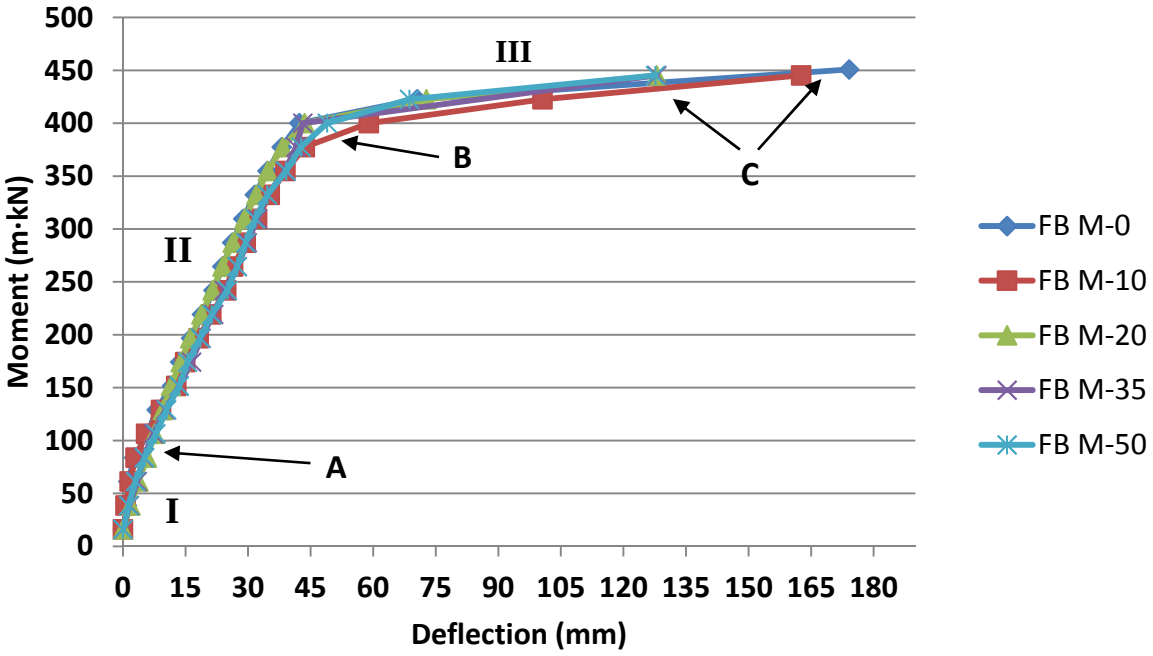

Figure 3.33. Moment vs. deflection at mid-span. Flexural behaviour test

All of the beams failed in flexure, as expected. The longitudinal tension steel yielded first, followed by the concrete crushing, which is a ductile mode of failure. In all of the cases investigated, three typical stages were identified (Figure 3.33): a first stage (I) between the start of the test and the occurrence of the first flexural crack (Point A), where all the beams displayed a steep linear elastic behaviour; a second stage (II) extended between the onset of cracking and the point of yielding (Point B); and a third stage (III) extended between yielding and failure (Point C), where concrete finally crushed in compression zone and beams failed.

As can be observed in Table 3.19, recycled aggregate concrete (RAC) beams, with the exception of FB-10 showed lower cracking moments and higher deflections than natural aggregate concrete (NAC) beam. This may be due to the lower splitting strength and the existence of two types of interfacial transition zones (ITZ) in the RAC beams. One ITZ

between natural aggregate and residual mortar in recycled aggregate and the other between residual mortar and fresh mortar, comparted with only one ITZ between the natural aggregate and the fresh mortar, in the conventional concrete beam.

Crack progression in the beams started with the appearance of the first flexural cracks in the region of maximum bending moment (mid-span). Then, additional cracks appeared between the load and the support regions and developed vertically as the load was increased. When the beam was close to failure, inclined flexure-shear cracks began to appear.

For all of the substitution percentages investigated, the ultimate bending moment did not differ from the reference value by more than 2.0%, and the yielding bending moment no more than 4.5%, which was reasonable given the effect of the concrete compressive strength on the flexural strength.

As can be observed in Table 3.19 that the deflections at mid-span at the moment of failure decreased as the substitution percentage increased, indicating a decrease in the ductility of the concrete. Specifically, when 50% of the total aggregate was replaced with recycled aggregate, the maximum mid-span deflection decreased by 27%.

Table 3.19. Values of the FB test

	FB-0	**FB-10**	**FB-20**	**FB-35**	**FB-50**
Cracking					
Bending moment at mid-span (m·kN) (M_{cr})	85	85	80	80	75
Deflection at mid-span (mm) (δ_{cr})	3	3	5	5	5.5
Yielding					
Bending moment at mid-span (m·kN) (M_y)	393	376	381	399	386
Deflection at mid-span (mm) (δ_y)	41	44	40	43	45
Failure					
Bending moment at mid-span (m·kN) (M_u)	450.0	444.3	444.3	444.3	447.3
Deflection at mid-span (mm) (δ_u)	174.1	162.6	> 128	> 128	127.7
Ductility ratio	4.25	3.70	> 3.2	> 2.98	2.84

The ductility ratio is defined as the ratio of the deflection at the ultimate load (δ_u) to the deflection at the yield of the reinforcement (δ_y). Meli [MELI 2010] also defined the ductility ratio as the quotient between the final strain and the elastic deformation of the material. The ductility ratio diminished as the content of recycled aggregate increased. For 50% replacement of the total aggregate, it decreased up to 33%.

In Figure 3.34 the yielding and ultimate bending moment are depicted for each tested beam. The theoretical ultimate bending moment was estimated for the average experimental concrete strengths obtained for each concrete batch, as well as the average properties of steel reinforcement, without applying any safety coefficient. As can be observed in figure, both the theoretical yielding bending moment and the theoretical ultimate bending moment are on the safe side with respect to their respective experimental results, for all the tested beams.

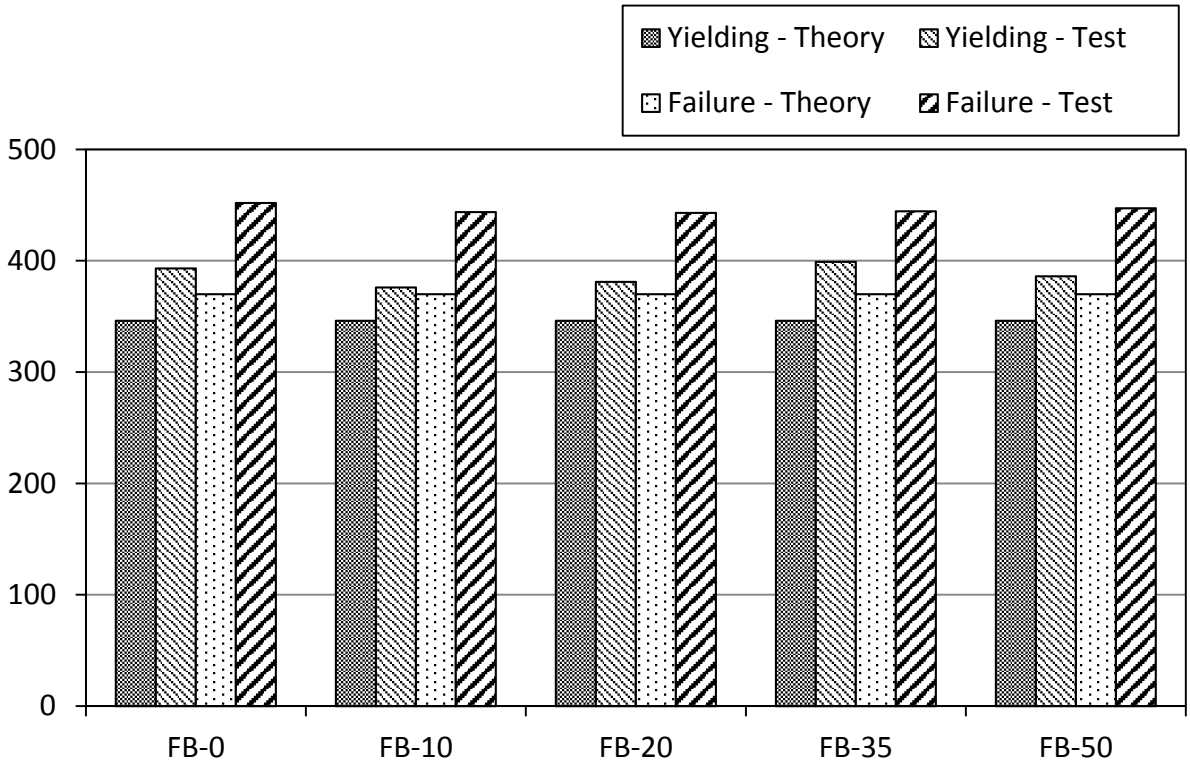

Figure 3.34. Theoretical vs. experimental yielding and failure moments

Different images of the flexural test performed for the different beams are shown in Figures 3.35 to 3.40.

Figure 3.35. Flexural test set-up

Figure 3.36. Linear displacement sensor for measuring deflection

Figure 3.37. FB M-0 Flexural failure

Figure 3.38. FB M-10 Flexural failure

Figure 3.39. FB M-35 Flexural failure

Figure 3.40. FB M-50 Flexural failure

3.4.4.2. Shear behaviour tests

The results of the flexural behaviour tests for each of the mix compositions are shown in Table 3.20 and the shear strength at support, which is the point that experiments the maximum shear force, vs. deflection at mid-span, are depicted in Figure 3.41. The moment

and shear strength included in table and figure consider the bending moment and shear, respectively, produced by the self-weight of the beam.

Table 3.20. Load vs. Deflection in shear behaviour tests

Load		V (kN)	M (m·kN)	Deflection (mm)				
ton	kN			SB M-0	SB M-10	SB M-20	SB M-35	SB M-50
0	0.0	11.4	16.0	0.00	0.00	0.00	0.00	0.00
2	19.6	21.2	28.8	0.11	0.51	0.63	0.35	0.40
4	39.3	31.0	41.5	1.12	0.94	-	-	0.73
4.3	42.2	32.5	43.4	-	-	-	1.11	-
4.5	44.2	33.5	44.7	-	-	1.88	-	-
6	58.9	40.8	54.3	1.84	2.53	-	-	1.43
6.3	61.9	42.3	56.2	-	-	-	1.85	-
6.5	63.8	43.3	57.5	-	-	3.25	-	-
8	78.6	50.7	67.1	2.99	4.05	4.27	-	2.48
8.3	81.5	52.1	69.0	-	-	-	2.93	-
10	98.2	60.5	79.8	4.29	6.34	-	4.02	4.05
10.5	103.1	62.9	83.0	-	-	6.58	-	-
12	117.8	70.3	92.6	7.34	9.13	7.83	6.93	7.25
14	137.5	80.1	105.4	9.27	12.01	9.53	8.73	10.32
16	157.1	89.9	118.1	11.26	13.83	11.31	10.93	12.53
18	176.8	99.8	130.9	13.63	16.02	13.85	12.86	14.06
20	196.4	109.6	143.7	16.33	17.58	15.48	15.05	15.95
22	216.0	119.4	156.4	17.70	19.89	17.99	16.88	-
23	225.9	124.3	162.8	-	-	-	-	18.99
24	235.7	129.2	169.2	19.82	22.31	-	18.35	20.38
24.5	240.6	131.7	172.4	-	-	20.06	-	-
26	255.3	139.0	182.0	21.93	24.15	21.71	20.08	22.31
28	275.0	148.9	194.7	23.36	26.28	23.30	22.51	24.28
30	294.6	158.7	207.5	24.85	28.51	-	24.56	27.36
30.5	299.5	161.1	210.7	-	-	26.45		
32	314.2	168.5	220.3	27.20	30.89			

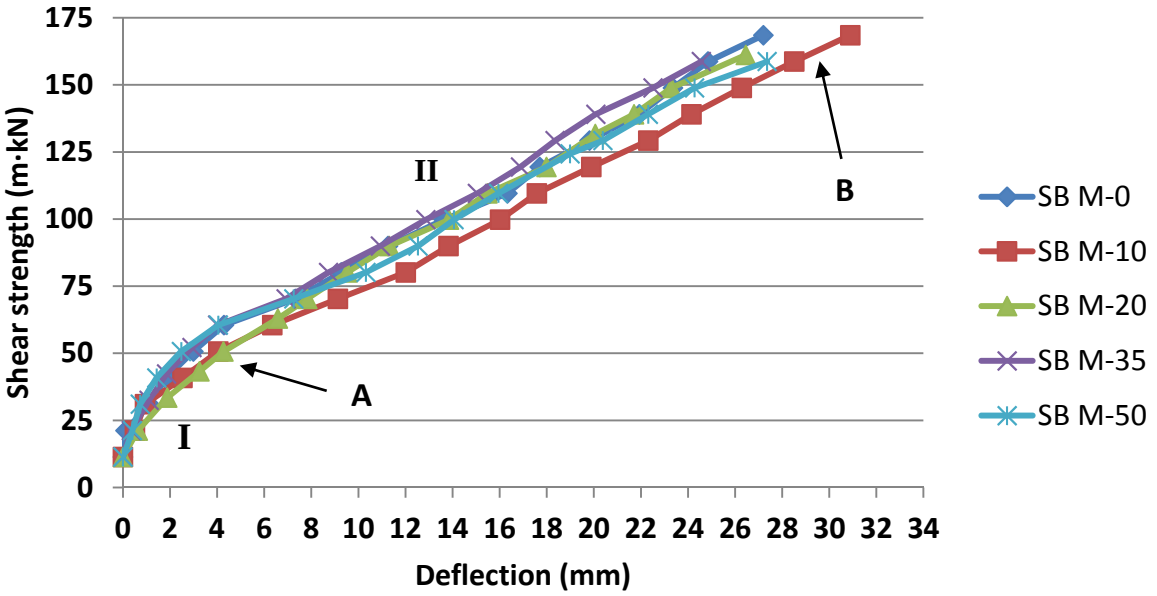

Figure 3.41. Shear strength at support vs. deflection at mid-span. Shear behaviour tests

The shear test results showed a brittle bond-shear failure for all of the substitutions investigated. In all of the cases, two typical stages were identified (Figure 3.41): the first stage (I) between the start of the test and the occurrence of the first flexural crack (Point A), where all the beams displayed a steep linear elastic behaviour; the second stage (II) extended linearly with a lower slope between the onset of cracking and shear failure (Point B), where concrete finally failed abruptly.

Crack progression in the beams started with the appearance of the first flexural cracks in the region of maximum bending moment (mid-span). Then, additional cracks appeared between the load and the support regions developing vertically as the load was increased. When the beams were close to failure, inclined flexure-shear cracks began to appear and a bigger shear crack was observed at the moment of failure.

As can be observed in Table 3.21, the substitution of natural aggregate by recycled aggregate decreased the cracking shear by 17% for all the replacement levels. The corresponding cracking deflection was also decreased by 41% for the highest replacement levels (SB-35 and SB-50). The ultimate shear for beam SB-10 was practically the same as that for the reference beam (SB-0) and the corresponding deflection was slightly higher. However, increasing the substitution percentage beyond 20% led to a slight decrease of the ultimate shear by 4-6%, with corresponding deflections similar to that obtained in the beam without recycled aggregate.

Table 3.21. Values of the SB test

	SB-0	SB-10	SB-20	SB-35	SB-50
Cracking					
Shear at support (kN) (Vr)	60	50	50	50	50
Deflection at mid-span (mm)	4.3	4.1	4.3	2.6	2.5
Failure					
Shear at support (kN) (Vr)	167.7	167.6	160.5	158.1	157.8
Deflection at mid-span (mm)	27.2	30.9	26.5	24.6	27.4

As in the previous case, the theoretical ultimate shear was determined and compared to the experimental results (see Figure 3.42).

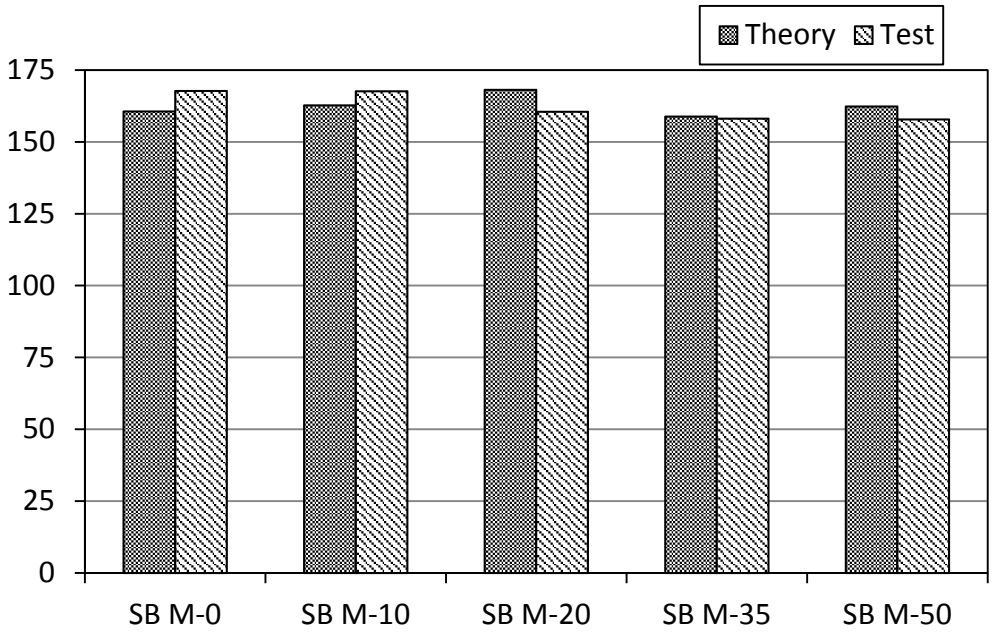

Figure 3.42. Theoretical vs. experimental shear failure

Analysing these values it can be seen that for a total aggregate replacement of 20% or more, the experimental value of ultimate shear is slightly smaller (at most 5%) than the theoretical prediction. Therefore, considering all the above results, the experimental ultimate shear, for beams with a replacement level between 10 and 50%, is approximately 95% of the theoretical ultimate shear obtained for the reference concrete beams.

Different images of the shear test performed for the different beams are shown in Figures 3.43 to 3.50.

Figure 3.43. Shear test set-up

Figure 3.44. Linear displacement sensor

Figure 3.45. SB-0 Shear crack

Figure 3.46. SB-0 Bond-Shear failure

Figure 3.47. SB-10 Shear crack

Figure 3.48. SB-10 Bond-Shear failure

Figure 3.49. SB-35 Bond-Shear failure

Figure 3.50. SB-50 Shear crack

3.5. Flexural behaviour tests in the CITEEC

The remaining five beams with higher shear reinforcement ratio were transported from the precast plant to the CITEEC and subjected to a flexural test controlled by displacement. The aim of this test was to obtain more information from the flexural tests such as the strains on concrete surface, deflections after the yielding point and deflections during the recovery of the beam after failure so as to delve into the post-peak behaviour and ductility.

The beams were again subjected to a four-point bending test, but in this case with a total span length of 5.70 m loading by two symmetrical concentrated loads. Schemes for the tests are depicted in Figures 3.51 and 3.52. The flexural test equipment was designed and used on previous research [VAZQ 2001, 2013a, 2013b and 2013c]. The load was applied to failure with a hydraulic actuator attached to a steel frame. The actuator was controlled by displacement with a 250 mm wire linear potentiometric transducer attached to the actuator and to the distribution beam. The displacement rate of the test was fixed to 0.05 mm/s. The deflection at mid-span was measured for each test with a 500 mm wire linear potentiometric transducer and the strains on both sides of the beam in two sections were measured with strain gauges fixed to the concrete surface. These gauges were used to calculate the curvature of the beam at every time of the test. The curvature is obtained as the slope of the line that joins the strain values of the gauges belonging to the same section [VAZQ 2001]. The force transmitted to the beam was measured with two load cells, each one placed between the beam and the corresponding support. Wire linear potentiometric transducers, load cells and strain gauges were all connected to the data acquisition device registering the measures every 0.1 s. During the tests, the crack widths and crack patterns were observed and marked on the surface of the beam for a later analysis.

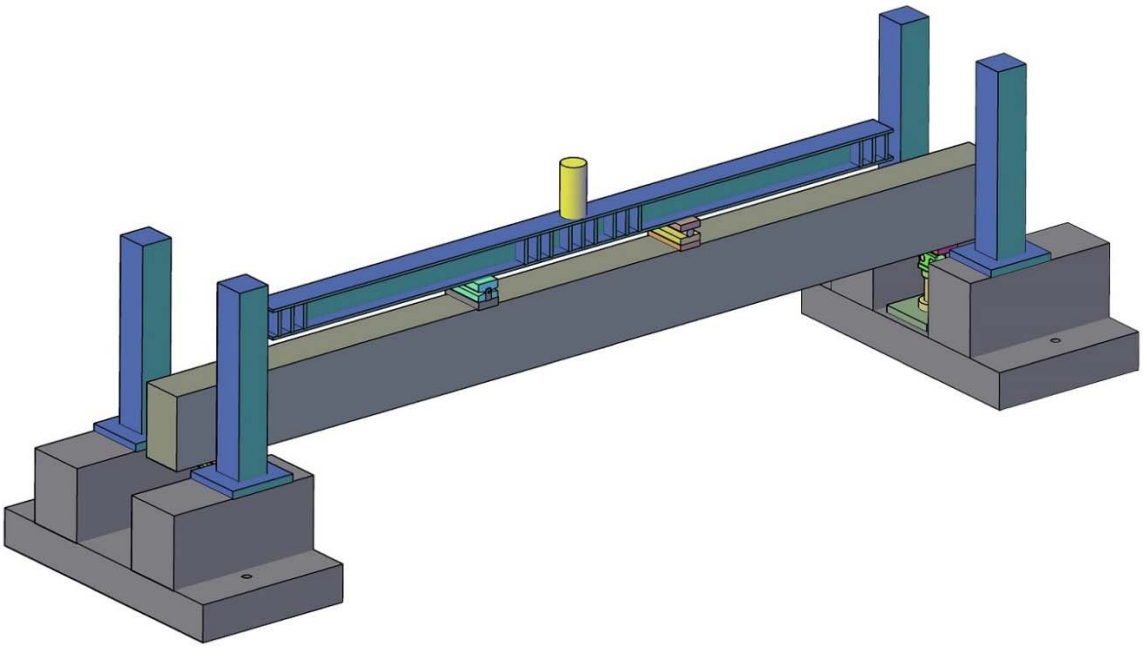

Figure 3.51. Model of flexural testing

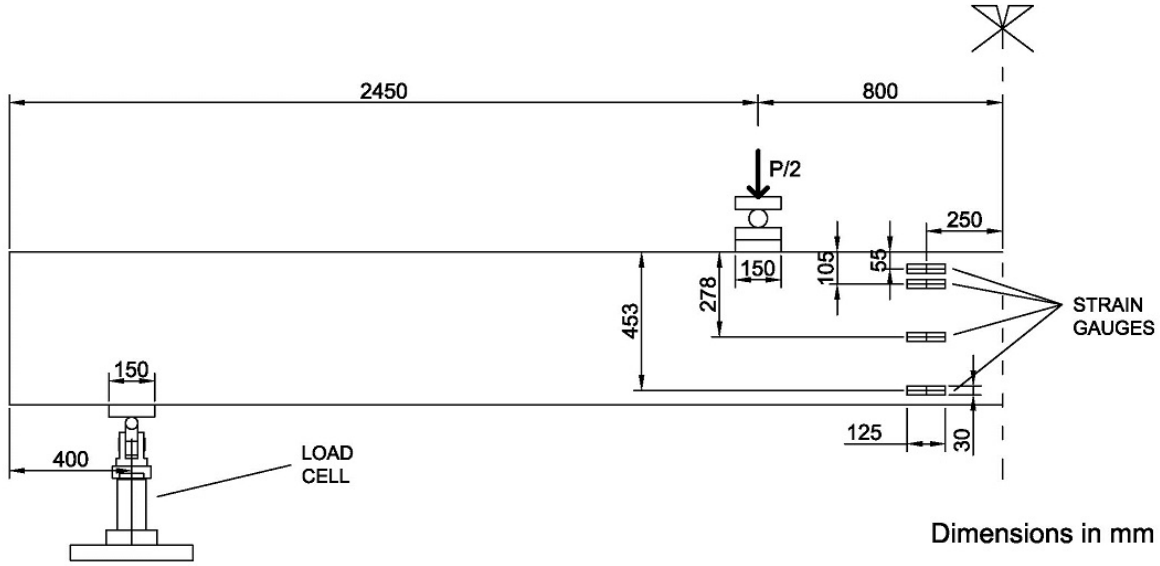

Figure 3.52. Schematic test set-up for flexural testing

The preparation of the test and disposal of the tested beam was performed according to the procedure described in Appendix 2. Different images of the flexural tests are shown in Figures 3.53 to 3.58.

Figure 3.53. Load cell

Figure 3.54. Beam ready to test

Figure 3.55. Linear potentiometric transducer attached to actuator

Figure 3.56. Linear potentiometric transducer for measuring deflections

Figure 3.57. Piece A between distribution steel profile and concrete beam

Figure 3.58. Piece B between distribution steel profile and concrete beam

3.5.1.Crack propagation and failure mode

As expected, all of the beams failed by the yielding of the reinforcement with extensive deflection, followed by the concrete crushing in the compression zone. This is a ductile mode of failure.

Crack progression in the beams started with the appearance of the first flexural cracks at mid-span in the range of 70-110 m·kN. Then, additional cracks appeared between the load

and the support regions and developed vertically as the load was increased. When the beam was close to failure, inclined flexure-shear cracks began to appear close to the supports.

The crack propagation and failure mode of all the beams are similar regardless of the replacement level of recycled aggregate.

3.5.2.Moment – deflection relationship

The bending moment vs. deflection diagrams at mid-span for each of the beams are depicted in Figures 3.59 and 3.60. The moment depicted in the figures includes the bending moment produced by the self-weight of the beams.

In FB-20 beam test, there was a problem with the hydraulic actuator setup at the beginning of the test. Therefore, the cracking moment was not appropriately registered.

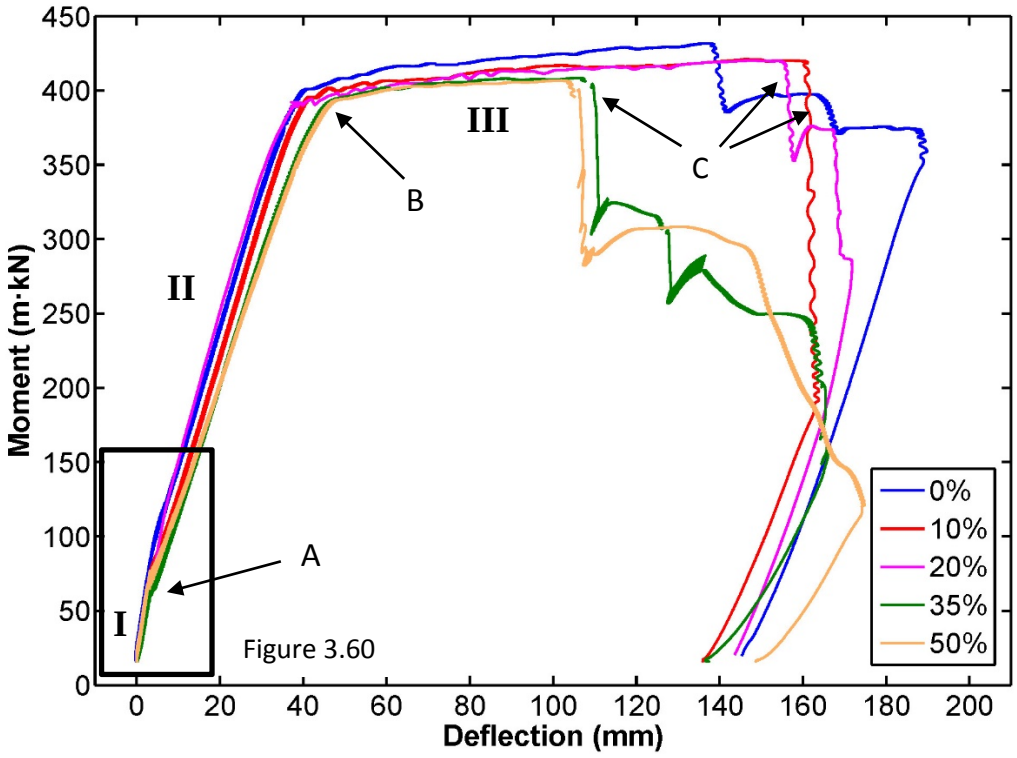

Figure 3.60

Figure 3.59. Moment vs. deflection at mid-span

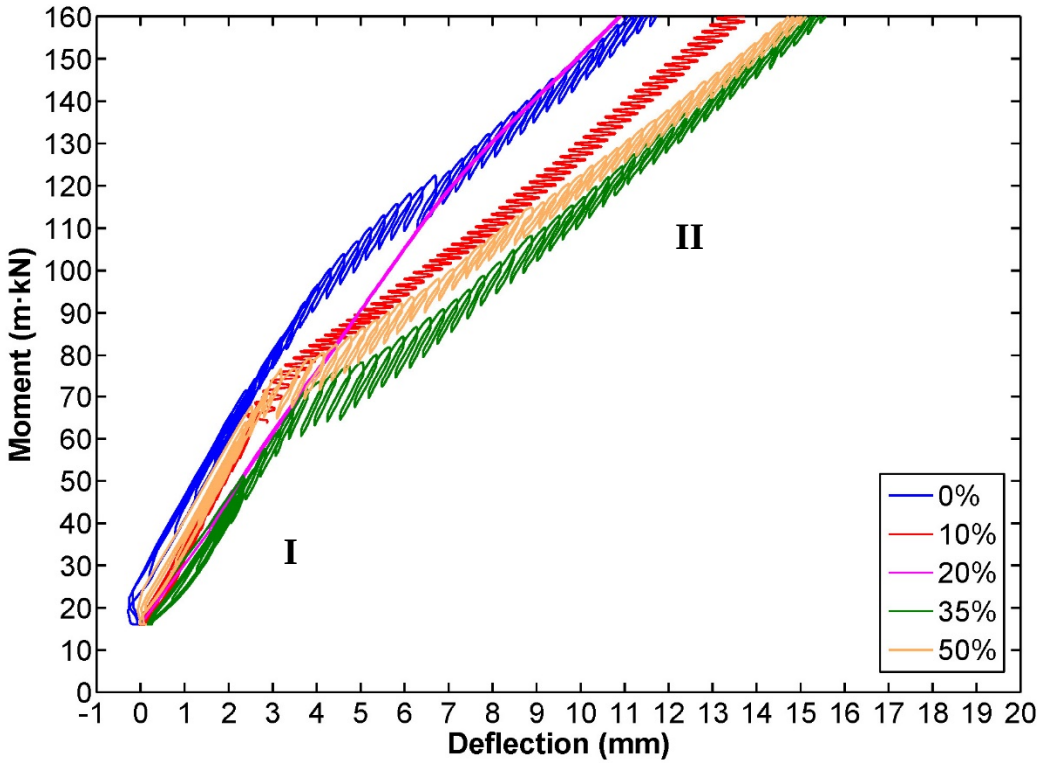

Figure 3.60. Moment vs. deflection at mid-span

In all of the cases investigated, three typical phases were again identified (Figure 3.59):

Phase I extended between the start of the test and the occurrence of the first flexural crack (Point A). In this phase, beams exhibited linear elastic behaviour due to the linear behaviour of the concrete and the passive reinforcements. Its slope is determined by concrete modulus of elasticity. The maximum moment of phase I was the cracking moment which is considerably lower for FB-35 and FB-50.

Phase II extended from the onset of cracking to the point of yielding (Point B). This phase was the cracked stage, which corresponded to the cross sectional behaviour under an increasing bending moment, for concrete already cracked in the tensioned zone of the cross section. During this phase, the bending moment increased approximately linearly with respect to the increase in the curvature (Figure 3.61) but with a much lower slope than that of phase I because of the loss of stiffness that the section exhibited due to cracking in the tensioned part of the cross section. This linearity was maintained until the passive reinforcement yielded.

Finally, phase III was the pre-failure stage, being extended between yielding and failure (Point C), where concrete finally crushed in compression zone and beams failed. During this phase, the passive reinforcement reached their yielding strength, which caused a decrease in the slope of the moment-curvature until it was zero in all of the beams (Figure 3.61). The

maximum bending moment was maintained while the curvature in the section increased. This behaviour implied fully developed reinforcement and, consequently, ductility.

The values achieved for the corresponding points and the ductility ratio of the beams are included in Table 3.22.

Analysing the failure deflection tendency, with a decrease as the replacement level raises, as well as the results obtained for the beams tested in the precast plant, the failure deflection for FB-0 was considered to happen at 165 mm. It can be observed in Figure 3.59 that at 140 mm there is a loss in the bending moment. After that, FB-0 curve continues with the same slope than it had after the yielding point. However, at 165 mm, there is another loss in the bending moment, but in this case the slope changes, being plain or even beginning to decrease. Therefore, 165 mm was considered as the failure deflection for FB-0.

Table 3.22. Values of the FB test (CITEEC)

	FB-0	**FB-10**	**FB-20**	**FB-35**	**FB-50**
Cracking					
Bending moment at mid-span (m·kN) (M_{cr})	100	80	-	70	70
Deflection at mid-span (mm) (δ_{cr})	4	3.5	-	3.5	3
Yielding					
Bending moment at mid-span (m·kN) (M_y)	375	370	350	350	350
Deflection at mid-span (mm) (δ_y)	35	37	31	38	39
Failure					
Bending moment at mid-span (m·kN) (M_u)	431.5	420.0	420.0	407.5	406.5
Deflection at mid-span (mm) (δ_u)	165	161	154	107	104
Ductility ratio	4.71	4.35	4.97	2.81	2.67

As can be observed in Table 3.22, RAC beams, with the exception of FB-20, showed lower cracking moment and slightly lower corresponding deflection than NAC beam as the replacement level increased. This may be due to the existence of two types of interfacial transition zones (ITZ) in the RAC beams. One ITZ between natural aggregate and residual

mortar in recycled aggregate and the other between residual mortar and fresh mortar, comparted with only one ITZ between the natural aggregate and the fresh mortar, in the conventional concrete beam.

For all of the substitution percentages investigated, the ultimate bending moment did not differ from the reference value by more than 5.8%, and the yielding bending moment no more than 6.7%, which was reasonable given the effect of the concrete compressive strength on the flexural strength.

Deflections at mid-span at the moment of failure were noticeably lower than FB-0 for the highest replacement levels (35 and 37% for FB-35 and FB-50, respectively), indicating a decrease in the ductility of the beam. However, for 10% and 20% replacement, deflections were slightly lower with a loss of 2.4 and 6.7%, respectively.

3.5.3.Moment – curvature relationship

The bending moment vs. curvature diagrams in a constant moment region (250 mm far from mid-span) are depicted in Figures 3.61 and 3.62. The curvature was computed from the compressive strain values provided by the strain gauges.

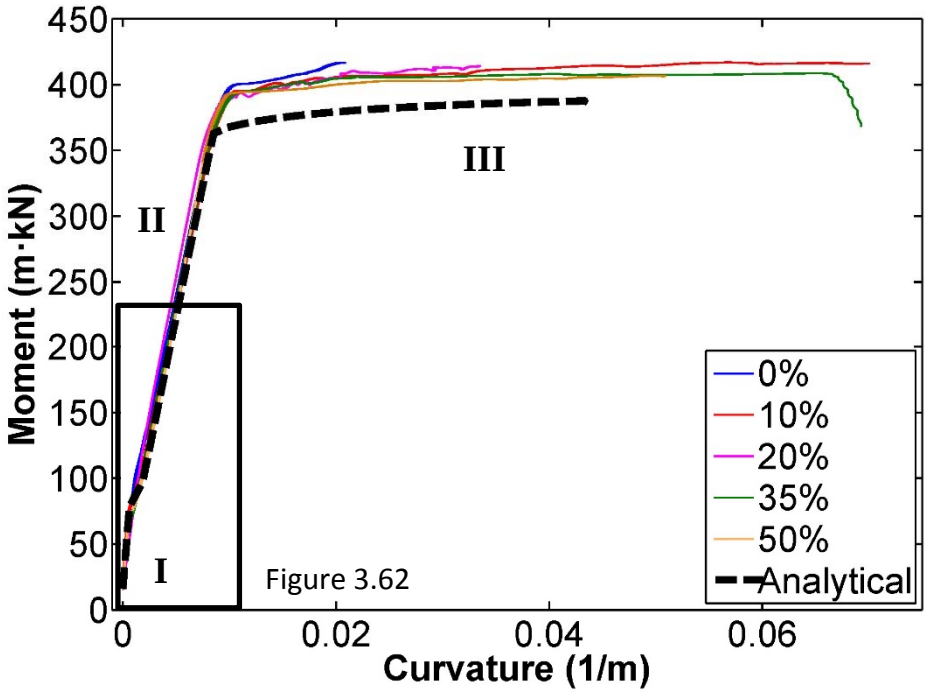

Figure 3.61. Moment vs. curvature 250 mm far from mid-span

As can be observed in Figure 3.61, the three stages with their break points are clearly identified. The curvatures of all tested beams are similar to each other with slight differences only appreciated if the area before cracking is zoomed in (Figure 3.62).

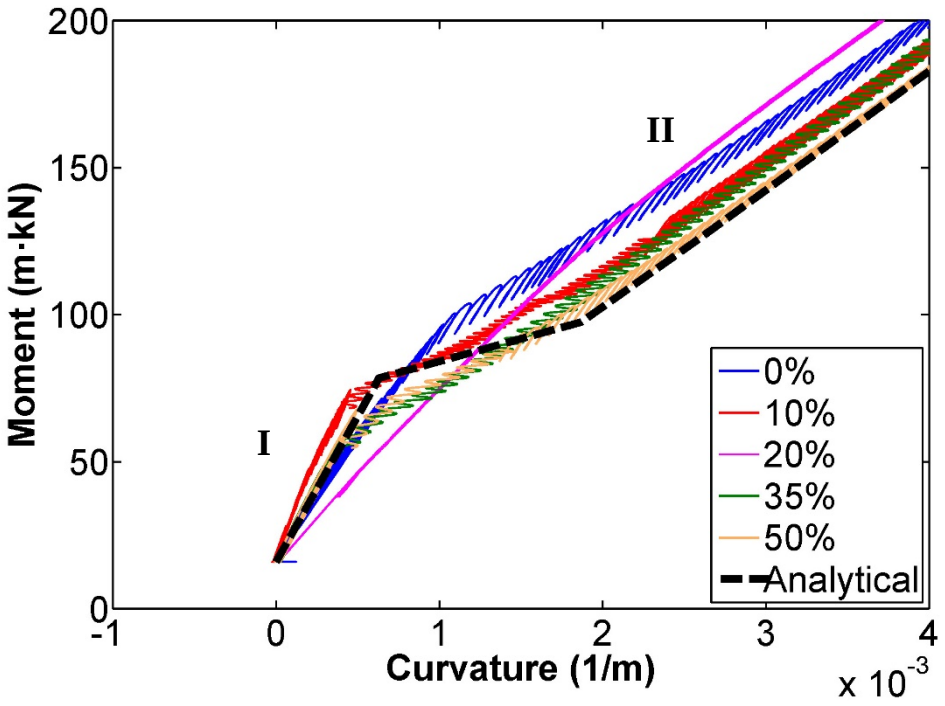

Figure 3.62. Moment vs. curvature

With the exception of the FB M-20, due to of the aforementioned problem with the actuator, there is tendency to decrease the curvature value for the cracking moment as the replacement ratio increases. The slope of this curve before cracking represents the stiffness of the beam and its elastic modulus. As can be appreciated in Figure 3.61, the stiffness is similar regardless of the replacement ratio.

However, the slope of the curves at the between the cracking and yielding point is practically identical for all of the beams.

From the yielding point to the failure of the beam, the extension of the curvature is not representative of the failure in the beam, since at some point of this stage, most strain gauges failed when cracks attained a certain width.

3.5.4.Ductility ratio

As said before, the ductility ratio is defined as the ratio of the deflection at the ultimate load (δ_u) to the deflection at the yield of the reinforcement (δ_y) [MELI 2010]. For replacement levels up to 20% of the total aggregate, the ductility ratio (Table 3.22) ranges from 4.35 to 4.97. However, for 35 and 50% replacement the degradation is significant, with a loss of up to 43% for FB-50 with regard to the beam without recycled aggregate.

3.5.5.Nominal moment analysis

In Figure 3.63 the yielding and ultimate bending moment are depicted for each beam tested. As can be observed, both the experimental yielding and ultimate bending moments are

lower than the corresponding theoretical moments in all the beams with recycled aggregate, being the difference lower as the replacement level increases due to the detrimental effect of the recycled aggregate on the concrete mechanical properties.

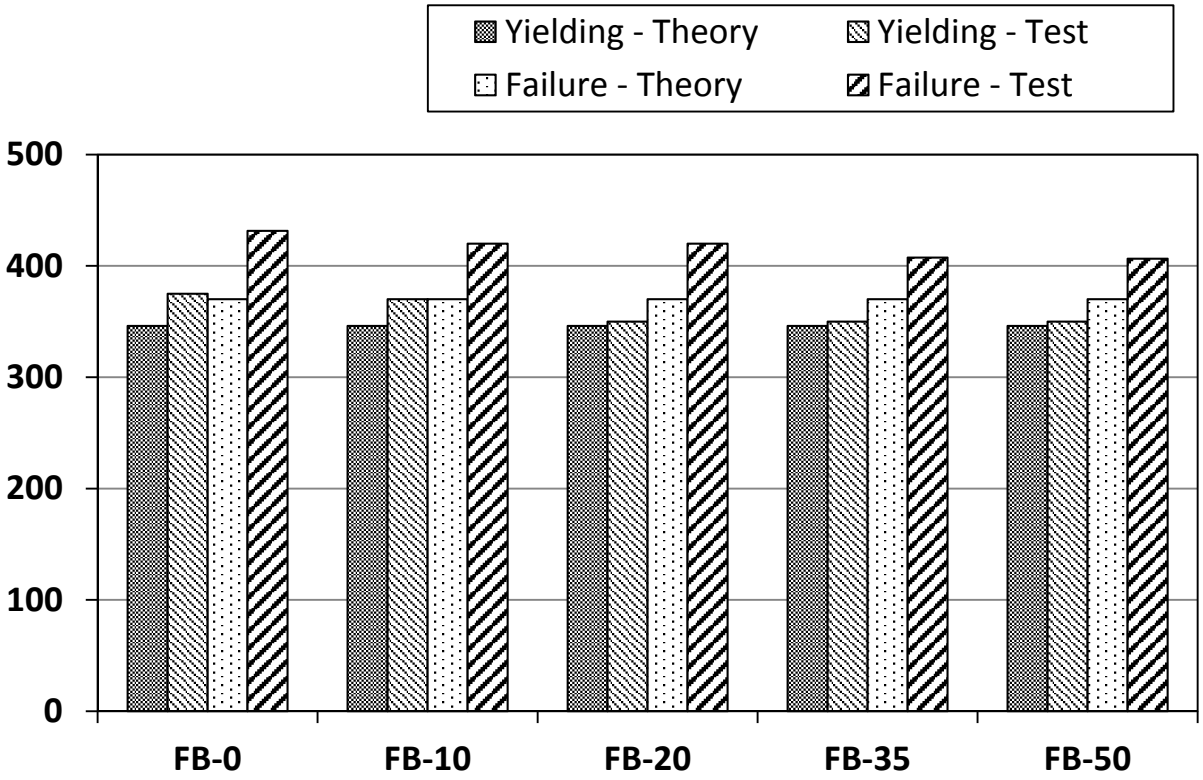

Figure 3.63. Theoretical vs. experimental yielding and failure moments

3.5.6.Crack pattern at failure

The crack pattern at failure on both sides of the beams is depicted in Figures 3.64 to 3.68. It can be observed that the crack patterns are similar regardless of the replacement ratio with recycled aggregate.

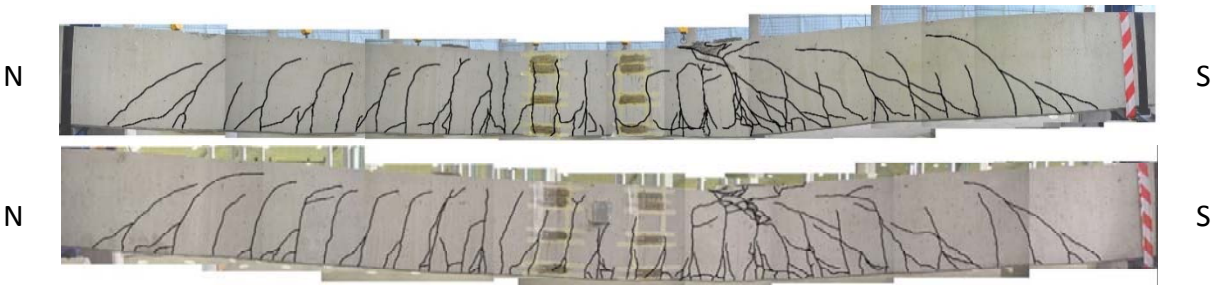

Figure 3.64. Cracking pattern at flexural failure. FB-0

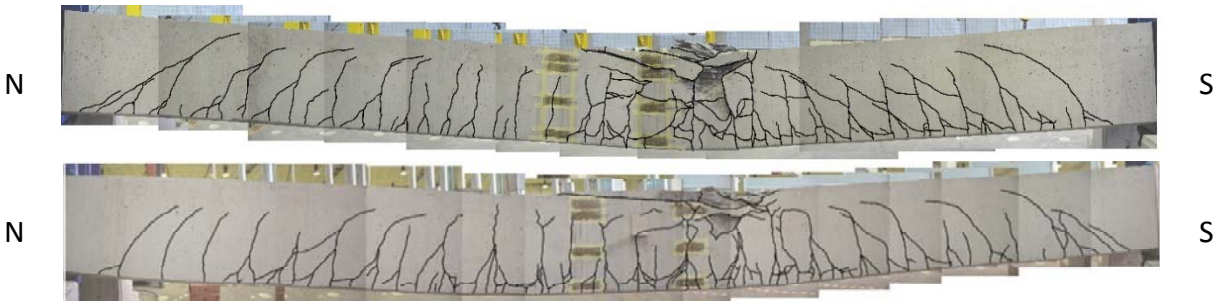

Figure 3.65. Cracking pattern at flexural failure. FB-10

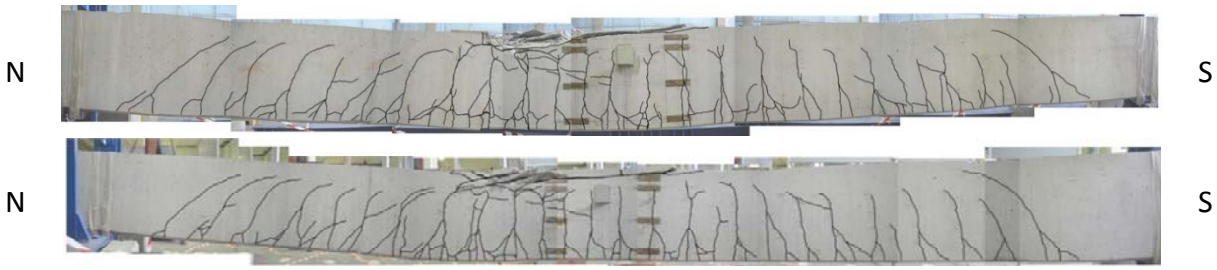

Figure 3.66. Cracking pattern at flexural failure. FB-20

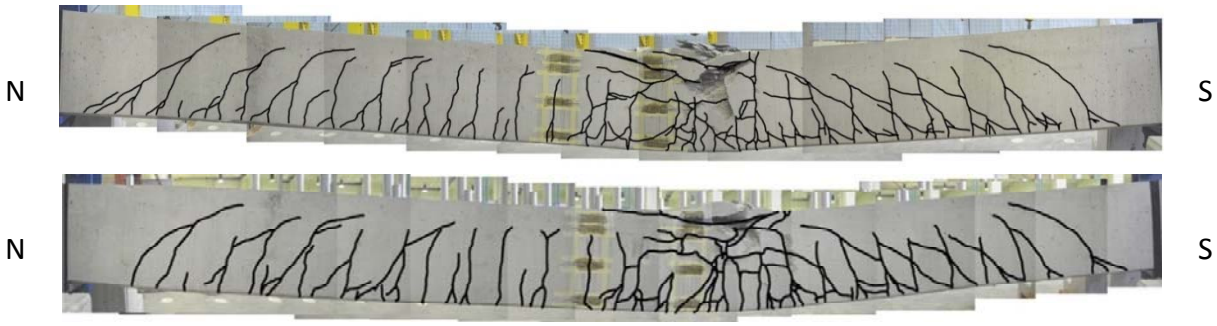

Figure 3.67. Cracking pattern at flexural failure. FB-35

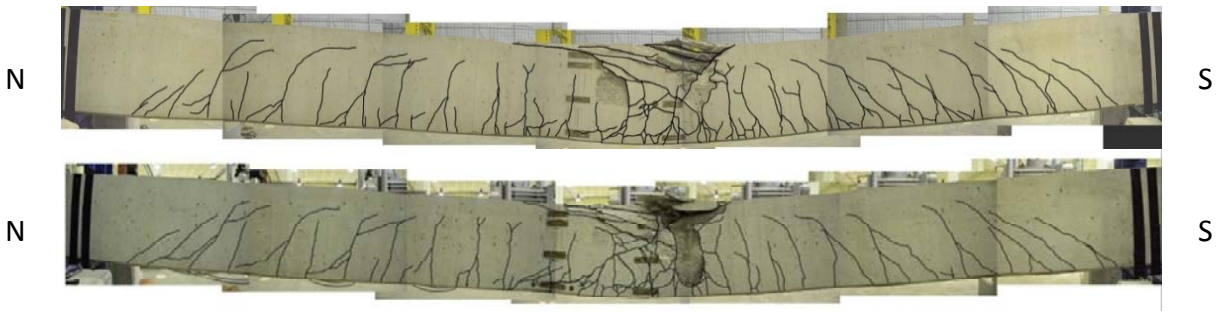

Figure 3.68. Cracking pattern at flexural failure. FB-50

From the previous crack pattern compositions, it can be observed that the distance between the top of the beam and the end of the crack is similar to the analytical value of *x=82 mm* for failure. This value represents the neutral axis depth corresponding to the compressive zone.

3.6. Results and discussion

3.6.1. Flexural behaviour test

All of the beams failed in flexure, as expected. The longitudinal tension steel yielded first, followed by the concrete crushing, which is a ductile mode of failure. Five beams with replacement levels of 0, 10, 20, 35 and 50% were tested in-situ in the precast plant and other five beams were tested in the CITEEC with a more accurate monitoring system.

The cracking moment of the beams tested in the precast plant decreased when fine and coarse recycled aggregate was incorporated. This loss of cracking strength was around 6% for FB-20 and FB-35 and by 12% for FB-50. When beams where tested in the CITEEC, the loss registered was greater, achieving losses of 20% for FB-10 and of 30% for FB-35 and FB-50. This loss of cracking strength agrees with the results obtained by Ignjatovic et al. [IGNJ 2013], with a loss of 10% when 100% coarse recycled aggregate was replaced; Lee et al. [LEE 2013] who concluded that the crack occurs earlier depending on the replacement level of recycled coarse aggregate; Knaack and Kurama [KNAA 2014] who noticed that Increased amounts of coarse recycled aggregate result in a reduction in the initial stiffness; and Seara-Paz [SEAR 2015], who observed that in both, the short-term and long-term analysis, the cracking moment decreases as the replacement level of coarse recycled aggregate increases due to the lower splitting tensile strength of recycled concrete.

The ultimate moment of RAC beams was slightly lower than the NCA beam as the replacement ratio of the total aggregate increased, with a maximum loss of 2.0% and 5.8% for FB-50, in the beam tested in the precast plant and the CITEEC, respectively. This loss of strength for such amount of recycled aggregate may be considered negligible and agrees with the results obtained by Sato et al. [SATO 2007], Choi et al. [CHOI 2012], Choi and Yun [CHOI 2013] who replaced fine and coarse recycled aggregate. On the other hand, Ignjatovic et al. [IGNJ 2013], Knaack and Kurama [KNAA 2014], Kang et al. [KANG 2014] and Seara-Paz [SEAR 2015] replaced only coarse aggregate. Similar results of nominal strength were observed by all of them, regardless of the replacement ratio and type of recycled aggregate.

Mid-span deflections at failure of beams tested in the precast plant was decreased as the substitution percentage increased, especially for the highest replacement ratios, with losses of up to 27% when 50% of the total aggregate was replaced. When beams were tested in the CITEEC, a similar trend was observed with losses of 35 and 37% for replacement levels of 35 and 50%, respectively. These results agree with the results obtained by Sato et al. [SATO 2007] and Choi and Yun [CHOI 2013], replacing fine and coarse recycled aggregate. On the other hand, agree also with the results of Knaack and Kurama [KNAA 2014], Arezoumandi et al. [AREZ 2015a] and Seara-Paz [SEAR 2015] replacing only coarse aggregate. All of them noticed that ultimate deflections of recycled concrete beams were larger than those with natural aggregates and increased for higher replacement levels.

The crack patterns observed were similar regardless of the replacement ratio. Crack spacing and crack width of NAC beam did not differ from RAC beams. This conclusion agrees with the results obtained by Sato et al. [SATO 2007], who did not appreciate significant difference in crack spacing; Choi and Yun [CHOI 2013] who concluded that the crack propagation of the beam with natural aggregate is similar to those of the recycled aggregate beams, regardless of the type of recycled aggregate; Choi et al. [CHOI 2012] who noticed that crack propagation of natural aggregate beams was similar to those of recycled aggregate concrete, regardless of the replacement ratio; Ignjatovic et al. [IGNJ 2013] who concluded that the crack spacing and width of NAC and RAC beams of the same reinforcement ratio can be considered similar; Lee et al. [LEE 2013] who noticed that in the crack occurrence and failure progress, generally crack shapes were found similar; and Kang et al. [KANG 2014] who observed that the overall crack pattern were similar.

The ductility ratio of the beams tested in the precast plant was lower as the replacement level increased, with losses of up to 33% for 50% replacement of the total aggregate. Similarly, when beams were tested in the CITEEC, a higher decrease was also observed for the highest replacement levels FB-35 and FB-50, with losses of 40% and 43%, respectively. This loss of ductility agrees with the results obtained by Choi et al. [CHOI 2012] who replaced fine and coarse recycled aggregate and Kang et al. [KANG 2014] replacing only coarse aggregate. Both of them observed that increasing the RCA replacement ratios of the specimens resulted in a decrease in ductility.

3.6.2.Shear behaviour test

The shear test results showed a brittle bond-shear failure for all of the substitutions investigated. Five beams with replacement levels of 0, 10, 20, 35 and 50% were tested in-situ in the precast plant.

The substitution of natural aggregate by recycled aggregate decreased the cracking shear by 17% for all the replacement levels. The corresponding cracking deflection was also decreased by 41% for the highest replacement levels (SB-35 and SB-50). The loss of cracking strength when recycled aggregate is incorporated agrees with the results obtained by González-Fonteboa and Martínez-Abella [GONZ 2007] replacing only coarse aggregate, who noticed that recycled concrete beams reached shear force at cracking in earlier load stages than conventional concrete beam.

The ultimate shear for beam SB-10 was practically the same as that for the reference beam (SB-0) and the corresponding deflection was slightly higher. However, increasing the substitution percentage beyond 20% led to a slight decrease of the ultimate shear by 4-6%, with corresponding deflections similar to that obtained in the beam without recycled aggregate. This slight loss of ultimate strength agrees with the results obtained by González-Fonteboa and Martínez-Abella [GONZ 2007] who noticed that recycled concrete beams

present almost the same shear force at failure as the conventional concrete beams with an equal amount of transverse reinforcement. Fathifazl et al. [FATH 2011] and Al-Zahraa et al. [AL-ZA 2011] noticed that beams with coarse recycled aggregate had even a higher shear strength compared to the beams made with natural aggregates. Arezoumandi et al. [AREZ 2014] observed that in terms of load deflection response, the behaviour of the coarse recycled aggregate and natural aggregate beams was virtually identical. However, in [AREZ 2014], where 50% replacement was also studied, there was slight difference in slope of load-deflection graphs after cracking.

Considering the results obtained in this experimental program, it may be concluded that the simultaneous use of up to 50% of fine and coarse recycled aggregates from the rejection of precast concrete members is feasible for producing self-compacting reinforced concrete beams. However, it would be necessary to perform durability tests in order to analyse the long-term behaviour of the recycled concrete beams.

Chapter 4. Prestressed Concrete Beams

4.1. Introduction

After analysing the feasibility of replacing fine and coarse recycled concrete aggregates in reinforced concrete, it was taken the decision to do a similar study with prestressed precast concrete elements.

First of all, it was taken the decision to do a preliminary study with prestressed pre-slabs and lower replacement ratios of recycled aggregate (0, 2, 4, 6, 8 and 10%). These elements were tested to failure to determine the loss of flexural and shear strength when the recycled aggregates are introduced in the mix. The fabrication procedure and test results are shown in Appendix 3. It was concluded that it is feasible to replace up to 10% of the total natural aggregate with recycled aggregate in this type of concrete and element, provided that the pre-slabs will not be subjected to excessive shear forces. These elements were placed in a real construction as a non-load bearing permanent formwork.

Due to the proper results of the preliminary tests, it was decided to do a more detailed study of the bond behaviour when recycled aggregate is introduced in the mix. So, a similar program to that of the reinforced beams was performed, but in this case with vibrated concrete, a recycled aggregate from a different source and prestressed concrete I-beams in place of reinforced rectangular beams. Different quantities of the total amount of natural aggregate (fine and coarse) were also replaced with recycled aggregate; and a detailed study was performed in the laboratory in order to evaluate their mechanical and durability properties. The resulting recycled concrete was used for the fabrication of pretensioned prestressed concrete beams in a precast plant. The beams were transported to the CITEEC and tested in order to study the influence of the recycled aggregate on the bond properties between the prestressing strand and the surrounding concrete.

4.2. Materials

The natural materials used for the present study were provided by the precast plant and are usually employed by this plant for the fabrication of precast elements. A detailed study was performed in the laboratory in order to analyse their properties and design a good mix composition.

The following materials were used in this study:

- Cement CEM I 52.5 R-SR 3. Holcim (Spain), S.A. Aenor Certificate: 015/001966
- Natural arkosic silica sand: 0/2 mm (NA-2 0/2) and 0/5 mm (NA-2 0/5) fractions (Figures 4.1 and 4.2). Source: Áridos Antelanos S.L. Sandás (Ourense)
- Natural amphibolite gravel: 4/12 mm (NA-2 4/12) and 10/20 mm (NA-2 10/20) fractions (Figures 4.3 and 4.4). Source: Canteras de Richinol, S.L. Lalín (Pontevedra)
- Recycled concrete aggregate: 0/12 mm (RCA-2 0/12) fraction (Figure 4.5).
- Sika Visocrete 80 superplasticizer

Figure 4.1. NA-2 0/2

Figure 4.2. NA-2 0/5

Figure 4.3. NA-2 4/12

Figure 4.4. NA-2 10/20

Figure 4.5. RCA-2 0/12

The recycled concrete aggregates for this study are were obtained from the crushing of old concrete sleepers (Figure 4.6) with a compressive strength higher than 35 MPa. These elements were taken to a construction and demolition waste (CDW) plant for recycling, where they were crushed and removed from impurities (Figure 4.7). After this process, the recycled aggregates were taken to the precast plant and to the laboratory.

Figure 4.6. Old concrete sleepers

Figure 4.7. Recycled concrete aggregate

The following properties were analysed for the materials used in this study:

- Particle size distribution
- Particle density and water absorption
- Particle shape. Flakiness index
- Classification of the constituents of coarse recycled aggregate
- Cement chemical composition

Particle size distribution

The particle size distribution of the aggregates was determined following the procedure of the UNE-EN 933-1:2012 and UNE-EN 933-2/1M:1999 Standards. The results are shown in Table 4.1 and Figure 4.8.

Table 4.1. Particle size distribution

Sieve size (mm)	Percentage passing (by weight)				
	NA-2 0/2	**NA-2 0/5**	**NA-2 4/12**	**NA-2 10/20**	**RCA-2 0/12**
0.063	2.5	1.0	0.0	0.1	1.5
0.125	8.6	1.9	0.1	0.1	4.2
0.25	20.1	7.5	0.1	0.1	6.6
0.5	42.2	25.7	0.1	0.2	9.9
1	71.4	51.0	0.1	0.2	14.8
2	98.1	78.5	0.2	0.2	25.4
4	100	95.4	0.4	0.2	47.0
5	100	98.0	2.0	0.3	54.4
5.6	100	98.5	4.4	0.3	59.5
6.3	100	99.0	14.9	0.6	70.2
8	100	99.8	45.7	1.7	84.6
10	100	100	77.4	6.6	95.7
11.2	100	100	92.9	13.6	98.2
12.5	100	100	98.2	32.8	99.7
14	100	100	99.6	56.3	99.7
16	100	100	100	77.7	100
20	100	100	100	97.7	100
25	100	100	100	100	100
31.5	100	100	100	100	100
63	100	100	100	100	100
Percentage of fines passing the 0,063 mm sieve (%)	2.5	1.0	0.1	0.1	1.1

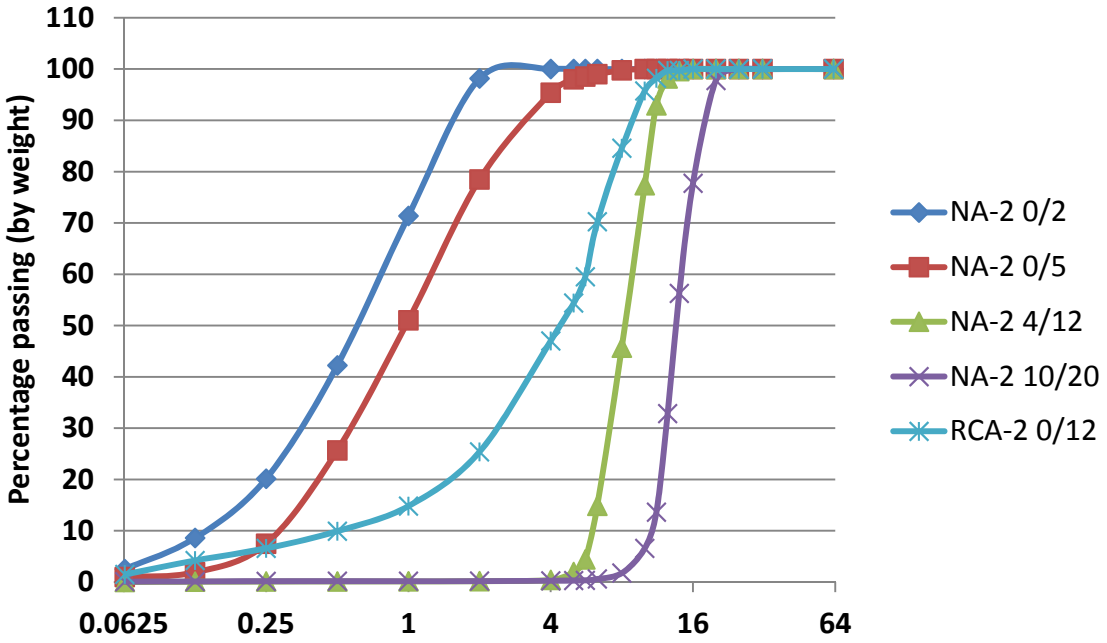

Figure 4.8. Particle size distribution

Particle density and water absorption

The particle density and water absorption of the aggregates was determined following the procedures of the UNE-EN 1097-6: 2001/A1: 2006 Standard. The results are showed in Table 4.2. The procedure, according to the mentioned Standard, is different depending of the size of the aggregate, for this reason the recycled aggregate was sieved in two fractions 0/4 and 4/12 for this test.

Table 4.2. Particle density and water absorption

	NA-2 0/2	NA-2 0/5	NA-2 4/12	NA-2 10/20	RCA-2 0/4	RCA-2 4/12
Bulk density of particles (ρa) Mg/m³	2.62	2.52	2.82	2.56	2.59	2.63
Density of particles after oven drying (ρrd) Mg/m³	2.56	2.46	2.76	2.53	2.24	2.32
Density of particles in saturated surface-dry condition (ρssd) Mg/m³	2.58	2.48	2.78	2.54	2.37	2.43
Water Absorption (WA24) %	0.89	0.95	0.75	0.44	5.99	5.09

As expected, the water absorption of both fractions of the recycled higher than the water absorption of the natural aggregate. Therefore, it needs to be considered when designing the mix composition.

Particle shape. Flakiness index

The particle shape test to obtain the flakiness index of the recycled aggregate was performed following the UNE-EN 933-3: 2012 Standard. The result is shown in Table 4.3.

Table 4.3. Particle shape test

Gravel	Flakiness index (%)
RCA-2 0/12	9

Classification of the constituents of coarse recycled aggregate

The classification of the constituents of the concrete recycled aggregate was performed following the procedure of the UNE-EN 933-11:2009/AC:2010 Standard. The results of the test are shown in Table 4.4.

Table 4.4. Classification of the constituents

Constituents	Description	RCA-2 0/12
FL (cm^3/kg)	Floating material	1.7
Rc (%)	Concrete, concrete products, mortar	13.3
Ru (%)	Unbound aggregate, natural stone	83.9
Rb (%)	Clay masonry units (bricks and tiles)	1.8
Ra (%)	Bituminous materials	0
Rg (%)	Glass	0
X (%)	Other: Cohesive (clay and soil), Miscellaneous: metals, non-floating wood and rubber, Gypsum plaster	0

The results in Table 4.4 show that almost all of the particles could be classified as Rc or Ru, as expected.

Chemical composition

Table 4.5 shows the chemical analysis results from X-ray fluorescence for all of the materials that were used for this study.

Table 4.5. Chemical composition (wt. %)

Component	NA-2 0/2 NA-2 0/5	NA-2 4/12 NA-2 10/20	AR-2 0/12	Cement
SiO_2	32.9	85.9	38.5	16.9
CaO	32.5	0.29	3.6	66.1
Al_2O_3	6.0	7.2	2.9	2.8
Fe_2O_3	3.0	0.21	12.3	5.2
MgO	1.7	0.065	31.1	1.4
K_2O	1.7	4.9	0.16	0.8
Na_2O	0.49	0.41	0.11	0.68
SO_3	0.40	*< 0.008*	0.10	3.5
TiO_2	0.36	0.083	0.17	0.29
P_2O_5	0.096	0.074	0.13	0.092
MnO	0.066	*< 0.003*	0.18	0.058
SrO	0.048	0.006	0.019	0.069
ZrO_2	0.031	0.008	*< 0.005*	0.009
CuO	0.018	0.007	0.016	0.096
Rb_2O	0.011	0.025	*< 0.005*	-
Cr_2O_3	*< 0.005*	*< 0.005*	0.49	-
NiO	*< 0.005*	*< 0.005*	0.47	-
Cl	-	-	-	0.076
V_2O_5	-	-	-	-
Br	-	-	-	-
Carbonates	-	-	-	0.99
ZnO	*< 0.005*	*< 0.005*	0.018	0.094
LOI (Lost on ignition)	20.5	0.5	9.4	1.82

As mentioned before, The Spanish Code on Structural Concrete [EHE 08] stablishes a series of requirements that the coarse aggregates should meet in order to achieve an appropriate concrete strength and durability. These requirements and the values obtained for the recycled aggregate used in this study are compared in Table 4.6.

Table 4.6. Aggregates Requirements

Property	Requirement	RCA-2 0/12
Fines content (< 0,063 mm) (%)	≤ 1,5	1.5
Sand content (< 4 mm) (%)	≤ 5	47
Flakiness index (%)	≤ 35	9
Los Angeles Coefficient	≤ 40	-
Water absorption (%)	≤ 5	5.09-5.99
Lightweight particles content (%)	≤ 1	0
Ceramic material content (%)	≤ 5	1.8
Asphalt content (%)	≤ 1	0
Other materials (glass, plastic, metal, etc.) (%)	≤1	0

Due to the high sand content of the recycled aggregate, it was not possible to perform the resistance to fragmentation test according to the UNE-EN 933-11:2009/AC:2010 Standard. As expected, the recycled aggregate RCA-2 0/2 does not satisfy the requirements established for sand content and water absorption. Therefore, this condition needs to be considered when designing the recycled concrete mixes.

4.3. Experimental program in laboratory

4.3.1. Mix proportions

The mix used in the precast concrete plant for vibrated concrete prestressed beams was used as a reference in the laboratory. In this way, 4 concrete mixes were fabricated with a water-to-cement ratio (w/c) of 0.45, one of them as a reference, without recycled aggregate (F-0), and the others with a replacement level of the total amount of aggregate (fine and coarse) by recycled aggregate of 8, 20 and 31% for F-8, F-20 and F-31, respectively.

Just like RCA-1 0/12, the excessive sand content (47%) in RCA-2 0/12, in comparison to the 5% recommended by the EHE, presents a great problem if solely the coarse natural aggregate is replaced, since the joint particle size distribution of the mix would be modified to a large extent. Hence, the decision was taken to replace the recycled aggregate in both, coarse natural aggregate 4/12 and fine natural aggregate 0/5 with a proportion of 53% and 47%, respectively, of the total amount of recycled aggregate introduced in the mixture. The goal of this kind of adjustment is getting a joint particle size distribution as similar as possible to the distribution of the reference concrete (F-0) as it can be seen in Figure 4.9.

The decision to select 8% as the first replacement ratio was taken according to the results obtained from the prestressed pre-slab tests explained in the previous chapter. According to the flexural test, 8% was the substitution percentage with a considerable amount of recycled aggregate (> 5%) in which the highest failure moment was obtained. The last replacement

ratio (31%), was the maximum possible, according to the replacement procedure explained in the previous paragraph, before the aggregate NA-2 4/12 was finished (Table 4.7).

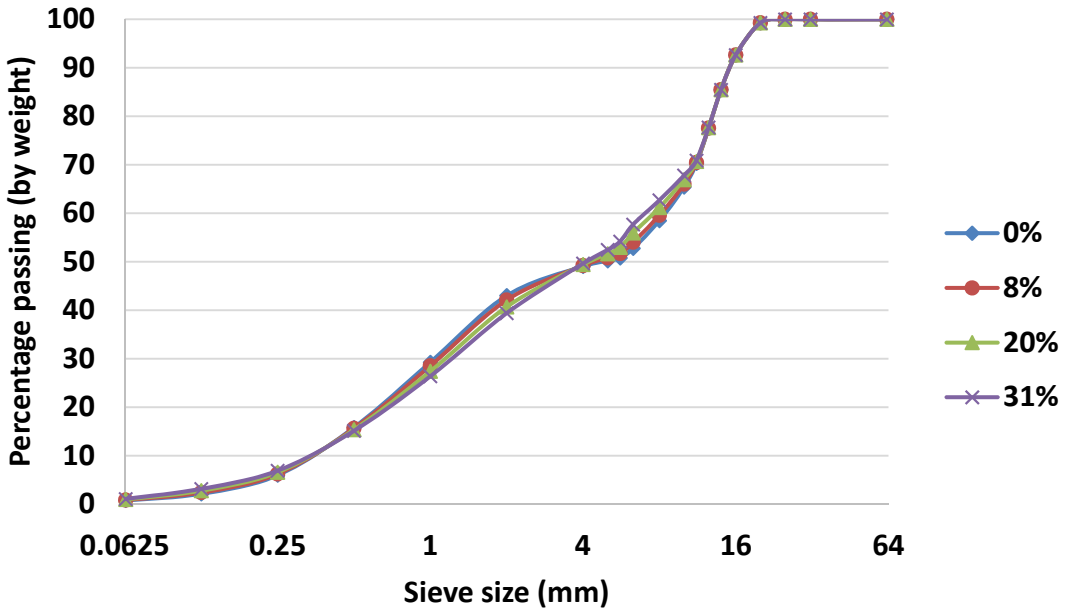

Figure 4.9. Joint particle size distribution

Due to the higher absorption of recycled aggregates in comparison with natural aggregates, the workability of the mixture is reduced. As explained in chapter 3 for the laboratory mixes, it was necessary to add an extra amount of water to the mixture to compensate this effect. It was calculated as the quantity necessary to saturate the recycled aggregates. The mix proportions for each replacement level are shown in Table 4.7 and the corresponding replacement level for each fraction, fine and coarse, are shown in Table 4.8.

Table 4.7. Mix proportions

	F-0 (Kg/m^3)	**F-8** (Kg/m^3)	**F-20** (Kg/m^3)	**F-31** (Kg/m^3)
CEM-I 52.5 R-SR 3	400	400	400	400
NA-2 0/2	308	308	308	308
NA-2 0/5	608	540	437	342
NA-2 4/12	300	223	108	0
NA-2 10/20	600	600	600	600
RCA-2 0/12	0	145	363	566
Water	180	180	180	180
Extra water	0	8	20	31
Superplasticizer	3.57	3.57	3.57	3.57
Effective w/c	0.45	0.45	0.45	0.45
w/c	0.45	0.47	0.50	0.53

Table 4.8. Replacement ratios

	M-8	M-20	M-31
% recycled aggregate with respect to total amount of aggregate	8	20	31
% recycled fine aggregate with respect to total amount of fine aggregate	7.4	18.7	29.0
% recycled coarse aggregate with respect to total amount of coarse aggregate	8.6	21.3	33.3

4.3.2. Mixing procedure and casting

For each of the mix proportions, it was decided to fabricate 2 batches of 60 litres because a great number of samples were needed for the different tests. The previous day to the concrete fabrication, the water content of each of the materials was determined following the UNE-EN 1097-5:2009 Standard, and the amount of water that would be added to the mix was adjusted in order to have the desired mix proportions. The mixing was made in a vertical axis mixer with two mixing blades and procedure for each of the replacement levels was as follows:

1. Moisten the mixer with a wet cloth.
2. Add natural sand and mix for 30 seconds.
3. Add cement and mix for 60 seconds.
4. Add coarse natural aggregate and recycled aggregate, and mix for 60 seconds.
5. Without stopping the mixer, add water slowly for 30 seconds and mix for 60 seconds.
6. Without stopping the mixer, add the superplasticizer slowly for 30 seconds and mix the necessary time until the power consumed by the mixer will be stabilized.

Immediately after mixing the materials, the slump test was performed according to the UNE-EN 12350-2:2009 Standard to evaluate the workability of the mixture. Cylinders 150 x 300 mm, cubes 100 mm and prisms 100 x 100 x 400 mm were cast following the UNE-EN 12390-2:2009 Standard and kept inside an environmental chamber between 16 hours and 3 days before demoulding. The curing conditions inside the chamber are 20±2 °C temperature and relative humidity higher than 95%. After demoulding, the samples continued inside the environmental chamber for an appropriate curing until the age of testing.

4.3.3. Fresh and hardened properties

For each of the mixes analysed, the workability through the slump test was studied in order to evaluate the fresh state properties; the density, compressive strength, flexural strength to

evaluate the hardened state properties; and the depth of penetration of water under pressure to evaluate the durability properties.

Workability

The slump test was performed according to the UNE-EN 12350-2:2009 Standard to assess the consistency of the concrete mix. The measured values for the different mixes are shown in Table 4.9.

Table 4.9. Slump test

Mix	Slump (cm)	Δ (%)
F-0	19	
F-8	21	7.9
F-20	22	13.2
F-31	22	13.2

As observed in Table 4.9, the slump increases as the replacement level raises for 8% and 20% replacement due to the free water content necessary to compensate the higher water absorption of the recycled aggregate. However, for 31% replacement the measured value does stabilize with respect to 20% replacement. Similar to the case of reinforced beams concrete, the reason may be due to that the effect of water absorption of the recycled aggregates on the consistency is more noticeable for higher replacement levels.

Density

Density of hardened concrete was measured following the UNE-EN 12390-7:2009 Standard for the cubes and cylinders tested at the age of 28 days. The measured values are shown in Table 4.10.

Table 4.10. Mean density

Mix	Mean density (Kg/m^3)	Δ (%)
F-0	2490	
F-8	2467	-0.92
F-20	2397	-3.73
F-31	2354	-5.46

As expected, the mean density of the hardened concrete was decreased as the replacement level raised because of the lower particle density of the recycled aggregate in comparison with the natural aggregate.

Compressive strength

The compressive strength was evaluated according to the UNE-EN 12390-3:2009/AC:2011 Standard. Three cubes were tested at 7 days and three at 28 days, calculating the mean value for each age. The results are shown in Table 4.11 and Figure 4.10.

Table 4.11. Compressive strength (cubic)

Mix	7 days		28 days	
	Compressive strength (MPa)	Δ (%)	Compressive strength (MPa)	Δ (%)
F-0	57.2		63.2	
F-8	57.2	0	62.5	-1.1
F-20	55.5	-3.0	61.5	-2.7
F-31	52.0	-9.1	57.6	-8.9

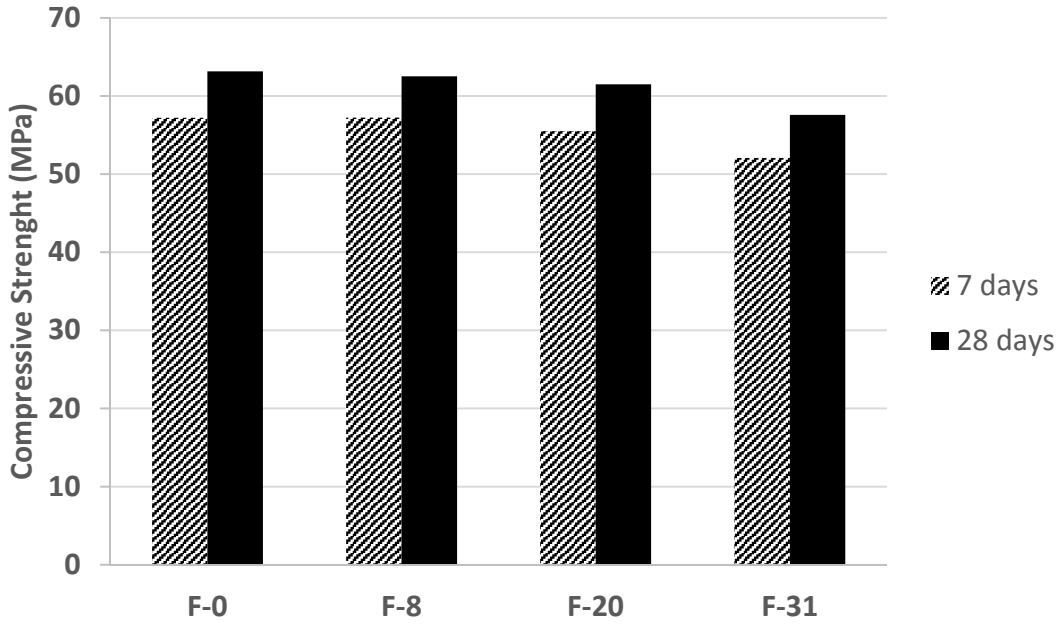

Figure 4.10. Compressive Strength

The data depicted in Figure 4.10 indicate that the compressive strength at 7 and 28 day slightly decreases when the natural aggregate is replaced by the recycled aggregate for replacement levels up to 20%. It decreases by 1.1 and 2.7% for 8 and 20% replacement, respectively. However, when 31% of the total aggregate is replaced, this decrease is sharper, with a loose of 8.9%. This may be due to the poor quality of recycled aggregate that is more noticeable for higher replacement levels.

Flexural strength

The flexural strength was calculated following the UNE-EN 12390-5:2009 Standard. Three prisms of 100 x100 x 400 mm were tested at the age of 28 days and the mean value was calculated. The results are shown in Table 4.12 and Figure 4.11.

Table 4.12. Flexural Strength

Mix	Flexural Strength (MPa)	Δ (%)	Δ (%)*
F-0	5.9		
F-8	7.2	22.0	
F-20	6.6	11.9	-8.3
F-31	6.3	6.8	-12.5

** With regard to F-8*

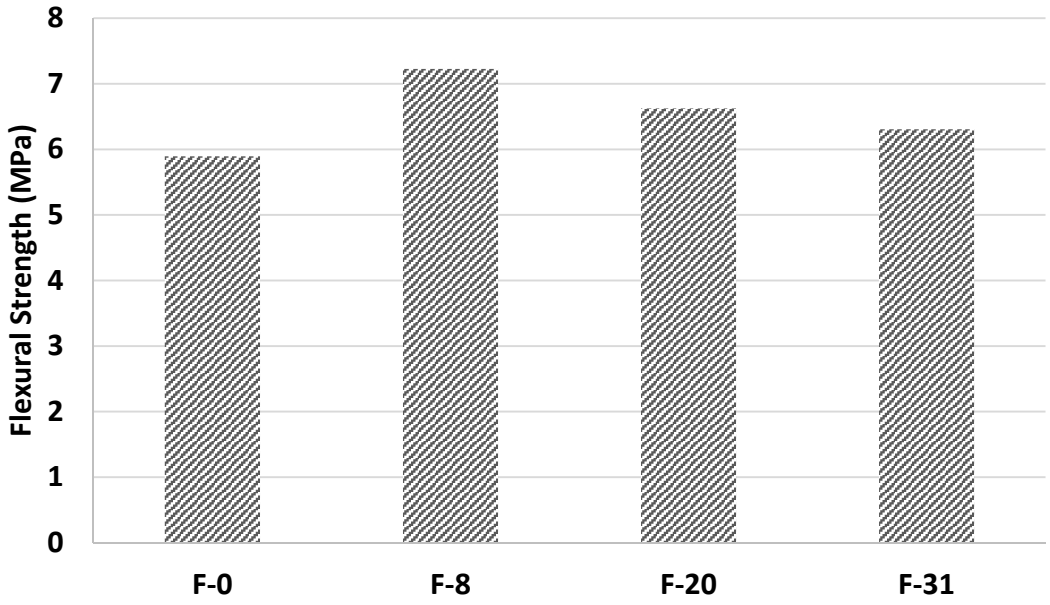

Figure 4.11. Flexural strength

The data depicted in Figure 4.11 indicate that from F-8 to F-31 there is a clear trend of the flexural strength to decrease (8.3 and 12.5% for F-20 and F-31, respectively, with regard to F-8) as the replacement level increases. However, the value obtained for F-0 is lower than the values obtained for the mixes with recycled aggregate. This result does not make sense and the reason might be a problem during the transport or curing of the samples at early age. Therefore, it should be dismissed.

Modulus of elasticity

The modulus of elasticity was calculated following the procedure of UNE 12390-13:2014 Standard. Two cylinders were tested for each age and the mean value was calculated. The results are shown in Table 4.13 and Figure 4.12.

Table 4.13. Modulus of elasticity

Mix	Test age	Elastic modulus (MPa)	Δ (%)
F-0	7 days	41400	
F-8	7 days	38000	-8.2
F-0	28 days	43300	
F-8	28 days	42000	-3.0
F-20	28 days	39900	-7.9
F-31	28 days	34800	-19.6

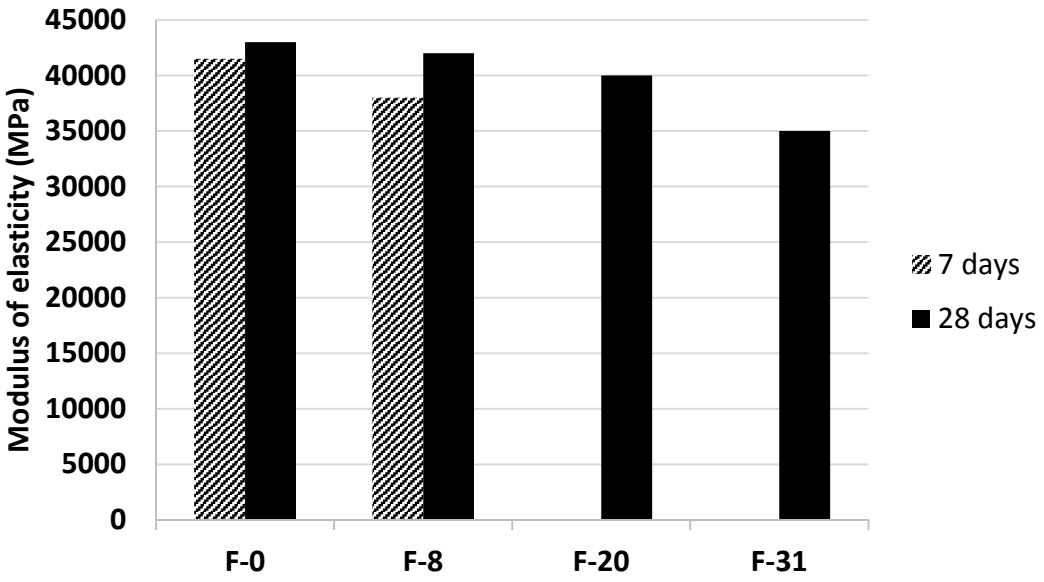

Figure 4.12. Modulus of elasticity

From the previous data, it can be concluded that the modulus of elasticity decreases as the replacement level increases, with a maximum loose of 19.6% for 31% replacement. Similar to the compressive strength results, the loose is sharper for highest replacement level due to the poorer quality of the recycled aggregate in comparison with the natural one.

Depth of penetration of water under pressure

The depth of penetration of water under pressure test was performed in order to evaluate the concrete permeability. It was evaluated according to the UNE-EN 12390-8:2009/1M:2011 Standard at an age older than 28 days. Three cylinders were tested for each replacement level and the measured values are shown in Table 4.14.

Table 4.14. Mean values of the maximum and mean depth of penetration of water under pressure

Mix		Max. depth (mm)	Mean depth (mm)
F-0		9	15
F-8		5	9
F-20		5	10
F-31		4	8
Limit imposed by EHE-08			
Environmental exposure IIIa, IIIb, IV, Qa, E, H, F, Qb (plain or reinforced concrete)	Mean value	50	30
	Maximum individual value	65	40
Environmental exposure IIIc, Qc, Qb (prestressed concrete)	Mean value	30	20
	Maximum individual value	40	27

The results obtained from the water penetration test show that penetration depth does not increase when recycled aggregate is introduced in the mix, being all of them lower than the required values stablished by the Spanish Code EHE-08.

4.3.4. Results and discussion

The following conclusions can be drawn from the experimental program performed in laboratory to evaluate the properties of the vibrated recycled concrete used for the fabrication of the prestressed beams:

All recycled concretes showed enough consistency at a fixed water-to-cement content 0.45. For F-8 and F-20 mixes, slump was increased 7.9 and 13.2%, respectively, due to the higher free water content. However, for F-31 mix the slump measured stabilized with respect to 20% replacement, probably because the effect of water absorption is more noticeable for higher replacement levels. This increase in the slump agrees with the results obtained for vibrated concrete by Khatib [KHAT 2005] with an increase of up to 11% in slump as the content of fine recycled concrete aggregate in the mixes was fully replaced; Kou and Poon [KOU 2009a]; [CLEAM] project, with an increase for small replacement ratios up to 10% of fine or coarse recycled aggregates; Chan and Pou [CHAN 2013] who observed that concrete containing 50% FRA had the highest initial slump. Mardani-Aghabaglou [MARD 2014] and Lotfy and Al-Fayez [LOTF 2015] noticed that mixtures exhibited equivalent fresh properties regardless of the RCA replacement level.

Density of hardened concrete was decreased 0.92, 3.73 and 5.46% for 8, 20, and 31% replacement of the total aggregate, respectively. The reason is the lower particle density of recycled aggregate in comparison with natural aggregate. This loss in density agrees with the results obtained by all of the researchers. Khatib [KHAT 2005] and Chan and Poon [CHAN

2013] registered weight losses up to 4% and 3.6%, respectively, for the total replacement of sand in vibrated concrete. On the other hand, Grdic et al [GRDI 2010] registered a decrease of 3.4% with full replacement of coarse aggregate in self-compacting concrete.

The compressive strength at 28 days decreased by 1.1, 2.7 and 8.9% for 8, 20, and 31% replacement of the total aggregate, respectively. These results agree with the losses obtained for vibrated concrete by Evangelista [EVAN 2007] with decreases of only 0.6, 3.4 and 3.7% for 10, 20 and 30% replacement, respectively, of FRA; Yaprak et al. [YAPR 2011] with losses by 4.3, 5.9 and 9.8% for 10, 20 and 30% replacement, respectively of FRA, and Chan and Poon [CHAN 2013], who noticed that the strength of the concrete mixtures decreased 12% as the replacement ratio of FRA increased from 0 to 100%. In self-compacting recycled concretes, the results agree with the obtained by Kou and Poon [KOU 2009b] who noticed that the incorporation of 25% and 50% of FRA as sand replacement did not significantly affected the 28 days compressive strength; and Grdic et al. [GRDI 2010] observed losses of 3.88% with 50% replacement t of CRA.

From the flexural strength test, with the exception of the incoherent value obtained for 0% replacement, general trend was that the flexural strength decreased as the replacement level increased with losses of 8.3 and 12.5% for 20 and 31% replacement, respectively, with regard to F8. This flexural strength loss agrees with the results obtained by Jang and Yun [JANG 2014] for vibrated concrete; and Khafaga [KHAF 2014] and Gesoglu et al. [GESO 2015b] for self-compacting concrete.

The modulus of elasticity at the age of 28 days decreased by 3.0, 7.9 and 19.6% for 8, 20 and 31% replacement of the total aggregate, respectively. This loss in the elastic modulus agrees with the results obtained for vibrated concrete by Corinaldesi and Marconi [CORI 2009] with losses of 20-30% when FRA is replaced. Pereira et al. [PERE 2012b] with losses between 9.5-17% for 100% replacement of the total content of sand. In self-compacting concrete mixtures, Gesoglu et al. [GESO 2015b] noticed that mixes with recycled aggregates had lower modulus of elasticity. It was reduced 13-18% in mixes with 100% replacement of CRA, 23-25% in mixes with 100% replacement of FRA and 28-34% in mixes with 100% replacement of CRA and FRA.

The depth of penetration of water under pressure test showed that penetration depth is not increased when recycled aggregate is introduced in the mix. These results agrees with the study performed by Grdic et al. [GRDI 2010], in which no water penetration was recorded on samples with 50% CRA and 100% CRA, whereas the control sample had a penetration of 10 mm.

Considering that the properties of this concrete are not badly affected by the simultaneous replacement of this type of fine and coarse concrete recycled aggregates, it might be concluded that it is feasible to replace up to 31% of the total amount of natural aggregate by

this particular recycled aggregate. However, it would be interesting to perform more durability tests to evaluate shrinkage performance, chloride-ion penetration, abrasion resistance and carbonation resistance, in order to evaluate the long-term behaviour since this concrete is utilised for the fabrication of prestressed elements that must avoid losses in the prestressing force.

4.4. Experimental program in precast plant

This experimental program consisted on the fabrication of 8 prestressed concrete beams with the mix composition studied in the laboratory. Half of them were cast with concrete containing only natural aggregates and the other 4 were cast with 8% substitution of the total aggregate (fine and coarse) with recycled aggregate.

The decision to make beams with only 0 and 8% replacement was taken according the results obtained from the pre-slab tests and the experimental program developed in the laboratory for the mix compositions. Replacement ratio of 8% showed negligible differences with regard to the reference concrete in terms of mechanical behaviour.

The aim of this new study was to analyse the bond behaviour between the reinforcing steel and the surrounding concrete and it was estimated that at least 3 beams of each replacement ratio would be necessary to test with different embedment length in order to determine the development length.

Transfer length, development length and bond strength were determined for both replacement levels in order to estimate the influence of recycled aggregate on the bond behaviour in prestressed concrete beams.

4.4.1. Geometry and reinforcement layout

Beams were fabricated in a prestressing bed of the precast plant according to the following geometry and reinforcement layout (Figures 4.13 – 4.20):

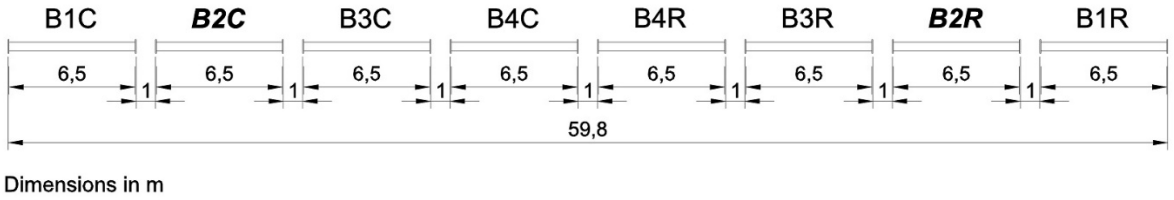

Figure 4.13. Prestressing bed distribution

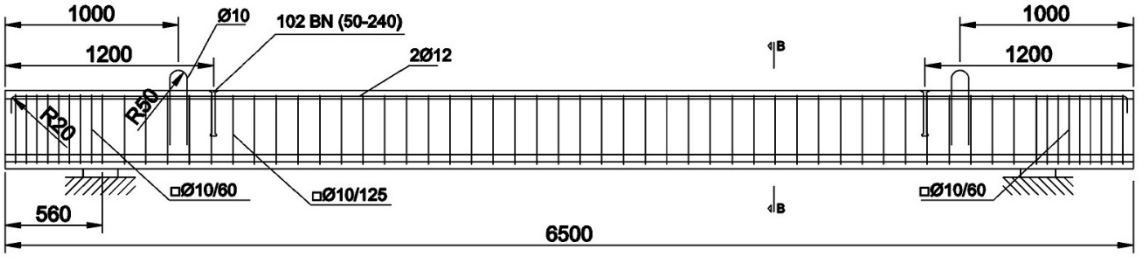

Figure 4.14. Geometry and reinforcement layout beams B1C, B3C, B4C, B1R, B3R and B4R

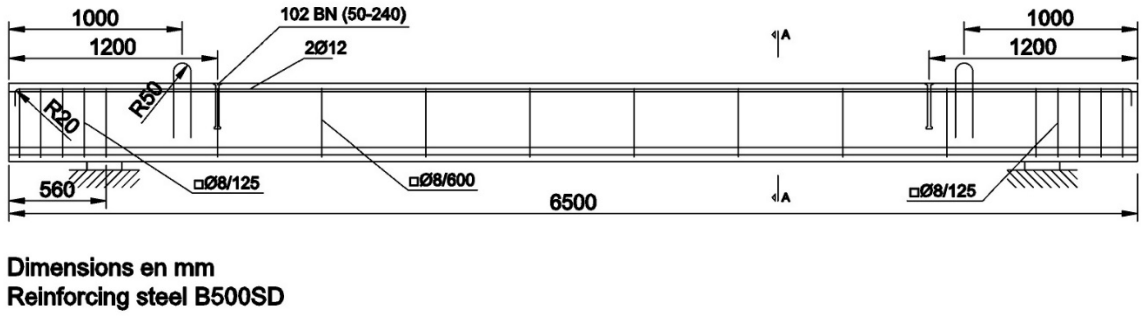

Figure 4.15. Geometry and reinforcement layout beams B2C and B2R

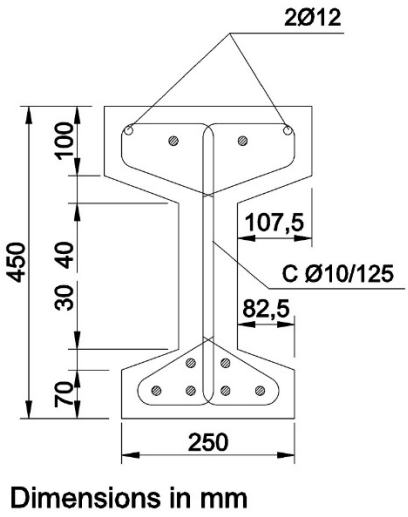

Figure 4.16. Cross-section B1C, B3C, B4C, B1R, B3R and B4R

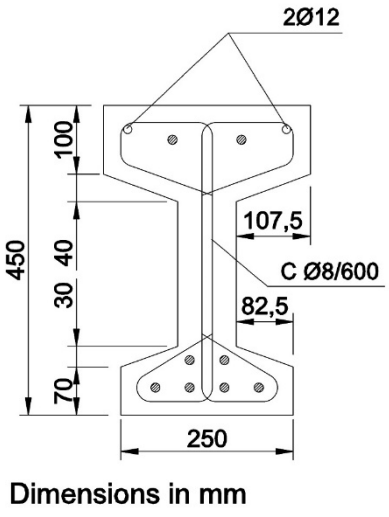

Figure 4.17. Cross section B2C and B2R

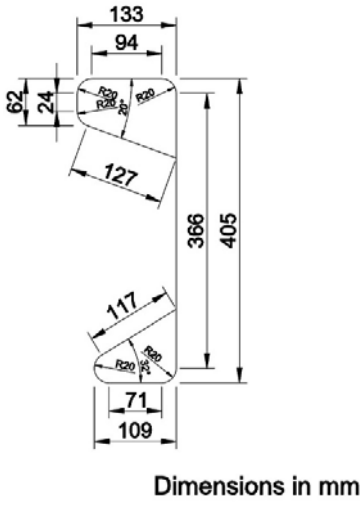

Figure 4.18. Stirrup

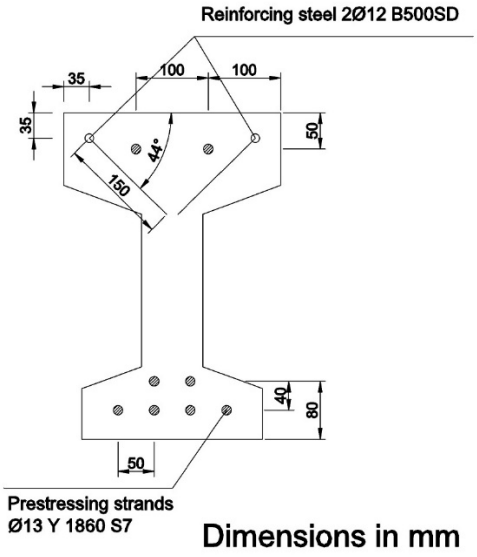

Figure 4.19. Longitudinal reinforcement

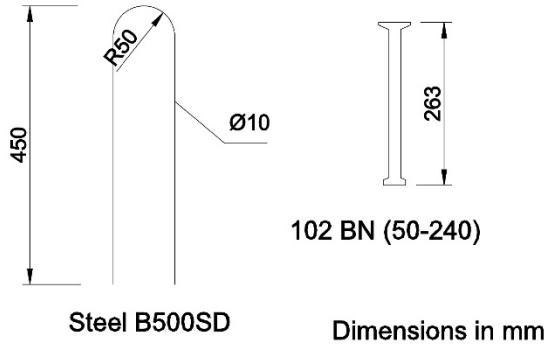

Figure 4.20. Lifting systems

As can be observed in Figures 4.14 and 4.15, shear reinforcement is different for B2C and B2R from the other beams. The reason was that these two beams were fabricated with less shear reinforcement (ø8/600 mm) than the others (ø10/125 mm), with the aim of being subjected to a shear failure test. The prestressing reinforcement consisted on 8 prestressing strands Y 1860 S7 with a nominal diameter of 13 mm, distributed as shown in Figure 4.19.

4.4.2. Fabrication of beams

Beams were fabricated and monitored following the procedure developed in Appendixes 4 and 5. After stressing strands, four strain gauges were adhered to strand no. 5 of each beam to determine the strain evolution during the fabrication and testing process (Figure 4.21). They were located at 1000 and 2750 mm far from each end of the beam. Six 200 KN load cells were placed on strands, 4 at the active anchor with special designed transition pieces and 2 at the passive anchor (Figure 4.22-4.24).

Figure 4.21. Strain gauge

Figure 4.22. Load cells active anchor

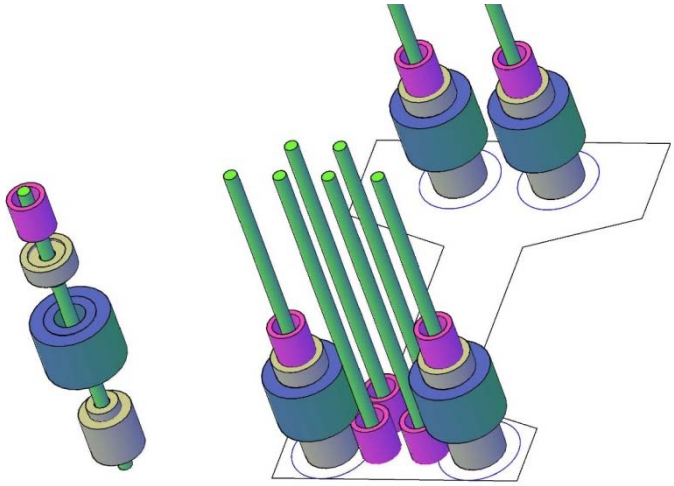

Figure 4.23. Load cell colocation with transition pieces at active anchor

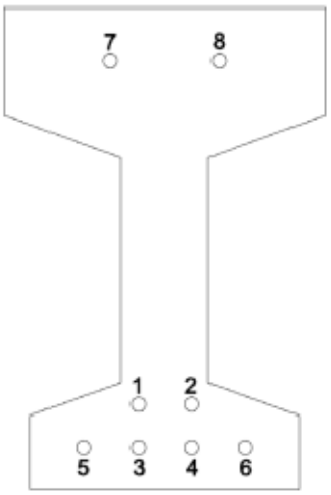

Figure 4.24. Strands numeration at active anchor

The force registered by the load cells when strands were stressed is shown in Table 4.15. Two shrinkage strain gauges were placed inside both sides of a beam of each type.

Table 4.15. Load cell force register at strands stressing

	Strand 5		Strand 6	Strand 7	Strand 8	
	Load cell 1 (kN)	Load cell 5 (kN)	Load cell 2 (kN)	Load cell 3 (kN)	Load cell 4 (kN)	Load cell 6 (kN)
Prestressing bed hydraulic actuator	-	-	-	16.82	21.38	21.34
Jack force (bar)						
50	15.10	15.86	17.02	-	-	-
100	37.35	38.49	37.90	34.52	36.82	38.38
150	-	-	60.00	53.00	55.54	53.43
200	76.93	79.27	79.00	72.30	75.12	73.04
250	96.38	97.38	98.50	89.24	93.63	91.45
300	118.00	118.00	120.60	107.40	112.29	110.09
330	130.10	130.30	131.00	117.50	121.73	119.82
No Jack	123.50	128.40	121.10	108.50	111.04	116.52

As well as the internal strain gauges, one gauge was adhered to a section of strand between two beams to check the elastic modulus of the steel (Figure 4.25). As seen in figure, stress registered by the load cells located on both sides of the strand is plotted against the strain registered by the gauge. The modulus of elasticity is calculated as the slope of these lines. The resulting mean value is around 210000 MPa, higher than the required value for this type of steel 190000 MPa.

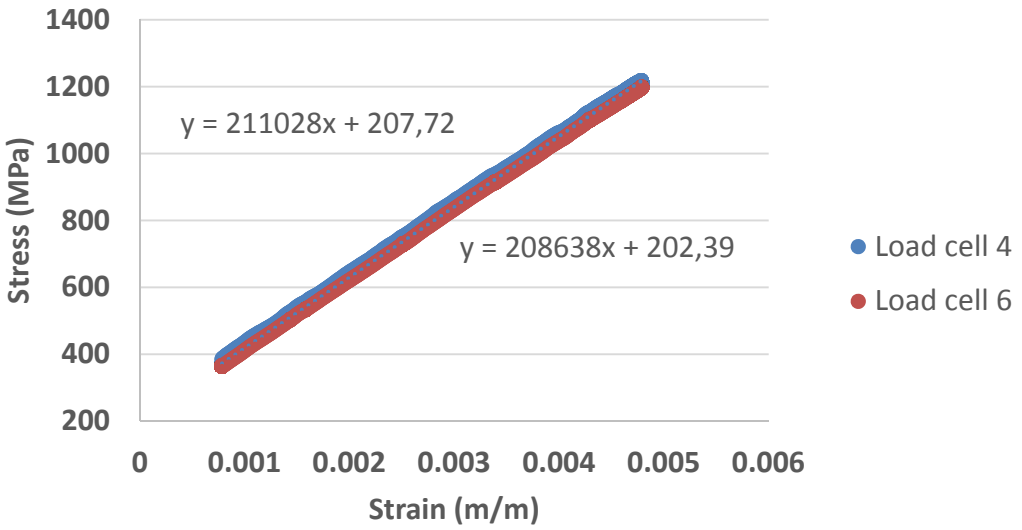

Figure 4.25. Stress vs. Strain (Strand 8)

As mentioned before, 4 beams were made of natural aggregate concrete (NAC) and the other 4 beams were made of 8% recycled aggregate concrete (RAC). It was necessary to prepare 3 batches of each mix composition to cast all of them (Figure 4.26). The slump test was performed for every mix (Figure 4.27) and 150x300 mm cylinders, 100x100x400 mm shrinkage prisms and 100 mm cubic samples were cast in order to have a quality control of the mixes (Figure 4.28).

During casting and concrete hardening, load cells and strain gauges were connected to a data acquisition system which was continuously registering the force transmitted by the prestressing strands and their strain. Moreover, several humidity and temperature dataloggers were installed in the precast plant in order to have a register of the curing environment.

Figure 4.26. Beams casting

Figure 4.27. Slump test

Figure 4.28. Quality control moulds

When beams gained enough strength, lateral formwork was removed and beams were named as indicated in Figure 4.13. DEMEC gauge points (Figure 4.29) were adhered on both ends of the bottom flange of one beam of each type (NAC and RAC) and were located 1500 mm far from each beam end every 50 mm. DEMEC points are necessary to determine the transfer length of the beams.

Figure 4.29. DEMEC gauge points

After releasing the prestressing force with the hydraulic actuator of the prestressing bed, strands between beams were cut (Figure 4.30). All of the beams were transported to the Centro de Innovación Tecnolóxica en Edificación e Enxeñería Civil (CITEEC) at the University of A Coruña, for being externally monitored and tested.

Figure 4.30. Strand cutting

4.4.3. Prestressing force transfer and immediate losses

Prestressing force was transferred to concrete 6 days after casting. The force was progressively released by the hydraulic actuator of the prestressing bed. During this process, immediate losses and free-end slips were measured for a better knowledge of the force transferred to concrete.

Linear displacement sensors were previously attached to the bottom flange strands in order to register their free-end slip at transference (Figure 4.31 and Table 4.16). These slips and that of the strands at the top flange of the beam were also measured with a depth gauge. Values are shown in Tables 4.17 and 4.18.

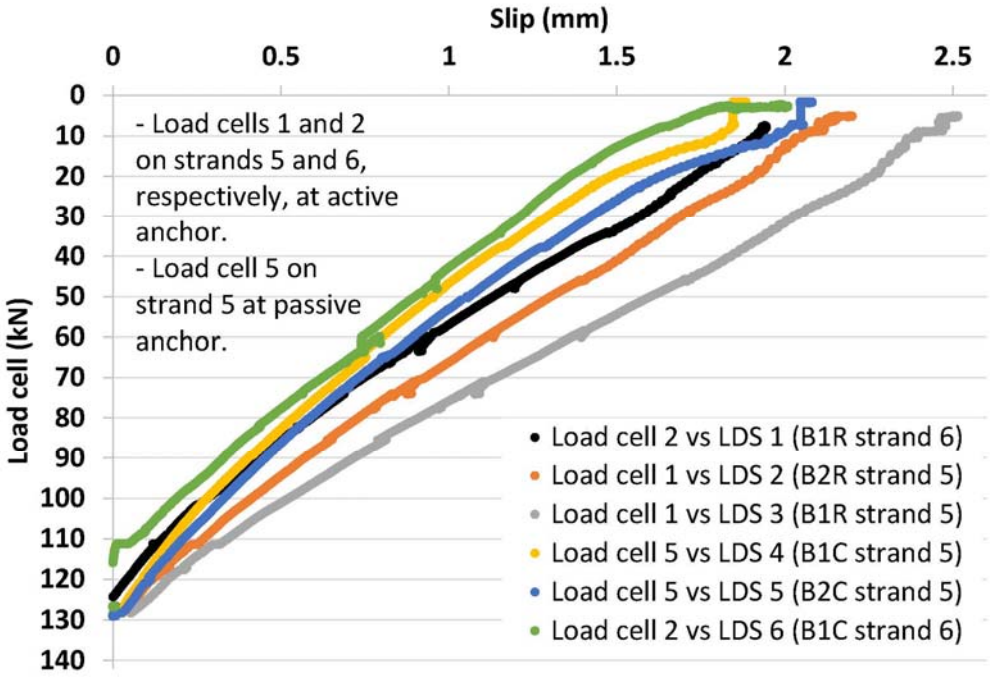

Figure 4.31. Free end-slip at transfer

Table 4.16. Free end-slip at transfer measured with linear displacement sensor

Linear displacement sensor	Position	Max. Free end-slip (mm)
LDS 1	B1R - North (Strand 6)	1.944
LDS 2	B2R - South (Strand 5)	2.200
LDS 3	B1R - North (Strand 5)	2.515
LDS 4	B1C - South (Strand 5)	1.884
LDS 5	B2C - North (Strand 5)	2.081
LDS 6	B1C - South (Strand 6)	2.009

As seen in Table 4.16 maximum slips registered with the linear displacement sensors are higher for recycled concrete beams with a maximum slip of 2.515 mm than in natural concrete beams with a maximum slip of 2.009 mm.

Table 4.17. Free-end slip at transfer measured with depth gauge. North side (mm)

Strand	B1R	B2R	B3R	B4R	B4C	B3C	B2C	B1C
1	2.3	1.2	1	0.9	1.6	1.8	1.7	-
2	1.8	0.8	0.5	1.1	1.3	3.1	0.6	-
5	2.1	-	1.6	1.8	2.2	1.7	4.7	-
6	2.1	0.8	0.6	1.6	2.4	1.1	1.4	-
7	1.9	1.8	1.8	2	2.6	2.8	2.7	2.6
8	3.2	2.5	1.8	1.8	2.5	2	2.2	2.4

Table 4.18. Free-end slip at transfer measured with depth gauge. South side (mm)

Strand	B1R	B2R	B3R	B4R	B4C	B3C	B2C	B1C
1	-	1.4	1.3	-	2.2	1.6	2.1	-
2	-	2	1.6	2.1	1.9	2.1	1.8	-
5	-	2.4	1.4	1.3	1.8	1.6	-	-
6	-	2	1.7	0.7	5.9	1.1	1.2	-
7	0.3	1.7	2.7	3.4	2.2	3.1	2.3	-
8	1.9	2.7	2.5	1.9	2.7	2.7	2.2	-

As seen in Tables 4.17 and 4.18, measures taken with the depth gauge are not as precise as measures taken with linear displacement sensors, but give an idea of the other strands' slip at transfer.

Camber and elastic shortening at the top and bottom flanges of the beam were measured before and after transfer with a measuring tape. These values are shown in Tables 4.19 and 4.20.

Table 4.19. Camber at mid-span after transfer

	B1R	B2R	B3R	B4R	B4C	B3C	B2C	B1C
Camber (mm)	4.5	7	7.5	8.2	7.4	4.2	5.9	4.8

Strain registered at transfer by internal strain gauges on strand 5 is useful to determine immediate losses after transfer. With a known elastic modulus and strand area, it is possible to determine the loss of prestressing force according to the deformation of the strand and the force registered by the load cell prior to release (Table 4.21).

Table 4.20. Elastic shortening at transfer

		Beam length (mm)							
	Flange	**B1R**	**B2R**	**B3R**	**B4R**	**B4C**	**B3C**	**B2C**	**B1C**
Before transfer	**Top**	-	6478	6493	6503	6501	6492	6508	6529
	Bottom	-	6438	6430	6456	6484	6465	6466	-
After transfer	**Top**	-	6475	6485	6503	6499	6491	6506	6525
	Bottom	-	6437	6426	6455	6479	6464	6462	-
		Elastic shortening (mm)							
	Top	-	3	8	0	2	1	2	4
	Bottom	-	1	4	1	5	1	4	-

Table 4.21. Immediate losses strand 5

	Strain at transfer (µm/m)	**Force loss (kN)**	**Immediate prestress losses (%)**
Beam B1R	-605.20	-12.71	- 9.90
Beam B3R	-612.05	-12.85	- 10.01
Beam B4R	-614.10	-12.90	- 10.05
Beam B4C	-533.28	-11.20	- 8.73
Beam B3C	-546.69	-11.48	- 8.95
Beam B1C	-460.69	-9.67	- 7.54

As seen in the previous table, immediate losses are by 25% higher for beams with recycled aggregate.

4.4.4. Quality control of the elements

For each of the mixes, the workability was studied through the slump test to evaluate the fresh state properties. Density and compressive strength at 7 and 28 days were also studied to evaluate the hardened state properties. Samples were kept inside an environmental chamber between 16 hours and 3 days before demoulding according to the UNE-EN 12390-2:2009 Standard. The curing conditions inside the chamber were 20±2 °C temperature and relative humidity higher than 95%. After demoulding, the samples continued inside the environmental chamber for an appropriate curing until the age of testing.

Workability

The slump test was performed according to the UNE-EN 12350-2:2009 Standard to assess the consistency of the concrete mix. The measured values for the different mixes are shown in Table 4.22.

Table 4.22. Slump test

Mix	Slump (cm)	Mix	Slump (cm)
NAC-1	25	RAC 8%-1	23
NAC-2	24	RAC 8%-2	25
NAC-3	25	RAC 8%-3	25

As observed in the table, the slump values obtained in the plant were higher than the values obtained in the laboratory (19 and 21 cm for F-0 and F-8, respectively). The main reason is that the quantity of superplasticiser added in the plant was by 40% higher than the quantity added in the laboratory (5 Kg/m^3 and 3.57 kg/m^3, respectively).

These values are higher than the limit established by de EHE for a liquid consistency (20 cm).

Density

Density of hardened concrete was measured following the UNE-EN 12390-7:2009 Standard for the cubes tested at the age of 28 days. The measured values are shown in Table 4.23.

Table 4.23. Mean density

Mix	Mean density (Kg/m^3)	Δ (%)
NAC	2483	
RAC 8%	2460	-0.93

As expected, the mean density of the hardened concrete was decreased due to the lower particle density of recycled aggregate in comparison with natural aggregate.

The loss of density is similar to that obtained in the laboratory for the same replacement level (-0.92%).

Compressive strength

The compressive strength was evaluated according to the UNE-EN 12390-3:2009/AC:2011 Standard. Three 100 mm cubes were tested at 7 and 28 days and the mean value was calculated. The results are shown in Table 4.24.

Table 4.24. Compressive strength (cubic)

Mix	7 days		28 days	
	Compressive strength (MPa)	Δ (%)	Compressive strength (MPa)	Δ (%)
F-0	60.4		68.2	
F-8	58.1	-3.8	66.3	-2.8

Similarly to the results obtained in the laboratory, the compressive strength at 7 and 28 day slightly decreases when 8% of the total natural aggregate is replaced by the recycled aggregate. However, the values obtained in plant are by 6.5% higher than the values obtained in the laboratory for both mix compositions.

4.5. Pull-Out Bond Tests

4.5.1. Introduction

Pull-Out bond tests were performed as part of the study on the loss of bond capacity when recycled aggregate is introduced in concrete. This test was designed to simulate the bond behaviour along the flexural bond length and it is based on the Moustafa Pull-Out Test [LOGA 1997] and the tests performed by Eiras-López [EIRA 2009] in his doctoral thesis. It consists on measuring the free-end slip of untensioned strands pulled from 150x300 mm concrete cylinders. For this test, 5 specimens were fabricated for the mix composition studied in laboratory with 0% replacement of the total aggregate and 5 samples for the mix with 8% replacement.

4.5.2. Specimens fabrication

Moulds for the fabrication of the specimens must be prepared at least one day before casting. Silicon is used and it is recommended to wait at least 24 hours for an appropriate hardening. Specimens were fabricated according to the following procedure:

The moulds used for this test were the typical moulds for casting 150x300 mm cylinders, but with the particularity of having a hole at the centre of the base, with an appropriate diameter for the prestressing strand (Figure 4.32).

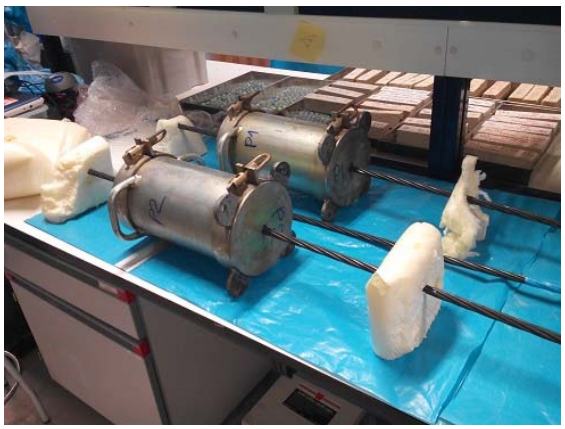

Figure 4.32. Pull-Out moulds

The section of strand tested has to be at least 1200 mm long. It was introduced through the hole of the base with the distribution depicted in Figure 4.33.

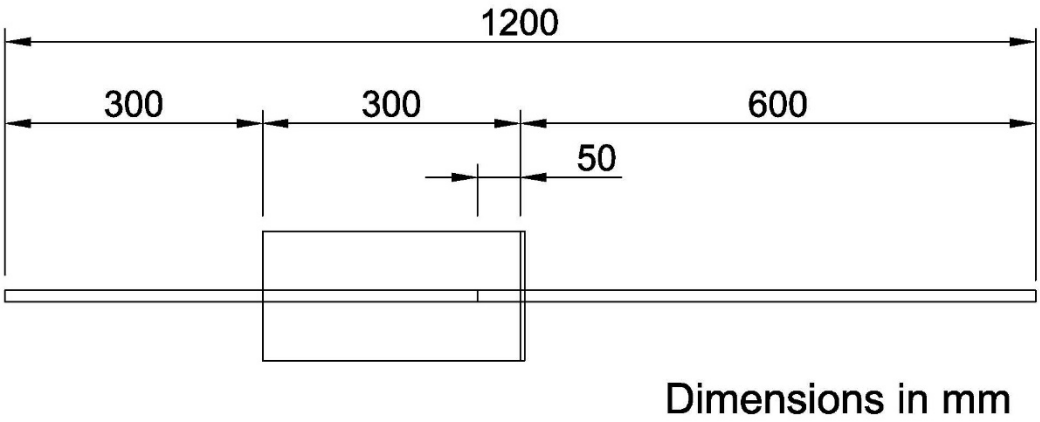

Figure 4.33. Strand distribution in mould

The first 50 mm of strand measured from the base of the mould were covered with insulating tape as a bond breaker, preventing from adhesion between steel and concrete at the bottom of the specimen (Figure 4.34).

The remaining void around the prestressing strand at the hole of the base was sealed with silicon on the outside surface to avoid water loss during the casting and hardening process (Figure 4.35).

Figure 4.34. Bond breaker

Figure 4.35. Silicon sealing

It is necessary to wait at least 24 hours until silicon hardens. After that, moulds were transported to a table with several holes through which strands were introduced. It is recommended to elevate the base of the mould from the table at least 10 cm. This space was used to support the weight of the strand against the table with special clams in order not to damage the silicon sealing.

After the moulds were cast, strands must remain completely vertical, so special pieces of porexpan with a central hole were designed to be adapted at the top side of the mould maintaining the necessary verticality (Figure 4.36).

Figure 4.36. Specimens after casting

Moulds must not be moved from the place where they were cast in order not to damage the silicon sealing between the strand and the mould base. It was necessary to wait 24 hours before being demoulded. Then, they were transported to an environmental chamber until the age of testing.

4.5.3.Test procedure

All specimens were tested at 28 days. The pull-out test consists on pulling the strand from the bottom of the specimen with a void hydraulic actuator while the free-end slip is registered. The force transmitted and the free-end slip are measured with a load cell and a linear displacement sensor, respectively.

Before placing the specimen on the hydraulic actuator, the strand was marked at a distance of 50 cm from the bottom face of the specimen (Figure 4.37). This mark is necessary to determine the length of strand subjected to test.

Then, the specimen was placed on the base of the hydraulic actuator according to the circle previously drawn to set the strand completely in the centre of the hole (Figure 4.38).

Figure 4.37. Mark to determine length subjected to test

Figure 4.38. Specimen on hydraulic actuator base

A 10 mm linear displacement sensor (LDS-10) was attached to the strand with a piece specially designed for this purpose, as shown in Figure 4.39. The LDS-10 was brought closer to the top face of the specimen in order to look for a surface of at least a 2x2 cm as flat as possible. This surface was smoothened and metallic piece of 1.5x1.5 cm was fixed with an epoxy. This piece offers the LDS-10 a plain surface to make contact and avoid reading errors (Figure 4.40).

Figure 4.39. Linear displacement sensor

Figure 4.40. Metal piece between LDS-10 and concrete surface

A 50 mm linear displacement sensor (LDS-50) was attached nearly closed to the hydraulic actuator with a clamp, making contact with the bottom side of the base, as shown in Figure 4.41. This LDS is necessary to control the test by displacement at a rate of 0.05 mm/s.

LDS-10 was tightened to the strand at its final position, making contact on the centre of the metallic piece but as open as possible (Figure 4.42); for example, when the data acquisition system is measuring 0.5 mm.

Figure 4.41. LDS-50 attached to hydraulic actuator

Figure 4.42. LDS-10 at its final position

Before introducing the load cell at the bottom of the strand, the hydraulic actuator was started to allow the oil to flow through the hoses and to check for proper operation.

The inner part of a grip was coated with molybdenum bisulfate or commercial grease for an easier removing of the wedge after the test.

The hydraulic actuator was completely closed and then, the load cell was introduced at the bottom side of the strand, followed by a transition piece, the grip and the wedge, as seen in Figure 5.43. It was necessary to use a hammer to hit the wedge and the grip until there was no gap between the load cell and the structure that supports the actuator.

After that, the distance between the mark located at 50 cm from the bottom face of the specimen and the end of the wedge was measured. The difference determines the strand length subjected to test (Figure 5.44).

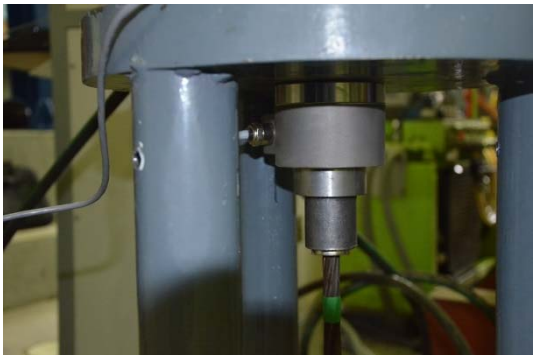

Figure 4.43. Load cell, transition piece, grip and wedge

Figure 4.44. Distance from wedge end to 50 cm mark

The test rate was established at 0.05 mm/s, the data acquisition system was configured to save data every 0.1 seconds and the test was finally initiated.

During the test, it is very important to observe the slip measured by LDS-10. The sensor has a maximum range of 10 mm and can be damaged if this value is exceeded. Therefore, the test must be always stopped before this happens.

When the slip detected was between 5 and 6 mm, the test was stopped, the hydraulic actuator returned to its initial position and data saved.

4.5.4.Results and discussion

The testing technique to simulate bond behaviour and calculate bond stress is depicted in Figure 5.45. τ is the bond stress, in MPa; ΔP is the force at which the strand is pulled by the actuator, in N; d_b the strand diameter, in mm; and L is the length of the strand embedded in concrete, in mm.

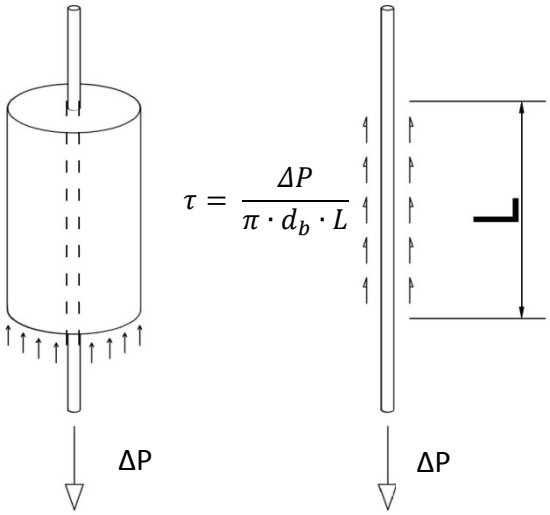

Figure 4.45. Testing technique to simulate bond behaviour

Considering the diameter of the strand as 12.9 mm and the embedded length as 250 mm, since the first 50 mm of the strand from the base of the mould were covered with insulating tape, the average bond stress of the 5 specimens made of solely natural aggregate and the 5 specimens with 8% replacement of the total aggregate are depicted in Figure 5.46.

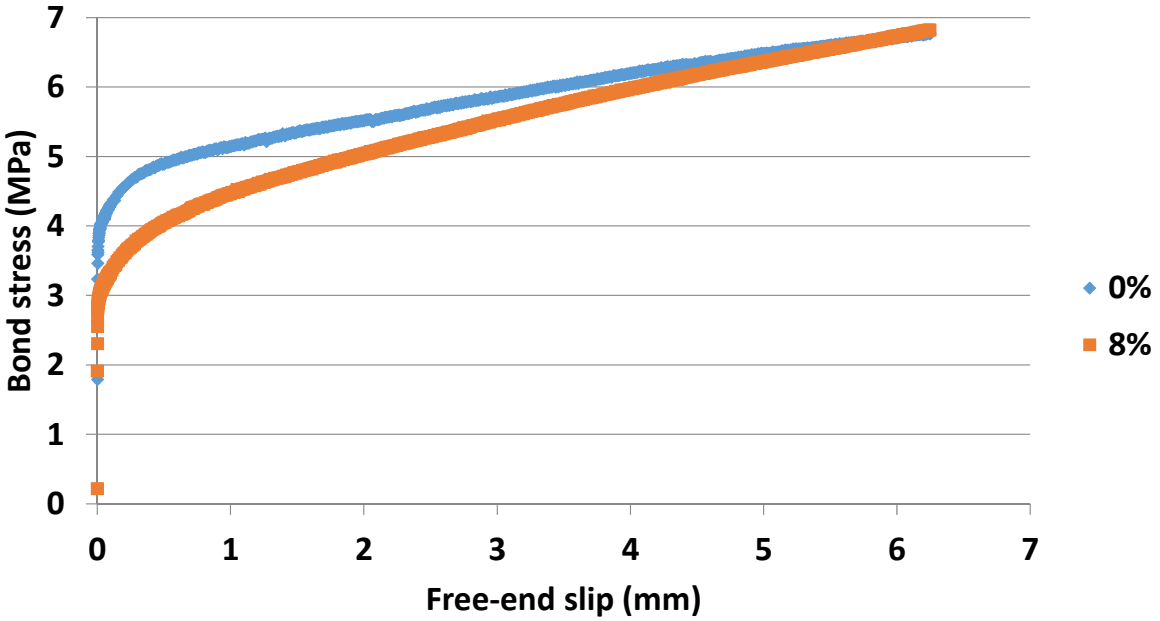

Figure 4.46. Average bond stress vs. Free-end slip

As can be observed in previous figure, the average bond stress was increased, without any slip, in both replacement ratios until a value of 3.84 and 2.93 MPa for 0 and 8% replacement, respectively. These values correspond to bond stress when a slip of 0.01 mm is achieved. Then, slip continued at a faster rate as the pulling force was increased.

The stress increase at the lower end causes a loss of contact by the Poisson effect in response to the strand diameter contraction. This loss of contact destroys the bond between strand and concrete, reducing friction and causing slip at the free end.

From the Pull-out test performed, it can be concluded that the bond stress at which the first slip occurs is approximately 24% lower when 8% of the total aggregate is replaced with recycled aggregate. This loss in bond behaviour is important, considering that only 8% of the total aggregate was replaced.

Chapter 5. Transfer and development length of prestressed concrete beams

5.1. Transfer length

5.1.1. Introduction

The transfer length (L_t) is defined as the distance from the end of the member over which the fully effective prestressing force is developed.

As mentioned in chapter 5, DEMEC gauge points adhered to the bottom flange surface of both ends of the beams were used to determine the transfer length.

5.1.2. Test procedure

The demountable mechanical strain gauge (DEMEC) consists of a standard or a digital dial gauge attached to an invar bar. A fixed conical point is mounted at one end of the bar, and a moving conical point is mounted on a knife edge pivot at the opposite end. The pivoting movement of this second conical point is measured by the dial gauge.

A setting out bar is used to position pre-drilled stainless steel discs which are attached to the structure using a suitable adhesive. Each time a reading has to be taken, the conical points of the gauge are inserted into the holes in the discs and the reading on the dial gauge noted. In this way, strain changes in the structure are converted into a change in the reading on the dial gauge.

With this method, transfer length is defined as the distance from the end of the member over which the strain measures are stabilized, which is an indicative of that the fully effective prestressing force has been developed.

Gauge points were adhered to the bottom flange surface of B1C and B1R every 50 mm along the first 1500 mm from each end of the same face of the beam. Measures were taken with a digital dial gauge attached to an invar bar 150 mm immediately before and after transferring the prestressing force, as well as at 7, 14, 28, 90 and 300 days after casting (Figure 5.1).

Figure 5.1. DEMEC Points measurement

Strain values were calculated comparing the reference values measured before transferring the prestressing force with the values taken at the different ages.

5.1.3. Results and discussion

The selected method to determine the transfer length was the 95% Average Maximum Strain Method (AMS) discussed by Russell [RUSS 1992]:

1. Plot the strain profile.
2. Determine the MAS for the specimen by computing the numerical average of all the strains contained within the strain plateau of the fully effective prestress force.
3. Multiply the AMS by 0.95 and construct a line corresponding to this value.
4. Transfer length is determined by the intersection of the 95% line with the strain profile.

An example of the procedure is shown in Figure 5.2 for the estimation of BC1 transfer length at 28 days.

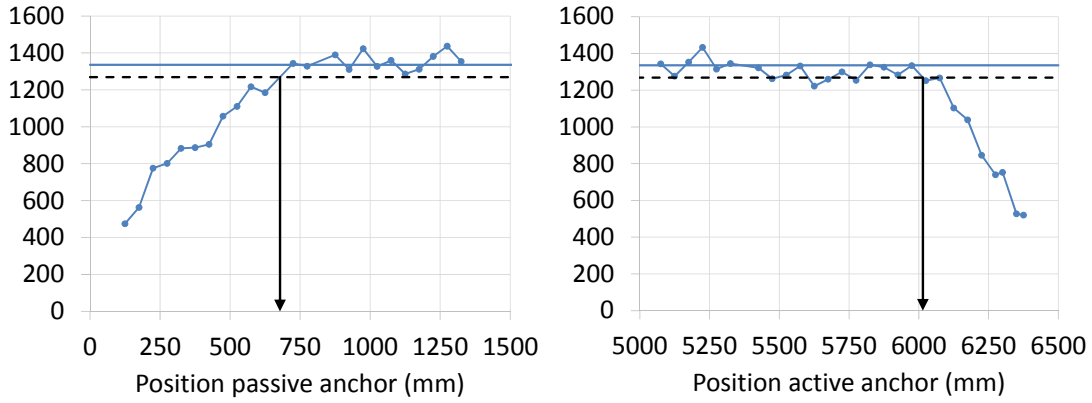

Figure 5.2. Transfer length B1C at 28 days with the 95% AMS method

Transfer length was determined with this method for both beams immediately after transfer and at 7, 14, 28, 90 and 300 days after casting. The strain values evolution is depicted in Figures 5.3 and 5.4 for B1C and B1R, respectively, at different ages.

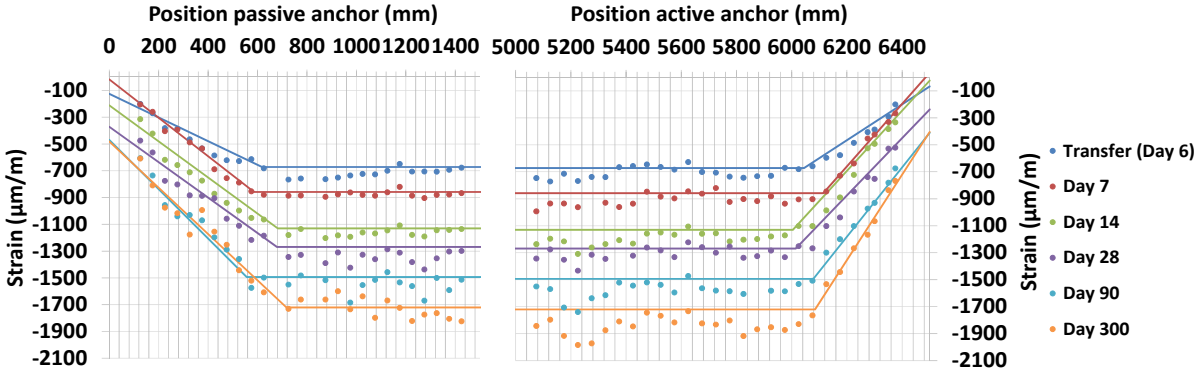

Figure 5.3. Transfer length B1C

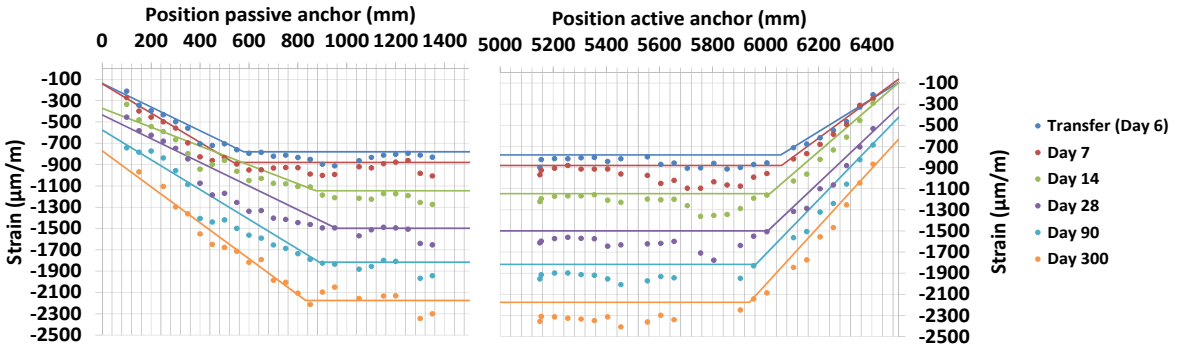

Figure 5.4. Transfer length B1R

Table 5.1 summarizes the transfer length and maximum strain value of the plateau at different ages on both sides of the beams.

Table 5.1. Transfer length and maximum strain

Age	B1C			B1R		
	Transfer length (mm)		Strain (μm/m)	Transfer length (mm)		Strain (μm/m)
	Passive anchor (North)	Active anchor (South)	Plateau	Passive anchor (North)	Active anchor (South)	Plateau
Transfer	618	455	-672	578	442	-780
Day 7	586	386	-858	537	440	-880
Day 14	683	496	-1131	874	484	-1146
Day 28	678	485	-1269	957	491	-1499
Day 90	556	422	-1494	888	537	-1816
Day 300	717	415	-1721	832	560	-2175
Max.	717	496	-1721	957	560	-2175

As seen in previous table, the detrimental effect of 8% replacement of recycled aggregate on transfer length and maximum strain is noticeable.

The transfer length of B1R is clearly higher than in B1C, especially at late ages. If the maximum values are compared, transfer length was increased 33 and 13%, at passive and active anchor, respectively, when 8% recycled aggregate was introduced in the mix. If the strain values of the plateaus are compared, they follow the same trend and increase with time. The strain value of the B1R plateau at the last measured age (300 days) was 26% higher than that of the B1C plateau.

This increase in transfer length agrees with the loss of bond detected in the pull-out tests, when the bond stress at which the first slip occurred (0.01 mm) was approximately 24% lower when 8% of the total aggregate was replaced with recycled aggregate.

Another detrimental effect of the recycled aggregate on transfer length can be observed in its evolution over time. If the transfer length measured immediately after transferring the prestressing force is compared with the maximum length, at both sides of the beams, it can be concluded that the increase of transfer length over time is higher for beams with recycled aggregate than in beams with only natural aggregate. In B1C, this value was increased 16 and 9% at passive and active anchor, respectively. While, in B1R the increase was considerably higher, 66 and 27 % at passive and active anchor, respectively.

As mentioned in Chapter 2, several authors proposed equations for transfer length based on the slip detected at transfer. These equations are summarized in Appendix 1 and the values introduced in the equations are included in Table 5.2. The predicted transfer lengths for each of the equations, considering an average value of the slip of 1.99 mm for natural

concrete beams and 2.24 mm for 8% recycled concrete beams, are shown in Table 5.3 and Figure 5.5.

Table 5.2. Values introduced in equations

	B1C		B1R	
	MPa	**ksi**	**MPa**	**ksi**
E_p	190000	27556.2	190000	27556
f_{pi}	1270	184	1270	184
f'_{ci}	48.32	7.01	46.48	6.74
f_{pe}, f_{se}	1016	147	1016	147
σ_{pd}, f_{pu}	1860	270	1860	270
f'_c	54.56	7.91	53.04	8.13
f_{ctd}	3.64	0.53	3.5	0.51
	mm	**in.**	**mm**	**in.**
δ	1.99	0.078	2.24	0.088
d_b	12.7	0.50	12.7	0.50
	mm2	**in.2**	**mm2**	**in.2**
A_s	100	0.155	100	0.155

Where E_p is the modulus of elasticity of the strand; f_{pi} is the strand stress before release; f'_{ci} is the compressive stress at transfer; f_{pe} and f_{se} are the effective stress in the prestressed reinforcement after all losses; σ_{pd} and f_{pu} are the stress in prestressed reinforcement at nominal strength; f'_c is the compressive strength of concrete at 28 days; f_{ctd} is the concrete tensile strength at transfer; δ is the slip of the prestressing strand at transfer; d_b is the diameter of the strand; and A_s is the cross-sectional area of the strand.

Table 5.3. Transfer length based on slip at transfer

	B1C (mm)	B1R (mm)
Guyon (mm) [GUYO 1953] and Larson et al. [LARS 2007]	595	670
Marshall and Krishnamurthy [MARS 1969]	754	800
Balázs [BALA 1992]	655	691
Balázs [BALA 1993]	707	766
Rose and Russell [ROSE 1997]	732	807
Russell and Burns [RUSS 1996]	577	650
Oh et al. [OH 2014]	704	750
Current research	717	957

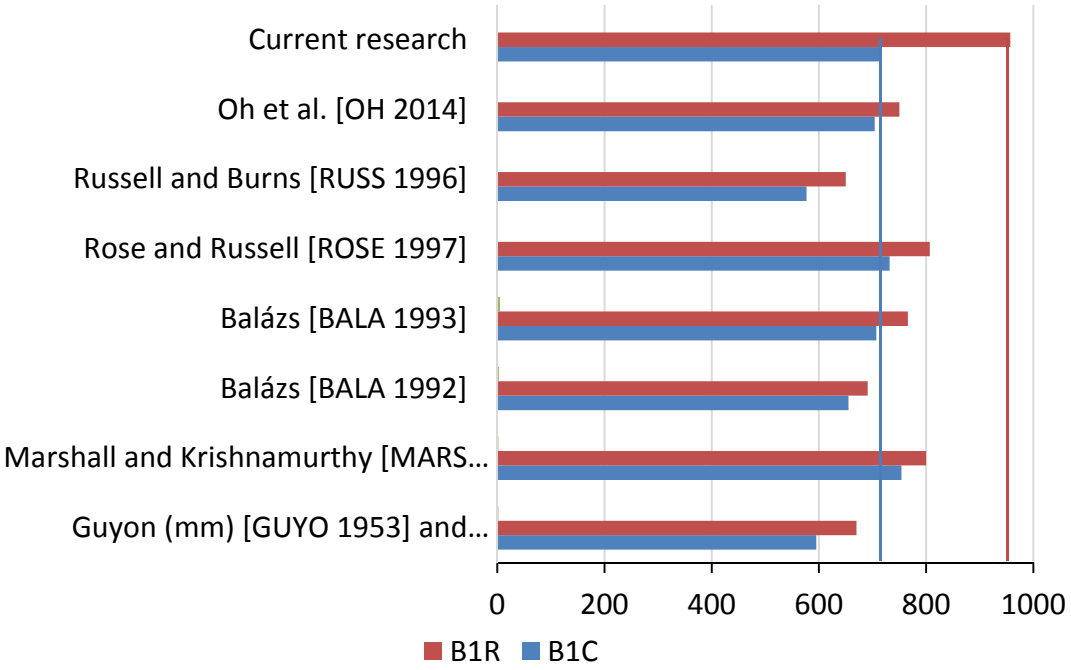

Figure 5.5. Transfer length based on slip at transfer

As can be observed in previous table, the maximum transfer length obtained from the DEMEC points measurements for B1C is in the range of values predicted by the proposed equations; specially, Balázs [BALA 1993] and Rose and Russell [ROSE 1997] with values very close to the experimental. However, in the case of B1R all the equations based on slip at transfer are non-conservative, with values significantly lower than the measured one.

Other authors and Codes propose equations to predict transfer length based on the prestressing force of the strand and properties of concrete at transfer (Table 5.4 and Figure 5.6). These equations are also summarized in Appendix 1 and the values introduced are included in Table 5.2.

Table 5.4. Transfer length based on strand and concrete properties

	B1C (mm)	B1R (mm)
Hanson and Kaar [HANS 1959]		
Kaar et al. [KAAR 1963]	624	623
ACI 318-63 - ACI 318-14		
Zia and Mostafa [ZIA 1977]	384	404
Martin and Scott [MART 1976]	1016	1016
AASHTO 92	635	635
Mitchell et al. [MITC 1993]	505	515
Deatherage et al. [DEAT 1994]	780	780
Buckner [BUCK 1995]	780	780
AASHTO 97	762	762
Russell and Burns [RUSS 1996]	936	936
Russell and Burns [RUSS 1997]	624	624
Lane [LANE 1998]	1055	1089
Mahmoud et al. [MAHM 1999]	500	513
Shahawy [SHAH 2001]	780	780
Eurocode 2 [CEN 2004]	263	274
Kose and Burkett [KOSE 2005]	1249	1267
Martí-Vargas et al. [MART 2006]	437	446
Martí-Vargas et al. [MART 2007a]	444	456
Ramirez and Russell [RAMI 2007]	576	587
EHE 2008 [EHE 2008]	458	458
MC – 2010 [MC 2010]	359	373
AASHTO LFRD 2012	762	762
Martí-Vargas et al. [MART 2012b]	532	546
Oh et al. [OH 2014]	459	465
Current research	717	957

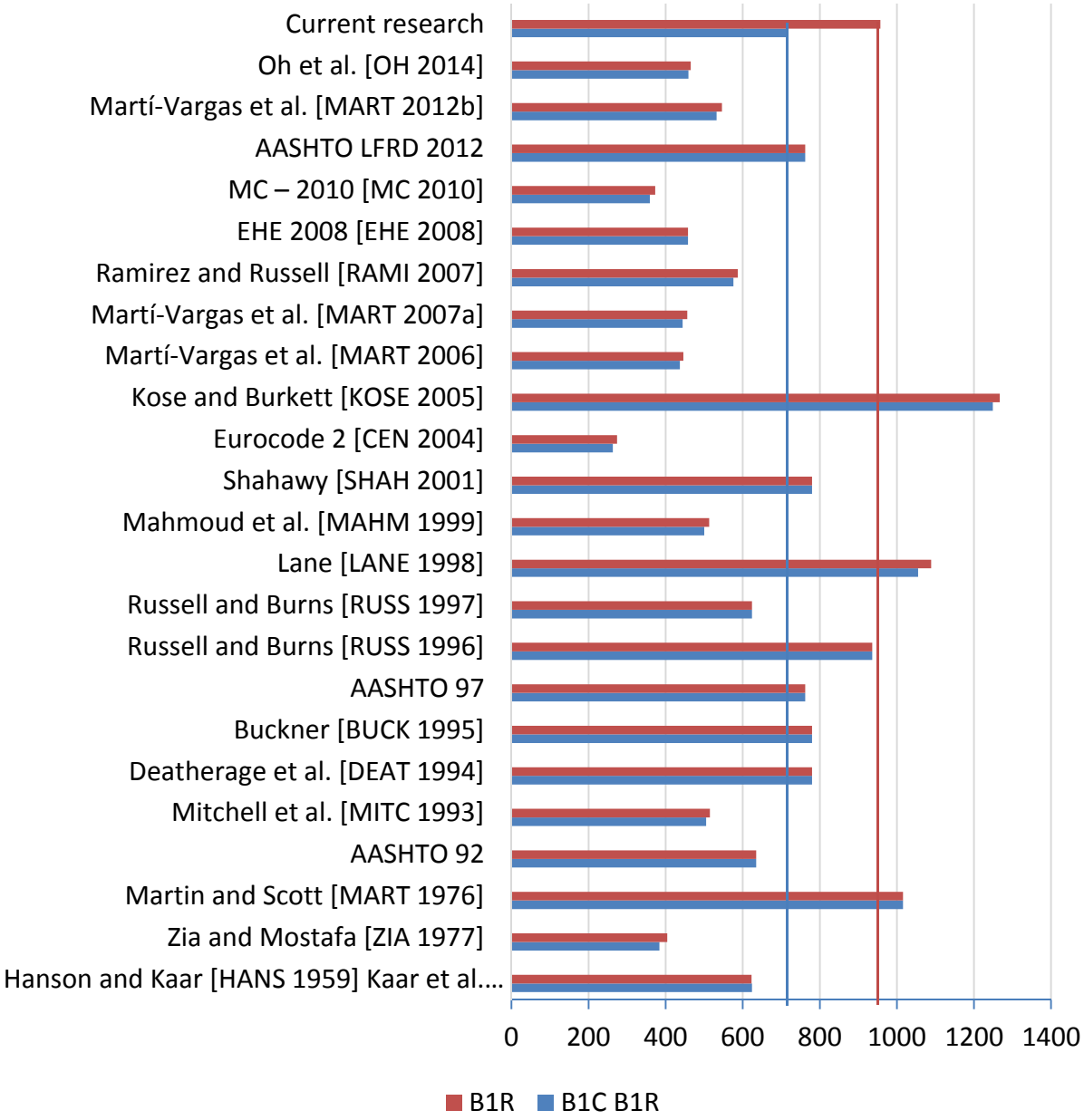

Figure 5.6. Transfer length based on strand and concrete properties

The experimental value of transfer length in B1C agrees with the value predicted by some of the proposed equations. It differs less than 9% from the equations proposed by Deatherage et al. and Buckner and Shahawy; and differs by 6% from the equation proposed by the AASHTO LFRD 2012. In the case of B1R, most equations propose values lower than the experimental one due to the presence of recycled aggregate and its lower bond performance. With the exception of Martin and Scott; Lane; and Kose and Burkett equations that predict higher values, all of the other equations are significantly non-conservative when 8% recycled aggregate is introduced in the mix composition.

If the experimental values of transfer length are compared with the experimental values of other authors when 12.7 mm strands are tested, transfer length in B1C agrees with the values obtained by Russell and Burns [RUSS 1996], who measured a transfer length of 749 mm for fully bonded strands; and Larson et al. [LARS 2007] with 740 mm for T-Shape specimens. Pozolo and Andrawes [POZO 2011a] measured a slightly higher value, 952 mm for T-Beams; and Floyd et al. [FLOY 2011] measured a shorter value, 511 mm, but in this case it was a light weight self-compacting concrete. Martí-Vargas et al. [MART 2012a] obtained transfer lengths between 400 and 550 mm with the ECADA test method, depending on the cement content and water/cement ratio; and Logan [LOGA 1997] obtained transfer lengths of 508 and 1143 mm at 21 days for strands with an average pull-out bond capacity exceeding 160 kN and less than 53.3 kN, respectively.

Studies on the influence of recycled aggregate on the transfer length have were not found, so it was not possible to compare the experimental results with that of the other authors.

5.2. Flexural bond length and development length

5.2.1. Introduction

The development length (L_d) is defined as required to develop the strand stress to ultimate stress at the ultimate flexural strength of the member. The tension reached at this point has to be the maximum stress of the prestressing steel. The difference between the transfer length and the development length is known as the flexural bond length (L_{fb}).

To determine development length, prestressed beams were subjected to a flexural test controlled by displacement at various embedment lengths.

5.2.2. Test procedure

The beams were subjected to a four-point bending test, with a total span length of 6.20 m, loading by two symmetrical concentrated loads. Schemes for the tests are depicted in Figures 5.7 - 5.9. The flexural test equipment was designed and used on previous research [VAZQ 2001, 2013a, 2013b and 2013c]. The load was applied with a hydraulic actuator attached to a steel frame. The actuator was controlled by displacement with a 250 mm wire linear potentiometric transducer attached to the actuator and to the distribution steel profile. The speed of the test was set to 0.05 mm/s. The deflection at mid-span was measured for each test with a 500 mm wire linear potentiometric transducer. The strain values on both sides of the beam in two sections were measured with strain gauges adhered to the concrete surface. Linear displacement sensors were attached to the bottom strands to register the free-end slip during the test. The force transmitted to the beams B3C, B4C and B4R was measured with two load cells, each of them placed between the beam and the

corresponding support and beams were tested to failure. While the force transmitted to the beams B3R, B1R and B1C was measured with an oil pressure transducer, previously calibrated, because one of the load cells was damaged in B4R test. For these last three beams, it was taken the decision to stop the test when the bending moment was higher than the nominal moment calculated. The aim of this decision was to avoid damaging the linear displacement sensors attached to the strands if an abrupt failure happened again.

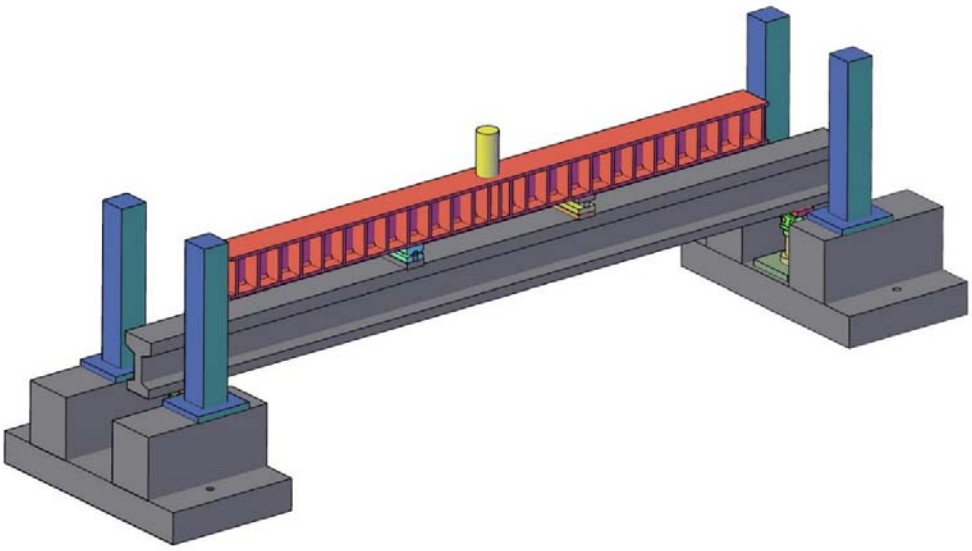

Figure 5.7. Development length test model

Wire linear potentiometric transducers, load cells, pressure transducer, strain gauges and linear displacement sensors were all connected to the data acquisition device registering the measures every 0.1 s. During the tests, the crack widths and crack patterns were observed and marked on the surface of the beam for a later analysis.

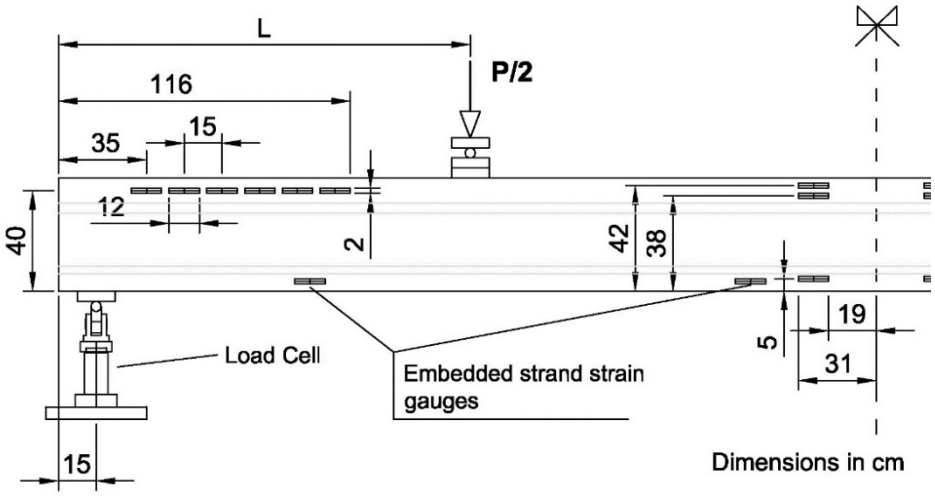

Figure 5.8. Schematic test set-up for B3C, B4C and B4R

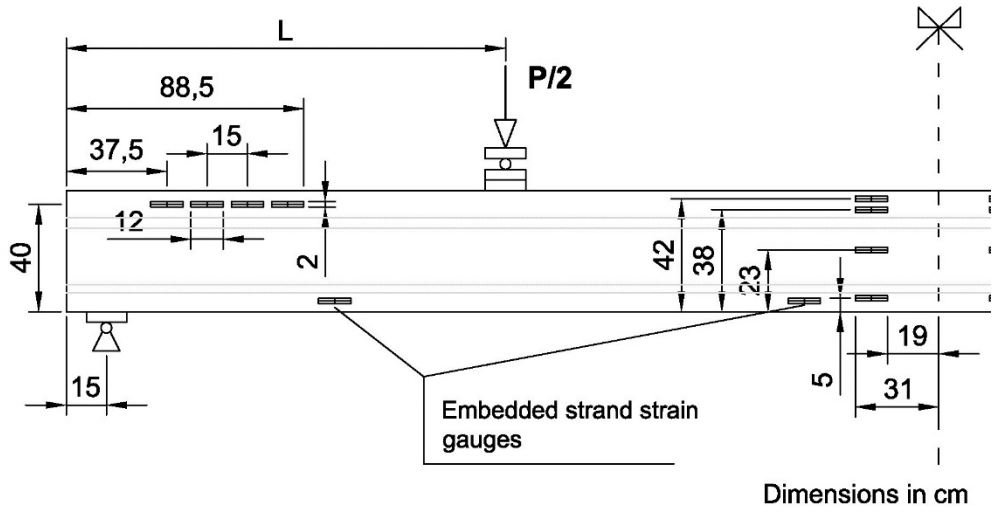

Figure 5.9. Schematic test set-up for B3R, B1R and B1C

The criterion used to determine the development length is a trial and error method which consists on trying an initial embedment length and decide, according to ultimate moment – nominal moment ratio, the strands slip values and the curve bending moment vs. deflection, if the following beam needs to be tested at a shorter or longer embedment length.

According to Ramirez and Russell [RAMI 2007], it is not uncommon for strand end slips to be measured even though a beam fails in flexure. Larson et al. [LARS 2007] established 0.25 mm as the limit established for additional slip occurred during loading. Andrawes and Pozolo [ANDR 2013] considered a slip of 1.6 mm as negligible. Mitchell et al. [MITC 1993] claimed that a small slip observed at the end of the strand prior to flexural crushing does not have to be considered a bond failure. The specimens which failed by first exhibiting significant strand slip, followed by a premature failure in either shear or flexure, were classified as bond failures. Kahn et al. [KAHN 2012] defined the development length as the minimum embedment length at which the girder failed in a flexural mode while reaching its theoretical flexural capacity with less than 2 mm bond slip.

Therefore, the criterion followed is depicted in Figure 5.10. If the ratio ultimate moment (M_u) – nominal moment (M_n) is lower than 1.0, there will be a Shear-Bond/Bond failure **(S-B/B)** when the maximum strand slip detected (δ) by the linear displacement sensors at bottom strands will be higher than 0.5 mm, this implies that the embedment length (L_e) is shorter than the development length (L_d); or a Flexural-Shear/Shear failure **(F-S/S)** when the maximum strand slip detected (δ) will be lower than 0.5 mm.

If the ratio ultimate moment (M_u) – nominal moment (M_n) is higher than 1.0, there will be a flexural failure **(F)** when the maximum strand slip detected (δ) by the linear displacement sensors at bottom strands will be lower than 0.5 mm, this implies that the embedment

length (L_e) is higher than the development length (L_d); or a Flexural Bond failure **(F-B)** when the maximum strand slip detected (δ) is higher than 0.5 mm, this implies that the embedment length (L_e) is close to the development length (L_d).

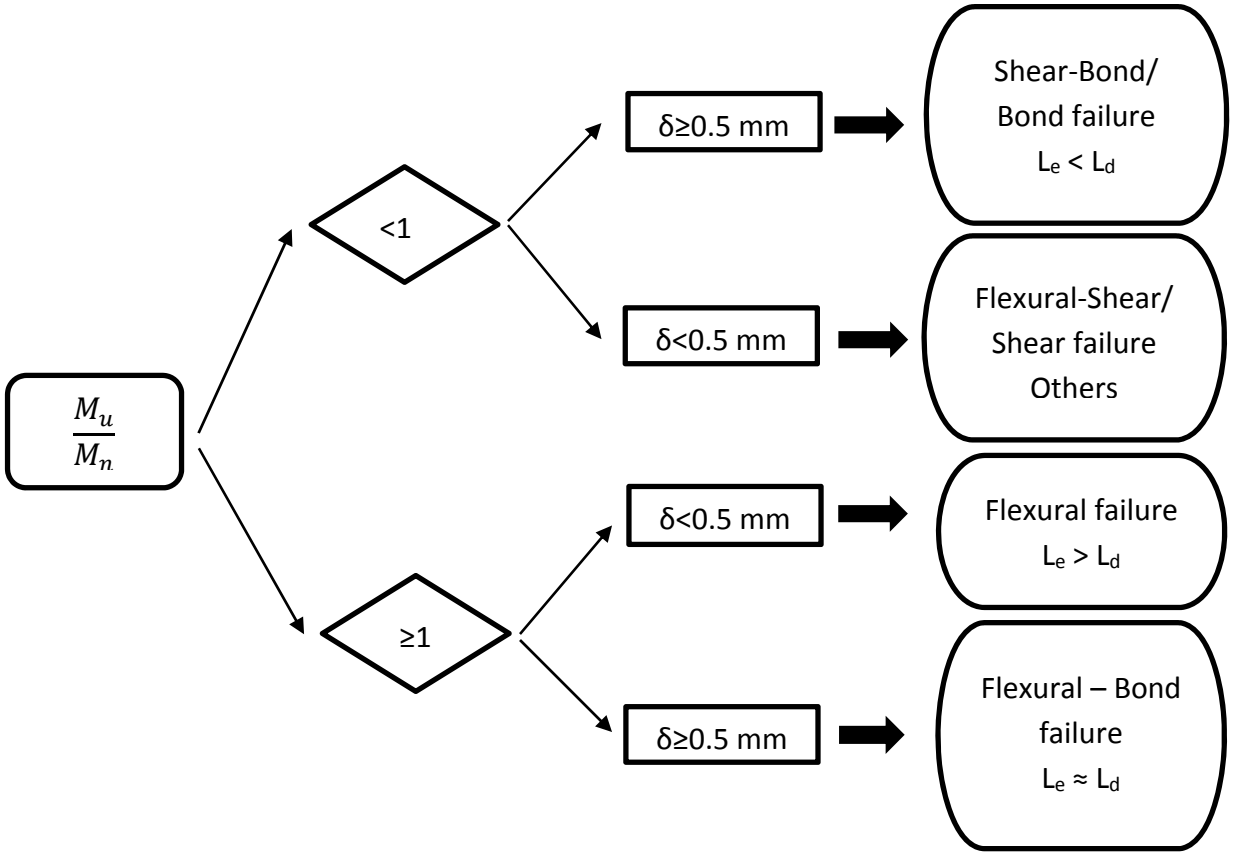

Figure 5.10. Criterion for determining development length

The development length is determined as the minimum embedment length for which maximum slip value detected at the bottom strands is lower than 0.5 mm.

5.2.3. Natural aggregate prestressed beams

Three identical beams were tested to determine the development length of prestressed beams made of natural aggregate concrete (NAC).

Beam B4C (1050 mm)

The first beam (B4C) was tested at an embedment length of 1050 mm. In this case, failure moment was lower than the calculated nominal moment and slip values were significantly higher than 0.5 mm at both ends of the beam. This resulted in a shear-bond failure, as can be seen in Figure 5.11.

Figure 5.11. Bond-shear failure (Beam B4C)

The blending moment vs. deflection of B4C test at mid-span is depicted in Figure 5.12.

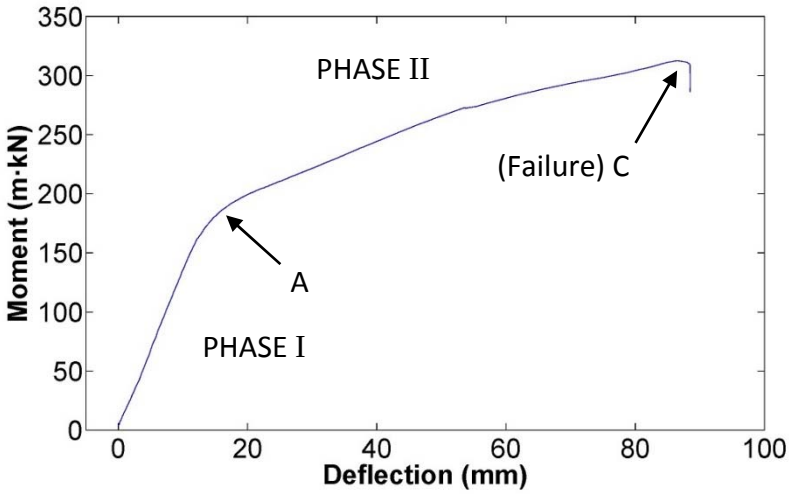

Figure 5.12. Moment vs. Deflection (Beam B4C)

As observed in previous figure, the yielding of the steel had not been reached when the beam failed (point C), since the bending moment of the beam continues increasing with the approximately the same slope than it had after the cracking moment. This is a brittle type of failure. The beam fails in Phase II without reaching Phase III. It can also be observed that the cracking moment (point A) was not reached before approximately 175 m·kN. This is an advantage that prestressed beams offer in contrast to reinforced beams, since the prestressing strands introduce a compressive force to the lower section of the beam, retarding the appearance of the first cracks.

The curvature of the beam calculated from the strain values measured during the test by the strain gauges adhered to the concrete surface is depicted in Figure 5.13.

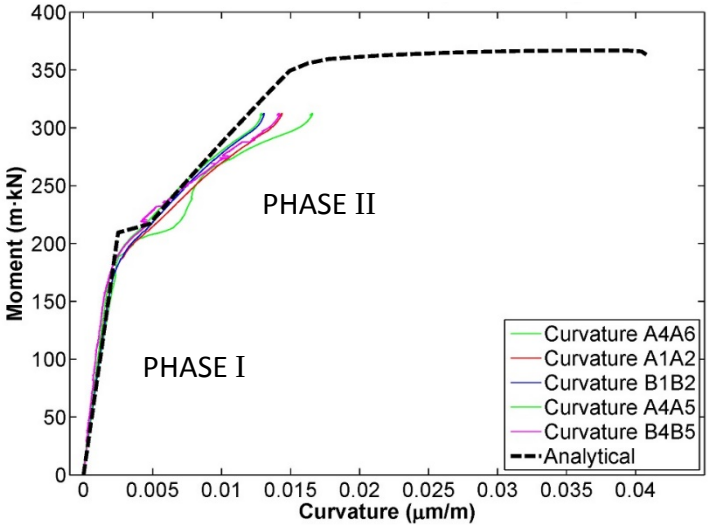

Figure 5.13. Moment vs. Curvature (Beam B4C)

As observed, the measured values are similar to the experimental value until the shear failure of the beam.

Figure 5.14 shows the evolution of the strand slip values at the bottom of the beam during the test.

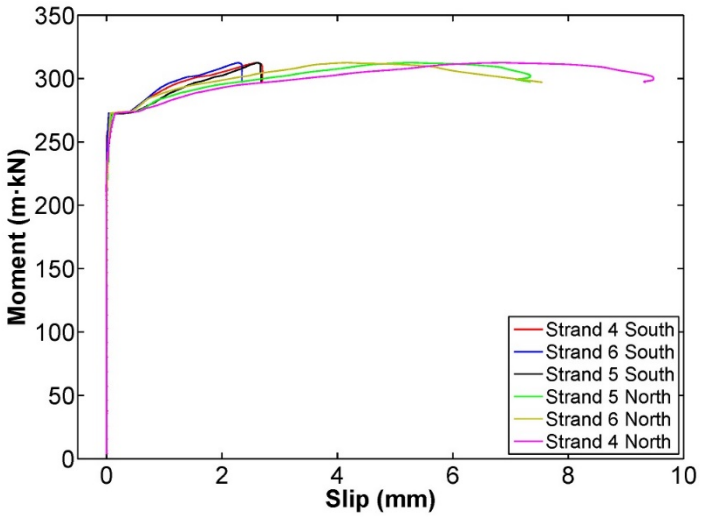

Figure 5.14. Moment vs. Slip (Beam B4C)

As seen in previous figure, slip values at the north end of the beam were more than three times larger than the values registered at south, and all of them larger than the value of 0.5 mm, fixed as a condition for bond failure. The reason may be that transfer length detected at north end was higher than that detected at south end. This implies that development length will be larger and will have a higher influence on slips.

In Figure 5.15, the strain values measured by the four strain gauges adhered to the lower level of prestressed strands (strand no. 5) are depicted. Two of them were placed at 1000 mm far from both ends of the beam the other two were placed at 2750 mm far from both ends. The values are compared with the analytical strain of the strand. The values registered by the strain gauges are similar to the analytical strain at mid-span. Due to the position of the applied loads, all of those sections are practically submitted to the same moment.

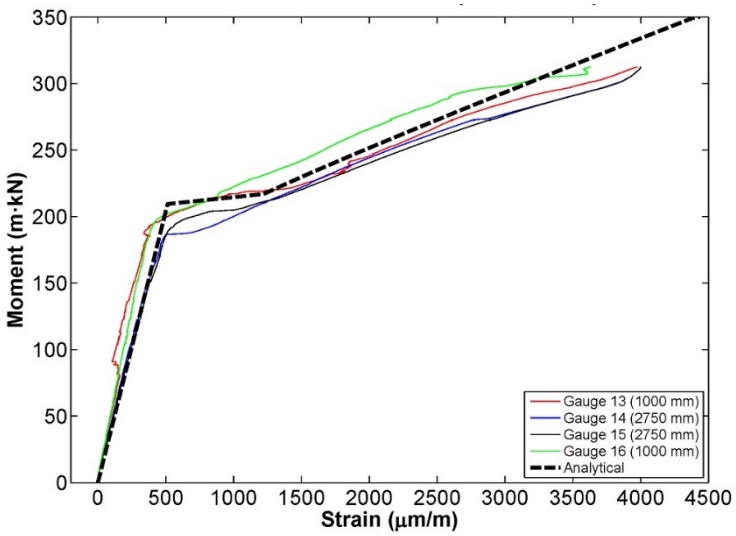

Figure 5.15. Moment vs. Strand strain (Beam B4C)

The strain values measured on the top flange of the beam by the strain gauges adhered to the concrete surface are depicted in Figure 5.16 with their corresponding distance to the end of the beam.

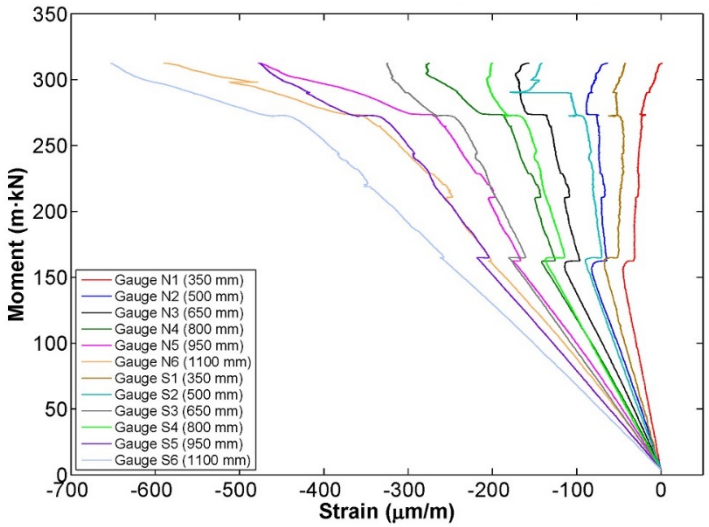

Figure 5.16. Moment vs. Strain on top flange (Beam B4C)

The stiffness of the beam can be calculated as the slope of the curve Moment-Curvature in Phase I (Figure 5.13). From this value, it is possible to get the elastic modulus (E) of the beam, since the inertia of the cross-section is known (Stiffness = E·I). These values are included in Table 5.5.

Table 5.5. Elastic modulus B4C

Stiffness (kN·m^2)	85398
Inertia (cm^4)	192944
Elastic modulus (MPa)	44260

Table 5.6 summarizes the maximum slip values registered for each of the monitored strands as well as the cracking and failure bending moments with their corresponding deflections.

Table 5.6. B4C test

	Moment (m·kN)	Deflection (mm)		Slip (mm) North	Slip (mm) South
Cracking	180	15	**Strand 4**	9.48	2.70
Failure	312	87	**Strand 5**	7.34	2.67
Nominal	366	-	**Strand 6**	7.55	2.34
Ductility	0				

The ductility ratio is defined as the ratio of the deflection at the ultimate load to the deflection at the yield of the reinforcement. In this case, this value is null since the yielding of steel was not reached before failing.

From this test, it could be concluded that the embedment length tested was lower than the development length of the beam. Therefore, it was necessary to increase the embedment length for the following test.

Beam B3C (1600 mm)

The second beam was tested at an embedment length of 1600 mm. In this case, failure moment was higher than the calculated nominal moment and slip values were lower than 0.5 mm at both ends of the beam. So, it was a flexural failure.

The blending moment vs. deflection of B3C test at mid-span is depicted in Figure 5.17.

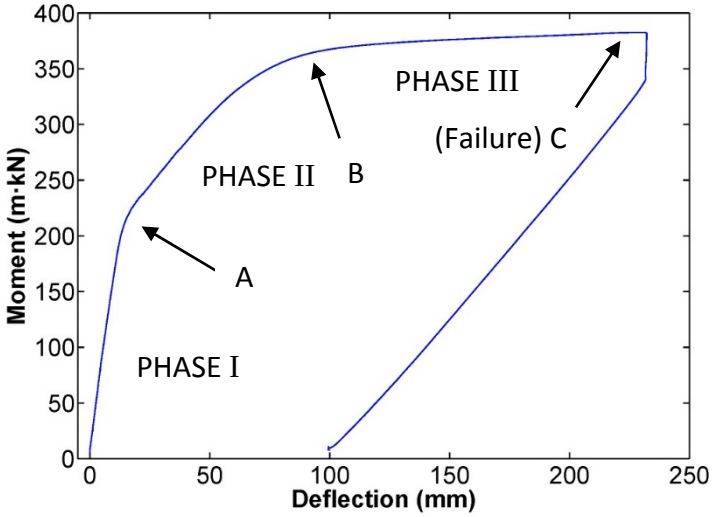

Figure 5.17. Moment vs. Deflection (Beam B3C)

Previous figure depicts the typical Moment-deflection diagram of a flexural failure. As can be observed, there are three stages with different slopes: a first stage between the onset of the test and the cracking moment (point A); a second stage between the cracking moment and the yielding moment (point B) with a lower slope; and a final stage nearly horizontal between the yielding moment and failure (point C). This is a flexural failure characterized by its ductility.

The curvature of the beam calculated from the strain values measured during the test by the strain gauges adhered to the concrete surface is depicted in Figure 5.18.

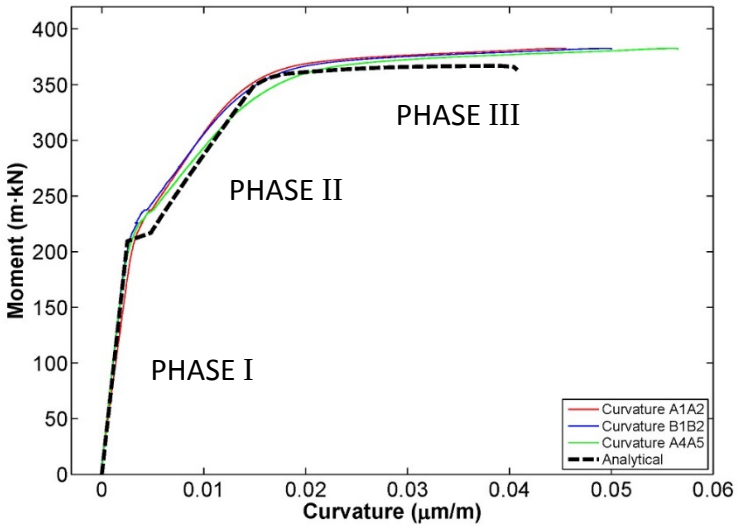

Figure 5.18. Moment vs. Curvature (Beam B3C)

The values measured by the strain gauges are similar to the analytical values.

Figure 5.19 shows the evolution of the strand slip values at the bottom of the beam during the test.

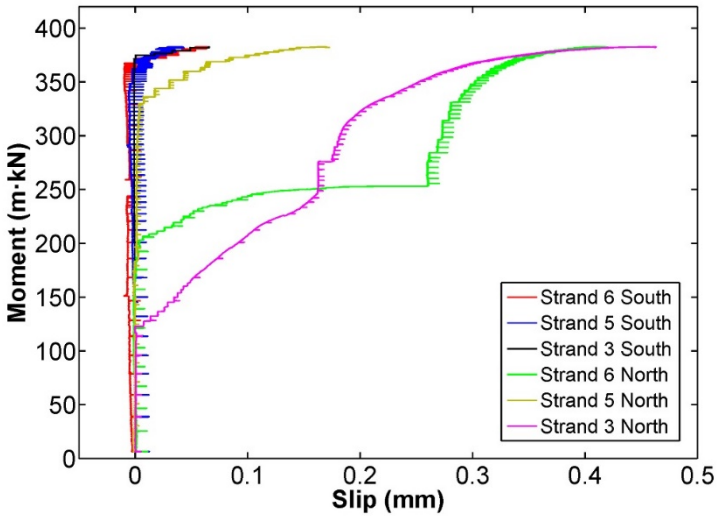

Figure 5.19. Moment vs. Slip B3C

As seen in previous figure, slip values at the north end of the beam were considerably higher than values at the south end, as happened in beam B4C. The reason may be again that transfer length at north end is higher than transfer length at south end, implying a larger development length with more influence on slips. However, all these values are lower than 0.5 mm, fixed as a condition for bond failure.

In Figure 5.20, the strain values measured by the four strain gauges adhered to the lower level of prestressed strands (strand no. 5) are depicted. Two of them were placed at 1000 mm far from both ends of the beam the other two were placed at 2750 mm far from both ends. The values compared to the analytical strain at mid-span are only similar in Gauges 18 and 19 because the gauges are placed in the zone between applied loads, that is, with the same moment than mid-span.

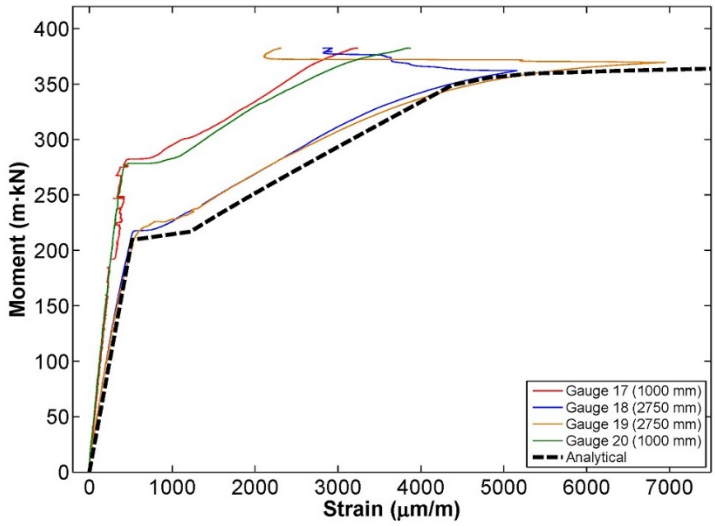

Figure 5.20. Moment vs. Strand strain (Beam B3C)

The strain values measured on the top flange of the beam by the strain gauges adhered to the concrete surface are depicted in Figure 5.21 with their corresponding distance to the end of the beam.

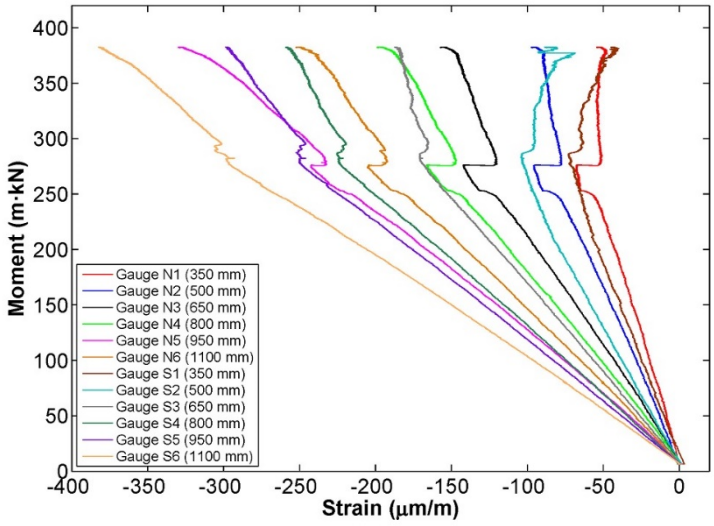

Figure 5.21. Moment vs. Strain on top flange (Beam B3C)

As said before, the stiffness of the beam can be calculated as the slope of the curve Moment-Curvature in Phase I (Figure 5.18). From this value, it is possible to get the elastic modulus (E) of the beam, since the inertia of the cross-section is known (Stiffness = E·I). The values are included in Table 5.7.

Table 5.7. Elastic modulus B3C

Stiffness (kN·m^2)	77188
Inertia (cm^4)	192944
Elastic modulus (MPa)	40005

Table 5.8 summarizes the maximum slip values registered for each of the monitored strands as well as the cracking, yielding and failure bending moments with their corresponding deflections.

Table 5.8. B3C test

	Moment (m·kN)	Deflection (mm)		Slip (mm) North	Slip (mm) South
Cracking	214	15	**Strand 3**	0.46	0.07
Yielding	330	60	**Strand 5**	0.17	0.04
Failure	382	232	**Strand 6**	0.42	0.06
Nominal	366	-			
Ductility	3.87				

From this test, it could be concluded that the embedment length tested was higher than the development length of the beam. Therefore, it was necessary to decrease the embedment length for the following test.

Beam B1C (1475 mm)

The third beam was tested at an embedment length of 1475 mm. In this case, the stop moment was also higher than the calculated nominal moment and slip values were lower than 0.5 mm at both ends of the beam. So, it was again a flexural failure.

The blending moment vs. deflection of B1C test at mid-span is depicted in Figure 5.22. It can be seen again, three clearly defined stages. A first stage from the start of the test to the cracking moment (point A); a second stage with a lower slope from the cracking moment to the yielding moment (point B); and a final stage nearly horizontal between the yielding moment and the stop of the test (point C). So, it is again a flexural failure which is a ductile type of failure.

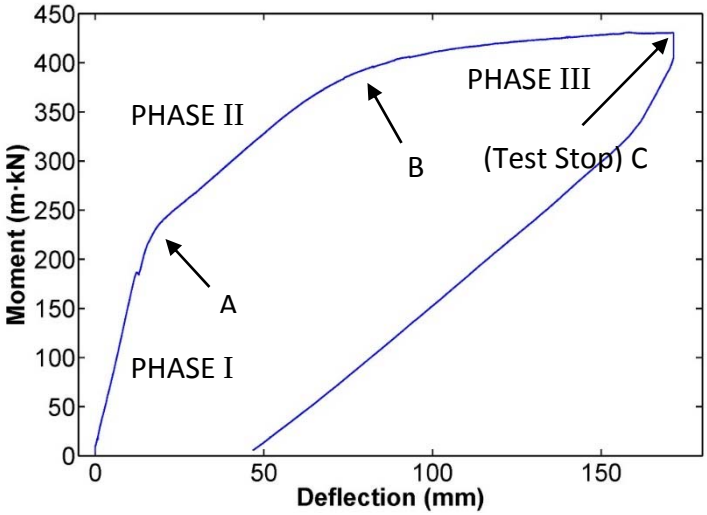

Figure 5.22. Moment vs. Deflection B1C

The curvature of the beam calculated from the strain values measured during the test by the strain gauges adhered to the concrete surface is depicted in Figure 5.23.

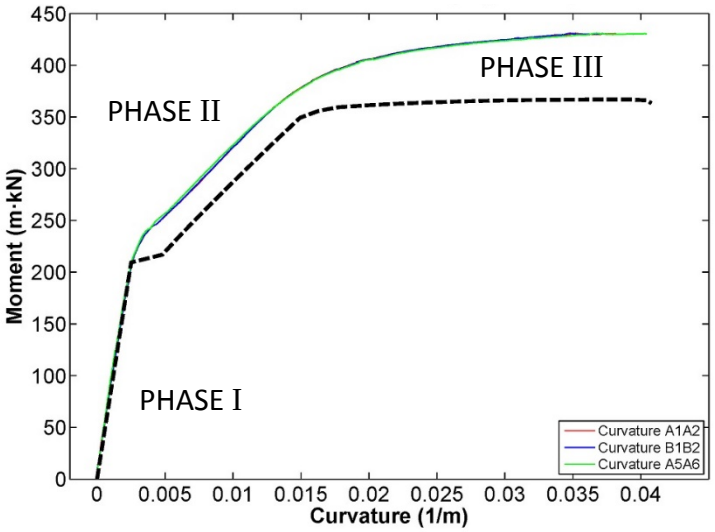

Figure 5.23. Moment vs. Curvature (Beam B1C)

Figure 5.24 shows the evolution of the strand slip values at the bottom of the beam during the test.

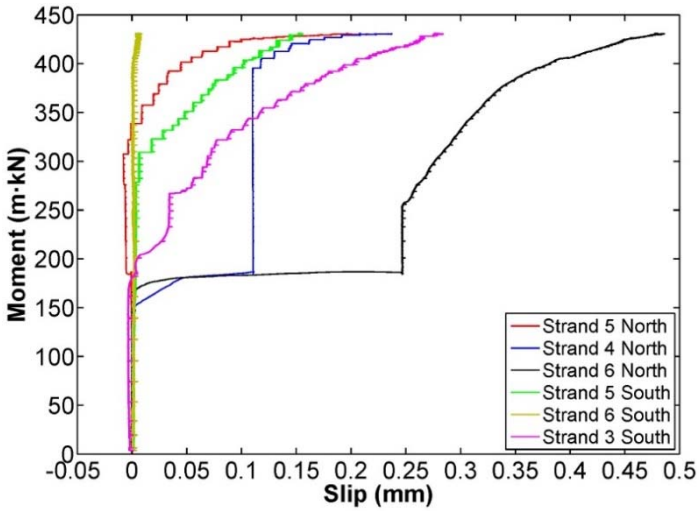

Figure 5.24. Moment vs. Slip B1C

As seen in previous figure, slip maximum slip value was registered at the north end of the beam due to the larger transfer length, while the minimum value was registered at the south end as happened in with B3C and B4C beams. The other slip values were in the range of 0.15 and 0.3 for both ends. All of them were lower than 0.5 mm, limit for considering bond failure.

In Figure 5.25, the strain values measured by the four strain gauges adhered to the lower level of prestressed strands (strand no. 5) are depicted. Two of them were placed at 1000 mm far from both ends of the beam the other two were placed at 2750 mm far from both ends. The values compared to the analytical strain at mid-span are closer in Gauges 22 and 23 because the gauges are placed in the zone between applied loads, that is, with the same moment than mid-span.

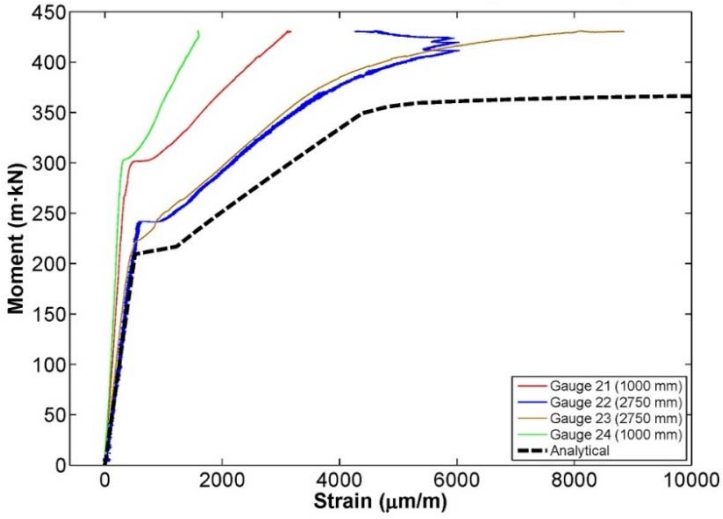

Figure 5.25. Moment vs. Strand strain (Beam B1C)

The strain values measured on the top flange of the beam by the strain gauges adhered to the concrete surface are depicted in Figure 5.26 with their corresponding distance to the end of the beam.

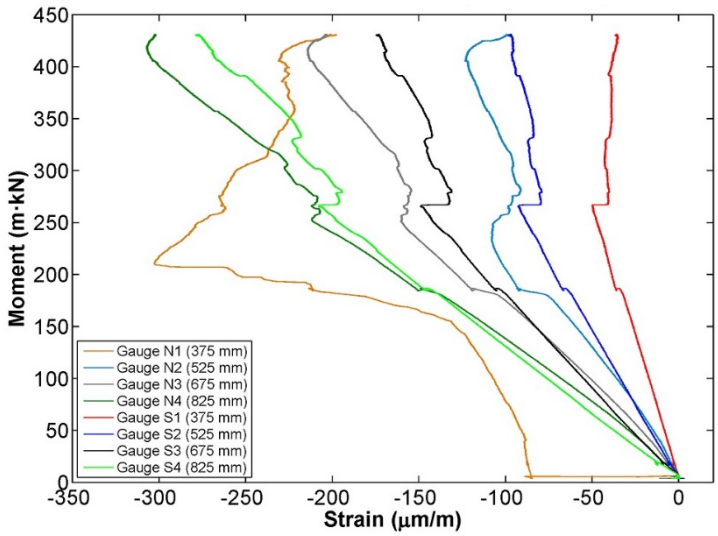

Figure 5.26. Moment vs. Strain on top flange (Beam B1C)

As said before, the stiffness of the beam can be calculated as the slope of the curve Moment-Curvature in Phase I (Figure 5.23). From this value, it is possible to get the elastic modulus (E) of the beam, since the inertia of the cross-section is known (Stiffness = E·I). The values are included in Table 5.9.

Table 5.9. Elastic modulus B1C

Stiffness (kN·m²)	81818
Inertia (cm⁴)	192944
Elastic modulus (MPa)	42405

Table 5.10 summarizes the maximum slip values registered for each of the monitored strands as well as the cracking, yielding and stop bending moments with their corresponding deflections.

Table 5.10. B1C test

	Moment (m·kN)	Deflection (mm)		Slip (mm) North	Slip (mm) South
Cracking	236	19	**Strand 3**	-	0.28
Yielding	380	70	**Strand 4**	0.24	-
Test stop	430	> 171	**Strand 5**	0.23	0.15
Nominal	366	-	**Strand 6**	0.48	0.005
Ductility	> 2.44				

From this test, it could be concluded that the embedment length was higher than the development length of the beam.

After analysing the results of the 3 tests, the development length of the beams made with solely natural aggregate was determined to in the range of (1050, 1475) mm.

5.2.4. Recycled aggregate prestressed beams

Three identical beams were also tested to determine the development length of prestressed beams with 8% replacement of the total aggregate with recycled aggregate.

Beam B4R (1850 mm)

The first recycled beam (B4R) was tested at an embedment length of 1850 mm. In this case, failure moment was similar to the calculated nominal moment and slip values were negligible at the north end of the beam but higher than 0.5 mm at the south end. This resulted in a flexural bond failure at the south end, causing the detachment of part of the bottom flange, as can be seen in Figure 5.27.

Figure 5.27. Failure at south end of B4R

The bending moment vs. deflection is depicted in Figure 5.28. As can be appreciated, there are again three stages clearly defined. The first one, from the start of the test to the cracking moment (point A); the second one with a lower slope from the cracking moment to the yielding moment (point B); and a final stage nearly horizontal between the yielding moment and failure (point C). So, the curve is typical of a flexural failure.

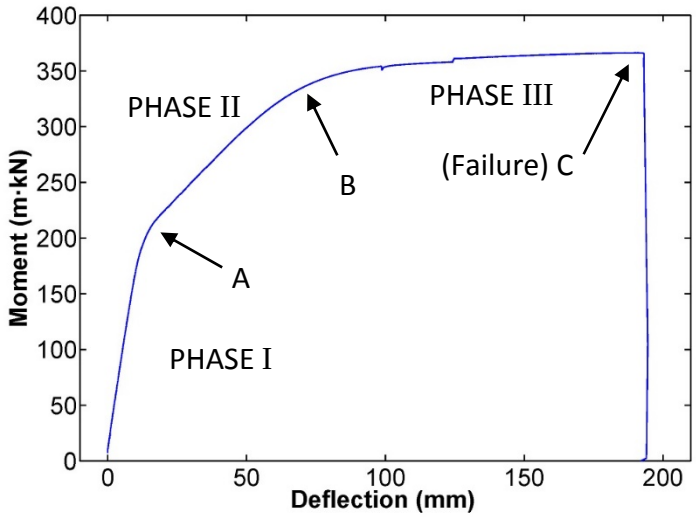

Figure 5.28. Moment vs. Deflection B4R

The curvature of the beam calculated from the strain values measured during the test by the strain gauges adhered to the concrete surface is depicted in Figure 5.29.

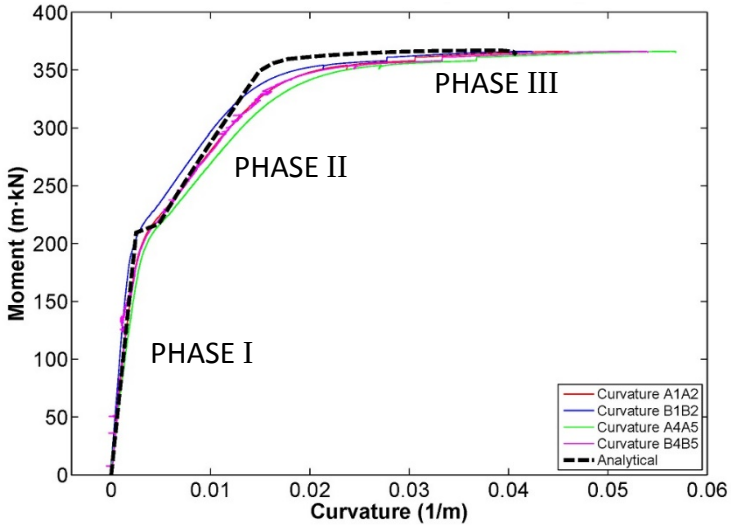

Figure 5.29. Moment vs. Curvature (Beam B4R)

Figure 5.30 shows the evolution of the strand slip values at the bottom of the beam during the test.

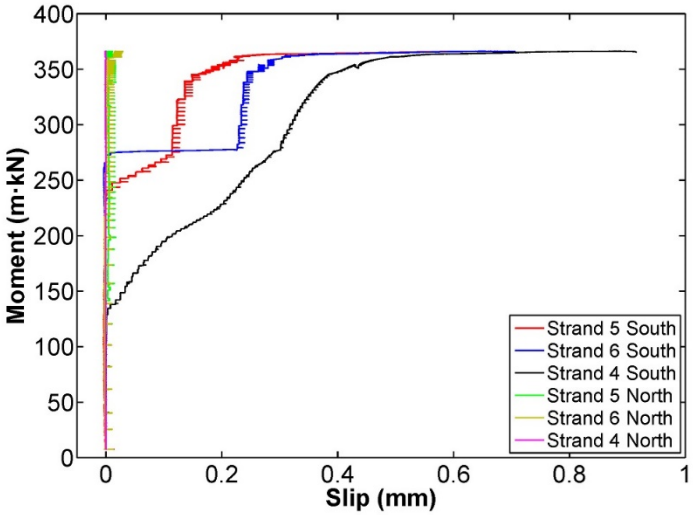

Figure 5.30. Moment vs. Slip B4R

As seen in previous figure, slip values registered at south end are considerably higher than the values registered at the north end, which were insignificant.

In Figure 5.31, the strain values measured by the four strain gauges adhered to the lower level of prestressed strands (strand no. 5) are depicted. Two of them were placed at 1000 mm far from both ends of the beam the other two were placed at 2750 mm far from both ends. The values compared to the analytical strain at mid-span are similar in Gauge 11 because it is placed in the zone between applied loads, that is, with the same moment than mid-span. The values registered by Gauge 10 should also be similar to Gauge 11, and Gauge 9 registered a strange vibration during the test. These last two gauges were located at the south end of the beam, where it failed abruptly, being an indicative of a bond problem.

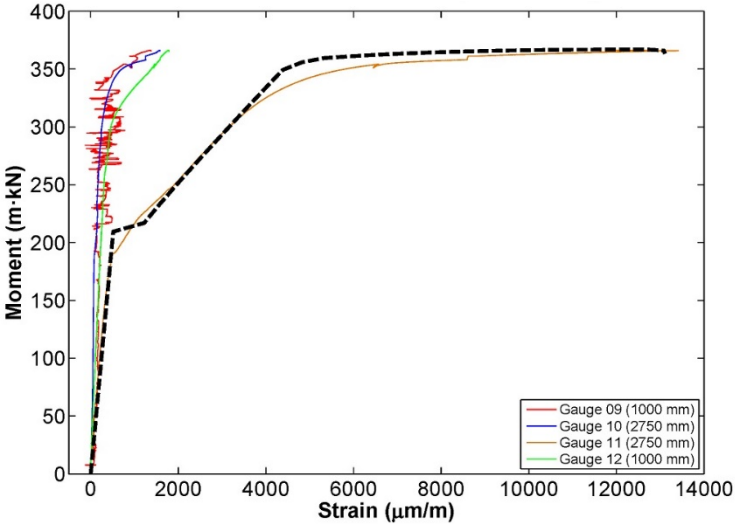

Figure 5.31. Moment vs. Strand strain (Beam B4R)

The strain values measured on the top flange of the beam by the strain gauges adhered to the concrete surface are depicted in Figure 5.32 with their corresponding distance to the end of the beam.

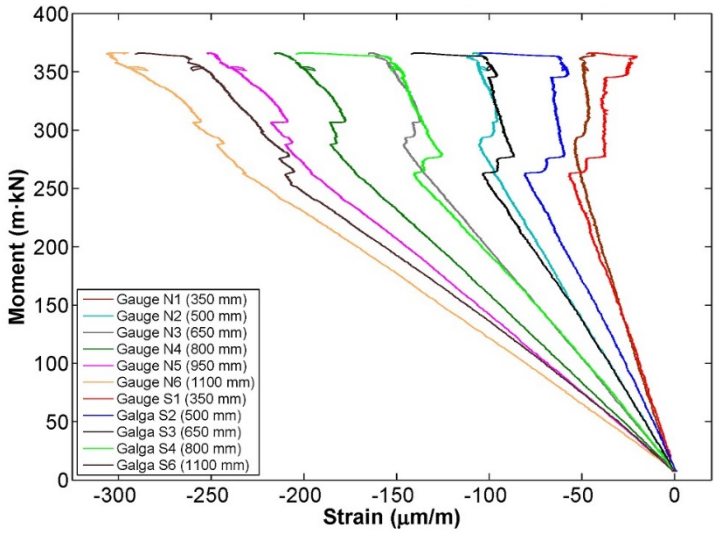

Figure 5.32. Moment vs. Strain on top flange (Beam B4R)

As said before, the stiffness of the beam can be calculated as the slope of the curve Moment-Curvature in Phase I (Figure 5.29). From this value, it is possible to get the elastic modulus (E) of the beam, since the inertia of the cross-section is known (Stiffness = E·I). The values are included in Table 5.11.

Table 5.11. Elastic modulus B4R

Stiffness (kN·m^2)	76439
Inertia (cm^4)	192944
Elastic modulus (MPa)	39617

Table 5.12 summarizes the maximum slip values registered for each of the monitored strands as well as the cracking, yielding and failure bending moments with their corresponding deflections.

Table 5.12. B4R test

	Moment (m·kN)	Deflection (mm)		Slip (mm) North	Slip (mm) South
Cracking	200	13	**Strand 4**	0	0.92
Yielding	340	74	**Strand 5**	0.01	0.70
Failure	366	193	**Strand 6**	0.02	0.71
Nominal	366	-			
Ductility	2.61				

From this test, it could be concluded that the difference between both ends of the beam with regard to the slip values detected is too big, especially if it is compared with the trend observed in natural aggregate beams. Slip values were higher than 0.5 mm at south end, being an indicative of a bond failure; while at north end, slip values were negligible. Contrary to natural aggregate beams, where slip measured at north end was always higher than at south end. Moreover, the detachment of part of the bottom flange of the beam may be an indicative of a defect of fabrication or an inadequate vibration of fresh concrete. Therefore, being not clear if the embedment length was higher or lower than the development length, it was decided to choose a higher embedment length for the following test.

Beam B3R (2200 mm)

The second recycled beam (B3R) was tested at an embedment length of 2200 mm. In this case, the stop of the test moment was higher than the calculated nominal moment and slip values were lower than 0.5 mm at both ends of the beam. So, it was a flexural failure.

The blending moment vs. deflection is depicted in Figure 5.33. As can be appreciated, there are three stages clearly defined. A first stage from the start of the test to the cracking moment (point A); a second stage with a lower slope from the cracking moment to the yielding moment (point B); and a final stage nearly horizontal between the yielding moment and the stop of the test (point C). So, it is a flexural failure characterized by its ductility.

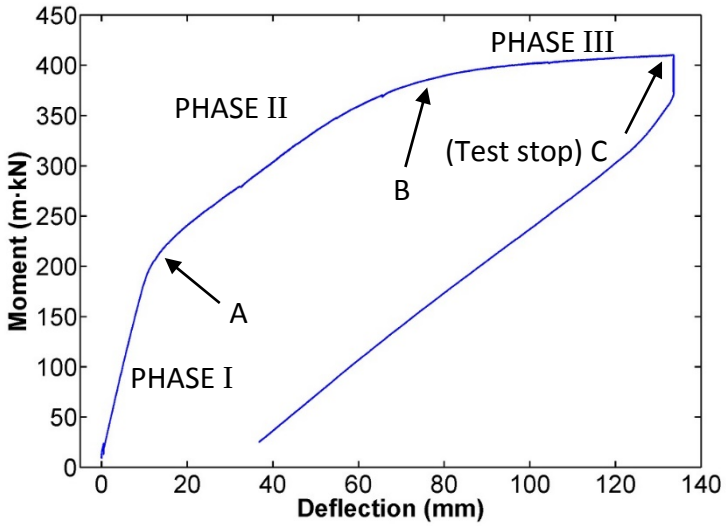

Figure 5.33. Moment vs. Deflection B3R

The curvature of the beam calculated from the strain values measured during the test by the strain gauges adhered to the concrete surface is depicted in Figure 5.34.

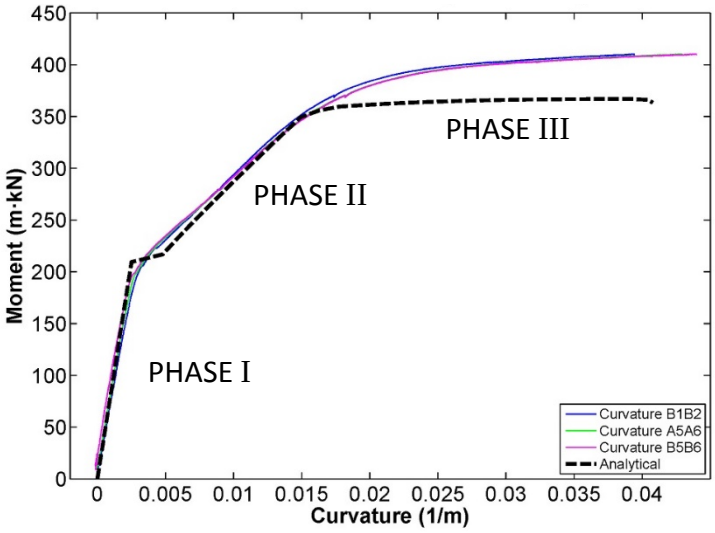

Figure 5.34. Moment vs. Curvature (Beam B3R)

Figure 5.35 shows the evolution of the strand slip values at the bottom of the beam during the test.

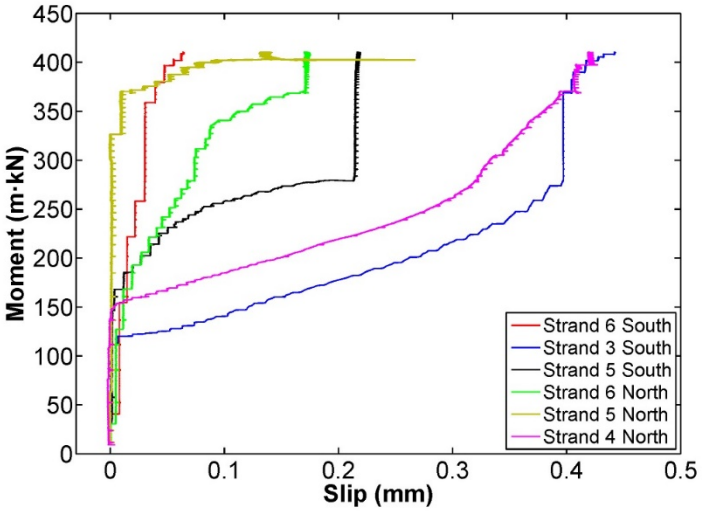

Figure 5.35. Moment vs. Slip B3R

As seen in previous figure, maximum slip values were similar at both ends of the beam, unlike in natural aggregate beams, where the maximum values were always registered at the north end. All the values were lower than 0.5 mm, limit for considering bond failure.

In Figure 5.36, the strain values measured by the four strain gauges adhered to the lower level of prestressed strands (strand no. 5) are depicted. Two of them were placed at 1000 mm far from both ends of the beam the other two were placed at 2750 mm far from both ends. The values compared to the analytical strain at mid-span are similar in Gauges 06 and

07 because the gauges are placed in the zone between applied loads, that is, with the same moment than mid-span.

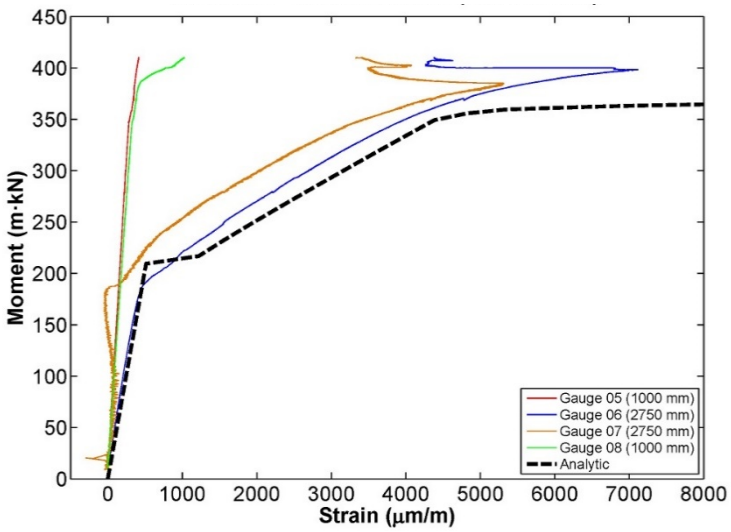

Figure 5.36. Moment vs. Strand strain (Beam B3R)

The strain values measured on the top flange of the beam by the strain gauges adhered to the concrete surface are depicted in Figure 5.32 with their corresponding distance to the end of the beam.

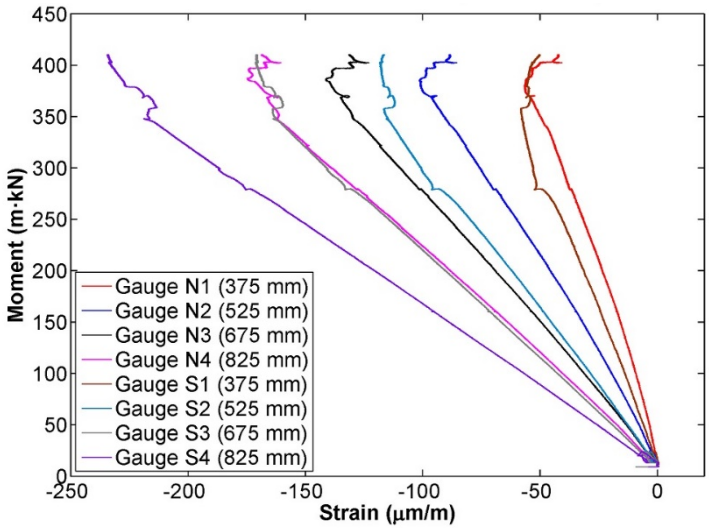

Figure 5.37. Moment vs. Strain on top flange (Beam B3R)

As said before, the stiffness of the beam can be calculated as the slope of the curve Moment-Curvature in Phase I (Figure 5.34). From this value, it is possible to get the elastic modulus (E) of the beam, since the inertia of the cross-section is known (Stiffness = E·I). The values are included in Table 5.13.

Table 5.13. Elastic modulus B3R

Stiffness (kN·m^2)	72222
Inertia (cm^4)	192944
Elastic modulus (MPa)	37432

Table 5.14 summarizes the maximum slip values registered for each of the monitored strands as well as the cracking, yielding and test stop bending moments with their corresponding deflections

Table 5.14. B3R test

	Moment (m·kN)	Deflection (mm)		Slip (mm) North	Slip (mm) South
Cracking	195	11	**Strand 3**	-	0.44
Yielding	350	56	**Strand 4**	0.42	-
Test stop	410	> 134	**Strand 5**	0.27	0.22
Nominal	366	-	**Strand 6**	0.17	0.06
Ductility	> 2.39				

From this test, it could be concluded that the embedment length tested was higher than the development length of the beam. Therefore, it was necessary to decrease the embedment length for the following test.

Beam B1R (1850 mm)

The third recycled beam (B1R) was tested again at an embedment length of 1850 mm. It was decided to repeat the test because both, the high slip values detected at south end in comparison with north end and the sudden detachment of the flange were suspicious of a manufacturing defect. In this case, stop test moment was higher than the calculated nominal moment and slip values were lower than 0.5 mm at both ends of the beam. So, it was again a flexural failure.

The blending moment vs. deflection is depicted in Figure 5.38. As can be appreciated, there are three stages such as in B4R. A first stage from the start of the test to the cracking moment (point A); a second stage with a lower slope from the cracking moment to the yielding moment (point B); and a final stage nearly horizontal between the yielding moment and the stop of the test moment (point C). So, it is a flexural failure.

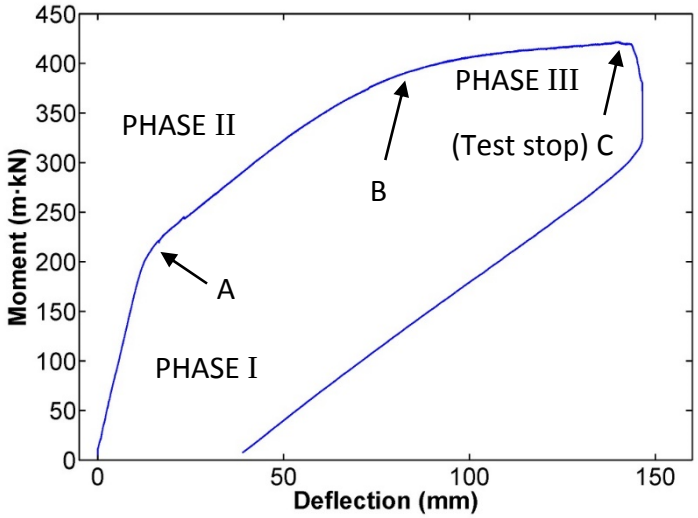

Figure 5.38. Moment vs. Deflection B1R

The curvature of the beam calculated from the strain values measured during the test by the strain gauges adhered to the concrete surface is depicted in Figure 5.39.

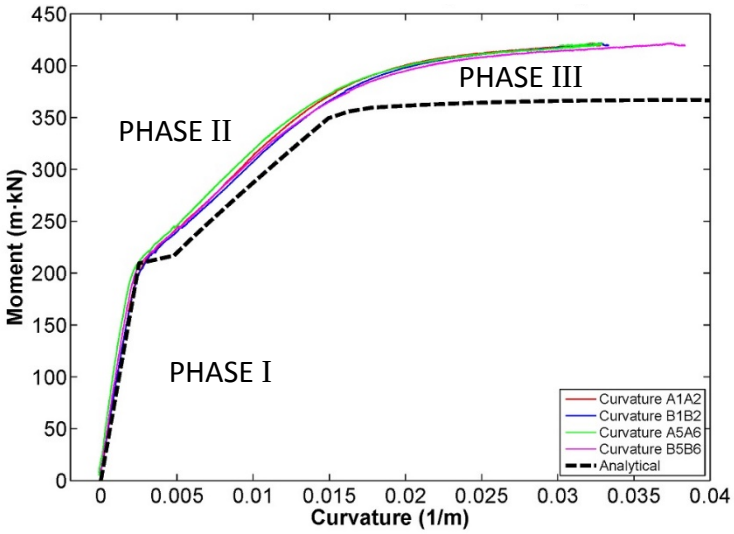

Figure 5.39. Moment vs. Curvature (Beam B1R)

Figure 5.40 shows the evolution of the strand slip values at the bottom of the beam during the test.

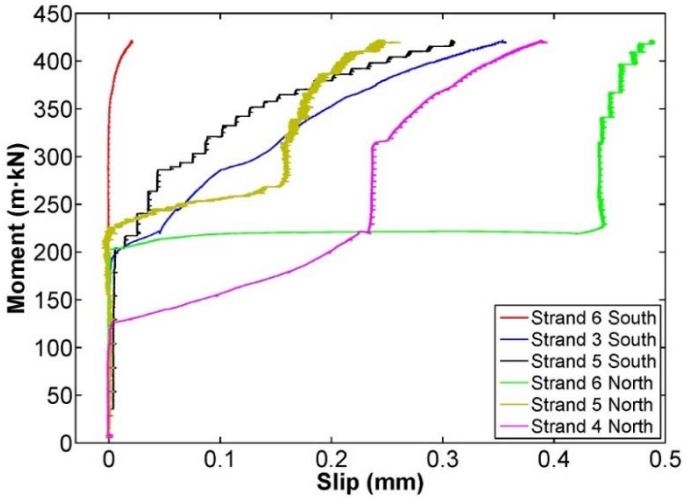

Figure 5.40. Moment vs. Slip B1R

Similar to natural aggregate beams, the maximum slip values were detected at the north end of the beam. Transfer length measured for recycled beams at north end was higher than transfer length measured at south end. So, it is an indicative of a larger development length with a higher influence on the slip values. All values were lower than 0.5 mm, limit established for not considering a bond failure.

In Figure 5.41, the strain values measured by the four strain gauges adhered to the lower level of prestressed strands (strand no. 5) are depicted. Two of them were placed at 1000 mm far from both ends of the beam the other two were placed at 2750 mm far from both ends. The values compared to the analytical strain at mid-span are similar in Gauges 02 and 03 because these gauges are placed in the zone between applied loads, that is, with the same moment than mid-span.

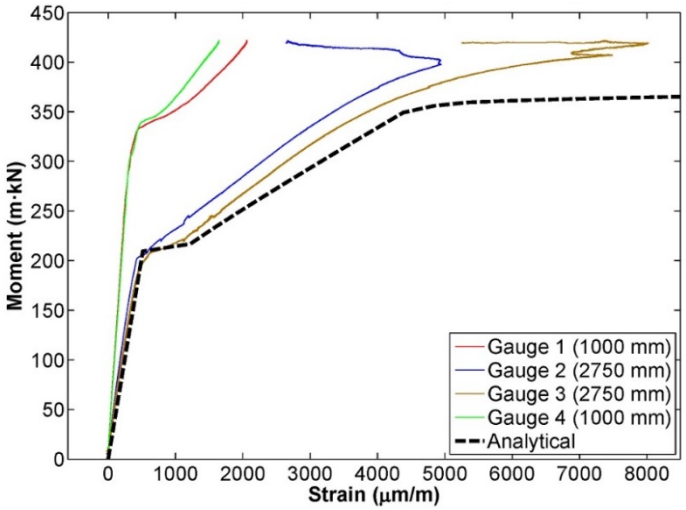

Figure 5.41. Moment vs. Strand strain (Beam B1R)

The strain values measured on the top flange of the beam by the strain gauges adhered to the concrete surface are depicted in Figure 5.42 with their corresponding distance to the end of the beam.

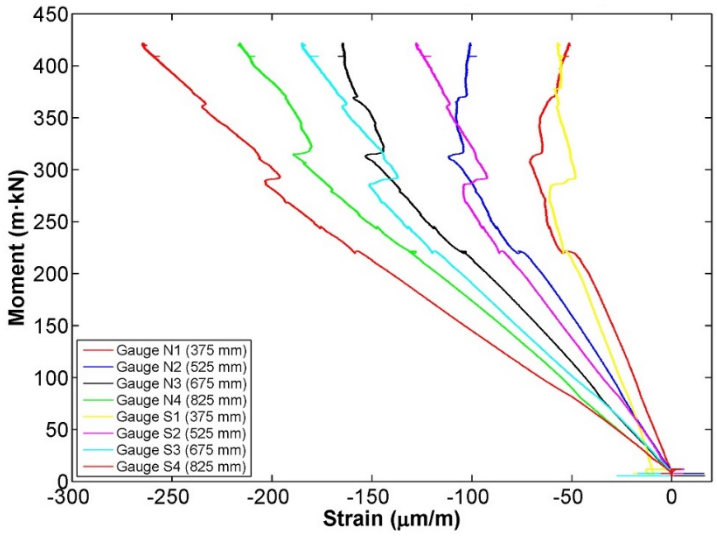

Figure 5.42. Moment vs. Strain on top flange (Beam B1R)

As said before, the stiffness of the beam can be calculated as the slope of the curve Moment-Curvature in Phase I (Figure 5.39). From this value, it is possible to get the elastic modulus (E) of the beam, since the inertia of the cross-section is known (Stiffness = E·I). The values are included in Table 5.15.

Table 5.15. Elastic modulus B1R

Stiffness (kN·m^2)	87761
Inertia (cm^4)	192944
Elastic modulus (MPa)	45485

Table 5.16 summarizes the maximum slip values registered for each of the monitored strands as well as the cracking, yielding and test stop bending moments with their corresponding deflections.

Table 5.16. B1R test

	Moment (m·kN)	Deflection (mm)		Slip (mm) North	Slip (mm) South
Cracking	200	12.5	**Strand 3**	-	0.35
Yielding	360	65	**Strand 4**	0.39	-
Test stop	420	>144	**Strand 5**	0.25	0.31
Nominal	366	-	**Strand 6**	0.49	0.02
Ductility	>2.21				

From this test, it could be concluded that the embedment length was higher than the development length of the beam.

After analysing the results of the 3 tests, the development length of the beams made with 8% replacement of recycled aggregate was determined to be ≤ 1850 mm.

5.2.5. Results and discussion

The results of the development length tests for both types of beams are summarized in Table 5.17 and the diagrams bending moment vs. deflection and bending moment vs. curvature including all of the beams are depicted in Figures 5.43 and 5.44, respectively.

Table 5.17. Development length results

Beam	L_e (mm)	M_{cr} (m·kN)	M_y (m·kN)	M_u (m·kN)	M_u/M_n	δ (mm)	D.F.	End	Max. slip (mm)	E (MPa)	Failure	Ld (mm)
B4C	1050	180	-	312	0.85	87	0	N S	9.48 2.70	42260	S-B Bond	L_d > 1050
B3C	1600	214	330	382	1.04	232	3.87	N S	0.46 0.07	40005	Flex. Flex.	L_d < 1600
B1C	**1475**	236	380	430	1.17	> 171	> 2.44	N S	0.48 0.28	42405	Flex. Flex.	L_d < 1475
B4R	1850	200	340	366	1.00	193	2.61	N S	0.02 0.92	39617	F-B Bond	L_d ≈ 1850
B3R	2200	195	350	410	1.12	> 134	> 2.39	N S	0.42 0.44	37432	Flex. Flex.	L_d < 2200
B1R	**1850**	200	360	420	1.15	> 144	> 2.21	N S	0.49 0.35	45485	Flex. Flex.	L_d < 1850

where: L_e is the embedment length, M_{cr} is the cracking moment, M_y is the yielding moment, M_u is the failure moment or test stop moment, depending on the beam, M_n is the calculated nominal moment, δ is the maximum deflection, *D.F.* is the ductility factor, E is the elastic modulus of the beam and L_d is the embedment length.

Following the criterion proposed, 1475 mm was determined as the maximum value development length of the beams made with solely natural aggregate. It was the maximum embedment length for which slip values lower than 0.5 mm were detected, in this case 0.48 mm at the north end. For the beams with 8% replacement of recycled aggregate, the maximum development length was stablished in 1850, being the maximum embedment length for which slip values lower than 0.5 mm were detected, in this case 0.49 mm at north end.

It can be concluded that there is an increase of 25% in maximum values of development length when 8% recycled aggregate is incorporated in the concrete mix. This may be due to

the worst properties of recycled aggregate in comparison with natural aggregate, which result in a loss of bond between the prestressed steel and the surrounding concrete. This difference is comparable with the loss of bond stress detected in the pull-out tests when the first slip (0.01 mm) occurred. In that case, bond stress was approximately 24% lower when 8% of the total aggregate was replaced with recycled aggregate. Therefore, the pull-out bond test accurately predicted the difference in the development length when recycled aggregate was incorporated.

Another interesting conclusion can be taken from the development length tests. Slip values were significantly higher at the north end of most of the beams. This fact may be correlated with the larger transfer length detected at the north end of the beams, implying a larger development length and a higher influence on the strand slip values.

In Figure 5.43, the bending moment is plotted against deflection at mid-span for the 6 beams.

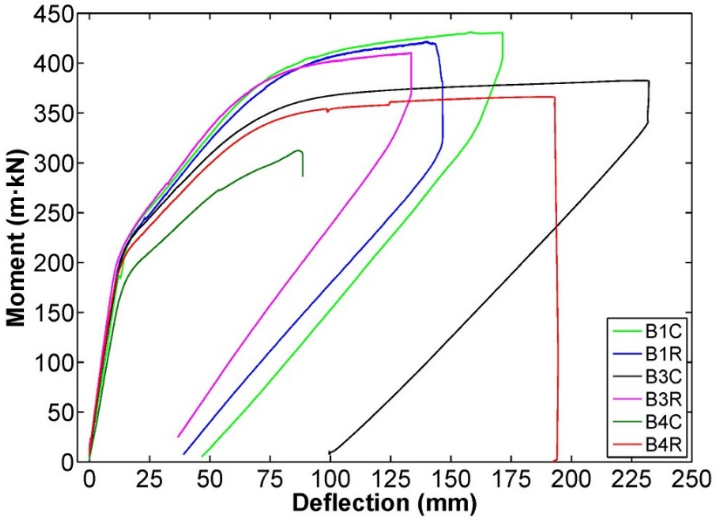

Figure 5.43. Moment vs. Deflection at mid-span. Development length tests

It is important to consider that B1C, B1R and B3R tests were stopped when the bending moment exceeded the nominal moment calculated, without waiting for the failure of the beam in order not to damage the measuring sensors. Therefore, the maximum deflections plotted are not the failure deflections of the 3 beams.

If the ultimate moments for the beams are observed, these values are in the range of 350 – 450 kN·m without a tendency to decrease when recycled aggregate is introduced in concrete. So, the ultimate moment is not apparently affected by 8% replacement of the total aggregate.

In Figure 5.44, the bending moment is plotted against the experimental and analytical curvature of the beams at a section located at 25 mm far from mid-span.

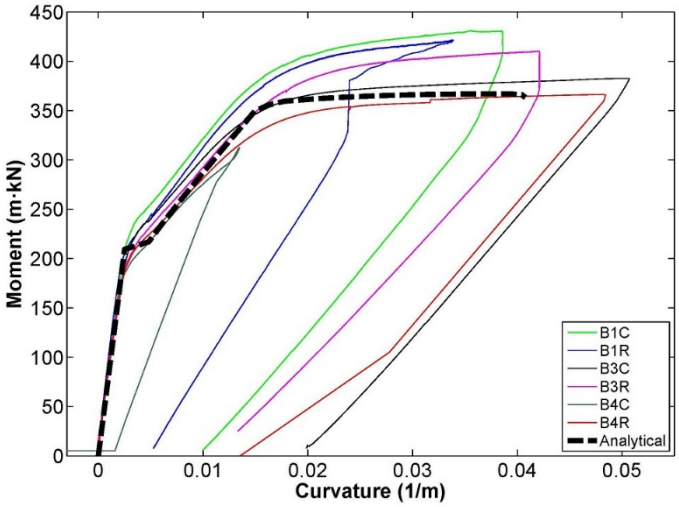

Figure 5.44. Moment vs. Curvature. Development length tests

Curvatures were calculated from the data proportioned provided by the strain gauges adhered to the concrete surface. Similarly to the previous figure, it is important to consider that the maximum curvatures for B1C, B1R and B3R are the curvatures when the test was stopped, not the failure curvatures.

Similar to the proposed equations for transfer length, several authors and codes proposed equations for estimating flexural bond length and development length based on the concrete and strand properties (Tables 5.18 - 5.19 and Figures 5.45 – 5.46). These equations are summarized in Appendix 1 and the values introduced are included in Table 5.2.

Table 5.18. Flexural bond length based on concrete and strand properties

	B1C (mm)	B1R (mm)
Hanson and Kaar [HANS 1959]		
Kaar et al. [KAAR 1963]	1555	1555
ACI 318-63 - ACI 318-14		
Zia and Mostafa [ZIA 1977]	1943	1943
Mitchell et al. [MITC 1993]	1172	1189
Deatherage et al. [DEAT 1994]	2331	2331
Buckner [BUCK 1995]	1541	1541
Lane [LANE 1998]	1638	1674
Shahawy [SHAH 2001]	1295	1295
Eurocode 2 [CEN 2004]	175	182
Kose and Burkett [KOSE 2005]	2647	2681

EHE 2008 [EHE 2008]	974	974
Model Code 2010 [MC 2010]	477	496
AASHTO LFRD 2012	1416	1416
Current research	758	893

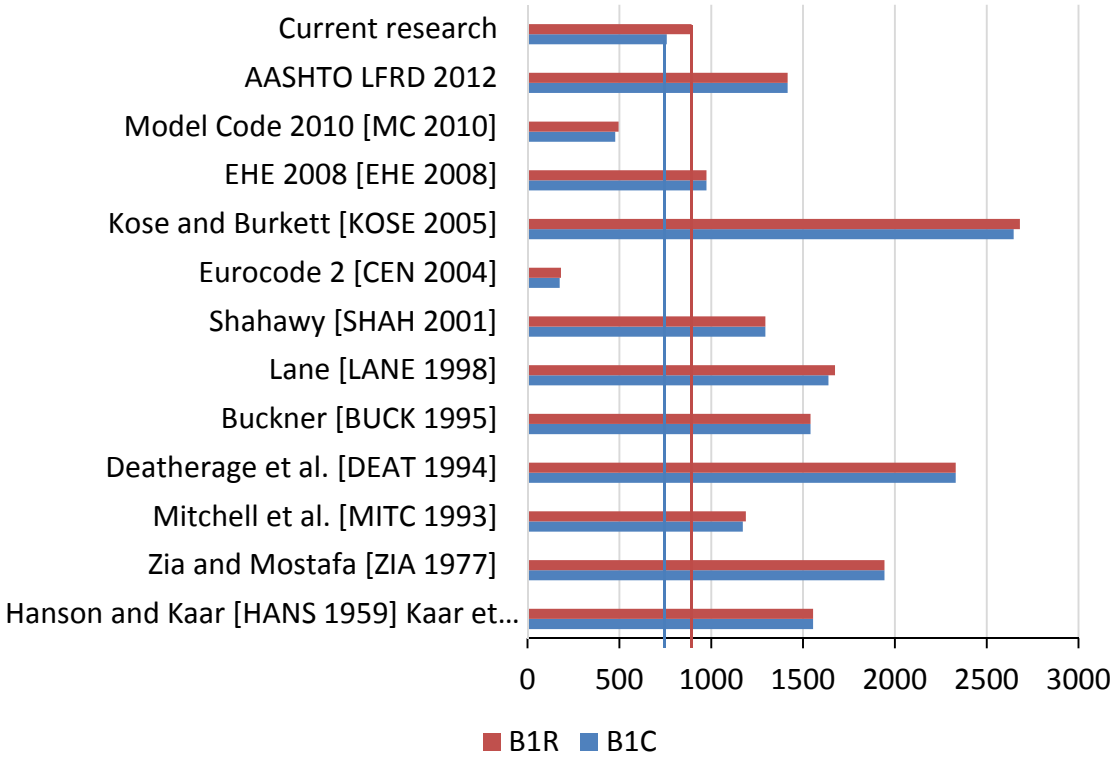

Figure 5.45. Flexural bond length based on concrete and strand properties

In the case of equations for predicting flexural bond length, most of them are over conservative for this particular case for both, natural and recycled concrete.

Table 5.19. Development length based on concrete and strand properties

	B1C (mm)	**B1R (mm)**
Hanson and Kaar [HANS 1959], Kaar et al. [KAAR 1963], ACI 318-63, ACI 318-14	2178	2178
Zia and Mostafa [ZIA 1977]	2327	2347
Mitchell et al. [MITC 1993]	1677	1704
Deatherage et al. [DEAT 1994]	3112	3112
Buckner [BUCK 1995]	2321	2321
Lane [LANE 1998]	2694	2764

Shahawy [SHAH 2001]	2075	2075
Eurocode 2 [CEN 2004]	491	510
Kose and Burkett [KOSE 2005]	3896	3948
Martí-Vargas et al. [MART 2006]	610	617
Ramirez and Russell [RAMI 2007]	1592	1617
EHE 2008 [EHE 2008]	1433	1433
MC – 2010 [MC 2010]	836	870
AASHTO LFRD 2012	2178	2178
Current research	1475	1850

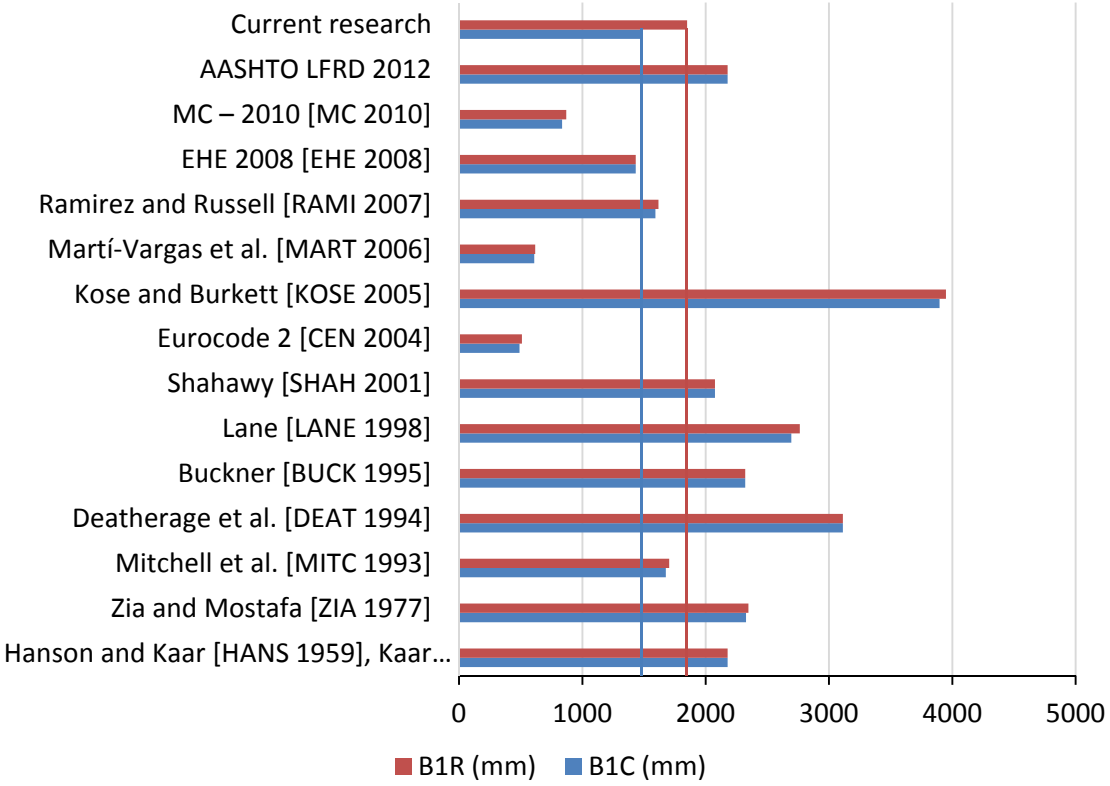

Figure 5.46. Development length based on concrete and strand properties

In the case of equations for predicting development length, the equation proposed by Ramirez and Russell agrees with the value obtained in B1C, even predicting a value slightly higher. However, the value obtained in B1R is significantly higher than the value predicted by the Ramirez and Russel equation.

From the experimental results performed by different authors with prestressed elements and 0.5 in. (12.7 mm strands) it can be concluded that some of them agree with the experimental values obtained for these beams. Larson et al. [LARS 2007] determined a

development length of 1470 mm and noticed an increase of the nominal capacity as the embedment length diminished during the tests. Logan [LOGA 1997] also observed a development length of 1473 mm with strands having an average pull-out capacity exceeding 160 kN, and 1854 mm with strands having a pull-out capacity less than 53.3 kN). Andrawes et al. [ANDR 2013] measured development length less than 1461 mm in I-Girders.

Studies on the influence of recycled aggregate on the development length were not found to date. Therefore, this research presents a first approach to the structural behaviour of prestressed recycled concrete.

Chapter 6. Conclusions and Future Lines of Research

6.1. Conclusions

The following conclusions can be drawn from the experimental work performed for this doctoral thesis:

6.1.1. Reinforced recycled concrete beams

Quality control of recycled concrete

The following conclusions can be established from the experimental program performed in laboratory to evaluate the properties of recycled self-compacting concrete, with replacement levels of 0, 20, 35 and 50% of the total aggregate (fine and coarse). These mix compositions were used for the fabrication of reinforced beams:

- All recycled concretes showed enough workability at a fixed water-to-cement content 0.50. For M-20 mix, the slump-flow increased 12% but no flow-segregation was noticed. This increase in the slump flow diameter may be due to the higher initial free water content.
- The density of hardened concrete decreased up to 1.3 % for 50% replacement of the total aggregate. It is expected since the density of the recycled aggregate is lower than that of the natural aggregate.
- The compressive strength slightly decreased by 3, 5 and 4% for 20, 35 and 50%, replacement of the total natural aggregate, respectively.
- The splitting tensile strength decreased up to 9% for 50% replacement of the total aggregate content.
- The modulus of elasticity decreased as the replacement level increased, with a maximum loss of 9 % for 50% replacement.

Considering that the properties of this concrete are not adversely affected by the simultaneous replacement of this type of fine and coarse concrete recycled aggregates, it might be concluded that it is feasible to replace up to 50% of the total amount of natural aggregate by this particular recycled aggregate. However, it would be interesting to perform durability tests in order to evaluate the long-term behaviour.

Flexural behaviour tests

Reinforced concrete beams were fabricated with the previously studied self-compacting recycled concrete and replacement levels of 0, 10, 20, 35 and 50% of the total aggregate (fine and coarse). These beams subjected to quality control flexural behaviour tests in the precast plant. Similar beams were monitored and tested under displacement control at the Center of Innovation in Building and Civil Engineering, CITEEC, University of La Coruña. These are the conclusions drawn from this research:

- All of the beams failed in flexure, as expected. The longitudinal tension steel yielded first, followed by the concrete crushing, which is a ductile mode of failure.
- The cracking moment of the beams tested in the precast plant decreased when fine and coarse recycled aggregate was incorporated. This loss of cracking strength was around 6% for FB-20 and FB-35 and by 12% for FB-50. When beams where tested in the CITEEC, the loss registered was greater, achieving losses of 20% for FB-10 and of 30% for FB-35 and FB-50.
- The ultimate moment of recycled beams was slightly lower than the natural aggregate beam as the replacement ratio of the total aggregate increased, with a maximum loss of 2% and 6% for FB-50, in the beam tested in the precast plant and the CITEEC, respectively.
- Mid-span deflections at failure of beams tested in the precast plant was decreased as the substitution percentage increased, especially for the highest replacement ratios, with losses of up to 27% when 50% of the total aggregate was replaced. When beams were tested in the CITEEC, a similar trend was observed with losses of 35 and 37% for replacement levels of 35 and 50%, respectively.
- The crack patterns observed were similar regardless of the replacement ratio. Crack spacing and crack width of NAC beam did not differ from RAC beams.
- The ductility ratio of the beams tested in the precast plant was lower as the replacement level increased, with losses of up to 33% for 50% replacement of the total aggregate. Similarly, when beams were tested in the CITEEC, a considerable decrease was also observed for the highest replacement levels FB-35 and FB-50, with losses of 40% and 43%, respectively.

Shear behaviour tests

Five beams with the same mix compositions (0, 10, 20, 35 and 50%) were also subjected to quality control shear behaviour tests in the precast plant. The following conclusions were drawn:

- The shear test results showed a brittle bond-shear failure for all of the substitutions investigated.
- The substitution of natural aggregate by recycled aggregate decreased the cracking shear by 17% for all the replacement levels. The corresponding cracking deflection was also decreased by 41% for the highest replacement levels (SB-35 and SB-50).
- The ultimate shear for beam SB-10 was practically the same as that for the reference beam (SB-0) and the corresponding deflection was slightly higher. However, increasing the substitution percentage beyond 20% led to a slight decrease of the ultimate shear by 4-6%, with corresponding deflections similar to that obtained in the beam without recycled aggregate.

Considering the results obtained from the flexural and shear behaviour tests in this experimental program, it may be concluded that the simultaneous use of up to 50% of fine and coarse recycled aggregates from the rejection of precast concrete members is feasible for producing self-compacting reinforced concrete beams. However, it would be necessary to perform durability tests in order to analyse the long-term behaviour of the recycled concrete beams.

6.1.2. Prestressed recycled concrete beams

Prestressed pre-slabs

The following conclusions can be drawn from the flexural and shear tests performed on prestressed pre-slabs:

- The failure bending moments achieved in flexural tests are similar, even higher than that of reference concrete with a maximum increase of 9 % for 4% replacement. Therefore, small amounts of recycled aggregate do not have a detrimental effect on the failure bending moment.
- The deflection achieved under the sustained load of 20 kN in flexural tests is increased as the replacement level raises with a maximum increase of 114% for 10% replacement. However, the deflection achieved at failure maintains a value between 50-60 mm, with the exception of the pre-slab with 2% replacement, in which the deflection is by 20% lower than the others values.
- In the shear behaviour tests, the ultimate shear remains unaffected for 2% replacement but it decreases around 25% for the remaining substitutions. Therefore, it

can be concluded that the recycled aggregate has a negative influence on the shear strength.

In accordance with the results obtained and due the absence of detailed studies of long-term behaviour, it is concluded that it is feasible to replace up to 10% of the total natural aggregate with recycled aggregate in this type of concrete and element, provided that the pre-slabs will not be subjected to excessive shear forces.

Quality control of prestressed concrete

The following conclusions can be drawn from the experimental program performed in laboratory to evaluate the properties of the vibrated recycled concrete used for the fabrication of the prestressed beams. Replacement levels of 0, 8, 20 and 31% replacement of the total aggregate (fine and coarse) were studied.

- All recycled concretes showed enough consistency at a fixed water-to-cement content 0.45. For F-8 and F-20 mixes, slump was increased 8 and 13%, respectively, due to the higher free water content. However, for F-31 mix the slump measured stabilized with respect to 20% replacement, probably because the effect of water absorption is more noticeable for higher replacement levels.
- Density of hardened concrete was decreased by 1, 4 and 5% for 8, 20, and 31% replacement of the total aggregate, respectively. The reason is the lower particle density of recycled aggregate in comparison with natural aggregate.
- The compressive strength at 28 days was decreased 1, 3 and 9% for 8, 20, and 31% replacement of the total aggregate, respectively.
- From the flexural strength test, with the exception of the incoherent value obtained for 0% replacement, general trend was that the flexural strength was decreased as the replacement level increased with losses of 8 and 13% for 20 and 31% replacement, respectively, with regard to F8.
- The modulus of elasticity at the age of 28 days was decreased 3, 8 and 20% for 8, 20 and 31% replacement of the total aggregate, respectively.
- The depth of penetration of water under pressure test showed that penetration depth is not increased when recycled aggregate is introduced in the mix.

Considering that the properties of this concrete are not adversely affected by the simultaneous replacement of this type of fine and coarse concrete recycled aggregates, it might be concluded that it is feasible to replace up to 31% of the total amount of natural aggregate by this particular recycled aggregate. However, it would be interesting to perform more durability tests to evaluate shrinkage performance, chloride-ion penetration, abrasion resistance and carbonation resistance, in order to evaluate the long-term behaviour since

this concrete is utilised for the fabrication of prestressed elements that must avoid losses in the prestressing force.

Prestressing force transfer

With the mix composition previously studied, four beams were fabricated with 0% replacement of the total aggregate and four beams with 8% replacement. The following conclusions can be drawn from the prestressing force transfer during the fabrication process of the beams:

- The mean value of slip registered at transfer with linear displacement sensors was 25% higher for recycled concrete beams, with a maximum slip of 2.515 mm, than in natural concrete beams, with a maximum slip of 2.009 mm.
- Great differences were not observed with regard to camber at mid-span and elastic shortening at transfer between natural and 8% recycled concrete beams.
- Immediate losses registered by strain gauges adhered to the steel strands were by 25% higher for beams with 8% replacement of recycled aggregate than in natural concrete beams.

Pull-Out bond tests

Pull-Out bond tests were performed to simulate the bond behaviour along the flexural bond length. Five specimens were fabricated for the mix composition studied in laboratory with 0% replacement of the total aggregate and five samples for the mix with 8% replacement. From these tests, it can be concluded that:

- The bond stress at which the first slip occurs (0.01 mm) was approximately 24% lower when 8% of the total aggregate is replaced with recycled aggregate. This loss in bond behaviour is important, considering that only 8% of the total aggregate was replaced.

Transfer length

DEMEC gauge points adhered to the bottom flange surface of both ends of the beam were used to determine the transfer length immediately after transfer and at 7, 14, 28, 90 and 300 days after casting. The following conclusions can be drawn:

- The detrimental effect of 8% replacement of recycled aggregate on transfer length and maximum strain was noticeable. The transfer length of the beams made with solely natural aggregate was determined as 717 mm (60ø), while the transfer length of the beams with 8% replacement of recycled aggregate was determined as 957 mm (75ø).
- The transfer length of the recycled concrete beam was clearly higher than in the natural concrete beam, especially at late ages. If maximum values are compared,

transfer length was increased by 33% and 13%, at passive and active ends, respectively, when 8% recycled aggregate was introduced in the mix.

- This increase in transfer length agrees with the loss of bond detected in the pull-out tests, when the bond stress at which the first slip occurred (0.01 mm) was approximately 24% lower when 8% of the total aggregate was replaced with recycled aggregate.
- Another detrimental effect of the recycled aggregate on transfer length can be observed in its evolution over time. If the transfer length measured immediately after transferring the prestressing force is compared with the maximum length, at both sides of the beams, it can be concluded that the increase of transfer length over time is higher for beams with recycled aggregate than in beams with only natural aggregate. In the natural concrete beam, this value was increased 16 and 9% at passive and active anchor, respectively. While, in recycled concrete beam, the increase was considerably higher, 66 and 27 % at passive and active anchor, respectively.
- Several authors proposed equations for transfer length based on the slip detected at transfer. The maximum transfer length obtained from the DEMEC points measurements for the natural concrete beam was in the range of values predicted by the proposed equations. However, in the case of B1R all the equations based on slip at transfer were non-conservative, with values up to 30% lower than the measured one.
- Other authors and Codes propose equations to predict transfer length based on the prestressing force of the strand and properties of concrete at transfer. The experimental value of transfer length in the natural concrete beam agrees with the value predicted by some of the proposed equations. However, In the case of recycled concrete beams, most equations propose values lower than the experimental one due to the presence of recycled aggregate and its lower bond performance.
- If the experimental values of transfer length are compared with the experimental values of other authors when 12.7 mm strands are tested, transfer length in natural concrete beams agrees with the values obtained.
- Studies on the influence of recycled aggregate on the transfer length have were not found, so it was not possible to compare the experimental results with that of the other authors.

Flexural bond length and development length

The beams were subjected to flexural tests at different embedment lengths and the slip values of strands during the test was registered. The development length of the beam was determined as the minimum embedment length for which maximum slip value detected at

the bottom strands was lower than 0.5 mm, reaching the nominal strength of the beam. The following conclusions were drawn from these tests:

- The development length of the beams made with solely natural aggregate was determined as 1475 mm. It was the maximum embedment length for which slip values lower than 0.5 mm were detected, in this case 0.48 mm at the north end.
- For the beams with 8% replacement of recycled aggregate, development length was stablished in 1850 mm, being the maximum embedment length for which slip values lower than 0.5 mm were detected (in this case 0.49 mm at North end).
- There was an increase of 25% in development length when 8% recycled aggregate is incorporated in the concrete mix. This may be due to the worst properties of recycled aggregate in comparison with natural aggregate, which result in a loss of bond between the prestressed steel and the surrounding concrete.
- This difference is comparable with the loss of bond stress detected in the pull-out tests when the first slip occurred, being by 24% lower when 8% of the total aggregate was replaced with recycled aggregate. Therefore, the pull-out bond test accurately predicted the difference in the development length when recycled aggregate was incorporated.
- Several authors and codes proposed equations for estimating flexural bond length based on the concrete and strand properties. However, most of them were excesively conservative for this particular case for both, natural and recycled concrete.
- With respect to equations predicting development length, the equation proposed by Ramirez and Russell agreed with the value obtained in conventional concrete beam, even predicting a value slightly higher. However, the value obtained in recycled concrete beam was by 14% higher than the value predicted by the Ramirez and Russel equation [RAMI 2007].
- From the experimental results performed by different authors with prestressed elements and 0.5 in. (12.7 mm strands) it can be concluded that some of them agreed with the experimental values obtained for these beams.
- With regard to the failure moment, large differences were not observed among the beams with recycled aggregates and the natural concrete beams, all values were in the range of 350 – 450 kN·m, regardless of the replacement ratio.
- Studies on the influence of recycled aggregate on the development length were not found to date. So, it was not possible to compare these results with that of previous authors.

Considering the results obtained from the test performed on prestressed concrete, it may be concluded that the bond loss is significant when 8% of the total aggregate is replaced

by fine and coarse recycled concrete aggregate. However, the failure moments are similar regardless of the amount of recycled aggregate. It would be necessary to perform durability tests in order to analyse the long-term behaviour when recycled aggregate is introduced in the mix.

6.2. Future Lines of Research

The study included in this doctoral thesis offers a good approach of the mechanical performance of concrete when fine and coarse recycled aggregates are incorporated. However, it would be interesting to evaluate its durability performance, especially when fine recycled aggregate is incorporated. Depending on the source of recycled aggregate, it may contain particles with detrimental effects on the reinforcing and prestressing steel. Therefore, durability tests are proposed as a future line of research. In particular:

- Shrinkage performance
- Abrasion resistance
- Chloride-ion penetration
- Water absorption by immersion
- Water absorption by capillarity
- Carbonation resistance
- Freeze-thaw

The preliminary study performed on prestressed pre-slab showed a good flexural behaviour for replacement levels up to 10% but a decrease in the ultimate shear strength of 25% for 10% replacement.

In the case of prestressed concrete beams, shear behaviour was not studied. It would be interesting to perform shear failure tests with an appropriate monitoring to study the loss of shear strength when recycled aggregate is introduced in the mix.

In this research, only two recycled aggregates were used for the fabrication of the beams. It would be a good idea to repeat the tests with recycled aggregates from different sources, with lower and higher quality. When prestressed recycled concrete was tested, the loss of bond performance was significant replacing solely 8% of the total aggregate. Maybe with a higher quality recycled aggregate, or replacing only the coarse fraction, the bond loss would be lower. The proposed study would offer a better understanding of the influence of recycled aggregates on reinforced and prestressed concrete.

Analytical models, numerical methods and finite element method are currently being applied so as to model the prestressed concrete beams, in a shared research project by the University of A Coruña and the Institute of Engineering of the National Autonomous

University of Mexico, so as to analyse the structural behaviour along the transfer length, the flexural bond length, stiffness, ductility and strength of the structural members object of this research, up to failure. Results of this research will allow a better understanding of the structural behaviour of recycled aggregate prestressed concrete girders.

References and Bibliography

References

[ABRI 1993] Abrishami, H. H., & Mitchell, D. (1993) Bond characteristics of pretensioned strand, *ACI Materials Journal*; 90 (3):228-235

[AGRE 2011] Agrela,F., Sánchez De Juan,M., Ayuso,J., Geraldes,V.L.,& Jiménez,J.R. (2011). Limiting properties in the characterisation of mixed recycled aggregates for use in the manufacture of concrete. Construction and Building Materials, Vol 25 (10), 3950-3955.

[ALAE 2011] Alaejos et al. (2011). Estudio prenormativo sobre la utilización de los RCDs en hormigón reciclado de aplicación estrucutral (Proyecto RECNHOR) y Reciclado de los RCDs como áridos de hormigones estructurales (Proyecto CLEAM). Ed. IECA. Madrid (España).

[AL-ZA 2011] Al-Zahraa, F., El-Mihilmy, & M., Bahaa, T. (2011). Experimental investigation of shear strength of concrete beams with recycled concrete aggregates. *International Journal of Materials and Structural Integrity, 5*(4), 291-310.

[ANDR 2013] Andrawes, B., Pozolo, A., & Chen, Z. (2013) Development length tests of full-scale prestressed self-consolidating concrete box and I-girders. *Journal of Bridge Engineering, 18(11), 1209-1218.*

[AREZ 2014] Arezoumandi, M., Smith, A., Volz, J., & Khayat, K. (2014). An experimental study on shear strength of reinforced concrete beams with 100% recycled concrete aggregate. *Construction & Building Materials, 53*, 612-620.

[AREZ 2015a] Arezoumandi, M., Smith, A., Volz, J., & Khayat, K. (2015). An experimental study on flexural strength of reinforced concrete beams with 100% recycled concrete aggregate. *Engineering Structures, 88*, 154-162.

[AREZ 2015b] Arezoumandi, M., Drury, J., Volz, J., & Khayat, K. (2015). Effect of recycled concrete aggregate replacement level on shear strength of reinforced concrete beams. *ACI Materials Journal, 112*(4), 559-568.

[AVRA 2016] Avramidis, I., Morfidis, K., Giaralis, A., Athanatopoulou, A., & Sextos, A. (2016). Eurocode-Compliant Seismic Analysis and Desing of R/C Buildings. Concepts, Commentary and Worked Examples with Flowcharts.

[BALA 1992] Balàzs. G. (1992) Transfer control of prestressing strands. *PCI Journal, V. 37, No.6, Nov. – Dec. 1992, pp. 60-71.*

[BALA 1993] Balàzs. G. (1993) Transfer length of prestressing strand as a function of draw-in and initial prestress, *PCI-Journal, V.38, No. 2, Mar.-Apr. 1993, pp. 86-93.*

[BRAV 2015a] Bravo, M., Bravo, M., de Brito, J., Pontes, J., & Evangelista, L. (2015). Mechanical performance of concrete made with aggregates from construction and demolition waste recycling plants. *Journal of Cleaner Production, 99*, 59-74.

[BRAV 2015b] Bravo, M., Bravo, M., de Brito, J., Pontes, J., & Evangelista, L. (2015). Durability performance of concrete with recycled aggregates from construction and demolition waste plants. *Construction & Building Materials, 77*, 357-369.

[BRUN 1987] Gru Brundtland, Mansour Khalid, Susanna Agnelli, et al. “Our Common Future ('Brundtland report') (21 May 1987)”.

[BUCK 1995] Buckner, C. D. (1995) A review of strand development length for pretensioned concrete members. *PCI Journal, 40(2), 84-105.*

[CARR 2015] Carro-López, D., Carro-López, D., González-Fonteboa, B., de Brito, J., Martínez-Abella, F., González-Taboada, I., & Silva, P. (2015). Study of the rheology of self-compacting concrete with fine recycled concrete aggregates. *Construction & Building Materials, 96*, 491-501.

[CEB-FIB] CEB-FIP (1989) Diagnosis and assessment of concrete structures - State of art report. CEB Bull 192:83–85

[CHAN 2013] Chan, D., & Poon, C. S. (2013). Effects of fine recycled aggregate as sand replacement in concrete. *Transactions - Hong Kong Institution of Engineers, 13*(4), 2-6.

[CHOI 2008] Choi, H. B., Yi, C. K., Cho, H. H., & Kang, K. I. (2010). Experimental study on the shear strength of recycled aggregate concrete beams. *Magazine of Concrete Research, 62*(2), 103-114.

[CHOI 2012] Choi, W., Yun, H., & Kim, S. (2012). Flexural performance of reinforced recycled aggregate concrete beams. *Magazine of Concrete Research, 64*(9), 837-848.

[CHOI 2013] Choi, W., & Yun, H. (2013). Long-term deflection and flexural behavior of reinforced concrete beams with recycled aggregate. *Materials in Engineering, 51*, 742-750.

[CORI 2004] Corinaldesi, V.,& Moriconi, G. (2004). Concrete and mortar performance by using recycled aggregates. Construction Demolition Waste. Conference paper.

[CORI 2009] Corinaldesi, V.,& Moriconi, G. (2009). Influence of mineral additions on the performance of 100% recycled aggregate concrete. *Construction & Building Materials, 23*(8), 2869-2876.

[CORI 2009b] Corinaldesi, V., Kew, H. Y., & Limbachiya, M. C. (2009). Environmentally-friendly self-compacting concrete for rehabilitation of concrete structures. *Excellence in Concrete Construction through Innovation - Proceedings of the International Conference on Concrete Construction 2009*, Pages 403-407.

[COUS 1990] Cousins, T. E., Johnston, D. W., & Zia, P. (1990) Transfer and development length of epoxy coated and uncoated prestressing strand. *PCI Journal, 35(4), 92-103.*

[COUS 1993] Cousins, T. E., Stallings, J. M. & Simmons, M. B. (1993) Effect of Strand Spacing on Development of Prestressing Strands. *Research Report, Alaska Department of Transportation and Public Facilities*, August 1993.

[DEAT 1994] Deatherage, J., Burdette, E., & Chew, C. (1994) Development length and lateral spacing requirements of prestressing strand for prestressed concrete bridge girders. *PCI Journal, 39(1), 70-83.*

[EIRA 2009] Estudio experimental de la capacidad adherente de las armaduras de pretensado. Tesis Doctoral. Universidade da Coruña. 2009.

[EURO 2011] European Commission (DG ENV). (2011). Service Contract on Management of Construction and Demolition Waste – SR1. A project under the Framework contract ENV.G.4/FRA/2008/0112. BIO Intelligence Service in association with ARCADIS and Institute European Enviromental Policy.

[ETXE 2015] Etxeberria,M.,&Vegas,I. (2015). Effect of fine ceramic recycled aggregate (RA) and mixed fine RA on hardened properties of concrete. Magazine of Concrete Research, Vol 67 (12), 645-655.

[EVAN 2007] Evangelista, L., & de Brito, J. (2007). Mechanical behaviour of concrete made with fine recycled concrete aggregates. *Cement Concrete Composites, 29*(5), 397-401.

[EVAN 2010] Evangelista, L., & de Brito, J. (2010). Durability performance of concrete made with fine recycled concrete aggregates. *Cement Concrete Composites, 32*(1), 9-14.

[EVAN 2014] Evangelista, L., & de Brito, J. (2014). Concrete with fine recycled aggregates: A review. *European Journal of Environmental and Civil Engineering, 18*(2), 129-172.

[FATH 2011] Fathifazl, G., Razaqpur, A. G., Burkan-Isgor, O., Abbas, A., Fournier, B., & Foo, S. (2011). Shear capacity evaluation of steel reinforced recycled concrete (RRC) beams. *Engineering Structures, 33*(3), 1025-1033.

[FHWA 1988] FHWA, "Memorandum," Federal Highway Administration, Washington, DC, October 26, 1988.

[FHWA 1996] FHWA, "Memorandum," Federal Highway Administration, Washington, DC, May 8, 1996.

[FLOY 2011] Floyd, R., Howland, M., & Micah Hale, W. (2011) Evaluation of strand bond equations for prestressed members cast with self-consolidating concrete. *Engineering Structures, 33(10), 2879-2887.*

[GEAR 2012] Guía española de áridos reciclados procedentes de residuos de construcción y demolición (RCD) Proyecto GEAR, 2012. GERD, Gremio de Entidades de Reciclaje de Derribos, Universidad Politécnica de Catalunya, Universidad Politécnica de Valencia, Universidad de A Coruña, Universidad de Oviedo, AITEMIN, INTROMAC y AIDICO, Madrid.

[GESO 2015a] Gesoglu, M., Güneyisi, E., Öz, H., Yasemin, M., & Taha, I. (2015). Durability and shrinkage characteristics of self-compacting concretes containing recycled coarse and/or fine aggregates. *Advances in Materials Science and Engineering, 2015*, 1-18.

[GESO 2015b] Gesoglu, M., Güneyisi, E., Öz, H., Taha, I., & Yasemin, M. (2015). Failure characteristics of self-compacting concretes made with recycled aggregates. *Construction & Building Materials, 98*, 334-344.

[GHEI 2012] Gheidari, M. H. N., & Salkhordeh, S. (2012). Laboratory investigation on the effect of adding different percentages of recycled concrete aggregates on the compressive strength of self-compacting concrete. *Ecology, Environment and Conservation, 18*(2), 215-218.

[GIRG 2005] Girgis, A. F. M., & Tuan, C. Y. (2005) Bond strength and transfer length of pretensioned bridge girders cast with self-consolidating concrete. *PCI Journal, 50(6), 72-87.*

[GOME 2009] Gomes,M.,&De Brito,J. (2009). Structural concrete with incorporation of coarse recycled concrete and ceramic aggregates: Durability performance. Materials and Structures/Materiaux et Constructions, Vol 42 (5), 663-675.

[GONZ 2007] González-Fonteboa, B., & Martínez-Abella, F. (2007). Shear strength of recycled concrete beams. *Construction & Building Materials, 21*(4), 887-893.

[GONZ 2009] González-Fonteboa, B., Martínez-Abella, F., Martínez-Lage, I., & Eiras-López, J. (2009). Structural shear behaviour of recycled concrete with silica fume. *Construction & Building Materials, 23*(11), 3406-3410.

[GONZ 2014] Gonzalez-Corominas,A.,&Etxeberria,M. (2014). Properties of high performance concrete made with recycled fine ceramic and coarse mixed aggregates. Construction and Building Materials, Vol 68, 618-626.

[GONÇ 2010] Gonçalves, P., & de Brito, J. (2010). Recycled aggregate concrete (RAC) – comparative analysis of existing specifications. *Magazine of Concrete Research, 62*(5), 339-346.

[GRDI 2010] Grdic, Z. J., Toplicic-Curcic, G. A., Despotovic, I. M., & Nenad, S. R. (2010). Properties of self-compacting concrete prepared with coarse recycled concrete aggregate. *Construction & Building Materials, 24*(7), 1129-1133.

[GUYO 1953] Guyon, Y. (1953) Pretensioned Concrete: Theoretical and Experimental Study. Paris, France. 1953, 711 pp.

[HANS 1959] Hanson, N. W., & Kaar, P. H. (1959) Flexural Bond Tests of Pretensioned Prestressed Beams, *ACI Journal, Proceedings V. 55, No. 7, Jan. 1959, pp. 783-803.*

[HOYE 1939] Hoyer, E., & Friederich, E. (1939) Beitrag zur Frage der Haftspannung in Eisenbeton-bauteilen; *Beton und Eisen; Vol. 50, No. 9, pp. 717-736*; Berlín.

[IGNJ 2013] Ignjatovic, I. S., Marinkovic, S. B., Miskovic, Z. M., & Savic, A. R. (2013). Flexural behavior of reinforced recycled aggregate concrete beams under short-term loading. *Materials and Structures, 46*(6), 1045-1059.

[JANE 1954] Janney, J.R. (1954) Nature of Bond in Pre-Tensioned Prestressed Concrete; *Journal of the American Concrete Institute; Vol. 25, No. 9, pp. 717-736; ACI*; May.

[JANG 2014] Jang, S., & Yun, H. (2015). Mechanical properties of ready-mixed concrete incorporating fine recycled aggregate. *Magazine of Concrete Research, 67*(12), 621-632.

[KAAR 1963] Kaar, P., LaFraugh, R., & Mass, M. (1963) Influence of Concrete Strength on Strand Transfer Length, *PCI Journal, V. 5, No. 8, October 1963, pp. 47-67.*

[KAHN 2012] Kahn, L., Dill, J., & Reutlinger, C. (2002). Transfer and development length of 15-mm strand in high performance concrete girders. *Journal of Structural Engineering, 128(7), 913-921.*

[KANG 2014] Kang, T. H. K., Kim, W., Kwak, Y. K., & Hong, S. G. (2015). Flexural testing of reinforced concrete beams with recycled concrete aggregates. *ACI Structural Journal, 112*(2), 239-240.

[KHAF 2014] Khafaga, S. A. (2014). Production of high strength self compacting concrete using recycled concrete as fine and/or coarse aggregates. *World Applied Sciences Journal, 29*(4), 465-474.

[KHAT 2005] Khatib, J. M. (2005). Properties of concrete incorporating fine recycled aggregate. *Cement and Concrete Research, 35*(4), 763-769.

[KNAA 2014] Knaack, A., & Kurama, Y. (2015). Behavior of reinforced concrete beams with recycled concrete coarse aggregates. *Journal of Structural Engineering (United States)*. Vol. 141, Issue 3, 1 March 2015, Article number B4014009.

[KIM 2011] Kim, H. Y., Chun, B. S., Park, T. H., & Ryou, J. S. (2011). An investigation of the recycling of waste concrete as a cementitious material. *Journal of Ceramic Processing Research, 12*(2), 202-206.

[KOSE 2005] Kose, M. M., & Burkett, W. R. (2005) Formulation of new development length equation for 0.6 in. prestressing strand. *PCI Journal, 50(5), 96-105.*

[KOSH 2014] Khoshkenari, A. G., Khoshkenari, A. G., Shafigh, P., Moghimi, M., & Mahmud, H. B. (2014). The role of 0–2mm fine recycled concrete aggregate on the compressive and splitting tensile strengths of recycled concrete aggregate concrete. *Materials in Engineering, 64*, 345-354.

[KOU 2009a] Kou, S. C., & Poon, C. S. (2009). Properties of concrete prepared with crushed fine stone, furnace bottom ash and fine recycled aggregate as fine aggregates. *Construction & Building Materials, 23*(8), 2877-2886.

[KOU 2009b] Kou, S. C., & Poon, C. S. (2009). Properties of self-compacting concrete prepared with coarse and fine recycled concrete aggregates. *Cement & Concrete Composites, 31*(9), 622-627.

[LANE 1998] Lane S.N. (1998) A new development length equation for pretensioned strands in bridge beams and piles. *Research FHWA-RD-98-116. Mclean, VA: Federal Highway Administration*.

[LARS 2007] Larson, K. H., Peterman, R. J., & Esmaeily, A. (2007) Bond characteristics of self-consolidating concrete for prestressed bridge girders. PCI Journal, 52(4), 44-57.

[LEE 2013] Lee, Y. T., Kim, S. H., Kim, J. H., Baek, S. K., Cho, Y. S., & Hong, S. U. (2013). Flexural behavior of high strength reinforced concrete beams by replacement ratio of recycled coarse aggregate. *Advanced Materials Research*, Vol. 680, pp. 230-233.

[LOGA 1997] Logan D. R. (1997) Acceptance criteria for bond quality of strand for pretensioned prestressed concrete applications. *PCI Journal, 42(2), 52–90.*

[LOTF 2015] Lotfi, S., Eggimann, M., Wagner, E., Mróz, R., & Deja, J. (2015). Performance of recycled aggregate concrete based on a new concrete recycling technology. *Construction & Building Materials, 95*, 243-256.

[MAHM 1999] Mahmoud Z.I., Rizkalla S.H., & Zaghloul E.R. (1999) Transfer and development lengths of carbon fiber reinforcement polymers prestressing reinforcing. *ACI Structural Journal 1999; 96(4):594–602.*

[MARD 2014] Mardani-Aghabaglou, A., Mardani-Aghabaglou, A., Tuyan, M., & Ramyar, K. (2014). Mechanical and durability performance of concrete incorporating fine recycled concrete and glass aggregates. *Materials and Structures,* 48(8), 2629-2640.

[MARS 1969] Marshall, W. T., & Krishnamurthy, D. (1969) Transmission length of prestressing tendons from concrete cube strengths at transfer*. Indian Concrete J, 43(7), 244-253,275.*

[MART 2003] Martí, J. R. (2003). Experimental Study on Bond of Prestressing Strand in High-Strength Concrete. [In Spanish.] Doctoral thesis, Polytechnic University of Valencia.

[MART 2006] Martí-Vargas, J. R., Arbaláez, C. A., Serna-Ros, P., Fernández-Prada, M. A., & Miguel-Sosa, P. F. (2006) Transfer and development lengths of concentrically prestressed concrete. *PCI Journal, 51(5), 74-85.*

[MART 2007a] Martí Vargas, J. R., Arbeláez, C. A., Serna-Ros, P., Navarro-Gregori, J., & Pallarés-Rubio, L. (2007) Analytical model for transfer length prediction of 13 mm prestressing strand. *Structural Engineering and Mechanics, 26(2), 211-229.*

[MART 2007b] Martí Vargas, J. R., Arbeláez, C. A., Serna-Ros, P., & Castro-Bugallo, C. (2007) Reliability of transfer length estimation from strand end slip. *ACI Structural Journal, 104(4), 487-494.*

[MART 2010] Martínez-Lage, I., Martínez-Abella, Fernández-Herrero, C., & Ordóñez, J. L. P. (2010). Estimation of the annual production and composition of C&D debris in Galicia (Spain). *Waste Management, 30*(4), 636-645.

[MART 2012] Martínez Lage, I., Martínez Abella, F., Vázquez Herrero, C., & Pérez Ordóñez, J. (2012). Properties of plain concrete made with mixed recycled coarse aggregate. *Construction & Building Materials, 37*, 171-176.

[MART 2012a] Martí Vargas, J. R., Serna, P., Navarro Gregori, J., & Bonet, J. L. (2012) Effects of concrete composition on transmission length of prestressing strands. *Construction & Building Materials, 27(1), 350-356.*

[MART 2012b] Martí Vargas, J. R., Serna, P., Navarro Gregori, J., & Pallarés, L. (2012) Bond of 13mm prestressing steel strands in pretensioned concrete members. *Engineering Structures, 41, 403-412.*

[MAS 2012] Mas, B., Cladera, A., Bestard, J., Muntaner, D., López, C.E., Piña ,S., et al. (2012). Concrete with mixed recycled aggregates: Influence of the type of cement. Construction and Building Materials, Vol 34, 430-441.

[MELI 2010] Meli R. (2010) Diseño Estructural [Structural Design] Segunda Edición. México DF: Limusa.

[MITC 1993] Mitchell, D., Cook, W. D., Khan, A. A., & Tham, T. (1993) Influence of High Strength Concrete on Transfer and Development Length of Pretensioning Strand. *PCI Journal, Vol. 38, No. 3, May-June, 52-66.*

[OH 2014] Oh, B. H., Lim, S. N., Lee, M. K., & Yoo, S. W. (2014) Analysis and prediction of transfer length in pretensioned, prestressed concrete members. *ACI Structural Journal, 111(3), 549-559.*

[PERE 2012a] Pereira, P., Evangelista, L., & de Brito, J. (2012). The effect of superplasticisers on the workability and compressive strength of concrete made with fine recycled concrete aggregates. *Construction Building Materials, 28*(1), 722-729.

[PERE 2012b] Pereira, P., Evangelista, L., & de Brito, J. (2012). The effect of superplasticizers on the mechanical performance of concrete made with fine recycled concrete aggregates. *Cement Concrete Composites, 34*(9), 1044-1052.

[PTI 2006] PTI. Recommendations for prestressed rock and soil anchors (revised 1996). Phoenix: Post-tensioning Institute; (2006).

[POZO 2011a] Pozolo, A., & Andrawes, B. (2011) Analytical prediction of transfer length in prestressed self-consolidating concrete girders using pull-out test results. *Construction & Building Materials, 25(2), 1026-1036.*

[POZO 2011b] Pozolo, A. M., & Andrawes, B. (2011) Transfer length in prestressed self-consolidating concrete box and I-girders. *ACI Structural Journal, 108(3), 341-349.*

[RAMI 2007] Ramirez J. A., & Russell B. W. (2007) Transfer, development, and splice length for strand/reinforcement in high-strength concrete. *Final report. West Lafayette (IN): Purdue University.*

[ROSE 1997] Rose, D. R., & Russell, B. W. (1997) Investigation of Standardized Tests to Measure the Bond Performance of Prestressing Strand. *PCI Journal, V.42, No. 4, July-Aug. 1997, pp. 56-80.*

[RUSS 1992] Russell, B. W. (1992) Design guidelines for transfer, development and debonding of large diameter seven wire strands in pretensioned concrete girders. Doctoral thesis, The Univ. of Texas at Austin, Austin, Texas.

[RUSS 1996] Russell, B. W., & Burns, N. H. (1996) Measured transfer lengths of 0.5 and 0.6 in. strands in pretensioned concrete. *PCI Journal, 41(5), 44-64.*

[RUSS 1997] Russell, B.W.; & Burns, N.H. (1997) Measurement of Transfer Lengths on Pretensioned Concrete Elements; *Journal of Structural Engineering; Vol. 123, No. 5, pp. 541-549.*

[SATO 2007] Sato, R., Maruyama, I., Sogabe, T., & Sogo, M. (2007). Flexural behavior of reinforced recycled concrete beams. *Journal of Advanced Concrete Technology, 5*(1), 43-61.

[SEAR 2014] Seara-Paz, S. Efecto de las deformaciones diferidas sobre la respuesta estructural a flexión y análisis del comportamiento adherente del hormigón reciclado. Tesis Doctoral. Universidade da Coruña.

[SHAH 1992] Shahawy, M.A., Issa, M., & Batchelor, B. (1992) Strand Transfer Lengths in Full Scale AASHTO Prestressed Concrete Girders. *PCI Journal, Vol. 37, No. 3, May-June, 84-96.*

[SHAH 2001] Shahawy, M. (2001) A critical evaluation of the AASHTO provisions for strand development length of prestressed concrete members. *PCI Journal, 46(4), 94 – 117.*

[SYMO 1999] Construction and demolition waste management practices, and their economic impacts. Report to DGXI, European Commission. Final Report February 1999. Report by Symonds, in association with ARGUS, COWI and PRC Bouwcentrum.

[TADR 1996] Tadros M. K., & Baishya M. C. (1996) Discussion of A review of strand development length for pretensioned concrete members. *PCI Journal 1996; 41(2):112–27.*

[TANG 2013] Tang, W. (2013). Fresh properties of self-compacting concrete with coarse recycled aggregate. *Advanced Materials Research.* Vols. 602-604 (2013) pp. 938-942.

[VAZQ 2001] Estudio comparativo de las propiedades de adherencia de cordones de pretensado en elementos prefabricados de hormigones de altas prestaciones iniciales. Tesis Doctoral. Universidade da Coruña. Diciembre, 2001.

[VAZQ 2013a] Vázquez Herrero, C., Martínez Lage, I., Aguilar, G., & Martínez Abella, F. (2013) Evaluation of strand bond properties along the transfer length of prestressed lightweight concrete members. *Engineering Structures, 49, 1048-1058.*

[VAZQ 2013b] Vázquez Herrero, C., Martínez Lage, I., & Martínez Abella, F. (2013) Transfer length in pretensioned prestressed concrete structures composed of high performance lightweight and normal-weight concrete. *Engineering Structures, 56, 983-992.*

[VAZQ 2013c] Vázquez Herrero, C., Martínez Lage, I., Vázquez Vázquez, H., & Martínez Abella, F. (2013) Comparative study of the flexural behavior of lightweight and normal weight prestressed concrete beams. *Engineering Structures, 56, 1868-1879.*

[VILL 2009] Villaverde, R. (2009). Fundamental Concepts of Eatrthquake Engineering.

[YAPR 2010] Yaprak, H., Aruntas, H. Y., Demir, I., Simsek, O., & Durmus, G. (2011). Effects of the fine recycled concrete aggregates on the concrete properties. *International Journal of Physical Sciences, 6*(10), 2455-2461.

[YUAN 2012] Yuan, Y., Ueda, T., & Chunlong, Y. U. (2012). SCC produced with recycled concrete aggregates. *Advanced Materials Research.* Vols. 512-515 (2012) pp. 2986-2989.

[ZIA 1977] Zia, P., & Mostafa, P. (1997) Development Length of Prestressing Strand, *PCI Journal, V. 22, No. 5, September-October 1977, pp. 54-66.*

Bibliography

ACHE Grupo de Trabajo2/5 "Hormigón reciclado". 2006. Coordinadora: P. Alaejos, Secretaría: M. Sánchez, Vocales: F. Aleza, M. Barra, M. Burón, J. Castilla, E. Dapena, M. Etxebarría, G. Francisco, B. Glez. Fonteboa, F. Mtnez. Abella, I. Mtnez. Lage, J.L. Parra, J.A. Polanco, M. Sanabria, E. Vázquez. Utilización de árido reciclado para la fabricación de hormigón estructural. ACHE Monografía M-11. Madrid. ISBN 84-89670-55-2.

Achtemichuk,S., Hubbard,J., Sluce,R.,& Shehata,M.H. (2009). The utilization of recycled concrete aggregate to produce controlled low-strength materials without using Portland cement. Cement and Concrete Composites, Vol 31 (8), 564-569.

Ajdukiewicz,A.B.,&Kliszczewicz,A.T. (2007). Comparative Tests of Beams and Columns Made of Recycled Aggregate Concrete and Natural Aggregate Concrete. Journal of Advanced Concrete Technology, Vol 5 (2), 259-273.

Andreu,G.,&Miren,E. (2014). Experimental analysis of properties of high performance recycled aggregate concrete. Construction and Building Materials, Vol 52, 227-235.

Bai,W.,Sun,B. 2010. Experimental study on flexural behavior of recycled coarse aggregate concrete beam. Applied Mechanics and Materials, Vol 29-32, 543-548.

Betat,E.F., Pereira,F.M.,& de Verney,J.C.K. (2009). Concretes produced with waste of agate processing: Assessment of compressive strength and cement content. Revista Materia, Vol 14 (3), 1047-1060.

Bhikshma,V.,&Kishore,R. (2010). Development of stress - strain curves for recycled aggregate concrete. Asian Journal of Civil Engineering, Vol 11 (2), 253-261.

De Brito,J.,&Alves,F. (2010). Concrete with recycled aggregates: The Portuguese experimental research. Materials and Structures/Materiaux et Constructions, Vol 43 (SUPPL. 1), 35-51.

de Brito,J.,&Robles,R. (2010). Recycled aggregate concrete (RAC) methodology for estimating its long-term properties. Indian Journal of Engineering and Materials Sciences, Vol 17 (6), 449-462.

Bustillo Revuelta,M. 2010. Manual de RCD y Áridos reciclados. Fueyo Editores. Madrid. ISBN 978-84-935279-7-6.

Cabral,A.E.B., Schalch,V., Molin,D.C.C.D.,& Ribeiro,J.L.D. (2010). Mechanical properties modeling of recycled aggregate concrete. Construction and Building Materials, Vol 24 (4), 421-430.

Casuccio,M., Torrijos,M.C., Giaccio,G.,& Zerbino,R. (2008). Failure mechanism of recycled aggregate concrete. Construction and Building Materials, Vol 22 (7), 1500-1506.

Chan,B. (2010). Recycled and secondary aggregates in concrete. Structural Engineer, Vol 88 (15-16), 12-13.

Chakradhara Rao,M., Bhattacharyya,S.K.,& Barai,S.V. (2011). Behaviour of recycled aggregate concrete under drop weight impact load. Construction and Building Materials, Vol 25 (1), 69-80.

Chan,D.,&Poon,C.S. (2006). Effects of fine recycled aggregate as sand replacement in concrete. Transactions Hong Kong Institution of Engineers, Vol 13 (4), 2-6.

Chen,M.-., Lin,J.-., Wu,S.-.,& Liu,C.-. (2011). Utilization of recycled brick powder as alternative filler in asphalt mixture. Construction and Building Materials, Vol 25 (4), 1532-1536.

Chidiroglou,I., O'Flaherty,F.,& Goodwin,A.K. (2009). Shear behavior of crushed concreate and bricks. Proceedings of Institution of Civil Engineers: Construction Materials, Vol 162 (3), 121-126.

Corinaldesi,V.,&Moriconi,G. (2010). Recycling of rubble from building demolition for low-shrinkage concretes. Waste Management, Vol 30 (4), 655-659.

Corinaldesi,V. (2010). Mechanical and elastic behaviour of concretes made of recycled-concrete coarse aggregates. Construction and Building Materials, Vol 24 (9), 1616-1620.

Corinaldesi,V. (2009). Mechanical behavior of masonry assemblages manufactured with recycled-aggregate mortars. Cement and Concrete Composites, Vol 31 (7), 505-510.

Debieb,F., Courard,L., Kenai,S.,& Degeimbre,R. (2010). Mechanical and durability properties of concrete using contaminated recycled aggregates. Cement and Concrete Composites, Vol 32 (6), 421-426.

Debieb,F., Courard,L., Kenai,S.,& Degeimbre,R. (2009). Roller compacted concrete with contaminated recycled aggregates. Construction and Building Materials, Vol 23 (11), 3382-3387.

Dhir,R.K.,&Paine,K.A. (2010). Value added sustainable use of recycled and secondary aggregates in concrete. Indian Concrete Journal, Vol 84 (3), 7-26.

Djerbi Tegguer,A. (2012). Determining the water absorption of recycled aggregates utilizing hydrostatic weighing approach. Construction and Building Materials, Vol 27 (1), 112-116.

Domingo,A., Lázaro,C., Gayarre,F.L., Serrano,M.A.,& López-Colina,C. (2010). Long term deformations by creep and shrinkage in recycled aggregate concrete. Materials and Structures/Materiaux et Constructions, Vol 43 (8), 1147-1160.

Domingo-Cabo,A., Lázaro,C., López-Gayarre,F., Serrano-López,M.A., Serna,P.,& Castaño-Tabares,J.O. (2009). Creep and shrinkage of recycled aggregate concrete. Construction and Building Materials, Vol 23 (7), 2545-2553.

Du,T., Wang,W., Liu,Z., Lin,H.,& Guo,T. (2010). The complete stress-strain curve of recycled aggregate concrete under uniaxial compression loading. Journal Wuhan University of Technology, Materials Science Edition, Vol 25 (5), 862-865.

Eguchi,K., Teranishi,K., Nakagome,A., Kishimoto,H., Shinozaki,K.,& Narikawa,M. (2007). Application of recycled coarse aggregate by mixture to concrete construction. Construction and Building Materials, Vol 21 (7), 1542-1551.

Etxeberria,M., Ainchil,J., Pérez,M.E.,& González,A. (2013). Use of recycled fine aggregates for Control Low Strength Materials (CLSMs) production. Construction and Building Materials, Vol 44, 142-148.

Etxeberria,M.,&Vázquez,E. (2010). Alkali silica reaction in concrete induced by mortar adhered to recycled aggregate. Materiales de Construccion, Vol 60 (297), 47-58.

Etxeberria,M., Marí,A.R.,& Vázquez,E. (2007). Recycled aggregate concrete as structural material. Materials and Structures/Materiaux et Constructions, Vol 40 (5), 529-541.

Etxeberria,M., Vázquez,E., Marí,A.,& Barra,M. (2007). Influence of amount of recycled coarse aggregates and production process on properties of recycled aggregate concrete. Cement and Concrete Research, Vol 37 (5), 735-742.

Etxeberria,M., Vázquez,E.,& Marí,A. (2006). Microstructure analysis of hardened recycled aggregate concrete. Magazine of Concrete Research, Vol 58 (10), 683-690.

Fernandez,I., Etxeberria,M.,& Marí,A.R. (2016). Ultimate bond strength assessment of uncorroded and corroded reinforced recycled aggregate concretes. Construction and Building Materials, Vol 111, 543-555.

Gao,S., Li,Q., Shang,Q. 2011. Quality evaluation of recycled fine aggregate based on the double-control concept of water demand ratio and strength ratio. Advanced Materials Research, Vol 168-170, 742-745.

García-González,J., Rodríguez-Robles,D., Juan-Valdés,A., Pozo,J.M.M.,& Guerra-Romero,M.I. (2014). Pre-saturation technique of the recycled aggregates: Solution to the water absorption drawback in the recycled concrete manufacture. Materials, Vol 7 (9), 6224-6236.

Gokce,A., Nagataki,S., Saeki,T.,& Hisada,M. (2004). Freezing and thawing resistance of air-entrained concrete incorporating recycled coarse aggregate: The role of air content in demolished concrete. Cement and Concrete Research, Vol 34 (5), 799-806.

Gómez-Soberón,J.M.V. (2003). Relationship between Gas Adsorption and the Shrinkage and Creep of Recycled Aggregate Concrete. Cement, Concrete and Aggregates, Vol 25 (2), 42-48.

Gonzalez-Corominas,A.,&Etxeberria,M. (2016). Effects of using recycled concrete aggregates on the shrinkage of high performance concrete. Construction and Building Materials, Vol 115, 32-41.

González Fonteboa,B. 2002. Hormigones con áridos reciclados procedentes de demoliciones: dosificaciones, propiedades mecánicas y comportamiento estructural a cortante. Universidade da Coruña. Tesis doctoral

González Fonteboa,B., Martínez,F., Carro,D.,& Eiras,J. (2010). Shear friction capacity of recycled concretes. Materiales de Construccion, Vol 60 (299), 53-67.

González,J.G., Robles,D.R., Valdés,A.J., Morándel Pozo,J.M., Romero,M.I.G. 2013. Influence of moisture states of recycled coarse aggregates on the slump test. Advanced Materials Research, Vol 742, 379-383.

González-Fonteboa,B., Martínez-Abella,F., Carro-López,D.,& Seara,S. (2011). Stress-strain relationship in axial compression for concrete using recycled saturated coarse aggregate. Construction and Building Materials, Vol 25 (5), 2335-2342.

González-Fonteboa,B.,&Martínez -Abella,F. (2005). Recycled aggregates concrete: Aggregate and mix properties. Materiales de Construccion, Vol 55 (279), 53-66.

Hebhoub,H., Aoun,H., Belachia,M., Houari,H.,& Ghorbel,E. (2011). Use of waste marble aggregates in concrete. Construction and Building Materials, Vol 25 (3), 1167-1171.

Ho,C.-.,Tsai,W.-. 2011. A study on the use of construction wastes as coarse aggregates on high performance concrete. Advanced Materials Research, Vol 163-167, 1525-1531.

Ho,C.-.,Tsai,W.-. 2011. Recycled concrete using crushed construction waste bricks subject to elevated temperatures. Advanced Materials Research, Vol 152-153, 1-10.

Hurley,J.,&Bush,R. (2007). The use of recycled aggregates in structural concrete. Concrete Engineering International, Vol 11 (3), 48-49.

Hwang,E.-.,&Hwang,T.-. (2007). Comparison of physical properties of pae polymer-modified mortars from recycled waste artificial marble and waste concrete fine aggregates. Journal of Industrial and Engineering Chemistry, Vol 13 (4), 585-591.

Ismail,S.,&Yaacob,Z. (2010). The possibility use of recycled fine aggregate in production of cement and sand bricks. International Journal of Materials Engineering Innovation, Vol 1 (3-4), 325-337.

Janković,K., Bojović,D.,& Nikolić,D. (2010). Some properties of concrete based on recycled bricks. Revista Romana de Materiale/ Romanian Journal of Materials, Vol 40 (3), 222-227.

Jiménez,J.R., Ayuso,J., Galvín,A.P., López,M.,& Agrela,F. (2012). Use of mixed recycled aggregates with a low embodied energy from non-selected CDW in unpaved rural roads. Construction and Building Materials, Vol 34, 34-43.

de Juan,M.S.,&Gutiérrez,P.A. (2009). Study on the influence of attached mortar content on the properties of recycled concrete aggregate. Construction and Building Materials, Vol 23 (2), 872-877.

Juan Valdés,A., Medina Martínez,C., Guerra Romero,M.I., Llamas García,B., Morán del Pozo,J.,& Tascón Vegas,A. (2010). Re-use of construction and demolition residues and industrial wastes for the elaboration or recycled eco-efficient concretes. Spanish Journal of Agricultural Research, Vol 8 (1), 25-34.

Katz,A. (2003). Properties of concrete made with recycled aggregate from partially hydrated old concrete. Cement and Concrete Research, Vol 33 (5), 703-711.

Kesegić,I., Bjegović,D.,& Netinger,I. (2009). Use of recycled brick as concrete aggregate. Gradjevinar, Vol 61 (1), 15-22.

Kesegić,I., Netinger,I.,& Bjegović,D. (2008). Recycled clay brick as an aggregate for concrete: Overview. Tehnicki Vjesnik, Vol 15 (3), 35-40.

Khalaf,F.M.,&DeVenny,A.S. (2004). Performance of brick aggregate concrete at high temperatures. Journal of Materials in Civil Engineering, Vol 16 (6), 556-565.

Kou,S.C., Poon,C.S.,& Etxeberria,M. (2014). Residue strength, water absorption and pore size distributions of recycled aggregate concrete after exposure to elevated temperatures. Cement and Concrete Composites, Vol 53, 73-82.

Kou,S.-., Poon,C.-.,& Etxeberria,M. (2011). Influence of recycled aggregates on long term mechanical properties and pore size distribution of concrete. Cement and Concrete Composites, Vol 33 (2), 286-291.

Lin,Y.-., Tyan,Y.-., Chang,T.-.,& Chang,C.-. (2004). An assessment of optimal mixture for concrete made with recycled concrete aggregates. Cement and Concrete Research, Vol 34 (8), 1373-1380.

López Gayarre,F., López-Colina Pérez,C., Serrano López,M.A.,& Domingo Cabo,A. (2014). The effect of curing conditions on the compressive strength of recycled aggregate concrete. Construction and Building Materials, Vol 53, 260-266.

López Gayarre,F., López-Colina,C., Serrano,M.A.,& López-Martínez,A. (2013). Manufacture of concrete kerbs and floor blocks with recycled aggregate from C&DW. Construction and Building Materials, Vol 40, 1193-1199.

López Gayarre,F. 2008. Influencia de la variación de los parámetros de dosificación y fabricación del hormigón reciclado estructural sobre sus propiedades físicas y mecánicas. Universidad de Oviedo. Tesis doctoral.

López-Gayarre,F., López-Colina,C., Serrano-López,M.A., García Taengua,E.,& López Martínez,A. (2011). Assessment of properties of recycled concrete by means of a highly fractioned factorial design of experiment. Construction and Building Materials, Vol 25 (10), 3802-3809.

López-Gayarre,F., Serna,P., Domingo-Cabo,A., Serrano-López,M.A.,& López-Colina,C. (2009). Influence of recycled aggregate quality and proportioning criteria on recycled concrete properties. Waste Management, Vol 29 (12), 3022-3028.

Kumutha,R.,&Vijai,K. (2010). Strength of concrete incorporating aggregates recycled from demolition waste. Journal of Engineering and Applied Sciences, Vol 5 (5), 64-71.

Lee,S.T., Moon,H.Y., Swamy,R.N., Kim,S.S.,& Kim,J.P. (2005). Sulfate attack of mortars containing recycled fine aggregates. ACI Materials Journal, Vol 102 (4), 224-230.

Li,X. (2009). Recycling and reuse of waste concrete in China. Part II. Structural behaviour of recycled aggregate concrete and engineering applications. Resources, Conservation and Recycling, Vol 53 (3), 107-112.

Limbachiya,M.C. (2010). Recycled aggregates: Production, properties and value-added sustainable applications. Journal Wuhan University of Technology, Materials Science Edition, Vol 25 (6), 1011-1016.

Limbachiya,M.C., Leelawat,T.,& Dhir,R.K. (2000). Use of recycled concrete aggregate in high-strength concrete. Materials and Structures/Materiaux et Constructions, Vol 33 (233), 574-580.

Lo,C.Y., Tam,V.W.Y.,& Kotrayothar,D. (2009). A simplified testing approach for recycled coarse aggregate in construction. Transactions Hong Kong Institution of Engineers, Vol 16 (4), 43-47.

Mačiulaitis,R., Vaičiene,M.,& Žurauskiene,R. (2009). The effect of concrete composition and aggregates properties on performance of concrete. Journal of Civil Engineering and Management, Vol 15 (3), 317-324.

Marinković,S., Radonjanin,V., Malešev,M.,& Ignjatović,I. (2010). Comparative environmental assessment of natural and recycled aggregate concrete. Waste Management, Vol 30 (11), 2255-2264.

Martín-Morales,M., Zamorano,M., Ruiz-Moyano,A.,& Valverde-Espinosa,I. (2011). Characterization of recycled aggregates construction and demolition waste for concrete production following the Spanish Structural Concrete Code EHE-08. Construction and Building Materials, Vol 25 (2), 742-748.

Matias,D., De Brito,J., Rosa,A.,& Pedro,D. (2013). Mechanical properties of concrete produced with recycled coarse aggregates - Influence of the use of superplasticizers. Construction and Building Materials, Vol 44, 101-109.

Mefteh,H., Kebaïli,O., Oucief,H., Berredjem,L.,& Arabi,N. (2013). Influence of moisture conditioning of recycled aggregates on the properties of fresh and hardened concrete. Journal of Cleaner Production, Vol 54, 282-288.

Bazán, E., Meli, R. (1999). Diseño Sísmico de Edificios.

Miranda,L.F.R.,&Selmo,S.M.S. (2006). CDW recycled aggregate renderings: Part I - Analysis of the effect of materials finer than 75 µm on mortar properties. Construction and Building Materials, Vol 20 (9), 615-624.

Murty,D.S.R.,&Durga,S.K. (2010). Performance of structural concrete with recycled coarse aggregate. Journal of Structural Engineering (Madras), Vol 37 (1), 26-30.

Obla,K.H. (2009). What to do with: Crushed, returned concrete. Concrete Producer, Vol 27 (9), 37-39.

Oikonomou,N.D. (2005). Recycled concrete aggregates. Cement and Concrete Composites, Vol 27 (2), 315-318.

Otsuki,N., Miyazato,S.-.,& Yodsudjai,W. (2003). Influence of recycled aggregate on interfacial transition zone, strength, chloride penetration and carbonation of concrete. Journal of Materials in Civil Engineering, Vol 15 (5), 443-451.

Pacheco-Torgal,F.,&Jalali,S. (2010). Reusing ceramic wastes in concrete. Construction and Building Materials, Vol 24 (5), 832-838.

Padmini,A.K., Ramamurthy,K.,& Mathews,M.S. (2009). Influence of parent concrete on the properties of recycled aggregate concrete. Construction and Building Materials, Vol 23 (2), 829-836.

Park,S.B., Lee,B.C.,& Kim,J.H. (2004). Studies on mechanical properties of concrete containing waste glass aggregate. Cement and Concrete Research, Vol 34 (12), 2181-2189.

Pereira,P., Evangelista,L.,& De Brito,J. (2012). The effect of superplasticizers on the mechanical performance of concrete made with fine recycled concrete aggregates. Cement and Concrete Composites, Vol 34 (9), 1044-1052.

Pereira,P., Evangelista,L.,& De Brito,J. (2012). The effect of superplasticisers on the workability and compressive strength of concrete made with fine recycled concrete aggregates. Construction and Building Materials, Vol 28 (1), 722-729.

Poon,C.S., Kou,S.C.,& Lam,L. (2007). Influence of recycled aggregate on slump and bleeding of fresh concrete. Materials and Structures/Materiaux et Constructions, Vol 40 (9), 981-988.

Poon,C.S.,&Lam,C.S. (2008). The effect of aggregate-to-cement ratio and types of aggregates on the properties of pre-cast concrete blocks. Cement and Concrete Composites, Vol 30 (4), 283-289.

Poon,C.-.,&Kou,S.-. (2009). Quality control of recycled aggregates derived from construction and demolition wastes. Sichuan Daxue Xuebao (Gongcheng Kexue Ban)/Journal of Sichuan University (Engineering Science Edition), Vol 41 (3), 248-257.

Poon,C.-., Kou,S.-., Wan,H.-.,& Etxeberria,M. (2009). Properties of concrete blocks prepared with low grade recycled aggregates. Waste Management, Vol 29 (8), 2369-2377.

Quaranta,N., Caligaris,M., López,H.,& Unsen,M. (2010). Working scheme for safe management of construction and demolition wastes containing hazardous substances. Vol 129 521-532.

Rahal,K. (2007). Mechanical properties of concrete with recycled coarse aggregate. Building and Environment, Vol 42 (1), 407-415.

Richardson,A., Allain,P.,& Veuille,M. (2010). Concrete with crushed, graded and washed recycled construction demolition waste as a coarse aggregate replacement. Structural Survey, Vol 28 (2), 142-148.

Salem,R.M., Burdette,E.G.,& Jackson,N.M. (2003). Resistance to freezing and thawing of recycled aggregate concrete. ACI Materials Journal, Vol 100 (3), 216-221.

Senthamarai,R., Manoharan,P.D.,& Gobinath,D. (2011). Concrete made from ceramic industry waste: Durability properties. Construction and Building Materials, Vol 25 (5), 2413-2419.

Senthamarai,R.M.,&Devadas Manoharan,P. (2005). Concrete with ceramic waste aggregate. Cement and Concrete Composites, Vol 27 (9-10), 910-913.

Da Silva Paula,M.M., De Lorenzi,V., Da Silva,L., Fiori,M.A.,& Bernardin,A.M. (2010). Leaching and solubility analysis of porcelain-recycled tile residues in clay bricks. International Journal of Applied Ceramic Technology, Vol 7 (2), 256-262.

Tabsh,S.W.,&Abdelfatah,A.S. (2009). Influence of recycled concrete aggregates on strength properties of concrete. Construction and Building Materials, Vol 23 (2), 1163-1167.

Tam,V.W.Y.,&Tam,C.M. (2009). Parameters for assessing recycled aggregate and their correlation. Waste Management and Research, Vol 27 (1), 52-58.

Topçu,I.B.,&Şengel,S. (2004). Properties of concretes produced with waste concrete aggregate. Cement and Concrete Research, Vol 34 (8), 1307-1312.

Torkittikul,P.,&Chaipanich,A. (2010). Utilization of ceramic waste as fine aggregate within Portland cement and fly ash concretes. Cement and Concrete Composites, Vol 32 (6), 440-449.

Valdés,G.A.,&Rapimán,J.G. (2007). Physical and mechanical properties of concrete bricks produced with recycled aggregates. Informacion Tecnologica, Vol 18 (3), 81-88.

Valdes,G.A.,&Rapiman,J.G. (2007). Physical and mechanical properties of concrete bricks produced with recycled aggregates; Propiedades fisicas y mecanicas de bloques de hormigon compuestos con aridos reciclados. Informacion Tecnologica, Vol 18 (3), 81-88.

Vegas,I., Ibañez,J.A., Lisbona,A., Sáez De Cortazar,A.,& Frías,M. (2011). Pre-normative research on the use of mixed recycled aggregates in unbound road sections. Construction and Building Materials, Vol 25 (5), 2674-2682.

Vegas,I., Azkarate,I., Juarrero,A.,& Frías,M. (2009). Design and performance of masonry mortars made with recycled concrete aggregates. Materiales de Construccion, Vol 59 (295), 5-18.

Xiao,J., Li,J.,& Zhang,C. (2005). Mechanical properties of recycled aggregate concrete under uniaxial loading. Cement and Concrete Research, Vol 35 (6), 1187-1194.

Xiao,J., Li,J.,& Zhang,C. (2006). On relationships between the mechanical properties of recycled aggregate concrete: an overview. Materials and Structures, Vol 39 (6), 655-664.

Xiao,J., Lu,D.,& Ying,J. (2013). Durability of recycled aggregate concrete: An overview. Journal of Advanced Concrete Technology, Vol 11 (12), 347-359.

Yang,K.-., Chung,H.-.,& Ashour,A.F. (2008). Influence of type and replacement level of recycled aggregates on concrete properties. ACI Materials Journal, Vol 105 (3), 289-296.

Yaprak,H., Aruntas,H.Y., Demir,I., Simsek,O.,& Durmus,G. (2011). Effects of the fine recycled concrete aggregates on the concrete properties. International Journal of Physical Sciences, Vol 6 (10), 2455-2461.

Yuan,X., Ruheng,W., Huachuan,Y. 2011. Experimental study on fundamental characteristic of recycled concrete. Advanced Materials Research, Vol 146-147, 1925-1929.

Zega,C.J.,&Di Maio,A.A. (2007). Effect of recycled coarse aggregate on concrete properties. Boletin Tecnico/Technical Bulletin, Vol 45 (2)

Zhang,X.-., Deng,S.-., Deng,X.-.,& Qin,Y.-. (2007). Experimental research on regression coefficients in recycled concrete Bolomey formula. Journal of Central South University of Technology (English Edition), Vol 14 (1 SUPPL.), 314-317.

Zhang,X.-., Deng,S.-.,& Qin,Y.-. (2007). Additional adsorbed water in recycled concrete. Journal of Central South University of Technology (English Edition), Vol 14 (1 SUPPL.), 449-453.

Zhao,W., Leeftink,R.B.,& Rotter,V.S. (2010). Evaluation of the economic feasibility for the recycling of construction and demolition waste in China-The case of Chongqing. Resources, Conservation and Recycling, Vol 54 (6), 377-389.

Zhu,H.-.,Li,X. 2009. Experiment on freezing and thawing durability characteristics of recycled aggregate concrete. Key Engineering Materials, Vol 400-402, 447-452.

Regulations

[ACI 318-63] ACI Committee 318, "Building Code Requirements for Reinforced Concrete", American Concrete Institute, Detroit, 1963, 144 pp.

[ACI 318-89] ACI Committee 318, "Building Code Requirements for Reinforced Concrete and Commentary (ACI 318-89/318R-89)", American Concrete Institute, Detroit, 1989, 353 pp.

[ACI 318-95] ACI Committee 318, "Building Code Requirements for Structural Concrete", American Concrete Institute, Farmington Hills, MI, 1995.

[ACI 318-99] ACI Committee 318, "Building Code Requirements for Structural Concrete" and "Commentary", American Concrete Institute, Detroit.

[ACI 318-02] ACI Committee 318, "Building Code Requirements for Structural Concrete" and "Commentary", American Concrete Institute, Farmington Hills, MI, 2002.

[ACI 318-05] ACI Committee 318, "Building Code Requirements for Structural Concrete" and "Commentary", American Concrete Institute, Farmington Hills, MI, 2005.

[ACI 318-08] ACI Committee 318, "Building Code Requirements for Structural Concrete" and "Commentary", American Concrete Institute, Farmington Hills, MI, 2008, 473 pp.

[AASHTO 92] AASHTO, Standard Specifications for Highway Bridges, 15th Edition, American Association of State Highway and Transportation Officials, Washington, D.C., 1992.

[AASHTO 96] AASHTO, Standard Specifications for Highway Bridges, 16th Edition, American Association of State Highway and Transportation Officials, Washington, D.C., 1996.

[AASHTO 97] AASHTO, LRFD, Specifications for Highway Bridges, Interim Revision, American Association of State Highway and Transportation Officials, Washington, D.C., 1997.

[AASHTO 04] "AASHTO LRFD Bridge Design Specifications", third edition. American Association of State Highway and Transportation Officials, Washington, D.C., 2004, 1450 pp.

[AASHTO 07] "AASHTO LRFD Bridge Design Specifications", 4th edition, Customary U.S. Units. American Association of State Highway and Transportation Officials, Washington, D.C., 2007.

[AASHTO 12] AASHTO LRFD Bridge Design Specifications", 6th edition, Customary U.S. Units. American Association of State Highway and Transportation Officials, Washington, D.C., 2012.

[CEN 1996] European Committee for Standardization. Eurocode 2: Design of concrete structures. Parts 1-4: General rules - Lightweight aggregate concrete with closed structure (in Spanish). Madrid. Aenor 1996.

[CEN 2004] Eurocode 2: design of concrete structures – Part 1–1: General Rules and Rules for Buildings. European standard EN 1992-1-1:2004. Comité Européen de Normalisation, Brussels, Belgium.

[EHE 2008] Instrucción de Hormigón Estructural. Ministerio de Fomento. España.

[MC 2010] FIB. Model Code 2010. First complete draft. Fib Bulletin No. 55, vol. 1. Lausanne: International Federation for Structural Concrete.

UNE 7-436-82: Método de ensayo para la determinación de las características de adherencia de las armaduras de pretensado.

UNE 83316:1996: Ensayos de hormigón. Determinación del módulo de elasticidad en compresión.

UNE-EN 933-1:2012. Tests for geometrical properties of aggregates - Part 1: Determination of particle size distribution - Sieving method.

UNE-EN 933-2/1M:1999. Test for geometrical properties of aggregates. Part 2: determination of particle size distribution. Test sieves, nominal size of apertures.

UNE-EN 933-3:2012. Tests for geometrical properties of aggregates - Part 3: Determination of particle shape - Flakiness index.

UNE-EN 933-5:1999/A1:2005. Test for geometrical properties of aggregates. Part 5: determination of percentage of crushed and broken surfaces in coarse aggregate particles.

UNE-EN 933-11:2009/AC:2010. Tests for geometrical properties of aggregates - Part 11: Classification test for the constituents of coarse recycled aggregate.

UNE-EN 1097-2:2010. Tests for mechanical and physical properties of aggregates - Part 2: Methods for the determination of resistance to fragmentation.

UNE-EN 1097-3:1999. Tests for mechanical and physical properties of aggregates. Part 3: determination of loose bulk density and voids.

UNE-EN 1097-5:2009. Tests for mechanical and physical properties of aggregates - Part 5: Determination of the water content by drying in a ventilated oven.

UNE-EN 1097-6:2014. Tests for mechanical and physical properties of aggregates - Part 6: Determination of particle density and water absorption.

UNE-EN 12350-8:2011. Testing fresh concrete - Part 8: Self-compacting concrete - Slump-flow test.

UNE-EN 12390-1:2013 (Versión corregida abril 2014). Testing hardened concrete - Part 1: Shape, dimensions and other requirements for specimens and moulds

UNE-EN 12390-2:2009/1M:2015. Testing hardened concrete - Part 2: Making and curing specimens for strength tests.

UNE-EN 12390-3:2009/AC:2011. Testing hardened concrete - Part 3: Compressive strength of test specimens.

UNE-EN 12390-5:2009. Testing hardened concrete - Part 5: Flexural strength of test specimens.

UNE-EN 12390-6:2010. Testing hardened concrete - Part 6: Tensile splitting strength of test specimens.

UNE-EN 12390-7:2009. Testing hardened concrete - Part 7: Density of hardened concrete.

UNE-EN 12390-8:2009. Testing hardened concrete - Part 8: Depth of penetration of water under pressure.

UNE-EN 12390-8:2009/1M:2011. Ensayos de hormigón endurecido. Parte 8: Profundidad de penetración de agua bajo presión.

UNE-EN 12390-13:2014. Testing hardened concrete - Part 13: Determination of secant modulus of elasticity in compression.

Appendix 1. Transfer, flexural bond and development length formulations

	Transfer length	Flexural bond length	Development length
Guyon [GUYO 1953]	$L_t = \alpha \frac{\delta E_p}{f_{pi}}$		
	δ = the strand end slip at the free end of a prestressed concrete member (mm) E_p = the modulus of elasticity of the prestressing strand (MPa) f_{pi} is the strand stress immediately before release (MPa) α = coefficient represents the shape factor of the bond stress distribution along the transfer zone (α=2 for uniform bond distribution and α=3 for linear descending bond distribution)		
Hanson and Kaar [HANS 1959] Kaar et al. [KAAR 1963] ACI 318-63 ACI 318-14	$L_t = \left(\frac{f_{se}}{3}\right) d_b$ (in.)	$L_{fb} = (f_{ps} - f_{se}) d_b$ (in.)	$L_d = L_t + L_{fb}$ (in.)
	f_{se} = effective stress in the prestressed reinforcement after all losses (ksi) f_{ps} = is the stress in the prestressed reinforcement at the critical section (ksi) d_b = is the nominal diameter of the strand (in.)		
Marshall and Krishnamurthy [MARS 1969]	$L_t = \sqrt{\frac{\delta}{K}}$ (mm)		
	δ = strand end slip (mm) K = 0.0000035 mm^{-1} for 12.7 mm seven wire strands		
Zia and Mostafa [ZIA 1977]	$L_t = \left[1.5 \left(\frac{f_{si}}{f'_{ci}}\right) d_b\right] - 4.6$ (in.)	$L_{fb} = 1.25(f_{su} - f_{se}) d_b$ (in.)	$L_d = L_t + L_{fb}$ (in.)
	f_{si} = the initial stress in strand before losses (ksi) f'_{ci} = the concrete compressive strength at transfer (ksi) f_{su} = ultimate strength of prestressing strand (ksi) f_{se} = effective stress in the prestressed reinforcement after all losses (ksi) d_b = nominal diameter of the strand (in.)		

Martin and Scott [MART 1976]	$L_t = 80d_b$		
Cousin et al. [COUS 1990]	$L_t = 0.5\left(\frac{U'_t\sqrt{f'_{ci}}}{B}\right) + \frac{f_{se}A_s}{\pi d U'_t\sqrt{f'_{ci}}}$	$L_{fb} = (f_{ps} - f_{se})\left(\frac{A_s/\pi d}{U'_d\sqrt{f'_c}}\right)$	$L_d = L_t + L_{fb}$
	$U'_t = U_t/\sqrt{f'_c}$; U_t = plastic bond stress for transfer length (psi). U'_t = 6.7 (uncoated strand); 10.6 (coated strand with low grit density); 16.5 (coated strand medium-high grit density) $U'_d = U_d/\sqrt{f'_{ci}}$; U_d = plastic bond stress for development length (psi). U'_d = 1.32 (uncoated strand); 4.55 (coated strand with low grid density); 6.40 (coated strand with medium-high grid density) B = the bond modulus (slope of bond stress curve in the elastic zone) (psi/in.) ≈ 300 psi/in. f_{se} = effective stress in the prestressed reinforcement after all losses (ksi) f_{ps} = stress in strand at flexural failure (ksi) A_s = cross-sectional area of strand (in^2) d = nominal strand diameter (in.) f'_{ci} = compressive strength at transfer (psi) f'_c = compressive strength at 28 days (psi)		
AASHTO 92	$50d_b$		
Balázs [BALA 1992]	$L_t = 105d_b\sqrt[4]{\frac{\delta^{3/2}}{f'_{ci}}}$ (mm)		
	d_b = nominal strand diameter (mm) δ = strand end slip (mm) f'_{ci} = compressive strength at transfer (MPa)		

Balázs [BALA 1993]	$L_t = \frac{111\delta^{0.625}}{f'_{ci}{}^{0.15}\left(\frac{f_{pi}}{E_p}\right)^{0.4}} \quad (mm)$		
	d_b = nominal strand diameter (mm) δ = strand end slip (mm) f'_{ci} = compressive strength at transfer (MPa) f_{pi} = strand stress immediately before release (MPa) E_p = modulus of elasticity of prestressing strand (MPa)		
Mitchell et al. [MITC 1993]	$L_t = 0.33 f_{pi} d_b \sqrt{\frac{3}{f'_{ci}}}$	$L_{fb} = (f_{ps} - f_{se}) d_b \sqrt{\frac{4.5}{f'_c}}$	$L_d = L_t + L_{fb}$
	f_{pi} = initial stress in prestressing strand just after release (ksi) d_b = nominal strand diameter (in.) f'_{ci} = compressive strength of concrete at time of release (ksi) f_{ps} = maximum stress in strand at nominal strength (ksi) f_{se} = stress in strand after losses (ksi)		
Deatherage et al. [DEAT 1994]	$L_t = \left(\frac{f_{si}}{3}\right) d_b$	$L_{fb} = 1.50(f_{ps} - f_{se}) d_b$	$L_d = L_t + L_{fb}$
	f_{si} = the initial stress in strand before losses (ksi) f_{ps} = stress in prestressed reinforcement at nominal strength (ksi) f_{se} = effective stress in prestressing steel after losses (ksi) d_b = nominal diameter of prestressed reinforcement (in.)		

Buckner [BUCK 1995]	$L_t = \left(\frac{f_{si}}{3}\right) d_b$	$L_{fb} = \lambda(f_{ps} - f_{se}) d_b$	$L_d = L_t + L_{fb}$
	f_{si} = the initial stress in strand before losses (ksi) f_{ps} = stress in prestressed reinforcement at nominal strength (ksi) f_{se} = effective stress in prestressing steel after losses (ksi) d_b = nominal diameter of prestressed reinforcement (in.) $1.0 \leq \left[\lambda = \left(0.6 + 40\varepsilon_{ps}\right) \quad or \quad \lambda = 0.72 + 0.102\frac{\beta_1}{w_p}\right] \leq 2.0$ ε_{ps}= strain corresponding to f_{ps}		
AASHTO 97	$60 d_b$		
Rose and Russell [ROSE 1997]	$L_t = 2\delta\frac{E_p}{f_{pi}} + 137.16 \qquad (mm)$		
	δ = strand end slip (mm) f'_{ci} = compressive strength at transfer (MPa) E_p = modulus of elasticity of prestressing strand (MPa)		
Russell and Burns [RUSS 1996]	$L_t = 290 L_{es}$ (in.) $L_t = \frac{f_{se}}{2} d_b \qquad (in.)$		
	L_{es} = measured end slip (in.) f_{se} = effective stress in prestressed reinforcement (after allowance for all prestress losses) (ksi)		
Russell and Burns [RUSS 1997]	$L_t = \left(\frac{f_{se}}{3}\right) d_b$ (in.)		
	f_{se} = effective stress in the prestressed reinforcement after all losses (ksi) d_b = is the nominal diameter of the strand (in.)		

Lane [LANE 1998]	$L_t = \frac{4f_{pt}}{f'_c} d_b - 5$	$L_{fb} = \frac{6.4(f_{ps} - f_{se})d_b}{f'_c} + 15$	$L_d = L_t + L_{fb}$
	f_{pt}= initial prestress prior to release (ksi) f'_c= compressive strength of concrete at 28 days (ksi) f_{ps} = stress in prestressed reinforcement at nominal strength (ksi) f_{se} = effective stress in prestressing steel after losses (ksi) d_b = nominal diameter of prestressed reinforcement (in.)		
Mahmoud et al. [MAHM 1999]	$L_t = \frac{f_{pi} d_b}{\alpha_t f'^{0.67}_{ci}}$	$L_{fb} = \frac{(f_{pu} - f_{pe})d_b}{\alpha_f f'^{0.67}_{c}}$	$L_d = L_t + L_{fb}$
	α_t= transfer length coefficient = 2.4 α_f = flexural bond length coefficient = 1.0≤α_f≤2.8 f'_{ci} = compressive strength of concrete at time of release (MPa) f'_c= compressive strength of concrete at 28 days (MPa) f_{pi} = effective prestress at transfer (MPa) f_{pu} = tensile strength of tendon (MPa) f_{pe} = effective prestress at loading (MPa) d_b = nominal diameter of strand (mm)		
Shahawy [SHAH 2001]	$L_t = \left(\frac{f_{si}}{3}\right) d_b$	$L_{fb} = \frac{f_{su} - f_{se}}{1.2} d_b$	$L_d = L_t + L_{fb}$
	f_{si} = the initial stress in strand before losses (ksi) f_{su} = stress in prestressed reinforcement at nominal strength (ksi) f_{se} = effective stress in prestressed reinforcement after all losses (ksi) d_b = nominal diameter of prestressed reinforcement (in.)		

Eurocode 2 [CEN 2004]	$L_t = \alpha_1 \alpha_2 \phi \frac{\sigma_{pm0}}{\eta_{p1} \eta_l f_{ctd}}$	$L_{fb} = \alpha_2 \phi \frac{(\sigma_{pd} - \sigma_{pm\infty})}{\eta_{p1} \eta_l f_{ctd}}$	$L_d = 1.2 L_t + L_{fb}$
	α_1= 1.0 (gradual release) or 1.25 (sudden release) α_2 = 0.25 (circular prestressed wires) or 0.19 (3 and 7 wires strands) ϕ = nominal diameter of the prestressing reinforcement (mm) σ_{pm0} = stress in prestressing strand just after release (MPa) η_{p1} = coefficient that accounts for the tendon type; 2.7 (wires) or 3.2 (3 and 7 wires strands) η_l = coefficient that accounts for the bond conditions; 1.0 (good conditions) or 0.7 (bad conditions) f_{ctd} = concrete tensile strength at transfer (MPa) σ_{pd} = stress in prestressed reinforcement at nominal strength (MPa) $\sigma_{pm\infty}$ = stress in prestressed reinforcement after all losses (MPa)		
Kose and Burkett [KOSE 2005]	$L_t = 95 \frac{f_{pi}(1 - d_b)^2}{\sqrt{f'_c}} \quad (in.)$	$L_{fb} = 8 + 400 \frac{(f_{pu} - f_{pi})(1 - d_b)^2}{\sqrt{f'_c}}$	$L_d = L_t + L_{fb}$
	f_{pi} is the stress in the prestressing strands prior to release (ksi) d_b is the nominal diameter of the strand, in in. f_{pu} is the ultimate tensile strength of the prestressing strand (ksi) $\sqrt{f'_c}$ is the square root of 28-day concrete compressive strength for the long-term transfer length measurements (psi)		
Martí-Vargas et al. [MART 2006]	$l_t = 29.85 - 0.0016 f'_{ci}$ (in.)	$l_{fb} = l_d - l_t$ (in.)	$l_d = 35.08 - 0.0014 f'_{ci}$ (in.)
	f'_{ci} = compressive strength of concrete at time of testing (psi)		

Martí-Vargas et al. [MART 2007a]	$L_t = \lambda \frac{f_{pi} A_p}{(4/3)\pi d_b 0.4 f'^{0.67}_{ci}}$		
	f_{pi} = stress in the prestressing at the time of prestress transfer (MPa) A_p = cross-sectional area of strand (mm²) d_b = nominal diameter of the strand (mm) f'_{ci} = concrete compressive strength at the time of prestress transfer (MPa) λ = 1.0 for the average value of transfer length 0.5 for the lower bound value of transfer length 1.5 for the upper bound value of transfer length		
Ramirez and Russell [RAMI 2007]	$l_t = \frac{120}{\sqrt{f'_{ci}}} d_b \geq 40 d_b$ (in.)	$l_{fb} = l_d - l_t$ (in.)	$l_d = \left[\frac{120}{\sqrt{f'_{ci}}} + \frac{225}{\sqrt{f'_c}}\right] d_b \geq 100 d_b$ (in.)
	f'_{ci} = concrete strength at release (ksi) d_b = diameter of prestressing strand (in.) f'_c = design concrete strength (ksi)		
Larson et al. [LARS 2007]	$L_{tr} = \frac{\Delta E_{ps}}{0.5 f_{si}}$		
	Δ = end slip, in in. E_{ps} = elastic modulus of the strand (ksi) f_{si} = average initial strand stress over the transfer length after release of prestressing (ksi)		

<table>
<tr><td rowspan="2">EHE 2008 [EHE 2008]</td><td>$L_t = \alpha_1\alpha_2\alpha_3\phi\frac{\sigma_{pi}}{4f_{bpd}(t)}$</td><td>$L_{fb} = \alpha_4\phi\frac{(\sigma_{pd}-\sigma_{pcs})}{4f_{bpd}}$</td><td>$L_d = L_t + L_{fb}$</td></tr>
<tr><td colspan="3">α_1= 1.0 (gradual release) or 1.25 (sudden release)
α_2= 1.0 (ultimate limit state) or 0.5 (service limit state)
ϕ = nominal diameter of the prestressing reinforcement (mm)
α_3 = 0.5 (for strands) or 0.7 (for indented or crimped wires)
α_4 = 0.8 (for strands) or 1.0 (for indented or crimped wires)
σ_{pi} = tendon stress before release (MPa)
$f_{bpd}(t)$ = bond stress when releasing (MPa) (Table 70.2.3 [EHE 2008])
σ_{pd} = stress in prestressed reinforcement at nominal strength (MPa)
σ_{pcs} = stress of the strand due to prestress after all losses</td></tr>
<tr><td rowspan="2">MC – 2010 [MC 2010]</td><td>$L_t = \alpha_{p1}\alpha_{p2}\alpha_{p3}\frac{7}{36}\phi\frac{\sigma_{pi}}{\eta_{p1}\eta_{p2}f_{ctd}}$</td><td>$L_{fb} = \frac{7}{36}\phi\frac{(\sigma_{pd}-\sigma_{pcs})}{\eta_{p1}\eta_{p2}f_{ctd}}$</td><td>$L_d = L_t + L_{fb}$</td></tr>
<tr><td colspan="3">α_{p1}= 1.0 (gradual release) or 1.25 (sudden release)
α_{p2}= 1.0 (moment and shear capacity considered) or 0.5 (verification of transverse stress in anchorage zone)
α_{p3} = 0.5 (for strands) or 0.7 (for indented or crimped wires)
η_{p1} = 1.2 (for 7-wire strands) or 1.4 (for indented and crimped wires)
η_{p2} = 1.0 (for all tendons with an inclination of 45°-90° with respect to the horizontal during concreting.
1.0 (for all horizontal tendons which are up to 250 mm from the bottom or at least 300 mm below the top of the concrete section during concreting)
0.7 (for all other cases)
ϕ = nominal diameter of the prestressing reinforcement (mm)
σ_{pi} = tendon stress before releasing (MPa)
f_{ctd} = f_{ctk} (t) / 1.50 is the lower design concrete tensile strength, for the transmission length at the time of release and for the anchorage length at 28 days
σ_{pd} = is de tendon stress under design load (MPa)
σ_{pcs} = tendon stress due to prestress after all losses (due to creep and shrinkage) (MPa)</td></tr>
</table>

AASHTO LFRD 2012	$L_t = 60d_b$	$L_{fb} = L_d - L_t$	$L_d = \kappa\left(f_{ps} - \frac{2}{3}f_{pe}\right)d_b$
	d_b = nominal diameter of the strand, in in. κ = 1.0 for pretensioned members with a depth of less than or equal to 24.0 in. 1.6 for pretensioned members with a depth greater than 24.0 in. f_{ps} = average stress in prestressing steel at the time for which the nominal resistance of the member is required (ksi) f_{pe} = effective stress in prestressing steel after losses (ksi)		
Martí-Vargas et al. [MART 2012b]	$L_T = \frac{2.5A_p}{\Sigma_p {f_{ci}}^{2/3}}\sigma_{pi}$	$L_{fb} = \frac{2.5A_p}{\Sigma_p {f_{ci}}^{2/3}}\left[1.6\left(\sigma_{pa} - \sigma_{pi}\right)\right]$	$L_d = L_t + L_{fb}$
	A_p = cross-sectional area of strand (mm^2) Σ_p = perimeter of the prestressing reinforcement (mm). f_{ci} = concrete compressive strength at the time of prestress transfer (MPa), in this cases coincides with the time of testing σ_{pa} is the maximum stress in strand at loading (for design stress, at nominal strength) (MPa). σ_{pi} is the effective stress in prestressing strand just after prestress transfer (MPa)		
Vázquez-Herrero et al. [VAZQ 2013a]	$l_{t,\max}(t) = \pi_1\pi_2 f_{pe}d_b/\left(4\tau_{min,TL}\right)$ (mm) $l_{t,\min}(t) = f_{pe}d_b/\left(4\tau_{max,TL}\right)$ (mm)		
	π_1 = 1 (favourable bond conditions); 1.43 (unfavourable bond conditions) π_2 = 1.0 (gradual transfer) ; 1.25 (sudden transfer) $\tau_{min,TL}$ = minimum value of the average bond stress that is expected for the transfer length at a generic age t. $\tau_{max,TL}$ = maximum value of the average bond stress that is expected for the transfer length at a generic age t. f_{pe} = effective prestress tension (MPa) d_b = diameter of the strand (mm)		

Vázquez-Herrero et al. [VAZQ 2013b]	$L_{t,min} = 2E_p\delta/(2f_{pi} - f_{pe})$ $L_{t,max} = \beta E_p\delta/(2f_{pi} - f_{pe})$		
	δ = the strand draw-in (mm) E_p = the elastic modulus of the strand (MPa) f_{pi} = the strand stress immediately before transfer (MPa) f_{pe} = the effective stress of the strand at the central zone of the structure β = an experimental coefficient		
Oh et al. [OH 2014]	$l_t = 8\sqrt{f_{pe}}\left(\frac{1}{f_{ci}}\right)^{1/3} {d_b}^{1.28}\left(\frac{1}{C - 20.0} + 0.25\right)$ $l_t = 183\Delta + 340$		
	f_{pe} = effective prestress after losses (MPa) f_{ci} = compressive strength at transfer (MPa) d_b = strand diameter (mm) C = concrete cover to the strand centre (mm) Δ = end-slip (mm)		

1 in. = 25.4 mm 1 ksi = 1000 psi = 6.895 MPa
1 mm = 0.0393701 in. 1 MPa = 0.1450 ksi

Appendix 2. Experimental procedure of beam flexural tests

The procedure described in this appendix was designed for the preparation and monitoring of flexural tests of reinforced and prestressed concrete beams in the Laboratory of Construction of the Centro de Innovación Tecnolóxica en Edificación e Enxeñaría Civil (CITEEC) at the University of A Coruña.

Previous security measures must be considered:

- Helmet and safety boots must be worn inside the laboratory of construction.
- The concrete blocks with the steel profile protections must be utilized on both sides of the beam during the test to avoid accidents if the beam becomes unstable or gets overturn during the test.
- An area must be delimited with security tape on the floor. It will be forbidden to enter when the beam will be placed inside.

Day 1

- Concrete blocks with the steel protections and the load cells must be placed at the exact position for the test.
- The beam must be lifted with two bridge cranes, and placed on wood or steel supports in an open area, with enough space to work on the surface of the beam. There must be a distance of at least 15 cm between the floor and the bottom surface of the beam. Both supports need to be located 30 cm far from both ends of the beam.
- The top surface must not have steel hooks to avoid the contact with the steel profile that transmits the load when testing. So, if necessary, they have to be sawed.
- Redefine the beam: centre, gauge positions and supports position.
- Place steel plates on both bottom sides of the beam. These plates provide a contact surface between the beam and the support steel cylinder. There are two options: in the first one, a lift table is necessary to lift the plate to its final position and put American tape around it and the beam. Other option can be performed with 3 people, two of

them will hold the plate from both sides of the beam and the third one will put American tape around the beam and the plate (Figure A2.1).

- Smooth the area where the gauges will be placed, clean the surface with acetone, redefine their position with a pencil and put adhesive tape around the area (Figure A2.2).

Figure A2.1 Support plates

Figure A2.2 Strain gauges position

- Put strain gauge adhesive PS on the area previously redefined, the adhesive must be covered with plastic sheets designed to create a flat surface.

Day 2

- Check that all of the strain gauges are working connecting them to the data acquisition device.
- Remove the plastic sheet covering the strain gauge adhesive.
- Clean a mirror or a piece of glass with acetone for chemical disinfection.
- Remove the plastics covering the strain gauges adhesive.
- For this task, two people are necessary:
  - Person A must extract the gauge from its protective case with gloves to avoid contamination and put it upside down on the glass surface. Person B must fix adhesive tape on the glass, covering the gauge with the long side of the tape parallel to the long side of the gauge.
  - Person A must lift carefully the adhesive tape from the mirror with the strain gauge at the same time that Person B must put cyanoacrylate on the area delimited for the strain gauge quickly. Immediately after, person A must put the strain gauge on its final position, progressively applying pressure with the finger, from one side to the other, to avoid the creation of air bubbles.
- Lift the beam with two bridge cranes and place it on the supports at its final position (Figures A2.3 and A2.4).

Figure A2.3 Load cell as support

Figure A2.4 Steel support

- Connect the strain gauges to the data acquisition device and check again that all of them are working.

Day 3

- Place the two neoprene plates (2 cm thick) on their final position on the top surface of the beam. This plates will absorb the irregularities of the top face.
- Place the contact steel pieces on the neoprene plates. These pieces will transmit the force between the steel profile and the beam (Figures A2.5 and A2.6).

Figure A2.5 Transmission piece A

Figure A2.6 Transmission piece B

- Lift the steel profile with two slings and two bridge cranes and put it on its final position on the contact steel pieces.
- Attach the hydraulic actuator to the steel frame. It is necessary to put the hydraulic actuator on a table and this table at the same time on the lift table.
- Connect oil hoses to the hydraulic actuator.
- Connect the Servosis with the wire linear potentiometric transducer that will control the test rate. Since the test will be controlled by displacement, it is very important to check an appropriate working before loading the beam opening and closing the cylinder rod. This check will be done attaching the potentiometric transducer to the hydraulic actuator with adhesive tape, and using a magnetic support to connect the wire of the transducer to the base of the cylinder rod.

Day 4

- The oil hoses must be disconnected from the hydraulic actuator.
- The steel frame with the actuator must be lifted with two slings and a bridge crane and put it in its final position. It is important to avoid contact between the bottom of the actuator and the steel profile, so the steel frame must be supported by steel pieces on the floor (Figure A2.7).
- Once the steel frame is placed, it has to be secured with threated steel plates to the ceiling of the floor below. For this task, 3 people are necessary, 2 of them holding the steel plate and the other one securing it with the thread.
- Connect again the oil hoses to the hydraulic actuator.
- If the beams are prestressed, attach the linear displacement sensors to the bottom strands at both ends of the beams with the pieces designed for this purpose. Find a flat contact surface to make contact on the beam, this surface must be smothered and 1.5 x 1.5 cm steel plates must be fixed with Araldite to create a flat contact surface.
- A steel L profile with a small hole drilled at the middle of one end, must be fixed with Araldite at mid-span of the beam. The vertical position must be decided according to tripod that will support the wire linear potentiometric transducer. The wire will be attached to the mentioned hole for registering the deflection during the test (Figure A2.8).

Figure A2.7 Steel plates under steel frame

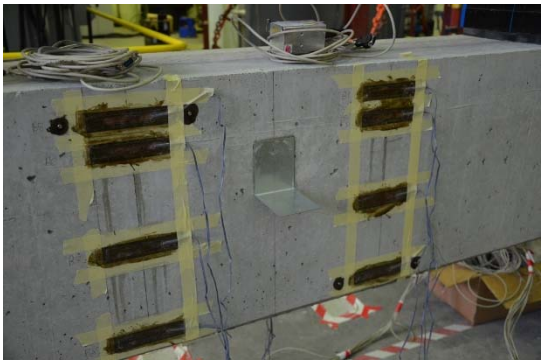

Figure A2.8 Steel profile for measuring deflection at mid-span

- The wire linear potentiometric transducer that controls the test rate will be attached to the hydraulic actuator and the wire attached to the steel profile with a magnetic support (Figure A2.9).
- Connect the load cells or hydraulic transducer, strain gauges, linear displacement sensors and potentiometric transducers to the data acquisition device and check that all of them registering adequate measures.
- Supports between the beam and the steel profile and supports must be secured with steel chains during the test.

- The steel profile must be secured to the bridge cranes with slings to avoid damages in case of an abrupt failure (Figure A2.10).

Figure A2.9 Wire linear potentiometric transducer

Figure A2.10 Steel profile secured with slings to the bridge cranes.

- The linear displacement sensors attached to the strands, in case of prestressed beams, must be as open as possible to take advantage of the total range in case of important slips. Dial gauges must also be fixed to the pieces which support the strands and make contact to the concrete surface (Figure A2.11).

Figure A2.11 Linear displacement sensors and dial gauges

Day 5

- Delimit a test zone around the beam with protections to avoid damages in case of an abrupt failure. It will be absolutely forbidden to enter this area until the end of the test.
- Initiate the data register by the data acquisition device.
- Initiate the test at desired rate, in this case 0.05 mm/s.
- Visualize on the computer monitor the load vs. deflection curve during the test. If the beam is prestressed, the test must be stopped before failure, that is, when the curve will be in the flat phase after yielding. The aim of the decision is to prevent linear displacement sensors attached to the strands form been damaged at failure.

- Once the hydraulic actuator has been stopped, the data acquisition device must continue registering data for at least one hour. Then the file must be saved.
- Dismantle the test.

The beam must be split into two parts by trained personnel and will be sent to a waste management company.

Appendix 3. Production and testing of prestressed concrete pre-slabs at a precast plant

A3.1. Introduction

After analysing the feasibility of a simultaneous replacement of fine and coarse recycled concrete aggregates in reinforced concrete beams, it was decided to replace the same recycled aggregate in other concrete elements fabricated in the same precast plant, in this case prestressed pre-slabs.

As mentioned in the literature review, previous studies were not found on the influence of recycled aggregates on the bond behaviour between prestressing steel and the surrounding concrete. Moreover, recycled aggregates are banned by most of the standards and codes for prestressed elements [GONÇ 2010]. Therefore, it was decided to perform an experimental program replacing small quantities of recycled aggregate (2, 4, 6, 8 and 10%) by the total amount of natural aggregate. The resulting pre-slabs were subjected to flexural and shear tests in order to analyse de influence of the recycled aggregate on the mechanical behaviour.

A3.2. Materials

The materials utilised for the fabrication of prestressed pre-slabs are the same as those utilised for the fabrication of the reinforced concrete beams. However, in this case, it is not a self-compacting concrete but a very dry vibrated concrete, so the mix composition is different and both the limestone filler and the superplasticizer are not used.

- Cement CEM-I 52.5 N/SR.
- Natural quartzite sand: 0/2.5 mm (NA-1 0/2.5) and 0/5 mm (NA-1 0/5) fractions.
- Natural granite gravel: 6/12 mm fraction (NA-1 6/12).

- Recycled concrete aggregate: 0/12 mm fraction (RCA-1 0/12).

As mentioned in Chapter 3, the recycled concrete aggregate was obtained from the existing waste of the precast plant: pieces and elements that were rejected or not sold. So, it is a high-quality recycled aggregate. The following properties were analysed for the materials used in the study: particle size distribution, particle density and water absorption, particle shape (flakiness index), resistance to fragmentation, classification of the constituents of coarse recycled aggregate and chemical composition. The results are included in Chapter 3.

A3.3. Mix proportions

Since the concrete elements were prestressed and the effect of recycled aggregates on the prestressing force was unknown, it was decided to replace low quantities of the total amount of natural aggregate (fine and coarse) with recycled aggregate, 2, 4, 6, 8 and 10% for P-2, P-4, P-6, P-8 and P-10, respectively. The mix which is used for these pre-slabs in the precast plant was taken as a reference concrete and, similarly to the reinforced beams, due to the higher sand content in the recycled aggregate the replacements were made in the fine natural aggregate 0/5 and the coarse natural aggregate 6/12, with the aim of getting a joint particle size distribution as closely as possible to the reference concrete mix.

During the fabrication of the pre-slabs, the addition of an extra amount of water to compensate the water absorption of the recycled aggregate was not considered because the replacement level was very low and this concrete composition looks for a very dry consistency. For the highest percentages, 8% and 10%, the production manager took the decision to decrease 10 litres per cubic metre the quantity of water in the mix because the resulting concrete consistency was not dry enough for its purpose.

Table A3.1 shows the mix proportions used for this study and Table A3.2 shows the replacement levels of total natural aggregate by recycled aggregate and the corresponding levels of the fine and coarse fraction.

Table A3.1. Mix proportions of prestressed pre-slabs

	P-0 (kg/m3)	**P-2** (kg/m3)	**P-4** (kg/m3)	**P-6** (kg/m3)	**P-8** (kg/m3)	**P-10** (kg/m3)
CEM-I 52,5 N/SR	320	320	320	320	320	320
NA-1 0/2.5	495	495	495	495	495	495
NA-1 0/5	495	475	455	435	415	395
NA-1 6/12	990	970	950	930	910	890
RCA-1 0/12	0	40	80	120	160	200
Water	160	160	160	160	150	150

Table A3.2. Replacement ratios of prestressed pre-slabs

	P-2	P-4	P-6	P-8	P-10
% recycled aggregates with respect to total amount of aggregates	2	4	6	8	10
% recycled fine aggregates with respect to total amount of fine aggregates	2	4	6	8	10
% recycled coarse aggregates with respect to total amount of coarse aggregates	2	4	6	8	10

A3.4. Geometry and reinforcement layout

The pre-slabs dimensions are 250 x 120 cm, with a 3 mm diameter reinforcing steel mesh B500S with a size of 115x245 mm and 12 prestressing 4 mm diameter wires (f_{pyk} = 1530 MPa) previously stressed to a force of 13.5 kN each wire. The cross-section is represented in Figure A3.1 and a 3D model is shown in Figure A3.2.

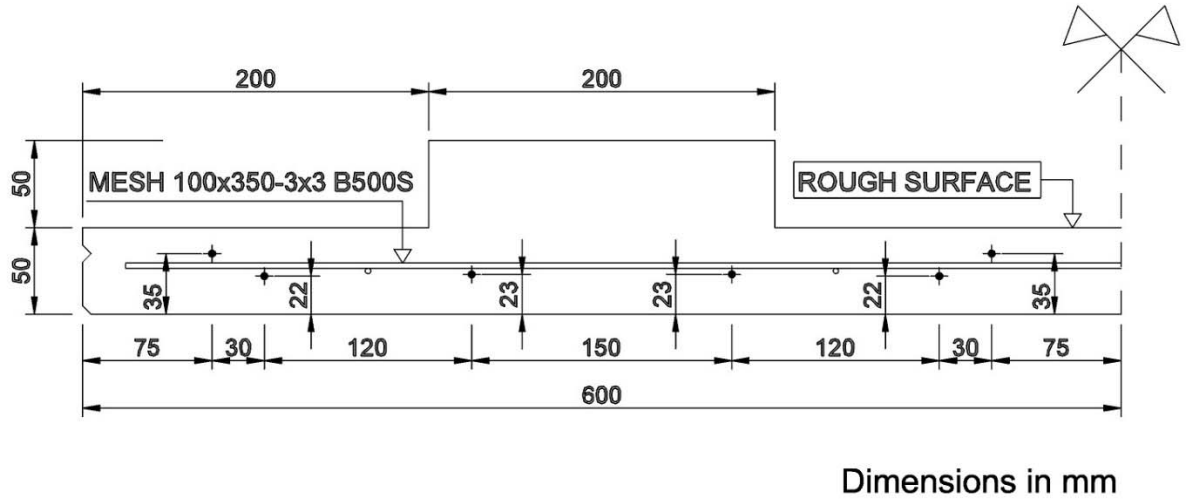

Figure A3.1. Cross-section of prestressed pre-slab

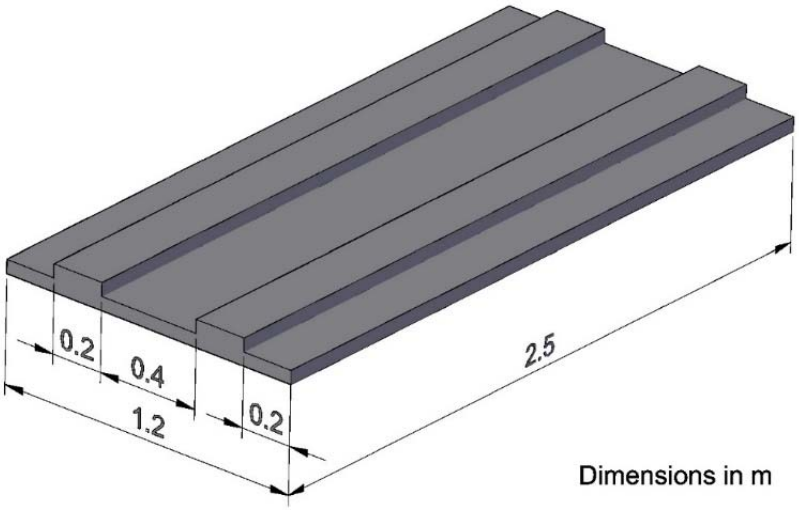

Figure A3.2. Model of a prestressed pre-slab

A3.5. Fabrication of the pre-slab specimens

For the fabrication of the pre-slab specimens, a 120 metres prestressing bed was prepared with the prestressing wires stressed to the necessary force and the steel mesh, as can be observed in Figure A3.3. Then, the concrete, it is spread, shaped and compacted with the aid of a moulding machine (Figure A3.4). In order to get and keep the desired shape of the pre-slab, it is necessary the mix have a very dry consistency.

Figure A3.3. Prestressing Bed

Figure A3.4. Moulding machine

A3.6. Quality control of the elements

The consistency of this type of concrete is so dry that it is not possible to compact cylinders 150 x 300 mm or cubes 100 mm with a conventional concrete vibrator. Therefore, for each replacement level, with the exception of 6%, two cubes 150 mm were fabricated and compacted on a vibrating table (Figures A3.5 and A3.6). Then, they were kept inside an

environmental chamber between 16 hours and 3 days before demoulding according to the UNE-EN 12390-2:2009 Standard. The curing conditions inside the chamber are 20±2 °C temperature and relative humidity higher than 95%. After demoulding, the samples were kept inside the environmental chamber again for an appropriate curing until the age of testing (28 days).

Figure A3.5. Sample compaction

Figure A3.6. Sample after compacting

In order to evaluate the mechanical properties with the different replacement levels, hardened concrete density tests were performed following the UNE-EN 12390-7:2009 Standard and compressive strength tests following the UNE-EN 12390-3:2009/AC:2011 Standard, both of them at the age of 28 days. The results of the density test are included in Table A3.3 and the results of compressive strength test are included in Table A3.4 and depicted in Figure A3.7.

Table A3.3. Hardened concrete density

Mix	Mean density (Kg/m^3)	Δ (%)
P-0	2356	
P-2	2356	0
P-4	2363	0.3
P-8	2361	0.2
P-10	2364	0.3

As can be observed in the Table A3.3, the mean density keeps practically constant regardless of the substitution percentage. Despite the recycled aggregate has a lower density than the natural aggregate, the replacement levels are so low that the influence on the concrete density is negligible.

Table A3.4. Compressive strength

Mix	Compressive strength (MPa)	Δ (%)
P-0	52.7	
P-2	50.7	-3.8
P-4	49.5	-6.1
P-8	50.5	-4.1
P-10	54.0	2.5

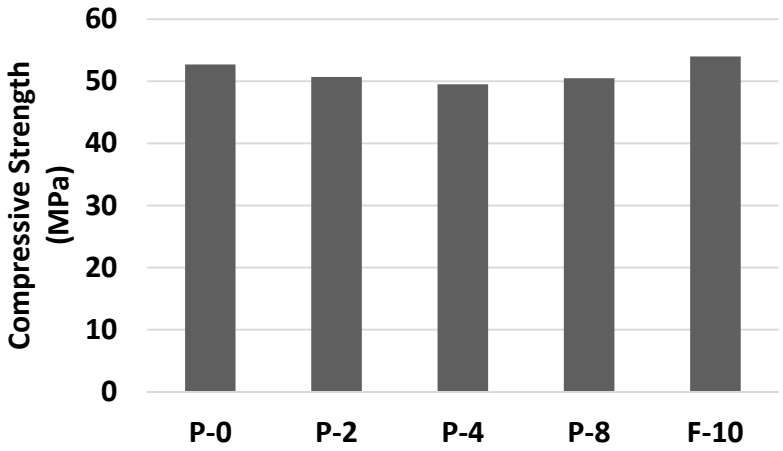

Figure A3.7. Compressive strength

As can be seen in Figure A3.7, the compressive strength slightly decreases for replacement levels up to 4% and increases again for 8 and 10%. The reason for this strength loss at the first percentages, is the worse quality of the recycled aggregate in comparison with the natural aggregate. For the highest percentages, 8% and 10%, the production manager took the decision to decrease 10 litres per cubic metre the amount of water in the mix because the concrete consistency was not dry enough for its purpose. When the water-to-cement relationship is reduced, the compressive strength increases, even if the amount of recycled aggregate is increased in small quantities. Therefore, it is possible to achieve similar compressive strengths reducing the amount of water for small replacement levels.

A3.7. Test of the pre-slabs in the precast plant

For each of the mixes, flexural and shear tests were performed in order to analyse the influence of the recycled aggregate on the flexural and shear behaviour of the pre-slabs. The supports were placed on both sides of the pre-slab and it was tested with a hydraulic actuator attached to a steel frame. A three-point loading setup with 2 ton (19.62 kN) increments was used, and the deflection at mid-span was measured for each specimen until failure. In the

flexural tests, the force was applied on mid-span (Figure A3.8), while in shear test, the force was applied 15 cm far from the support (Figure A3.9).

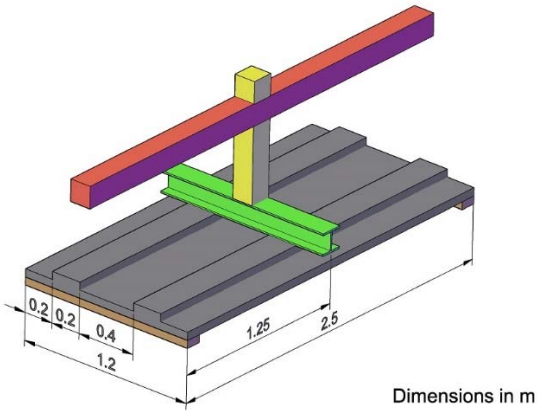

Figure A3.8. Schematic test set-up for flexural testing

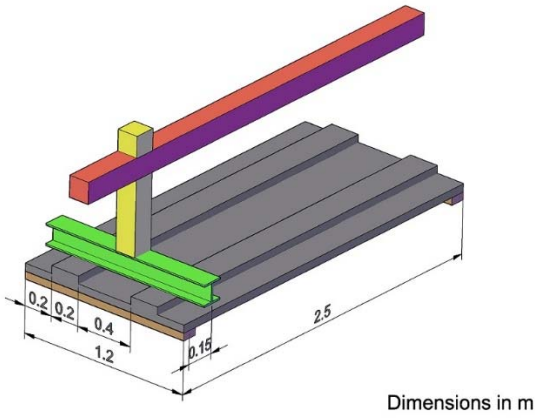

Figure A3.9. Schematic test set-up for shear testing

A3.7.1. Flexural behaviour tests

The result of the flexural tests for a sustained load of 20 kN are included in Table A3.5 and the results at failure are included in Table A3.6 and are depicted in Figures A3.10 and A3.11 for a better understanding.

Table A3.5. Flexural tests on prestressed pre-slabs at sustained load

Pre-slab	Load (kN)	Moment (m·kN)	Deflection (mm)	Δ (%)
P-0	20	11.02	7	
P-2	20	11.05	6	-14.3%
P-4	20	11.04	8.5	21.4%
P-6	20	11.06	12	71.4%
P-8	20	11.14	12	71.4%
P-10	20	11.07	15	114.3%

Table A3.6. Flexural tests on prestressed pre-slabs at failure

Pre-slab	Failure Load (kN)	Moment (m·kN)	Δ (%)	Deflection (mm)	Δ (%)
P-0	25	13.48		52	
P-2	26	14.00	3.9	38	-26.9
P-4	27.5	14.73	9.3	52	0
P-6	25	13.52	0.3	57	9.6
P-8	26	14.11	4.7	56	7.7
P-10	25	13.54	0.4	49	-5.8

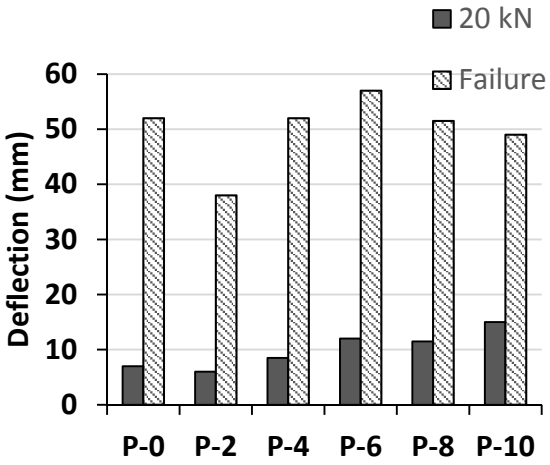

Figure A3.10. Deflection reached in flexural tests

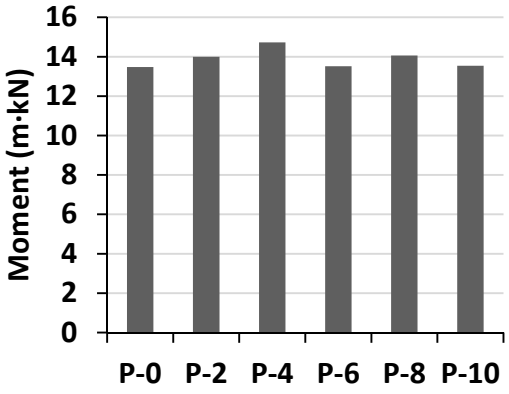

Figure A3.11. Bending moment at failure in flexural tests

The deflection at mid-span for a sustained load of 20 kN (Figure A3.10) was increased as the replacement level raises, being the value obtained for P-10 more than twice the value obtained for the reference concrete P-0. This effect is detrimental from the point of view of the mechanical properties, since the deflections are higher under the same load conditions.

As can be observed in Figure A3.11, the ultimate bending moment was increased by 3.9% and 9.3% for P-2 and P-4, respectively. For the remaining substitution percentages, the bending moment was decreased and keeps between 13.5-14.0 m·kN, being slightly higher than the value obtained for the reference concrete pre-slab P-0, without recycled aggregate. It can be concluded that the failure bending moment is not negatively affected by the low replacement levels of recycled aggregate.

The deflection reached at mid-span at failure (Figure A3.10) does not follow the same trend than in the case of the sustained load. The logical trend would be that for higher failure bending moments, the deflection was increased, under the same fabrication and test conditions. However, the failure bending moment of P-2 is by 4% higher than P-0 but the deflection is by 27% lower, even replacing the 2% of natural aggregate by recycled aggregate. In the pre-slab P-4, the failure bending moment was increased again but the deflection is similar to the deflection reached by P-0. For replacement levels higher than 4%, the effect of recycled aggregate becomes noticeable. Although the failure bending moment was increased for 2% and 4% replacement, the deflections achieved by higher replacement ratios are in the order of the value reached by the reference pre-slab P-0. It can be noticed that between P-4 and P-6, the bending moment was decreased by 9% and the deflection was increased by 10%. In the remaining replacement ratios, it can be observed that for P-8, the bending moment was

slightly increased but the deflection was similar to the deflection reached by the reference pre-slab P-0. Finally, in the case of P-10, both the bending moment and the deflection achieved similar values to P-0.

With the exception of FP-2, it can be concluded that the deflection reached in the failure bending moment remains between 50 and 60 mm, with maximum deviations of 10% with regard to the reference concrete FP-0.

Figures A3.12-A3.15 show different images of the flexural behaviour tests.

Figure A3.12. Flexural test P-0

Figure A3.13. Flexural test P-0

Figure A3.14. Flexural test P-6

Figure A3.15. Flexural test P-10

A3.7.2. Shear behaviour tests

The result of the shear tests on the pre-slabs are included in Table A3.7 and depicted in Figure A3.16 for a better understanding.

Table A3.7. Shear tests on prestressed pre-slabs at failure

Pre-slab (%)	Load (kN)	Shear (kN)	Moment (m·kN)	Δ Moment (%)
P-0	60	56.40	9.00	
P-2	60	56.40	9.00	0%
P-4	44	41.36	6.60	-27%
P-6	45	42.30	6.75	-25%
P-8	45	42.30	6.75	-25%
P-10	45	42.30	6.75	-25%

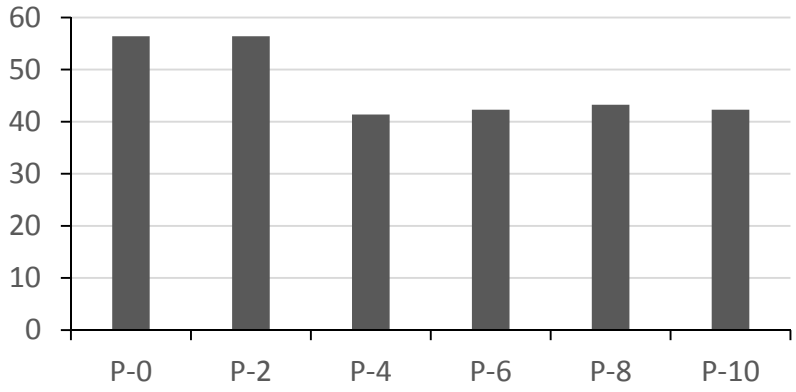

Figure A3.16. Shear strength at failure in shear tests

As can be observed in Figure A3.16, the ultimate shear reached by the pre-slab with a 2% replacement (P-2) at failure is similar to the value achieved by the reference pre-slab P-0, so the effect of this small replacement of natural aggregate by recycled aggregate is not noticeable. However, for higher replacement levels (P-4 to P-10) the ultimate shear is approximately 25% lower than the value achieved by the reference pre-slab P-0. Therefore, it can be concluded that the replacement of natural aggregate with recycled aggregate has a detrimental effect on the shear strength for substitution percentages higher than 2%.

Figures A3.17-A3.20 show different images of the shear behaviour tests.

Figure A3.17. Shear test P-0

Figure A3.18. Shear test P-2

Figure A3.19. Shear test P-6

Figure A3.20. Shear test P-10

A3.8. Results and discussion

The following conclusions can be drawn from the prestressed pre-slab tests:

For small replacement levels, the concrete density remains practically unaffected regardless of the replacement ratio. Similarly, the compressive strength slightly influenced, with variations in the range of -6.1% to 2.5% for 4% and 10% replacement, respectively. These negligible differences in compressive strength agree with the results obtained by [EVAN 2007] and [YAPR 2011] with loses of 0.6% and 4.6%, respectively, for 10% replacement of fine recycled aggregate; and [MARD 2014] with loses of 0.6% for 15% replacement of fine recycled aggregate.

The failure bending moments achieved in flexural tests are similar, even higher than that of reference concrete with a maximum increase of 9.3% for 4% replacement. Therefore, small amounts of recycled aggregate do not have a detrimental effect on the failure bending moment.

The deflection achieved under the sustained load of 20 kN in flexural tests is increased as the replacement level raises with a maximum increase of 114% for 10% replacement. This effect

is detrimental, since for the same sustained load, the deflections are higher. However, the deflection achieved at failure maintains a value between 50-60 mm, with the exception of the pre-slab with 2% replacement, in which the deflection is by 20% lower than the others values.

In the shear behaviour tests, the ultimate shear remains unaffected for 2% replacement but it decreases around 25% for the remaining substitutions. Therefore, it can be concluded that the recycled aggregate has a negative influence on the shear strength.

In accordance with the results obtained and due the absence of detailed studies of long-term behaviour, it is concluded that it is feasible to replace up to 10% of the total natural aggregate with recycled aggregate in this type of concrete and element, provided that the pre-slabs will not be subjected to excessive shear forces.

Appendix 4. Monitoring and production procedure of precast prestressed concrete beams

The fabrication of the prestressed beams was scheduled for 9 working days according to the following procedure:

DAY A: Thursday, January 22nd, 2015

- Position the formworks which separate the beams along the prestressing bed.
- Position the stirrups and the steel reinforcement (Figure A4.1 and A4.2).

Figure A4.1. Stirrups B1R, B3R, B4R, B1C, B3C and B4C

Figure A4.2. Stirrups B2R and B2C

- Position all the prestressing strands.
- Place the transition pieces and corresponding load cells in strand C7 (active anchor) and strand C8 (active and passive anchors) as depicted in Figures A4.3 and A4.4. Register the current measures from the load cells and place the wedges and grips in strands C7 and C8.

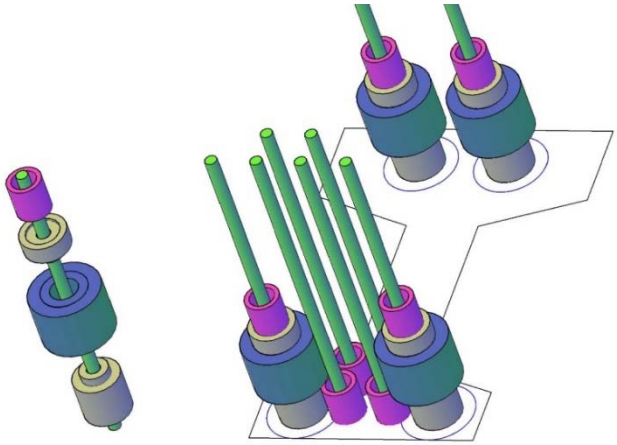

Figure A4.3. Position of transition pieces and load cells

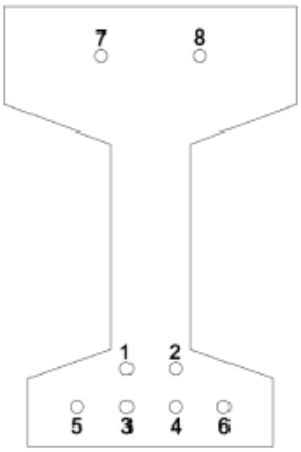

Figure A4.4. Strand numbering

- Place the wedges and grips in both sides of strands C1 to C4.
- Transfer the initial prestressing force to strands C1 – C4, C7 and C8 with the prestressing bed hydraulic actuator.
- Place two strain gauges on strand C8 in a zone located between two beams with the aim of registering the strain caused by the prestressing of the strand.
- Transfer the 100% prestressing force to strands C1 to C4.
- Place the transition pieces and corresponding load cells in strands C5 and C8, in active anchor, and C5 in passive anchor. Register the current measures.
- Transfer the 100% prestressing force to strands C5 to C8 (Figure A4.5). The force must be transferred progressively by the jack with increments of 50 bar. Between every increment, the corresponding force registered by the load cells must be recorded.

Figure A4.5. Strand pulled by the jack

DAY B: Friday, January 23rd, 2015

- Fabricate trial natural concrete mixes.
- Place again the formworks which separate beams on their final position with a separation between consecutive beams of at least 1 m. Measure and register the final position of the beams on the prestressing bed according to the separating formwork.
- Set the geometric position and adhere the strain gauges on strand C5 according to the procedure described in Appendix 5. The gauges will be placed solely on beams B1C, B3C, B4C, B1R, B3R and B4R. Four gauges will be adhered on each beam at a distance of 1000 and 2750 mm far from each side of the beam (Figure A4.6).
-

Figure A4.6. Strain gauge on strand

DAY C: Monday, January 26th, 2015

- Fabricate more trial natural concrete mixes and recycled aggregate concrete mixes.
- Protect strain gauges according to procedure (Appendix 5).
- Placing temperature sensors in several beams and shrinkage strain gauges in B1R and B1C hooked to the reinforcing steel (Figures A4.7 and A4.8).

Figure A4.7. Internal temperature sensor

Figure A4.8. Internal shrinkage gauge

- Close and secure the lateral formwork after being applied the releasing agent.
- Prepare the moulds for casting: cylinders, shrinkage prisms and cubes (Figure A4.9).

Figure A4.9. Mould for quality control samples

- Review the position of the sensors, and check if the humidity and temperature dataloggers installed in the plant are registering data.
- Connect the strain gauges to the data acquisition device and check correct functioning.

DAY D: Tuesday, January 27th, 2015

- Initiate the data register in the data acquisition device
- During the mixing procedure, the weight of every different material added to the mixture must be noted (cement, aggregates, admixtures and water), as well as the power consumed by the mixer checked with a multimeter surrounding the corresponding phase of the electric cable. At the end of the mixing process, the power consumed should be stabilized.
- The slump test must be performed immediately after the mix procedure be finished (Figure A4.10)
- Beam casting and concrete vibration (Figure A4.11). Simultaneously, the shrinkage prisms, cylinders and quality control samples must be cast. The superficial concrete temperature must be measured with a laser thermometer.

Figure A4.10. Slump test

Figure A4.11. Concrete vibration

- When the concrete begin to harden, DEMEC points fixed to nails must be introduced in the concrete surface of beams V1C, V1R, V4C, V4R and shrinkage prisms for the evaluation of concrete shrinkage.
- Beams, cylinders and shrinkage prisms must be covered with plastics with the aim of avoiding the loss of moisture (Figure A4.12). Environment dataloggers must be kept between the beam and the plastic. When concrete begins to harden, the surface of the beams must be moistened from time to time.
- Quality control sampled must wrapped with plastic film with the aim of avoiding a loss of moisture. They must be taken to an environmental chamber for an adequate curing (Figure A4.13).

Figure A4.12. Beams covered

Figure A4.13. Environmental chamber

- Measure again the superficial temperature of the beams before leaving and cover the beams, cylinders and prisms surface with wet papers under the plastic to avoid drying cracks.
- Save de file created by the data acquisition device and start a new one.

DAY 1: Wednesday, January 28th, 2015

- Save de file created by the data acquisition device and start a new one.
- Measure the shrinkage DEMEC points inside prisms and beams at the beginning of the day.
- Measure the beams superficial temperature with the laser thermometer.
- Moisten the papers on the beams, cylinders and prisms surface every 2 hours.
- Demould and identify all the samples with exception of the shrinkage prisms. The samples will be kept inside water recipients in the environmental chamber.

- Perform non-destructive tests (NDT) (Figures A4.14 and A4.15) and test two cubic samples of both mix compositions at approximately 24 hours after casting. Analysis of the results and their deviation and decide if it is necessary to test a third cubic sample.

Figure A4.14. Ultrasonic pulse velocity test

Figure A4.15. Rebound hammer test

- Download the temperature data from the internal and external dataloggers, estimation of the equivalent age, maturity of the beams and their corresponding compressive strength.
- Remove the formwork of the beams and dry the surface bottom the top and bottom flanges of the beams B1R and B1C with acetone for adhering the PS before fixing the DEMEC points.
- Adhere PS along the first 1500 mm of both ends of B1R and B1C, solely on one side of the beam. Adhere also 20 cm of PS at 2750 mm from both ends of beams B1C, B3C, B4C, B1R, B3R and B4R, at the top flange (5 and 15 cm from the top surface) and at the centre of the bottom flange.
- Measure the beams superficial temperature with the laser thermometer.
- Moisten the papers in the beams and concrete samples.
- Measure the shrinkage DEMEC points inside beams and prisms.
- Save de file created by the data acquisition device and start a new one.

DAY 2: Thursday, January 29th, 2015

- Save de file created by the data acquisition device and start a new one.
- Measure the shrinkage DEMEC points inside beams and prisms.
- Measure the superficial temperature of the beams.
- Perform non-destructive tests, and compressive strength test in cubic samples.
- Download of the maturity data of the beams and cubic samples and calculate the maturity of the beams.
- Demould the shrinkage prisms and keep them next to the beams.
- Measure the shrinkage prisms and their superficial temperature.

- Visual inspection of cracks on the beams. If a crack is found, it must be noted with the date and painted with a pencil on the concrete surface.
- Mark the position of the DEMEC points on the PS surface of the beams. The points along 1500 mm from both ends of the bottom flange of B1C and B1R need to be separated 5 cm. The other points need to be separated 15 cm.
- The DEMEC points must be fixed with Cyanoacrylate and named as follows: “Number of Beam”-“C/R”- “North/South” “Number of point”. For example, 1C-N3 would be placed on the beam B1C, on the north end and it would be the third point, starting from the end of the beam (Figure 4.16).

Figure A4.16. DEMEC points

- Measure the shrinkage DEMEC points inside beams and prisms.
- Measure the superficial temperature of the beams.
- Save de file created by the data acquisition device and start a new one.

DAY 3: Friday, January 30th, 2015

- Save de file created by the data acquisition device and start a new one.
- Measure the shrinkage DEMEC points inside beams and prisms.
- Measure the superficial temperature of the beams.
- Download the maturity data from the dataloggers and evaluate the maturity.
- Perform non-destructive tests and compressive strength tests.
- At end of the day measure again the shrinkage DEMEC points inside beams and prisms, and superficial temperature of the beams.
- Save de file created by the data acquisition device and start a new one.

DAY 6: Monday, February 2nd, 2015

- Save de file created by the data acquisition device and start a new one.

- Measure the shrinkage DEMEC points inside beams and prisms, and superficial temperature of the beams.
- Measure the distance between the DEMEC points on the surface of the beam.
- Measure the distance between a mark on every strand and the beam face with a depth gauge, at both ends of all of them.
- Measure the camber and distance between both ends of the beams at the top and bottom flange
- Measure the distance between the DEMEC points on the surface of the beam immediately before transferring the prestressing force.
- Attach linear displacement sensors to the bottom strands to measure their slip at transfer (Figure A4.17).

Figure A4.17. Linear displacement sensors attached to strands

- Check the proper measuring of the linear displacement sensors, load cells and strain gauges. Data need to be recorded at least every second.
- Measure the distance between the DEMEC points on the surface of the beam immediately before transferring the prestressing force.
- The prestressing force must be released gradually by the hydraulic actuator of the prestressing bed.
- The strands between beams must be cut at a distance of at least 30 cm far from the end of the beams with the aim of attaching linear displacement sensors during the flexural tests. The strand free ends must be covered with insulating tape to avoid injuries.
- Measure the camber and the distance from both ends of the beams at the top and bottom flange.
- Measure the distance between the DEMEC points on the surface of the beam after transferring the prestressing force.
- Measure the strands slip from the previous mark with a depth gauge.
- Perform non-destructive tests and compressive strength tests.

- Save de file created by the data acquisition device and start a new one.

DAY 7: Tuesday, February 3rd, 2015

- Save de file created by the data acquisition device.
- Prepare the beams to be transported to the CITEEC (Figure A4.18).
- Store the instrumentation devices and material.
- Prepare a zone in the CITEEC for the beams.
- Transport the beams from the precast plant to the CITECC.
- Place the beams on their final position in the CITEEC until the date of testing (Figure A4.19).

Figure A4.18. Beams in precast plant

Figure A4.19. Beams in CITEEC

Appendix 5. Procedure for strain gauge fixing to prestressing strand

A5.1. Strand surface preparation

- First of all, the strand where the strain gauges will fixed must be cleaned with acetone.
- Mark areas on the strand of approximately 50 mm, where the gauges will placed with a permanent marker.
- Degrease the area of the strand with the degreaser CSM-2 (Figure A5.1) and a clean gauze.
- Polish the strand surface around its perimeter with a polishing brush (Figure A5.2).

Figure A5.1. Degreaser CSM-2

Figure A5.2. Polishing brush

- Polish the wires surface with 220-grit silicon carbide wet-or-dry paper (SCP-1) (Figure A5.3), during at least 5 minutes, taking special care of the zone between wires.
- Polish again the wires surface, but this time with 320-grit silicon carbide wet-or-dry paper (SCP-2) (Figure A5.4), during at least 5 minutes, taking special care of the zone between wires.

Figure A5.3. SCP-1

Figure A5.4. SCP-2

- Clean the strand surface with Conditioner A (Figure A5.5) and a gauze GSP-1 (Figure A5.6), and dry the surface with another gauze. This action must be done only in one direction in order not to deposit contaminants.
- Clean again the area with Conditioner A and a cotton swab CSP-1 in only one direction. Dry the surface with a gauze in one direction.

Figure A5.5. Conditioner A

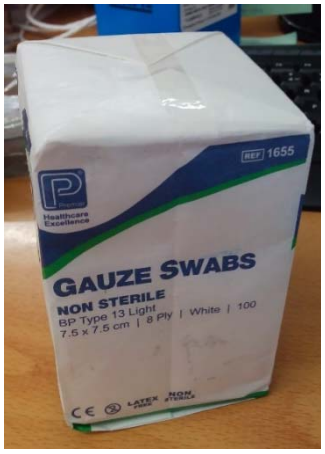

Figure A5.6. GSP-1 Gauzes

Figure A5.7. Neutralizer 5A

- Clean the area with Neutralizer 5A (Figure A5.7) and a gauze. Dry the surface with another gauze GSP-1. This action must be done only in one direction in order not to deposit contaminants.
- Clean again with a cotton swab CSP-1 and Neutralizer 5A in only one direction and dry the surface with a gauze. This step is very important to neutralize the Conditioner A utilised.
- The surface must be completely clean.

- Mark the position of the strain gauge on the wire of the strand with a 4H pencil (hard), or a marker which paints on steel.
- From the mark on the strand, which points the gauge end, stick a Teflon tape (Figure A5.8) of at least 2 cm. This tape will avoid contact between the gauge electric wires and the strand.
- Cover the Teflon tape with a gauze to avoid deposits of contaminants.

Figure A5.8. Teflon tape

A5.2. Strain gauge preparation

- Clean a mirror or a piece of glass with acetone for chemical disinfection.
- Extract the gauge from its protective case with gloves to avoid contamination and out it upside down on the glass surface. Fix adhesive tape on the glass, covering the gauge as shown in Figure A5.9, with the long side of the tape, being perpendicular to the short side of the gauge.
-

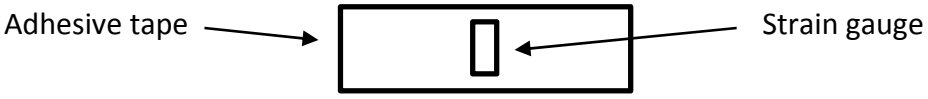

Figure A5.9. Adhesive tape and strain gauge

- Lift carefully the adhesive tape from the mirror with the strain gauge and fix it to the selected wire of the strand according to the marks.
- Attach the strain gauge wires to the strand with two cable ties to avoid possible damages caused by an abrupt pulling of the cable.

A5.3. Cyanoacrylate application

- Lift the adhesive tape at the short side progressively up to the gauge will be completely lifted (Figure A5.10), put a drop of cyanoacrylate and push from the opposite side to fix the gauge and avoid the creation of air bubbles.

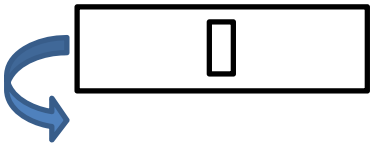

Figure A5.10. Adhesive tape lifting

- Apply pressure with the finger for at least a minute. Then, use a clamp and a piece of thin neoprene to apply pressure for at least 2 minutes.
- After that time, remove the clamp and cover the gauge with adhesive tape to avoid the entrance of moisture.
- Check the appropriate functioning of the strain gauge with a multimeter or connecting it to the data acquisition device.

A5.4. Strain gauges and cables protection

- Warm the surface that will be protected with a dryer if the temperature is lower than 10 °C.
- Put a strip of Teflon tape covering the strain gauge and the electric wires.
- Apply M Coat B (Figure A5.11) on the strain gauge cable and on the Teflon tape to improve their adherence and protect them.
- Prepare pieces of butile with a cut for protecting the gauge as shown in Figure A5.12:

Figure A5.11. M Coat B

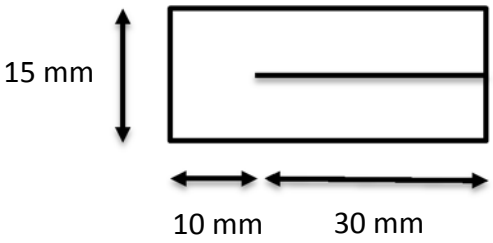

Figure A5.12. Piece of butile

-
- Prepare larger pieces of butile to cover the previous ones (Figure A5.13).

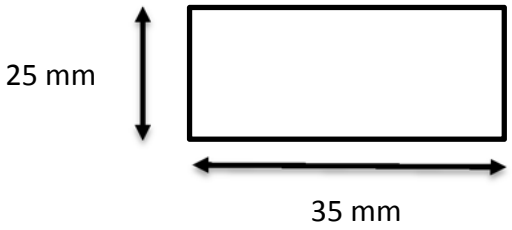

Figure A5.13. Cover piece of butile

- Put the piece of butile with the cut surrounding the strain gauge and leaving the cable over the part without cut.
- Prepare wax a drop it over the strain gauge in the resulting hole surrounded by the piece of butile.
- Put the cover piece of butile over the first one and push them with the fingers until they will be completely merged.
- Check the adequate functioning of the strain gauges.
- Cut pieces of the adhesive aluminium strip with the following size (Figure A5.14) and do the middle fold.

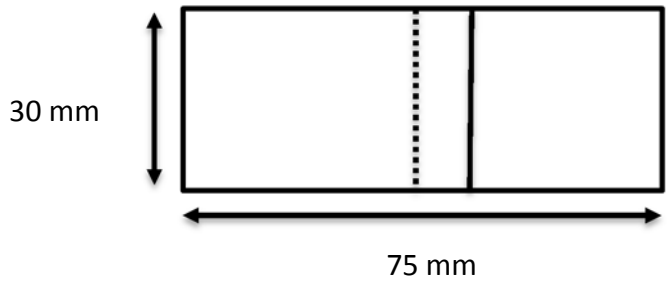

Figure A5.14. Aluminium tape

- The area of the stand will be covered with this piece of aluminium tape. Then, M-COAT B will be put on the contact surface between the aluminium tape and the strand and on the cable that will be embedded in concrete.

Appendix 6. Extended summary in Spanish

A6.1. Introducción y objetivos

El rápido desarrollo urbano de las últimas décadas con el hormigón como principal material de construcción, ha originado una reducción de los recursos naturales disponibles en algunas partes del mundo. La extracción de materias primas tiene un impacto importante en el medio ambiente, modificando el curso y lecho de los ríos, originando problemas de estabilidad en laderas y dañando el paisaje natural. Al mismo tiempo, millones de toneladas de escombros procedentes de residuos de construcción y demolición son generados y van directamente a vertederos sin un tratamiento previo o selección que podría dar lugar a una posible reutilización.

De acuerdo con el Plan Nacional de Gestión de Residuos de Construcción y Demolición (2001-2006), aproximadamente la mitad de los residuos de construcción y demolición producidos en España están compuestos de ladrillo, azulejo y cerámica, y sobre el 20% están compuestos de hormigón y mortero. Estos residuos pueden ser reutilizados como áridos reciclados para la fabricación de hormigón después de ser machacados y cribados. Varios estudios han sido realizados hasta la fecha por diferentes autores con resultados muy prometedores [GEAR 2002].

La mayor parte de los países tienen normativas sobre el uso del árido reciclado en hormigón. En particular, la Instrucción española de Hormigón Estructural [EHE 08] define "hormigón reciclado" como un hormigón producido exclusivamente con árido reciclado del machaqueo de piezas de hormigón, y recomienda limitar el porcentaje de sustitución al 20% cuando se usa en hormigón estructural. Por lo tanto, excluye el árido reciclado fino y los áridos con un origen diferente al hormigón (árido reciclado mixto, asfalto, etc.).

En otros países, las normativas con respecto al uso de árido reciclado son diferentes. En algunas de ellas se permiten porcentajes de sustitución más altos de árido grueso de hormigón en hormigón estructural, como en Alemania y Japón con un 35%, o incluso en

Holanda y Dinamarca, que se permite un 100% de sustitución. Con respecto al uso de árido reciclado fino de hormigón, está permitido su uso en Brasil con un 100% de sustitución para hormigón no estructural, en Japón hasta un 100% para estructuras menos exigentes, en Holanda solamente si el árido grueso es natural, en Suiza con un 100% de sustitución incluso en hormigón estructural, 20% en Dinamarca para ambientes no agresivos y 100% en Rusia para hormigón no pretensado.

Después de analizar varios estudios sobre el uso de árido reciclado fino de hormigón, se puede concluir que es viable fabricar hormigón con árido reciclado fino y obtener un comportamiento similar al del hormigón fabricado exclusivamente con áridos naturales. Por lo tanto, es demasiado conservativo considerar inaceptable su uso para la fabricación del hormigón.

Esta tesis tiene como finalidad llevar un paso adelante el reciclado del hormigón. Hasta ahora, la mayor parte de las investigaciones se han centrado en reemplazar únicamente diferentes ratios de la fracción gruesa con árido reciclado de diferentes fuentes. El número de estudios realizados substituyendo la fracción fina es inferior, y cuando se sustituyen ambas suele realizarse de manera independiente. Este proceso conlleva un importante gasto de energía puesto que los áridos necesitan ser cribados para obtener las fracciones deseadas.

En esta tesis doctoral se propone reemplazar simultáneamente la fracción fina y gruesa sin tener que cribar el árido reciclado bruto. Es necesario analizar previamente la granulometría del árido reciclado para determinar su porcentaje de partículas finas (< 4 mm). A la hora de fabricar el hormigón, el árido reciclado se introduce directamente en la mezcla como sustitución del árido total, quitando las cantidades correspondientes de las fracciones fina y gruesa naturales, según el porcentaje de finos previamente determinado.

Con este método es posible obtener una granulometría conjunta similar a la del árido total, independientemente del porcentaje de sustitución. Además, la fracción fina se introduce en la mezcla de hormigón en lugar de ser rechazada y se evita el correspondiente gasto energético al cribar.

Este método de sustitución no solo se ha probado en hormigón armado, sino también en hormigón pretensado. Hasta ahora no se han encontrado estudios sobre el uso de áridos reciclados en hormigón pretensado. Por lo tanto, esta investigación ofrece una primera aproximación a la pérdida de capacidad adherente entre los cordones de pretensado y el hormigón que los envuelve.

Por lo tanto, dos son los objetivos principales de esta tesis:

El primer objetivo consiste en analizar la viabilidad de reemplazar porcentajes de substitución más altos que el límite del 20% recomendado por la EHE-08 para árido grueso en hormigón estructural. Pero en este caso, tanto la fracción fina como gruesa serán reemplazadas. La substitución será simultánea en las fracciones fina y gruesa, de acuerdo con la granulometría del árido reciclado, sin haber sido sometido a un proceso previo de cribado. Por consiguiente, se realizarán ensayos estructurales para caracterizar la rigidez, resistencia y ductilidad de vigas armadas de hormigón reciclado en comparación con las de hormigón convencional. Por lo tanto, se evaluará el comportamiento estructural de vigas de hormigón reciclado.

El segundo objetivo será estudiar la viabilidad de fabricar vigas de hormigón pretensado cuando se introducen áridos reciclados en la mezcla. Las vigas de hormigón pretensado se fabrican y monitorizan en la planta de prefabricados, usando un hormigón reciclado y un hormigón de referencia con una resistencia a compresión similar. Después de transferir el pretensado en planta, se determinan las pérdidas de pretensado y la longitud de transmisión. Después, las vigas son monitorizadas y sometidas a ensayos a flexión por control de desplazamiento, permitiendo determinar su rigidez, resistencia, ductilidad y longitud de anclaje. En resumen, se evaluará el comportamiento estructural de las vigas de hormigón pretensado.

Estos objetivos superan el alcance de la actual instrucción del hormigón estructural EHE-08, tanto en materiales como en los requerimientos sísmicos incluidos en esta normativa nacional. Los resultados de esta tesis pueden apoyar un incremento más allá del 20% recomendado para árido reciclado grueso por la EHE-08 e incluso permitir la incorporación de la fracción fina.

A6.2. Metodología y resultados

La metodología seguida para lograr los objetivos mencionados anteriormente se puede resumir en cuatro etapas que tuvieron lugar en orden cronológico:

La primera etapa incluye un análisis de la legislación actual y estudios realizados hasta la fecha sobre el uso de árido reciclado de hormigón para la fabricación de hormigón además del comportamiento adherente entre los cordones pretensados y el hormigón. La información fue buscada en libros, revistas científicas y en ponencias de congresos. Después de analizar toda la información se diseñó una campaña experimental para estudiar la posibilidad de sustituir porcentajes superiores de árido reciclado a los permitidos por las normativas actuales en hormigón estructural incluyendo la fracción fina.

La segunda etapa describe la primera parte de la campaña experimental. Esta parte incluye:

- Estudio detallado de las principales propiedades de los materiales utilizados en las mezclas de acuerdo con las normativas UNE-EN.
- Ensayos de laboratorio para evaluar la evolución de las propiedades mecánicas del hormigón autocompactante cuando el 0, 20, 35 y 50% del árido total (fino y grueso) es reemplazado por árido reciclado. Estos ensayos fueron realizados conforme a las normativas UNE-EN.
- Fabricación de vigas armadas con porcentajes de sustitución del 0, 10, 20, 35 y 50% del árido total en una planta de prefabricados.
- Ensayos de flexión y cortante de las vigas in-situ en la planta de prefabricados, midiendo en todos ellos la flecha en el centro de la viga. Estos ensayos se hacen a modo de estudio preliminar sobre la pérdida de propiedades mecánicas cuando se introduce el árido reciclado en el hormigón en diversas proporciones.
- Ensayos a flexión controlados por desplazamiento en la Universidade da Coruña con esas vigas, siguiendo el proceso descrito en el Anexo 2 de este documento. La carga aplicada es monitorizada con células de carga, la flecha en centro luz se registra con un transductor potenciométrico de hilo y las deformaciones son medidas con galgas de deformación adheridas a la superficie del hormigón.

La tercera fase describe la segunda parte de la campaña experimental. Esta parte incluye:

- Estudio preliminar del comportamiento mecánico del hormigón convencional pretensado cuando el árido reciclado se introduce en la mezcla en ratios inferiores al 10% del árido total. Para ello, se sometieron a ensayos a flexión y cortante prelosas pretensadas con porcentajes de sustitución del 0, 2, 4, 6, 8 y 10% del árido total.
- Estudio detallado de las principales propiedades de los materiales utilizados en las mezclas de acuerdo con las normas UNE-EN.
- Ensayos de laboratorio para evaluar la evolución de las propiedades mecánicas cuando 0, 8, 20 y 31% del árido total (fino y grueso) es reemplazado. Estos ensayos se realizan de acuerdo con las normas UNE-EN.
- Fabricación y monitorización de vigas pretensadas tipo I con porcentajes de sustitución del 0 y 8% en una planta de prefabricados, siguiendo los procedimientos descritos en los anexos 4 y 5.
- Mediada de la penetración de los cordones y longitud de transmisión inmediatamente después de la transferencia del pretensado.
- Medida de las deformaciones con puntos DEMEC adheridos a la superficie del hormigón en ambas caras de la viga. Estas medidas son tomadas inmediatamente antes y después de transferir el pretensado y a 7, 14, 28, 90 y 300 días.
- Ensayos a flexión con diferentes puntos de aplicación de la carga siguiendo el procedimiento descrito en el anexo 2. La flecha es medida en centro luz con transductor potenciométrico de hilo, la carga aplicada a la viga es registrada con

células de carga en el caso de las 3 primeras vigas ensayas y con un transductor de presión de aceite en las 3 siguientes, la penetración de los cordones en la viga durante el ensayo es registrada con sensores lineales de desplazamiento sujetos a los cordones y los valores de deformación son medidos con galgas de deformación adheridas a la superficie del hormigón.

La última etapa incluye el procesado y posterior análisis de todos los datos obtenidos durante la campaña experimental y su comparación con las predicciones analíticas. Estos resultados son comparados con los de otros autores y se obtienen una serie de conclusiones y recomendaciones.

A6.3. Conclusiones

Se pueden extraer las siguientes conclusiones del trabajo experimental realizado para esta tesis doctoral:

Vigas armadas de hormigón autocompactante reciclado

De la campaña experimental realizada en laboratorio para evaluar las propiedades mecánicas del hormigón reciclado autocompactante, con porcentajes de sustitución del 0, 20, 35 y 50% del árido total (fino y grueso) y que después fueron utilizadas para la fabricación de las vigas armadas, se puede deducir que:

- Todos los hormigones reciclados mostraron suficiente fluidez con una relación agua cemento fijada de 0.50. Para la mezcla del 20%, el diámetro de la torta se incrementó un 12% sin observarse signos de segregación. Este incremento puede ser debido al elevado contenido inicial de agua libre en la mezcla.
- La densidad del hormigón endurecido disminuyó hasta un 1.3% para una sustitución del 50% del contenido total de árido. Una disminución es esperada puesto que la densidad del árido reciclado es inferior a la del árido natural.
- La resistencia a compresión disminuyó ligeramente un 2.7, 4.9 y 4.1% para las sustituciones del 20, 35 y 50% de contenido de árido total, respectivamente.
- La resistencia a tracción indirecta disminuyó hasta un 9.3% para el 50% de sustitución de árido total.
- El módulo de elasticidad disminuyó según aumentaba el porcentaje de sustitución, con una pérdida máxima del 9.5% para la sustitución del 50%.

Considerando que las propiedades del hormigón no se vieron significativamente afectadas por la sustitución simultánea de este tipo de árido reciclado fino y grueso, se podría concluir que es viable reemplazar hasta un 50% de la cantidad total de árido natural por este árido reciclado en particular. Sin embargo, sería interesante realizar ensayos de durabilidad para evaluar el comportamiento a largo plazo.

De las vigas armadas ensayadas a flexión, tanto en la planta de prefabricados como en el CITEEC de la Universidade da Coruña, con porcentajes de sustitución del 0, 10, 20, 35 y 50% de sustitución del árido total, se pueden deducir las siguientes conclusiones:

- Todas las vigas rompieron a flexión como era de esperar. La armadura pasiva inferior plastificó primero, seguida de la rotura del hormigón a compresión en la capa superior, siendo un tipo de rotura dúctil.
- El momento de fisuración de las vigas ensayadas en la planta de prefabricados disminuyó cuando el árido reciclado fino y grueso fue incorporado. Esta pérdida de resistencia a fisuración fue alrededor de un 6% por FB-20 y FB-35 y alrededor de un 12% para FB-50. Cuando las vigas se ensayaron en el CITEEC, la pérdida registrada fue mayor, alcanzando pérdidas del 20% para FB-10 y de un 30% para FB-35 y FB-50.
- El momento último de las vigas recicladas fue ligeramente inferior al de las vigas de hormigón natural según se incrementaba el porcentaje de sustitución, con una pérdida máxima del 2.0% y del 5.8% para FB-50, en la viga ensayada en la planta de prefabricados y en la viga ensayada en el CITEEC, respectivamente.
- Las flechas en el centro de la viga en el momento de rotura en la planta de prefabricados disminuyeron según el porcentaje de sustitución se incrementaba, especialmente para porcentajes altos de sustitución, con pérdidas de hasta un 27% cuando el 50% del árido total es reemplazado. Cuando las vigas fueron ensayadas en el CITEEC, se observó una tendencia similar con pérdidas del 35 y 37% para FB-35 y FB-50, respectivamente.
- Los patrones de fisuración observados fueron similares independientemente del porcentaje de sustitución. La distancia entre fisuras y su espesor fue similar en todas las vigas.
- El ratio de ductilidad de las vigas ensayadas en la planta de prefabricados disminuyó según se incrementaba el porcentaje de sustitución, con pérdidas de hasta un 33% para el 50% de sustitución del árido total. De manera similar, cuando las vigas fueron ensayadas en el CITEEC, se observó una disminución mayor para los porcentajes de sustitución más altos, con pérdidas del 40 y 43% para FB-35 y FB-50, respectivamente.

De las vigas armadas ensayadas a cortante en la planta de prefabricados se pueden deducir las siguientes conclusiones:

- Los ensayos mostraron una rotura frágil a cortante para todas las sustituciones investigadas, como era de esperar.
- La sustitución de árido natural por reciclado disminuyó la fuerza de fisuración en un 17% para todos los porcentajes de sustitución. La flecha correspondiente en el centro de la viga, a la que se produjo la fisuración, también disminuyó, en este caso hasta un 41% para los porcentajes de sustitución superiores (SB-35 y SB-50).

- El cortante de fallo para la viga SB-10 fue prácticamente el mismo que el de la viga de referencia (SB-0) y la flecha correspondiente fue ligeramente superior. Sin embargo, incrementando el porcentaje de sustitución más allá del 20% produjo una ligera disminución del cortante de fallo de entre 4-6%, con las flechas correspondientes similares a las obtenidas en la viga sin árido reciclado.

Considerando los resultados obtenidos de los ensayos a flexión y cortante en esta primera campaña experimental, se puede concluir que la sustitución simultánea de hasta un 50% de árido fino y grueso de hormigón procedente de piezas descartadas es viable para fabricar vigas armadas de hormigón autocompactante. Sin embargo, sería necesario realizar ensayos de durabilidad con el fin de analizar el comportamiento a largo plazo de las vigas de hormigón reciclado.

Vigas pretensadas de hormigón convencional reciclado

Del estudio previo realizado en prelosas pretensadas con árido reciclado con sustituciones de hasta el 10% del árido total se puede concluir que:

- Los momentos últimos de fallo alcanzados en los ensayos de flexión son similares e incluso ligeramente superiores al del hormigón de referencia. Por lo tanto estas pequeñas cantidades de árido reciclado no tienen un efecto perjudicial sobre el comportamiento a flexión de estos elementos.
- En los ensayos a cortante, el cortante último no se ve afectado con la sustitución del 2%, sin embargo, para sustituciones superiores disminuye un 25%. Por lo tanto, se puede concluir que tiene un efecto negativo sobre la resistencia a cortante.

De los ensayos realizados en el laboratorio para evaluar las propiedades del hormigón convencional utilizado para la fabricación de las vigas pretensadas con porcentajes de sustitución del 0, 8, 20 y 31% del árido total se pueden deducir las siguientes conclusiones:

- Todos los hormigones reciclados mostraron suficiente consistencia con una relación agua/cemento fijada de 0.45. Para las mezclas F-8 y F-20, la medida del cono de Abrams se incrementó un 8 y 13 %, respectivamente, debido al mayor contenido de agua libre de mezcla. Sin embargo, para la mezcla F-31 el cono se estabilizó con respecto al 20% de sustitución, probablemente debido a que el efecto de la absorción de agua se hace más notable para porcentajes de sustitución elevados.
- La densidad del hormigón endurecido disminuyó un 1, 4 y 5% para las sustituciones del 8, 20 y 31% del árido total, respectivamente.
- La resistencia a compresión a 28 días disminuyó 1, 3 y 9% para el 8, 20 y 31% de sustitución del árido total, respectivamente.
- De los ensayos de resistencia a flexión en probetas prismáticas, con excepción del resultado incoherente obtenido para el 0% de sustitución, la tendencia general fue que la resistencia a flexión disminuyó según se incrementaba el porcentaje de

sustitución, con pérdidas del 8 y 13% para F-20 y F-31, respectivamente, con respecto a F-8.
- El módulo de elasticidad a la edad de 28 días disminuyó un 3, 8 y 20% para el 8, 20 y 31% de sustitución del árido total, respectivamente.
- La profundidad de penetración de agua bajo presión no se incrementó cuando el árido reciclado se introdujo en la mezcla.

Considerando que las propiedades del hormigón no se vieron significativamente afectadas por la sustitución simultánea de este tipo de árido reciclado fino y grueso, se podría concluir que es viable reemplazar hasta un 31% de la cantidad total de árido natural por este árido reciclado en particular. Sin embargo, sería interesante realizar ensayos de durabilidad para evaluar la retracción del hormigón, la penetración de ion cloruro, resistencia a la abrasión y la resistencia a la carbonatación para evaluar el comportamiento a largo plazo puesto que este hormigón se utiliza para la fabricación de elementos pretensados que deben evitar pérdidas en la fuerza de pretensado transmitida por los cordones.

Del proceso de transferencia del pretensado durante la fabricación de las vigas con un 0 y un 8% de sustitución del árido reciclado se pueden extraer las siguientes conclusiones:

- El valor medio de la penetración registrada por cordón de pretensado en la viga al transferir fue un 25% superior en las vigas de árido reciclado.
- No se apreciaron grandes diferencias con respecto a la contraflecha y el acortamiento elástico.
- Las pérdidas instantáneas registradas por las galgas internamente adheridas a los cordones de pretensado fueron un 25% superiores para las vigas con un 8% de sustitución de árido reciclado.

Los ensayos Pull-Out fueron realizados para simular el comportamiento adherente a lo largo de la longitud adicional de anclaje. De estos ensayos se puede concluir que la tensión adherente a la que se produce el primer desplazamiento (0.01 mm) es aproximadamente un 24% más baja cuando el 8% del árido total se sustituye por árido reciclado.

De las medidas de longitud de transmisión con puntos DEMEC en el ala inferior de la viga se puede concluir que:

- El efecto negativo de la sustitución del 8% del árido total es perfectamente observable.
- La longitud de transmisión en las vigas de árido reciclado es claramente superior a la de las vigas de árido natural, especialmente a mayores edades. Si se comparan los valores máximos, la longitud de transmisión desciende un 33 y un 13% en los anclajes pasivo y activo, respectivamente.

- Otro efecto negativo del árido reciclado en la longitud de transmisión se puede observar en su evolución a lo largo del tiempo. Si la longitud medida inmediatamente después de transferir el pretensado se compara con el valor máximo medido a lo largo del tiempo a ambos lados de la viga, se puede concluir que este incremento es mayor en las vigas de hormigón reciclado.

De los ensayos a flexión realizados para determinar la longitud de anclaje en las vigas pretensadas se puede concluir que:

- La longitud de anclaje determinada para las vigas fabricadas únicamente con árido natural fue de 1475 mm. Mientras que para las vigas con un 8% de árido reciclado fue de 1850 mm, es decir un 25% superior. Estas fueron las máximas distancia del extremo de la viga al punto de aplicación de la carga para la que el valor de penetración del cordón registrado fue inferior a 0.5 mm.
- Esta diferencia es comparable a la diferencia registrada en los ensayos Pull-Out para la tensión de adherencia en la que se registra el primer deslizamiento.
- Con respecto al momento de fallo de las vigas en los ensayos a flexión, no se observaron grandes diferencias entre ellos relacionadas con la incorporación de árido reciclado a la mezcla. Todos los valores estaban en un rango de 350 – 450 kN, independientemente de estar fabricadas de hormigón reciclado o natural.

Considerando los resultados obtenidos de estos ensayos en hormigón pretensado se puede concluir que la pérdida de adherencia es significativa cuando sustituimos un 8% del árido total en la mezcla. Sin embargo, los momentos de fallo son similares independientemente del porcentaje de sustitución. Sería necesario realizar ensayos de durabilidad para analizar el comportamiento a largo plazo cuando se introduce el árido reciclado en la mezcla.

Appendix 7. Extended summary in Galician

A7.1. Introdución e obxectivos

O rápido desenvolvemento urbano das últimas décadas co formigón como principal material de construción, orixinou unha redución dos recursos naturais dispoñibles nalgunhas partes do mundo. A extracción de materias primas ten un impacto importante no medio ambiente, modificando o curso e leito dos ríos, orixinando problemas de estabilidade en ladeiras e danando a paisaxe natural. Ao mesmo tempo, millóns de toneladas de cascallos procedentes de residuos de construción e demolición son xerados e van directamente a vertedoiros sen un tratamento previo ou selección que podería dar lugar a unha posible reutilización.

De acordo co Plan Nacional de Xestión de Residuos de Construción e Demolición (2001-2006), aproximadamente a metade dos residuos de construción e demolición producidos en España están compostos de ladrillo, azulexo e cerámica, e sobre o 20% están compostos de formigón e morteiro. Estes residuos poden ser reutilizados como áridos reciclados para a fabricación de formigón despois de ser machucados e cribados. Varios estudos foron realizados ata a data por diferentes autores con resultados moi prometedores [GEAR 2002].

A maior parte dos países teñen normativas sobre o uso do árido reciclado en formigón. En particular, a Instrución española de Formigón Estrutural [EHE 08] define "formigón reciclado" como un formigón producido exclusivamente con árido reciclado do machaqueo de pezas de formigón, e recomenda limitar a porcentaxe de substitución ao 20% cando se usa en formigón estrutural. Por tanto, exclúe o árido reciclado fino e os áridos cunha orixe diferente ao formigón (árido reciclado mixto, asfalto, etc.).

Noutros países, as normativas con respecto ao uso do árido reciclado son diferentes. Nalgunhas delas permítense porcentaxes de substitución máis altos de árido groso de formigón en formigón estrutural, como en Alemaña e Xapón cun 35%, ou mesmo en Holanda e Dinamarca, que se permite un 100% de substitución. Con respecto ao uso do árido reciclado fino de formigón, está permitido o seu uso en Brasil cun 100% de

substitución para formigón non estrutural, en Xapón ata un 100% para estruturas menos esixentes, en Holanda soamente se o árido groso é natural, en Suíza cun 100% de substitución mesmo en formigón estrutural, 20% en Dinamarca para ambientes non agresivos e 100% en Rusia para formigón non pretensado.

Despois de analizar varios estudos sobre o uso do árido reciclado fino de formigón, pódese concluír que é viable fabricar formigón con árido reciclado fino e obter un comportamento similar ao do formigón fabricado exclusivamente con áridos naturais. Por tanto, é demasiado conservativo considerar inaceptable o seu uso para a fabricación do formigón.

Esta tese ten como finalidade levar un paso adiante a reciclaxe do formigón. Ata agora, a maior parte das investigacións centráronse en substituír unicamente diferentes procentaxes da fracción grosa con árido reciclado de diferentes orixes. O número de estudos realizados substituíndo a fracción fina é inferior, e cando se substitúen ambas adoita realizarse de maneira independente. Este proceso leva un importante gasto de enerxía posto que os áridos necesitan ser cribados para obter as fraccións desexadas.

Nesta tese doutoral proponse substituír simultaneamente a fracción fina e grosa sen ter que cribar o árido reciclado bruto. É necesario analizar previamente a granulometría do árido reciclado para determinar a súa porcentaxe de partículas finas (< 4 mm). Á hora de fabricar o formigón, o árido reciclado introdúcese directamente na mestura como substitución do árido total, quitando as cantidades correspondentes das fraccións fina e grosa naturais, segundo a porcentaxe de finos previamente determinado.

Con este método é posible obter unha granulometría conxunta similar á do árido total, independentemente da porcentaxe de substitución. Ademais, a fracción fina introdúcese na mestura de formigón en lugar de ser rexeitada e evítase o correspondente gasto enerxético ao cribar.

Este método de substitución non só probouse en formigón armado, senón tamén en formigón pretensado. Ata agora non se atoparon estudos sobre o uso de áridos reciclados en formigón pretensado. Por tanto, esta investigación ofrece unha primeira aproximación á perda de capacidade adherente entre os cordóns de pretensado e o formigón que os envolve.

Por tanto, dous son os obxectivos principais desta tese:

O primeiro obxectivo consiste en analizar a viabilidade de substituír porcentaxes de substitución máis altos que o límite do 20% recomendado pola EHE-08 para árido groso en formigón estrutural. Pero neste caso, tanto a fracción fina como grosa serán substituídas. A substitución será simultánea nas fraccións fina e grosa, de acordo coa granulometría do árido reciclado, sen ser sometido a un proceso previo de cribado. Por conseguinte,

realizaranse ensaios estruturais para caracterizar a rixidez, resistencia e ductilidade de vigas armadas de formigón reciclado en comparación coas de formigón convencional. Por tanto, avaliarase o comportamento estrutural de vigas de formigón reciclado.

O segundo obxectivo será estudar a viabilidade de fabricar vigas de formigón pretensado cando se introducen áridos reciclados na mestura. As vigas de formigón pretensado fabrícanse e monitorízanse na planta de prefabricados, usando un formigón reciclado e un formigón de referencia cunha resistencia a compresión similar. Despois de transferir o pretensado en planta, determínanse as perdas de pretensado e a lonxitude de transmisión. Despois, as vigas son monitorizadas e sometidas a ensaios a flexión por control de desprazamento, permitindo determinar a súa rixidez, resistencia, ductilidade e lonxitude de ancoraxe. En resumo, avaliarase o comportamento estrutural das vigas de formigón pretensado.

Estes obxectivos superan o alcance da actual instrución do formigón estrutural EHE-08, tanto en materiais como nos requirimentos sísmicos incluídos nesta normativa nacional. Os resultados desta tese poden apoiar un incremento máis aló do 20% recomendado para árido reciclado groso pola EHE-08 e mesmo permitir a incorporación da fracción fina.

A7.2. Metodoloxía e resultados

A metodoloxía seguida para lograr os obxectivos mencionados anteriormente pódese resumir en catro etapas que tiveron lugar en orde cronolóxica:

A primeira etapa inclúe unha análise da lexislación actual e estudos realizados ata a data sobre o uso do árido reciclado de formigón para a fabricación de formigón ademais do comportamento adherente entre os cordóns pretensados e o formigón. A información foi buscada en libros, revistas científicas e en publicacións en congresos. Despois de analizar toda a información deseñouse unha campaña experimental para estudar a posibilidade de substituír porcentaxes superiores de árido reciclado aos permitidos polas normativas actuais en formigón estrutural incluíndo a fracción fina.

A segunda etapa describe a primeira parte da campaña experimental. Esta parte inclúe:

- Estudo detallado das principais propiedades dos materiais utilizados nas mesturas de acordo coas normativas UNE-EN.
- Ensaios de laboratorio para avaliar a evolución das propiedades mecánicas do formigón autocompactante cando o 0, 20, 35 e 50% do árido total (fino e groso) é substituído por árido reciclado. Estes ensaios foron realizados conforme ás normativas UNE-EN.
- Fabricación de vigas armadas con porcentaxes de substitución do 0, 10, 20, 35 e 50% do árido total nunha planta de prefabricados.

- Ensaios de flexión e cortante das vigas in-situ na planta de prefabricados, medindo en todos eles a frecha no centro da viga. Estes ensaios fanse a modo de estudo preliminar sobre a perda de propiedades mecánicas cando se introduce o árido reciclado no formigón en diversas proporcións.
- Ensaios a flexión controlados por desprazamento na Universidade da Coruña con esas vigas, seguindo o proceso descrito no Anexo 2 deste documento. A carga aplicada é monitorizada con células de carga, a frecha en centro luz rexístrase cun transductor potenciométrico de fío e as deformacións son medidas con galgas de deformación adheridas á superficie do formigón.

A terceira fase describe a segunda parte da campaña experimental. Esta parte inclúe:

- Estudo preliminar do comportamento mecánico do formigón convencional pretensado cando o árido reciclado se introduce na mestura en cocientes inferiores ao 10% do árido total. Para iso, sometéronse a ensaios a flexión e cortante prelosas pretensadas con porcentaxes de substitución do 0, 2, 4, 6, 8 e 10% do árido total.
- Estudo detallado das principais propiedades dos materiais utilizados nas mesturas de acordo coas normas UNE-EN.
- Ensaios de laboratorio para avaliar a evolución das propiedades mecánicas cando 0, 8, 20 e 31% do árido total (fino e groso) é substituído. Estes ensaios realízanse de acordo coas normas UNE-EN.
- Fabricación e monitorización de vigas pretensadas tipo I con porcentaxes de substitución do 0 e 8% nunha planta de prefabricados, seguindo os procedementos descritos nos anexos 4 e 5.
- Mediada da penetración dos cordóns e lonxitude de transmisión inmediatamente despois da transferencia do pretensado.
- Medida das deformacións con puntos DEMEC adheridos á superficie do formigón en ambas as caras da viga. Estas medidas son tomadas inmediatamente antes e despois de transferir o pretensado e a 7, 14, 28, 90 e 300 días.
- Ensaios a flexión con diferentes puntos de aplicación da carga seguindo o procedemento descrito no Anexo 2. A frecha é medida en centro luz con transductor potenciométrico de fío, a carga aplicada á viga é rexistrada con células de carga no caso das 3 primeiras vigas ensaias e cun transductor de presión de aceite nas 3 seguintes, a penetración dos cordóns na viga durante o ensaio é rexistrada con sensores lineais de desprazamento suxeitos aos cordóns e os valores de deformación son medidos con galgas de deformación adheridas á superficie do formigón.

A última etapa inclúe o procesado e posterior análise de todos os datos obtidos durante a campaña experimental e a súa comparación coas predicións analíticas. Estes resultados son comparados cos doutros autores e obtéñense unha serie de conclusións e recomendacións.

A7.3. Conclusións

Pódense extraer as seguintes conclusións do traballo experimental realizado para esta tese doutoral:

Vigas armadas de formigón autocompactante reciclado

Da campaña experimental realizada en laboratorio para avaliar as propiedades mecánicas do formigón reciclado autocompactante, con porcentaxes de substitución do 0, 20, 35 e 50% do árido total (fino e groso) e que despois foron utilizadas para a fabricación das vigas armadas, pódese deducir que:

- Todos os formigóns reciclados mostraron suficiente fluidez cunha relación auga cemento fixada de 0.50. Para a mestura do 20%, o diámetro da torta incrementouse un 12% sen observarse signos de segregación. Este incremento pode ser debido ao elevado contido inicial de auga libre na mestura.
- A densidade do formigón endurecido diminuíu ata un 1.3% para unha substitución do 50% do contido total de árido. Unha diminución é esperada posto que a densidade do árido reciclado é inferior á do árido natural.
- A resistencia a compresión diminuíu lixeiramente un 2.7, 4.9 e 4.1% para as substitucións do 20, 35 e 50% de contido de árido total, respectivamente.
- A resistencia a tracción indirecta diminuíu ata un 9.3% para o 50% de substitución de árido total.
- O módulo de elasticidade diminuíu segundo aumentaba a porcentaxe de substitución, cunha perda máxima do 9.5% para a substitución do 50%.

Considerando que as propiedades do formigón non se viron significativamente afectadas pola substitución simultánea deste tipo de árido reciclado fino e groso, poderíase concluír que é viable substituír ata un 50% da cantidade total de árido natural por este árido reciclado en particular. Con todo, sería interesante realizar ensaios de durabilidade para avaliar o comportamento a longo prazo.

Das vigas armadas ensaiadas a flexión, tanto na planta de prefabricados como no CITEEC da Universidade dá Coruña, con porcentaxes de substitución do 0, 10, 20, 35 e 50% de substitución do árido total, pódense deducir as seguintes conclusións:

- Todas as vigas romperon a flexión como era de esperar. A armadura pasiva inferior plastificou primeiro, seguida da rotura do formigón a compresión na capa superior, sendo un tipo de rotura dúctil.
- O momento de fisuración das vigas ensaiadas na planta de prefabricados diminuíu cando o árido reciclado fino e groso foi incorporado. Esta perda de resistencia a fisuración foi ao redor dun 6% por FB-20 e FB-35 e ao redor dun 12% para FB-50.

Cando as vigas ensaiáronse no CITEEC, a perda rexistrada foi maior, alcanzando perdas do 20% para FB-10 e dun 30% para FB-35 e FB-50.

- O momento último das vigas recicladas foi lixeiramente inferior ao das vigas de formigón natural segundo incrementábase a porcentaxe de substitución, cunha perda máxima do 2.0% e do 5.8% para FB-50, na viga ensaiada na planta de prefabricados e na viga ensaiada no CITEEC, respectivamente.
- As frechas no centro da viga no momento de rotura na planta de prefabricados diminuíron segundo a porcentaxe de substitución incrementábase, especialmente para porcentaxes altas de substitución, con perdas de ata un 27% cando o 50% do árido total é substituído. Cando as vigas foron ensaiadas no CITEEC, observouse unha tendencia similar con perdas do 35 e 37% para FB-35 e FB-50, respectivamente.
- Os patróns de fisuración observados foron similares independentemente da porcentaxe de substitución. A distancia entre fisuras e o seu espesor foi similar en todas as vigas.
- O cociente de ductilidade das vigas ensaiadas na planta de prefabricados diminuíu segundo se incrementaba a porcentaxe de substitución, con perdas de ata un 33% para o 50% de substitución do árido total. De maneira similar, cando as vigas foron ensaiadas no CITEEC, observouse unha diminución maior para as porcentaxes de substitución máis altos, con perdas do 40 e 43% para FB-35 e FB-50, respectivamente.

Das vigas armadas ensaiadas a cortante na planta de prefabricados pódense deducir as seguintes conclusións:

- Os ensaios mostraron unha rotura fráxil a cortante para todas as substitucións investigadas, como era de esperar.
- A substitución de árido natural por reciclado diminuíu a forza de fisuración nun 17% para todas as porcentaxes de substitución. A frecha correspondente no centro da viga, á que se produciu a fisuración, tamén diminuíu, neste caso ata un 41% para as porcentaxes de substitución superiores (SB-35 e SB-50).
- O cortante de fallo para a viga SB-10 foi practicamente o mesmo que o da viga de referencia (SB-0) e a frecha correspondente foi lixeiramente superior. Con todo, incrementando a porcentaxe de substitución máis aló do 20% produciu unha lixeira diminución do cortante de fallo de entre 4-6%, coas frechas correspondentes similares ás obtidas na viga sen árido reciclado.

Considerando os resultados obtidos dos ensaios a flexión e cortante nesta primeira campaña experimental, pódese concluír que a substitución simultánea de ata un 50% de árido fino e groso de formigón procedente de pezas descartadas é viable para fabricar vigas armadas de formigón autocompactante. Con todo, sería necesario realizar ensaios de durabilidade co fin de analizar o comportamento a longo prazo das vigas de formigón reciclado.

Vigas pretensadas de formigón convencional reciclado

Do estudo previo realizado en prelosas pretensadas con árido reciclado con substitucións de ata o 10% do árido total pódese concluír que:

- Os momentos últimos de fallo alcanzados nos ensaios de flexión son similares e mesmo lixeiramente superiores ao do formigón de referencia. Por tanto estas pequenas cantidades de árido reciclado non teñen un efecto prexudicial sobre o comportamento a flexión destes elementos.
- Nos ensaios a cortante, o cortante último non se ve afectado coa substitución do 2%, con todo, para substitucións superiores diminúe un 25%. Por tanto, pódese concluír que ten un efecto negativo sobre a resistencia a cortante.

Dos ensaios realizados no laboratorio para avaliar as propiedades do formigón convencional utilizado para a fabricación das vigas pretensadas con porcentaxes de substitución do 0, 8, 20 e 31% do árido total pódense deducir as seguintes conclusións:

- Todos os formigóns reciclados mostraron suficiente consistencia con unha relación auga/cemento fixada de 0.45. Para as mesturas F-8 e F-20, a medida do cono de Abrams incrementouse un 8 e 13 %, respectivamente, debido ao maior contido de auga libre de mestura. Con todo, para a mestura F-31 o cono estabilizouse con respecto ao 20% de substitución, probablemente debido a que o efecto da absorción de auga faise máis notable para porcentaxes de substitución elevados.
- A densidade do formigón endurecido diminuíu un 1, 4 e 5% para as substitucións do 8, 20 e 31% do árido total, respectivamente.
- A resistencia a compresión a 28 días diminuíu 1, 3 e 9% para o 8, 20 e 31% de substitución do árido total, respectivamente.
- Dos ensaios de resistencia a flexión en probetas prismáticas, con excepción do resultado incoherente obtido para o 0% de substitución, a tendencia xeral foi que a resistencia a flexión diminuíu segundo incrementábase a porcentaxe de substitución, con perdas do 8 e 13% para F-20 e F-31, respectivamente, con respecto a F-8.
- O módulo de elasticidade á idade de 28 días diminuíu un 3, 8 e 20% para o 8, 20 e 31% de substitución do árido total, respectivamente.
- A profundidade de penetración de auga baixa presión non se incrementou cando o árido reciclado introduciuse na mestura.

Considerando que as propiedades do formigón non se viron significativamente afectadas pola substitución simultánea deste tipo de árido reciclado fino e groso, poderíase concluír que é viable substituír ata un 31% da cantidade total de árido natural por este árido reciclado en particular. Con todo, sería interesante realizar ensaios de durabilidade para avaliar a retracción do formigón, a penetración de ión cloruro, resistencia á abrasión e a resistencia á carbonatación para avaliar o comportamento a longo prazo posto que este

formigón utilízase para a fabricación de elementos pretensados que deben evitar perdas na forza de pretensado transmitida polos cordóns.

Do proceso de transferencia do pretensado durante a fabricación das vigas cun 0 e un 8% de substitución da árido reciclado pódense extraer as seguintes conclusións:

- O valor medio da penetración rexistrada por cordón de pretensado na viga ao transferir foi un 25% superior nas vigas de árido reciclado.
- Non se apreciaron grandes diferenzas con respecto á contraflecha e o acortamiento elástico.
- As perdas instantáneas rexistradas polas galgas internamente adheridas aos cordóns de pretensado foron uns 25% superiores para as vigas cun 8% de substitución de árido reciclado.

Os ensaios Pull-Out foron realizados para simular o comportamento adherente ao longo da lonxitude adicional de ancoraxe. Destes ensaios pódese concluír que a tensión adherente á que se produce o primeiro desprazamento (0.01 mm) é aproximadamente un 24% máis baixa cando o 8% do árido total substitúese por árido reciclado.

Das medidas de lonxitude de transmisión con puntos DEMEC na á inferior da viga pódese concluír que:

- O efecto negativo da substitución do 8% do árido total é perfectamente observable.
- A lonxitude de transmisión nas vigas de árido reciclado é claramente superior á das vigas de árido natural, especialmente a maiores idades. Se se comparan os valores máximos, a lonxitude de transmisión descende un 33 e un 13% nas ancoraxes pasivo e activo, respectivamente.
- Outro efecto negativo do árido reciclado na lonxitude de transmisión pódese observar na súa evolución ao longo do tempo. Se a lonxitude medida inmediatamente despois de transferir o pretensado compárase co valor máximo medido ao longo do tempo a ambos os dous lados da viga, pódese concluír que este incremento é maior nas vigas de formigón reciclado.

Dos ensaios a flexión realizados para determinar a lonxitude de ancoraxe nas vigas pretensadas pódese concluír que:

- A lonxitude de ancoraxe determinada para as vigas fabricadas unicamente con árido natural foi de 1475 mm. Mentres que para as vigas cun 8% de árido reciclado foi de 1850 mm, é dicir un 25% superior. Estas foron a máximas distancia do extremo da viga ao momento de aplicación da carga para a que o valor de penetración do cordón rexistrado foi inferior a 0.5 mm.

- Esta diferenza é comparable á diferenza rexistrada nos ensaios Pull-Out para a tensión de adherencia na que se rexistra o primeiro deslizamiento.
- Con respecto ao momento de fallo das vigas nos ensaios a flexión, non se observaron grandes diferenzas entre eles relacionadas coa incorporación de árido reciclado á mestura. Todos os valores estaban nun rango de 350 - 450 kN, independentemente de estar fabricadas de formigón reciclado ou natural.

Considerando os resultados obtidos destes ensaios en formigón pretensado pódese concluír que a perda de adherencia é significativa cando substituímos un 8% do árido total na mestura. Con todo, os momentos de fallo son similares independentemente da porcentaxe de substitución. Sería necesario realizar ensaios de durabilidad para analizar o comportamento a longo prazo cando se introduce o árido reciclado na mestura.